Synthesis, Characterization, Electrochemistry, and Ring-Opening Polymerization of Heavier Group 13 Bridged Metallocenophanes

A Thesis Submitted to the College of

Graduate Studies and Research

in Partial Fulfillment of the Requirements

for the Degree of Doctor of Philosophy

in the Department of Chemistry

University of Saskatchewan

Saskatoon

By

Jörg A. Schachner

Permission to Use

In presenting this thesis in partial fulfilment of the requirements for a Postgraduate degree from the University of Saskatchewan, I agree that the Libraries of this University may make it freely available for inspection. I further agree that permission for copying of this thesis in any manner, in whole or in part, for scholarly purposes may be granted by the professor or professors who supervised my thesis work or, in their absence, by the Head of the Department or the Dean of the College in which my thesis work was done. It is understood that any copying or publication or use of this thesis or parts thereof for financial gain shall not be allowed without my written permission. It is also understood that due recognition shall be given to me and to the University of Saskatchewan in any scholarly use which may be made of any material in my thesis.

Requests for permission to copy or to make other use of material in this thesis in whole or part should be addressed to:

Head of the Department of Chemistry

University of Saskatchewan

Saskatoon, Saskatchewan (S7N 5C9)

Canada

ABSTRACT

The synthesis of two types of metallocenophanes is described: strained, ring-tilted [1]metallocenophanes with Al and Ga in bridging positions and Fe and Ru as transition elements and unstrained [1.1]ferrocenophanes with Al, Ga and In in bridging positions. [1]Metallocenophanes are potential monomers for the synthesis of organometallic polymers via ring-opening polymerization (ROP). After the successful synthesis of various starting monomers using the concept of intramolecular coordinating ligands, four different pathways of ROP were investigated. However, only one of these pathways proved successful in obtaining polymeric material. The starting monomers showed a surprising stability against commonly used initiators. This was attributed to an overly steric protection by the intramolecular coordinating ligands, thereby blocking the initiators, and a reduced ring strain, a consequence of the size of the bridging element.

[1.1]Ferrocenophanes belong to a class of dinuclear complexes where the two redox-active iron atoms are in close proximity with restricted flexibility. [1.1]Ferrocenophanes with Al, Ga and In in bridging positions were investigated. The redox properties of previously published [1.1]ferrocenophanes showed a fully reversible, stepwise, one-electron oxidation (FeII/FeII → FeII/FeIII → FeIII/FeIII). After the initial oxidation of the first iron center, a stable, mixed-valent monocationic species is created. The removal of a second electron from the second iron center therefore is more difficult, and occurs at higher potential to create the dicationic species. The difference in potential for the stepwise oxidation is directly related to the delocalization of the charge in the mixed-valent species. This delocalization mainly depends on the electronic properties of the bridging element. Depending on the bridging

group 13 element, very different electrochemical properties were observed. For the alumina[1.1]ferrocenophane, no delocalization was detected, and a one-step, two-electron oxidation at the same potential was observed. For the inda[1.1]ferrocenophane, a more complex electrochemistry was observed that we attributed to an isomerization of the compound in solution. Only the investigated galla[1.1]ferrocenophane showed the expected stepwise oxidation-reduction behavior.

ACKNOWLEDGMENTS

I would like to thank Prof. Jens Müller for all his support and guidance during my time as a PhD student in his group at the University of Saskatchewan.

I would like to thank the University of Saskatchewan and the Department of Chemistry for accepting me as a PhD candidate and providing financial support. I would also like to thank the staff at the Saskatchewan Structural Science Center, especially Dr. J. Wilson Quail, for their help and support.

I would like to thank my colleagues and friends Clinton Lund and Landon Ziffle for all their help and support, both in my academic career as well as my private life.

I would like to thank my parents Klaus and Eva and my brother Schoko for always helping and encouraging me in so many ways, and supporting me in obtaining this degree.

LIST OF FIGURES

Figure page

LIST OF SCHEMES

Scheme page

LIST OF TABLES

Table page

LIST OF ABBREVIATIONS

Abbreviation

[1]FeCP ..... [1]ferrocenophane
[1]RuCP ..... [1]ruthenocenophane
[1.1]CoFeCP ..... [1.1]cobaltoferrocenophane
[1.1]CoCP ..... [1.1]cobaltocenophane
[1.1]FeRuCP ..... [1.1]ferroruthenocenophanes
[1.1]RuCP ..... [1.1]ruthenocenophane
anROP ..... anionic ring-opening polymerization
BHT 2,6-di-*tert*-butyl-4-methylphenol
CN ..... coordination number
COD 1,5-cyclooctadiene
COT ..... cyclooctatetraene
Cp ..... cyclopentadienyl
Cp* ..... pentamethylcyclopentadienyl
Cy ..... cyclohexyl
CV ..... Cyclic Voltammetry
dba ..... dibenzylideneacetone
dmpe ..... dimethylphosphinoethane
DSC ..... Differential Scanning Calorimetry
GPC ..... Gel Permeation Chromatography
LALLS ..... low-angle Laser Light Scattering
MCP ..... metallocenphane
M_n ..... number average molecular weight
M_w ..... weight average molecular weight
MO ..... molecular orbital
MS ..... Mass Spectrometry
PDI ..... poly-dispersity index
phROP ..... photolytic ring-opening polymerization
PMDTA ..... N,N',N',N'',N''-pentamethyldiethylenetriamine
r ..... radius
ROP ..... ring-opening polymerization
thROP ..... thermal ring-opening polymerization
TMEDA ..... N,N,N',N',-tetramethylethylenediamine
tmROP ..... transition metal catalyzed ring-opening polymerization
VT-NMR ..... variable temperature NMR spectroscopy
WAXS ..... wide-angle X-ray Scattering

TABLE OF CONTENTS

page

CHAPTER 1
INTRODUCTION

1.1 [1]Metallocenophanes

[1]Metallocenophanes ([1]MCPs) are strained, ring-tilted cyclic complexes consisting of two cyclopentadienyl rings, a transition metal M that is π-bound to each cyclopentadienyl ring in a η^5-fashion and one bridging element E that is σ-bound to each cyclopentadienyl ring and a ligand of the general form R_x (Figure 1-1). The ligand R_x can be simply σ- or π-bound ligands (in these cases x = 1 or 2) or can be spirocyclic or contain intramolecular coordinating donors.

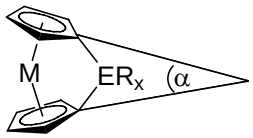

Figure 1-1. Schematic representation of an ER_x-bridged [1]metallocenophane with tilt angle α.

The introduction of the bridging element distorts the coplanar arrangement of the cyclopentadiene rings in the parent metallocene resulting in a ring tilt thereby forcing the two *ipso* carbons of the cyclopentadienyl rings closer to the transition metal. In addition to the ring tilt there is a considerable bond angle distortion at the *ipso* carbon-element bond. Both distortions results in ring strain that is usually indicated by the tilt angle α which can be determined by X-ray crystallography. For main-group bridging

elements, another analytical tool that indicates the amount of ring strain is the ^{13}C NMR shift of the *ipso* carbons of the cyclopentadienyl rings, which are shifted upfield with respect to the parent metallocene. This shift however rather gives a trend than an absolute measurement of ring tilt, because values cannot be attributed to a single structural parameter alone, as will be discussed later. In the case that the bridging elements are transition metals, the trend is actually reversed, with the *ipso* carbon atoms showing a downfield shift in the ^{13}C NMR spectra. An in-depth review on bent metallocenes and ring strain was published by Green.[1]

Although initially believed to be too unstable to be isolated because "intramolecular cyclization would produce an impossibly strained system",[2] there have been two synthetic pathways established that yield [1]MCPs, which are commonly referred to as the dilithiation route (Scheme 1-1 **A**) and the fly-trap route (Scheme 1-1 **B**).

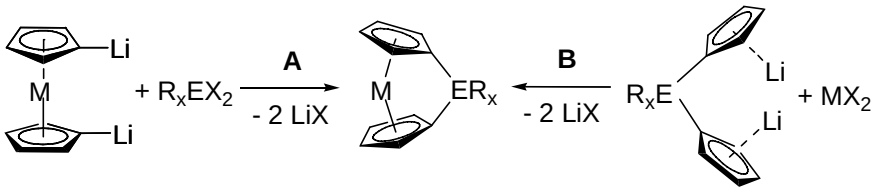

Scheme 1-1. Two main pathways to synthesize [1]MCPs. Dilithiation route **A** and fly-trap route **B**.

When applicable, the dilithiation route **A** is preferable because it gives higher yields. Amongst other side reactions, route **B** has a tendency to yield low molecular weight oligomeric materials, likely from polycondensation type reactions, which competes with [1]metallocenophane cyclization. Dilithiation of metallocene can be achieved cleanly with alkyl-lithium reagents in the presence of a base like N,N,N',N'-

tetramethylethylenediamine (TMEDA) or N,N',N',N'',N''-pentamethyldiethylenetriamine (PMDTA). The dilithiated metallocene can be isolated and stored or generated *in situ*. Depending on the metallocene, adducts with these bases of different stoichiometry are formed. For dilithioferrocene, a crystal structure determination revealed the structure to be a 3:2 adduct of 1,1'-dilithioferrocene with TMEDA, equivalent with dilithioferrocene · 2/3 TMEDA.[3] For dilithioruthenocene, the mono-adduct 1,1'-dilithioruthenocene · TMEDA is obtained, although no crystal structure data is available to confirm this.[4] For ease of readability, the TMEDA adduct part will be omitted from here on and the starting complexes simply referred to as dilithioferrocene and dilithioruthenocene, respectively. Some metallocenes, however, are not accessible from dilithiation due to decomposition of the metallocene. In these cases, the desired [1]MCP can be prepared via a dilithiation of the $R_xE(CpH)_2$ precursor using alkyl-lithium reagents or other strong bases and subsequent reaction with the respective metal source, usually metal halides. All new [1]MCPs discussed within this thesis have been prepared via dilithiation route **A**.

1.1.1 Group 4-Bridged [1]Metallocenophanes

The series of Ti-, Zr- and Hf-bridged [1]FeCPs was reported by Gautheron *et al.* from reactions of dilithioferrocene and the respective R_xECl_2 metal halide [ER_x = $TiCp_2$ (**1a**), = $Ti(C_5H_4tBu)_2$ **(1b)**; $ZrCp_2$ (**2a**), $Zr(C_5H_4tBu)_2$ (**2b**); $HfCp_2$ (**3a**), $Hf(C_5H_4tBu)_2$ **(3b)**].[5] Complex **2b**, which contains *tert*-butyl groups on the Zr-bound cyclopentadienyl rings, was fully characterized by X-ray crystallography and displayed with $\alpha = 6.0°$ the smallest tilt angle reported for a [1]FeCP to date (Figure 1-2).

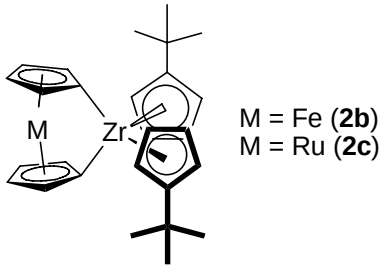

Figure 1-2. Zircona[1]metallocenophanes **2b** (M = Fe) and **2c** (M = Ru).

It is interesting to note that the *ipso* carbon ^{13}C resonances of **1b**, **2b** and **3b** were shifted downfield to 150-180 ppm. This is the exact opposite of what is usually observed for main group-bridged [1]MCPs.[5]

An example of a zirconium-bridged [1]ruthenocenophane ([1]RuCP) was reported by Manners *et al.* (Figure 1-2).[6] The zirconium-bridged complex **2c** [ER_x = $Zr(C_5H_4tBu)_2$] contained the same ligands as **2b**. The bigger size of the ruthenium atom in **2c** over the iron atom in **2b** increased the tilt angle of **2c** to $\alpha = 10.4°$. In the ^{13}C NMR spectrum a similar downfield shift of the cyclopentadienyl *ipso* carbon to 165 ppm was observed.

1.1.2 Group 13-Bridged [1]Metallocenophanes

The only examples of group 13-bridged [1]FeCPs were published by Braunschweig and Manners with boron as a bridging element.[7] To date, these complexes are the only [1]metallocenophanes bridged by a second row element. The successful synthesis was achieved using aminoboranes equipped with bulky ligands to obtain bora[1]ferrocenophanes **4a** [ER_x = $BN(SiMe_3)_2$] and **4b** [ER_x = $BN(SiMe_3)(tBu)$] (Figure 1-3).

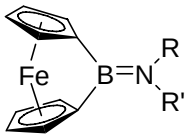

4

Figure 1-3. Aminobora[1]ferrocenophanes. [R = R' = $SiMe_3$ (**4a**); R = $SiMe_3$, R' = *t*Bu (**4b**); R = R' = *i*Pr (**4c**)].

Complex **4a** was structurally characterized by X-ray crystallography and the largest tilt angle to date for a [1]MCP of $\alpha = 32.4(2)°$ was reported. This is a result of the small covalent radius of boron (CN = 3, r = 0.82 Å) (CN = coordination number).[8] From Differential Scanning Calorimetry (DSC) a ring-opening exotherm of 95 kJ/mol was measured. In 2000, an additional derivative was published by Manners *et al.*, equipped with *iso*-propyl groups [ER_x = $BN(iPr)_2$ (**4c**)]. Various ring-opening polymerization (ROP) experiments were described and an unprecedented reactivity towards metal carbonyls was observed.[9] Under irradiation with UV-light, the carbonyl complex [$Fe(CO)_5$] inserted into the Fe-(η^5-C_5H_4) bond of **4c** (Scheme 1-2).

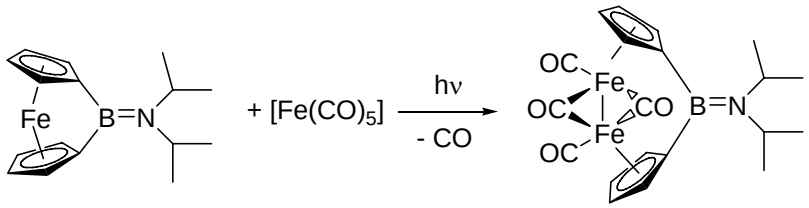

4c

Scheme 1-2. Insertion of a [$Fe(CO)_4$] fragment into the Fe-(η^5-C_5H_4) bond of **4c** under UV-light irradiation.

1.1.3 Group 14-Bridged [1]Metallocenophanes

To date, [1]MCPs bridged by a single carbon atom are unknown. Due to the small covalent radius of carbon (CN = 4, r = 0.77 Å),[8] the tilting of the cyclopentadienyl rings would presumably result in an unfavorable, highly strained species. [1]MCPs of the heavier congeners Si, Ge, and Sn are known, with the most examples reported for sila[1]ferrocenophanes. The majority of synthesis and the fundamental work on ROP were contributed by the Manners group since 1992.

The very first isolations of strained [1]MCPs were reported in 1975 by Osborne and Whiteley, a diphenylsilane-bridged [1]FeCP [ER_x = $SiPh_2$ (**5a**)] and a spirocyclic sila[1]ferrocenophane [ER_x = $Si(\eta^5\text{-}C_5H_4)_2Fe$ (**5b**)] (Figure 1-4).[10] Complex **5a** is moderately strained with a tilt angle of α = 19.1(10)°.[11] The synthesis of **5b** was later revisited by Manners *et al.* and a full structural characterization performed, with a measured tilt angle of α = 19.4(2)° (Figure 1-4).[12]

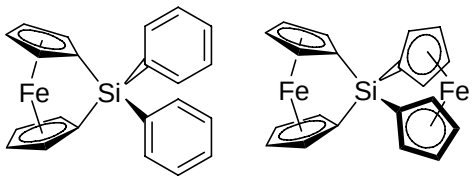

5a **5b**

Figure 1-4. The very first reported examples of [1]metallocenophanes.

Sila[1]ferrocenophanes bear some advantages over other main-group elements. There is a wide variety of high purity silanes commercially available to readily react with dilithioferrocene. Many of the so-obtained strained [1]FeCPs are thermally robust enough to be sublimed without decomposition, which is important for their purification

as monomers. After polymerization, the polymers are air stable, which allows for facile analysis and gives access to a wide variety of applications. For large substituents on the bridging silicon (R and R' in Figure 1-5) even the monomers are air stable (e.g. **5a**-**b**).

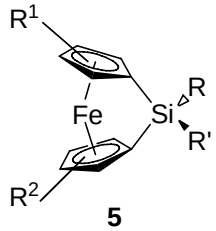

5

Figure 1-5. Sila[1]ferrocenophane **5** with various substituents on the bridging silicon (R, R') and the cyclopentadienyl rings (R^1, R^2).

Table 1-1. Selected structural parameters for fully characterized examples of **5**.

	R	R'	R^1	R^2	α[j]	*ipso* C[k]	Ref.
5a	Ph	Ph	H	H	19.1(10)	31.0[a]	10,13
5b	$(\eta^5\text{-}C_5H_4)_2Fe$		H	H	19.4(2)	30.6[a]	10,11
5c	$(CH_2)_3$		H	H	20.61(8)	31.9[b]	12
5d	Me	Me	H	H	20.8(5)	33.5[b]	14,15
5e	Cl	Cl	H	H	19.2(4)	36.1[b]	16,17
5f	OC_6H_4-*p*-NO_2	OC_6H_4-*p*-NO_2	H	H	18.6(2)	34.9[a]	18
5g	Fc[d]	Fc[d]	H	H	20-22[e]	34.8[a]	19
5h	H	H	H	H	19.1(1)	21.3[b]	20
5i	Me	Cl	H	H	19.4(3)	33.8[b]	17,21
5j	CH_2Cl	Cl	H	H	19.08	31.4[b]	22
5k	CH_2Cl	Ph	H	H	20.4(1)	30.0[b]	23
5l	Me	Ph	H	H	21.0(2)	32.2[b]	24,25
5m	Me	N[f]	H	H	21.0(2)	34.8[a]	19
5n	Cl	O[g]	H	H	19.08	31.4[c]	22
5o	Me	Ar'[h]	H	H	21.27(1)	37.4[b]	26
5p	CH_2Cl	Ar'[h]	H	H	21.4	35.2[b]	23
5q	Ph	Ph	3-*t*Bu	3'-*t*Bu	18.81	29.7[b]	27
5r	Me	Me	3-Me	3'-Me	18.6(3)	32.2[b]	28
5s	Me	Me	Me	Me	16.1(3)	25.6[b]	28
5t	Me	Me	3,4-$SiMe_3$	3',4'-$SiMe_3$	26.3(2)	[i]	29
5u	Me	Me	2,4-*t*Bu	2',4'-*t*Bu	20.3(1)	[i]	29

[a] $CDCl_3$; [b] C_6D_6; [c] $CDCl_2$; [d] Fc = $(C_5H_4)Fe(C_5H_5)$; [e] disordered structure; [f] N = $N(CH_2)_3SiMe_2(CH_2)_2SiMe_2$; [g] O = $CH_2N(Me)C(Me)=O$; [h] Ar' = $(C_6H_4)CH_2N(Me)_2$; [i] ^{13}C NMR data not reported; [j] [°]; [k] [ppm].

From structural data obtained by X-ray crystallography some connections can be drawn between structural parameters and substituents. For [1]FeCPs with unsubstituted cyclopentadienyl rings **5a-p** (R^1 = R^2 = H) the changes in tilt angle α are marginal between 19.08 and 21.27(1)°, indicating that the substituents R and R' in **5** are not influencing the ring tilt significantly. For hypercoordinated complexes **5m-p** the change of coordination geometry from tetrahedral to trigonal bipyramidal on the silicon atom induces structural changes that are reflected by a new reactivity. For example, **5o-p** show one elongated cyclopentadienyl *ipso* C-Si bond *trans* to the incoming nitrogen donor respectively [Si-N = 1.919(2) Å and 1.891(2) Å (**5o**); = 1.909(2) Å and 1.879(2) Å (**5p**)] (Figure 1-6).[26]

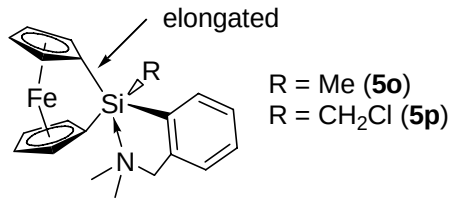

Figure 1-6. Hypercoordinated sila[1]ferrocenophanes **5o-p** showing an elongated C-Si bond *trans* to the N-donor.

In both complexes the nitrogen donor could be quaternized using MeOTf resulting in a four-coordinated complex with the now cationic nitrogen group bent away from the silicon. This strategy was pursued later on to derivatize polyferrocenylsilanes with pending amine functionalities to make them water soluble.[30] When complex **5p** was dissolved in CH_2Cl_2, it underwent an internal cyclization to yield a new cationic spirocyclic [1]FeCP containing a quaternary nitrogen atom (Scheme 1-3).[23] From variable temperature NMR spectroscopy (VT-NMR) experiments, the free energy of exchange for the dimethylamino groups in both complexes was measured, which

indicated a slightly stronger Si···N interaction in solution for **5p** [in CD_2Cl_2: $\Delta G^{\neq}_{181.15}$ = 35.0 kJ/mol (**5o**); $\Delta G^{\neq}_{177.15}$ = 37.6 kJ/mol (**5p**)], although this was not reflected by the Si-N distance found in the solid state by X-ray crystallography [Si-N = 2.7763(17) Å (**5o**); = 2.876(2) Å (**5p**)]. The cyclization was also observed in the solid state for crystals of **5p** over several weeks, indicating that reactions between the CH_2Cl group and the NMe_2 functionality in **5p** are involved (Scheme 1-3).

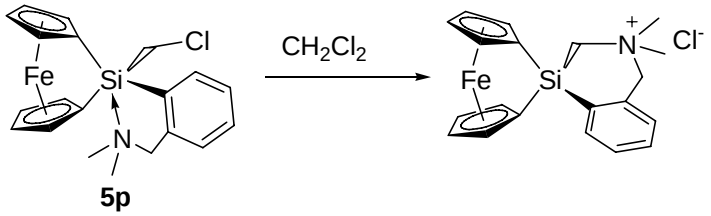

5p

Scheme 1-3. Intramolecular cyclization of **5p**.

A pronounced structural change is observed when substituents on the cyclopentadienyl rings are introduced (R^1 and R^2, Figure 1-5). Introduction of electron donating *tert*-butyl groups in the complex **5q**[27] or methyl groups in the complex **5s**[28] are reflected by an even higher upfield shift of the *ipso* carbon atoms compared to cyclopentadienyl unsubstituted [1]FeCPs, even though the tilt angles α are decreased. Because of the bridging element in [1]MCps, rotation of the cyclopentadienyl ligands is suppressed and restricted to an eclipsed conformation. In the silylated complex **5t** the trimethylsilyl groups on both cyclopentadienyl rings are therefore also eclipsed, resulting in steric repulsion and an increased tilt angle of α = 26.3(2)° (Figure 1-7).

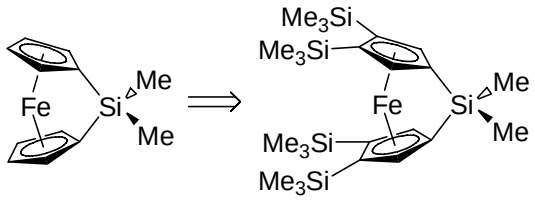

5d, α = 20.8(5)° **5t**, α = 26.3(2)°

Figure 1-7. Increase in ring tilt going from **5d** (α = 20.8(5)°) to **5t** (α = 26.3(2)°) because of steric repulsion of the trimethylsilyl groups in **5t**.

Fully methylated complex **5s** (R^1 = Me, Scheme 1-4) and 2,3,4,5-tetramethylated complex **5v** are examples where the fly-trap route has been employed (R^1 = H, Scheme 1-4). Complex **5v** has not been characterized by X-ray crystallography. The respective precursor was dilithiated at low temperature with *n*BuLi in a donor solvent like DME or THF to yield the precursor $Li_2[(C_5H_4)(C_5Me_4)SiMe_2]$ and $Li_2[(C_5Me_4)_2SiMe_2]$, respectively. Upon reaction with $FeCl_2$ in THF ring closing occurs to yield **5s** or **5v** (Scheme 1-4).

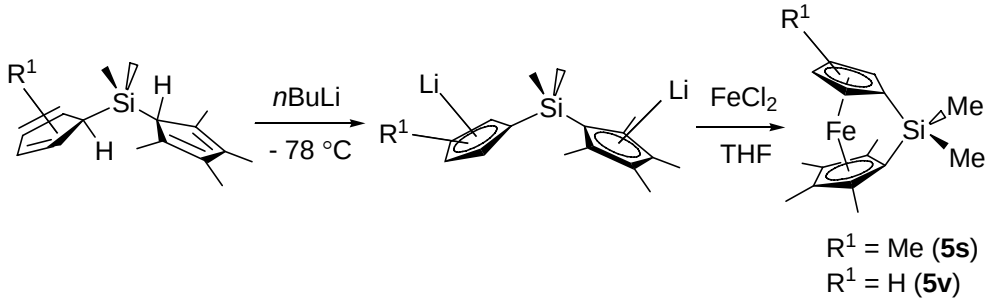

Scheme 1-4. Synthesis of **5s** and **5v** via the fly-trap route.

Chloro-substituted sila[1]metallocenophanes like **5e** and **5i-j** can be used for subsequent substitution reactions either at low temperatures on the monomer without ring-opening or after polymerization to derivatize the obtained polyferrocenes. Low-

temperature substitution reactions enable access to monomers that cannot be synthesized by a direct route, thereby providing access to a wider variety of ligands at the bridging silicon atom. For example, **5o-p** were synthesized from complexes **5i-j** at low temperature by addition of Li[(2-C_6H_4)CH_2NMe_2 without formation of ring-opened side products. In a similar manner, alkyne groups can be introduced (Scheme 1-5).[31]

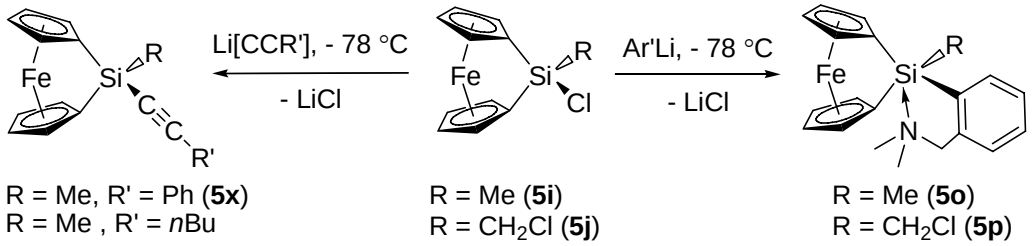

Scheme 1-5. Low-temperature synthesis of **5o-p** and alkyne-substituted (**5x**) [1]FeCPs from **5i-j** without formation of ring-opened side products (Ar'Li = Li[(2-C_6H_4)CH_2NMe_2]).

Beside these fully characterized complexes discussed above, there are various other examples of silicon-bridged [1]FeCPs that have been characterized by spectroscopic and other standard analytical techniques, but not necessarily by X-ray diffraction. Examples contain various alkyl and alkenyl [ER_x = $Si(CH_2CH_2CF_3)_2$, $Si(CHCH_2)_2$, $Si(nC_{17}H_{38})_2$, $Si(Nor)_2$ (Nor = 5-norbornyl)][25], alkoxy [ER_x = $Si(OCH_2Ph)_2$, $Si(OtBu)_2$, $Si(OiPr)_2$[32]; $Si(OMe)_2$, $Si(OEt)_2$, $Si(OCH_2CF_3)_2$, $Si(OnBu)_2$, $Si(OHex)_2$, $Si(OC_{12}H_{25})_2$, $Si(OC_{18}H_{38})_2$, $Si(OPh)_2$, $Si(OC_6H_4$-*p*-*t*$Bu)_2$, $Si(OC_6H_4$-*p*-$Ph)_2$[18]], amino [ER_x = $Si(NMe_2)$][33] or acetylide [ER_x = $Si(CCnBu)_2$ (**5w**)[34], Si(Me)(CCPh) (**5x**), Si(Me)(CC*n*Bu), $Si(CCPh)_2$[31]] ligands. Cyclopentadienyl substituted complexes include the substituted [1]FeCP [ER_x = $SiCl_2$, R^1 = 2-$CH(Me)NMe_2$][35] (Figure 1-5), the 2,3,4,5-tetramethylated [1]FeCP [ER_x = $SiMe_2$, R^1 =

Me (**5v**)][28] (Scheme 1-4) and the 3,3'-bis(trimethyl)silylated [1]FeCP [ER_x = $SiMe_2$, R^1 = 3-$SiMe_3$, R^2 = 3'-$SiMe_3$] (Figure 1-5).[36]

The first example of a germa[1]ferrocenophane contained a diphenylgermylene bridge [ER_x = $GePh_2$ (**6a**)].[11] A tilt angle of α = 16.6° was reported,[13] which is smaller compared to the respective silane **5a** (α = 19.1(10)°). The incorporation of a larger bridging element usually results in reduced ring strain (CN = 4, covalent radii in Å Si: r = 1.17; Ge: r = 1.22).[8] A spirocyclic germa[1]ferrocenophane [ER_x = $Ge(\eta^5\text{-}C_5H_4)_2Fe$ (**6b**)] was published by Osborne *et al.,* and was isostructural to the spirocyclic silane **5b**, but no yield or spectroscopic data was reported.[37] The synthesis of **6b** was later revisited by Manners *et al*.[12] A yield for **6b** of 3 - 5% and full structural data, including a ring tilt of α = 19.1(5)° were reported, which is very similar to the isostructural silane **5b** (α = 19.4°). The dimethylgermylene-bridged [1]FeCP [ER_x = $GeMe_2$ (**6c**)] and diethylgermylene-bridged [1]FeCP [ER_x = $GeEt_2$ (**6d**)], including full structural characterization of **6c**, were published by Manners *et al.*[38,39] For complex **6c,** a ring tilt of α = 19.0(9)° was reported. The Fe-Ge distance in **6c** was found to be 2.804(2) Å, which is only 18% longer than the sum of covalent radii (2.38 Å). ^{57}Fe Mössbauer spectroscopy provided evidence for a weak dative bond between Fe and Ge.[39] Similar ^{57}Fe Mössbauer spectroscopy results were reported for **6b**.[11] Pannell *et al.* reported the synthesis of di(*n*-butyl)germylene-bridged [1]FeCP [ER_x = Ge*n*Bu_2 (**6e**)]. However, full characterization of the new complex was not attempted, because **6e** was used *in situ* for ring-opening polymerization (ROP).[40] Later the same group published four new unsymmetrical substituted germa[1]ferrocenophanes [ER_x = GeMeCl (**6f**), Ge*t*BuCl

(**6g**), GePhCl (**6h**), GeFcPh (**6i**)].[41] Complex **6h** was characterized by X-ray crystallography and displayed a tilt angle of $\alpha = 18.4°$.

A rather unusual germa[1]ferrocenophane was reported by Togni *et al*.[42] From reaction of dichlorogermol (1,1-dichloro-1-germa-2,3,4,5-tetramethyl-cyclopentadiene) with dilithioferrocene a spirocyclic germol-bridged [1]FeCP [ER_x = $Ge(Me_4C_4)$ (**6j**)] was obtained, displaying a tilt angle of $\alpha = 18.9°$ (Figure 1-8).

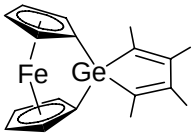

6j

Figure 1-8. Germacyclopentadienyl-bridged [1]ferrocenophane **6j**.

First attempts to synthesize a stanna[1]ferrocenophane using the starting compounds Me_2SnCl_2, Ph_2SnCl_2 or Et_2SnCl_2 were unsuccessful and yielded mainly polymeric materials.[11,43] Seyferth *et al.* were able to isolate small amounts of the unstrained stanna[1.1]ferrocenophanes **21a-b** and characterized them by MS (see Chapter 1.3.2).[43] The first successful synthesis of a stanna[1]ferrocenophane was accomplished by Manners *et al*.[44] Via low-temperature reaction of tBu$_2$SnCl$_2$ with dilithioferrocene followed by a quick and cold work-up the isolation of tin-bridged [1]FeCP **7a** [ER_x = SntBu$_2$] was achieved. Complex **7a** was fully characterized and showed a ring tilt of $\alpha = 14.1(2)°$, which is significantly smaller than that found for the lighter congeners silicon and germanium (CN = 4, Sn: r = 1.40 Å).[8] Steric protection at the tin atom proved to be vital. An attempted synthesis using nBu$_2$SnCl$_2$ instead of tBu$_2$SnCl$_2$ was unsuccessful, only polymeric material was isolated. A second example

employing sterically demanding groups on the tin atom was reported starting from Mes_2SnCl_2 (Mes = 2,4,6-trimethylphenyl) to yield the new [1]FeCP **7b** [ER_x = $SnMes_2$].[45] Complex **7b** showed a tilt angle of α = 15.2(2)°, similar to **7a**. As observed for other [1]FeCPs bearing sterically demanding ligands on the bridging element, **7a-b** are air stable. Surprisingly though, after several days **7a** started to polymerize in the solid state, whereas **7b** was stable indefinitely and showed no signs of polymerization (see Chapter 1.2.5). Stanna[1]ferrocenophane **7c** [ER_x = $Sn^{iPr}Ph_2$], employing the bulky ligand ^{iPr}Ph (= 2,4,6-tri(isopropyl)phenyl), was published by Pannell *et al.*[46] Complex **7c** showed a ring tilt of α = 14.7° and proved to be exceptionally inert towards ring-opening. For example, ring-opening did not occur under hydrolytic conditions in water or in refluxing methanol, but only under more drastic conditions on a column using wet silica gel. In comparison, **7b** was slowly hydrolyzed by excess methanol to give a ring-opened product over a period of six days.[47]

A second example of a [1]RuCP was published by Manners *et al.* and contained a di(mesityl)tin bridge [ER_x = $SnMes_2$ (**7d**)]. The complex was isolated in low yield from a low-temperature reaction in THF, with the side products being presumably polymeric material. A single-crystal X-ray diffraction showed three independent molecules of **7d** in the unit cell, displaying tilt angles of α = 20.9(3)°, 20.2(3)° and 20.8(4)°, respectively. Complex **7d** was significantly more tilted than **7b**, as expected for the introduction of the larger ruthenium atom over the iron atom.

1.1.4 Group 15-Bridged [1]Metallocenophanes

The first synthesis of a strained [1]MCPs bridged by a group 15 element was reported in 1980 by Osborne and Whiteley.[11] The phenylphosphanediyl-bridged [1]FeCP **8a** [ER_x = PPh] displayed a ring strain of $\alpha = 26.7°$.[13] The complex was only moderately air stable and retained its reactivity as a conventional phosphine in reactions with other transition metal complexes. An inversion at the phosphorous atom by NMR spectroscopy (100 MHz) was not observed up to 70 °C. Independently, Seyferth and Whiters synthesized **8a** and reported on the new methylphosphanediyl-bridged [1]FeCP **8b** [ER_x = PMe] and phenylarsanediyl-bridged [1]FeCP **9a** [ER_x = AsPh].[43] No tilt angles were reported for the new [1]FeCPs, and the reactivity as a donor ligand towards transition metals was investigated. Also, the first ROP experiments with alkyl-lithium reagents were performed and the possibility to obtain oligomeric material from these reactions was concluded (see Chapter 1.2.2). Another contribution to phosphanediyl and arsanediyl-bridged [1]FeCPs included cyclopentadienyl ring substituted ferrocenophanes (Figure 1-9) which were published by Cullen *et al.*[48] This work included the first fully structural characterized arsa[1]ferrocenophane **9b** [ER_x = AsPh, R = $CH(Me)NMe_2$] by single-crystal X-ray diffraction (Figure 1-9).

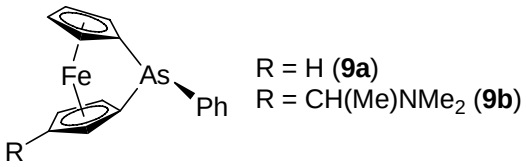

Figure 1-9. Examples of arsa[1]ferrocenophanes.

The reported tilt angle of $\alpha = 22.9°$ indicated a less strained molecule compared to phospha[1]ferrocenophanes, which was expected for the introduction of the heavier congener As (CN = 3, covalent radii in Å: P 1.10, As 1.21).[8] Manners *et al.* expanded the series of monomers to a chlorophosphanediyl-bridged [1]FeCP [ER_x = PCl (**8c**)] and synthesized two more cyclopentadienyl substituted phenylphosphanediyl-bridged monomers, [$(C_5H_3nBu)Fe(C_5H_4)$]PPh (**8d**) and [$(C_5H_3SiMe_3)_2Fe$]PPh (**8e**).[49] It was also demonstrated that the bridging P(III) atom in **8e** can be cleanly oxidized to P(V) with elemental sulfur to quantitatively yield the phenylphosphanediyl sulfide-bridged [1]FeCP **8f** [ER_x = P(S)Ph]. Complexes **8c-f** were fully characterized by X-ray crystallography and showed tilt angles α between 25.3(3)° and 27.0(6)°. Miyoshi *et al.* further investigated the coordination of **8a** to a series of different metal fragments, including the two fully characterized complexes [**8a**→$FeCp(CO)_2$]$^+$ ($\alpha = 25.0°$) [50] and [**8a**→$W(CO)_5$] ($\alpha = 25.6°$)[51] (Figure 1-10).

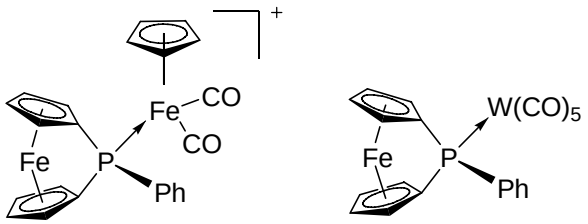

[**8a**→$Fe(Cp)(CO)_2$]$^+$ [**8a**→$W(CO)_5$]

Figure 1-10. Fully characterized examples of phospha[1]ferrocenophane **8a** coordinated to two different transition metals.

Miyoshi was initially interested in P-C bond activation. By coordinating various metal complexes to **8a** and irradiating them with UV light, a ring slippage was observed

(Scheme 1-18, page 40) that eventually led to the discovery of a new pathway to produce polyferrocenes, namely photolytic ROP (see chapter 1.2.4).[51,52]

In 1999 Herberhold *et al.* synthesized two phospha[1]ferrocenophanes [ER_x = $PN(iPr)_2$ (**8g**), P(tmp) (**8h**)] (tmp = 2,2',6,6'-tetramethylpiperidine) bearing bulky alkyamino groups. The attempted synthesis employing a less bulky diethylamino substituent (ER_x = $PNEt_2$) only led to unidentified products. A crystal structure analysis of **8g** revealed a tilt angle of α = 27.8°. Complex **8g** retained the characteristics of a phosphine ligand by coordinating the fragment [$Pt(PPh_3)_2$] or could be oxidized with sulfur and selenium.

In 2000, Brunner *et al.* published a comprehensive article on the synthesis of phospha[1]ferrocenophanes containing chiral ligands including their reactivity and ROP.[53] The chiral phospha[1]FeCPs **8i** [ER_x = P(-)Men] (Men = menthyl) and **8j** [ER_x = P(-)Bor] (Bor = bornyl) were obtained from their respective chiral starting compounds (-)$MenPCl_2$ and (-)$BorPCl_2$ and dilithioferrocene (Figure 1-11).

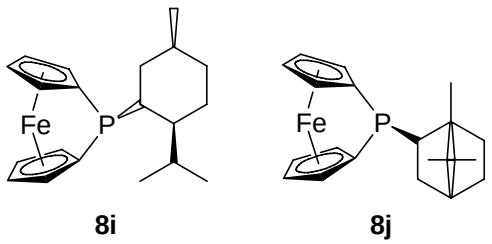

8i **8j**

Figure 1-11. Chiral phospha[1]ferrocenophanes. Menthyl substituted **8i** and bornyl substituted **8j**.

Brunner *et al.* also investigated the coordination chemistry of **8a** and **8i**. Complex **8a** coordinated to the half-sandwich complex [$MnCp^*(CO)_2THF$] to give the new complex [**8a**→$MnCp^*(CO)_2$], which was fully characterized by X-ray

crystallography. When two equivalents of **8i** were reacted with [Pd(COD)Cl_2], the trinuclear heterobimetallic complex [**8i**→$PdCl_2$←**8i**] was obtained. The complex was characterized by X-ray crystallography and contained a square planar Pd center with *trans* chlorine substituents and displayed C_2 symmetry.

1.1.5 Group 16-Bridged [1]Metallocenophanes

The first reported group 16-bridged [1]FeCP contained a "naked" sulfur atom with no ligands attached [E = S **10**] (Figure 1-12).[54] Complex **10** was obtained in low yield from the reaction of dilithioferrocene with $(PhSO_2)_2S$. A structural characterization by X-ray crystallography revealed a tilt angle of α = 31.05(10)°, which constitutes the second highest ring strain of a [1]FeCP to date.

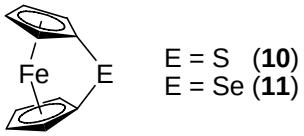

Figure 1-12. Ligand free group 16-bridged [1]FeCPs.

This ring strain was also reflected by a large upfield shift of the *ipso* carbon ^{13}C NMR resonance at 14.3 ppm. From a DSC experiment a ring-opening exotherm of 130 ± 20 kJ/mol was measured, the largest one for any [1]FeCP.[55] In the same publication, the first selena[1]ferrocenophane was reported from reaction of dilithioferrocene with $(S_2CNEt_2)_2Se$ [E = Se (**11**)].[55] A tilt angle of α = 26.4(2)° and a ring-opening exotherm of 110 ± 20 kJ/mol was reported (CN = 2, covalent radii in Å: S 1.04, Se 1.17).[8] ROP experiments of **10** and **11** yielded insoluble materials, which was rationalized by the

lack of organic substituents in **10** and **11**, which usually facilitate dissolution of polyferrocenes in organic solvents. In order to obtain a more soluble polyferrocenylsulfide that can be characterized by gel permeation chromatography (GPC), the ring-methylated complex **10a** was synthesized as a mixture of isomers from dilithiodimethylferrocene and $(PhSO_2)_2S$ (Figure 1-13).

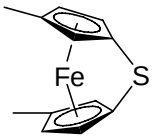

10a

Figure 1-13. Ring-methylated [1]FeCP **10a**.

The enantiomer $[(3,3'\text{-}MeC_5H_3)_2Fe]S$ of **10a** was isolated as single crystals and characterized by X-ray crystallography and a tilt angle of $\alpha = 31.46(8)°$ was measured. This value is slightly higher than that of the parent complex **10** (by 0.4(1)°), which is opposite to the trend in silicon-bridged [1]FeCPs.

1.2 Ring-Opening Polymerization

In general there are two synthetic pathways that yield polymers, polycondensation and polymerization.[56] Polycondensation is a step-growth process, where bi-functional monomers undergo a series of condensation reactions with simultaneous elimination of small molecules, for example H_2O or LiCl. Polyurethane, the product of the condensation of diols and diisocyanates, is also classified as a polycondensation even though no small molecules are eliminated during the process. In a step-growth process, the polymer weight initially increases very slowly. Monomers

react with monomers to dimers, dimers react with monomers to trimers, dimers and dimers react to give tetramers etc. Only after some time, when higher oligomers are present, the polymer weight increases significantly until eventually high molecular weight polymers are formed. Reactions occur between any different-sized species present. Polymerization on the other hand is a chain-growth process. A so-called initiator reacts with the starting monomer, thereby creating a highly reactive center that can attack another monomer, which propagates the chain. Because the initiator does not get incorporated into the growing chain, the repeating unit has the same composition as the monomer. Polymer weight growth occurs only at the reactive site of the growing polymer chain, unreacted monomers do not react with other monomers. If polycondensation and polymerization are compared side by side, the following characteristics are observed. In chain-growth polymerization at any given conversion rate high molecular weight polymer is always present together with initiator and monomer, but no intermediate oligomers. The only change over time and increasing conversion is the concentration of polymer molecules. In a step-growth process high molecular weight polymer is obtained only near complete conversion. Thus in polycondensation polymer weight and concentration are dependent on conversion, unlike in polymerization. In chain-growth polymerization, the polymer weight is constant over the percent conversion, in step-growth polycondensation the polymer weight increases exponentially with the percent conversion. A polymerization is referred to as living when the initiation is rapid and no termination or chain-transfer reactions occur. This means polymerization continues until all monomer is consumed, upon which the remaining ends of the polymer chain remain active or living. This gives access to

end group control and block-copolymers. Addition of more monomer of the same type to a living end further propagates the chain. Addition of a different monomer initiates the formation of a controlled block-copolymer. The polymer weight can be controlled by initiator to monomer ratio.

Ring-opening polymerization (ROP) is a special case of chain-growth polymerization. Although it does display all the characteristics of a chain-growth process, the rate propagation constants are similar to step-growth polycondensations, several magnitudes lower than in linear olefin polymerization for example. That is why polymer weight does show a dependence on conversion, which increases linear in the case of a living ROP. Under very stringent conditions a living polymerization can also be achieved for ROP. Initial attempts to synthesize organometallic polymers employed polycondensation routes.[57-59] Those attempts were in general rather unsuccessful, because of the metal atoms "annoying tendency to dimerize".[57] Many of the desired properties of a macromolecule are only observed above certain molecular weights. Polycondensation requires highly purified, bi-functional starting materials at extremely exact starting stoichiometries. For example, to achieve 200 repeating units via polycondensation, assuming 100% conversion of monomer to polymer, the starting ratios of monomers must be 0.99 : 1.00 or better.[60] This can be easily achieved for unreactive, air stable organic monomers, which are often commercially available in high grades of purity. Since many of the organometallic monomers have to be synthesized first and are very reactive and air sensitive, achieving high grades of purity and exact starting stoichiometries becomes very challenging. These drawbacks usually led to incomplete conversion of starting monomers and formation of low molecular weight

oligomers and polymers. Chain-growth process polymerizations do not suffer from stringent stoichiometry or even impurities as long as they do not interfere with the propagating center. Therefore, high molecular weight polymers can be obtained even at incomplete monomer conversion. ROP had already been established as a powerful synthetic tool to synthesize high molecular weight organic and organic/inorganic hybrid polymers including polyamides, polyethers, polyolefins, polyacetylenes, polycarbonates, polycarbosilanes, polysiloxanes and polyphosphazenes.[60,61] ROP of organometallic monomers, however, that would yield polymers containing the metal in the backbone of the polymer would only become feasible with the discovery of strained [1]MCPs. The first polymer that contained ferrocene was obtained from the radical polymerization of vinyl ferrocene.[62] Many of the attractive and desired electrical, optical, magnetic, preceramic or catalytic properties of organometallic polymers though are only obtained if the metal is incorporated into the backbone of the polymer chain, not as a side group functionality.

1.2.1 Thermal Ring-Opening Polymerization

Thermal ring-opening polymerization (thROP) was the first pathway described in literature to yield high molecular weight polymetallocenes employing strained [1]MCPs. In 1992 Manners *et al.* described thROP of **5a** and **5d**.[63] From a DSC experiment it was found that **5d** melts at 78 °C and shows an exothermic peak from 120-170 °C, which integrated to 80 kJ/mol. Complex **5a** melted at 196 °C and showed a similar exothermic peak from 200-235 °C, with an exotherm of 60 kJ/mol. When **5d**

was heated to 130 °C in an evacuated flame sealed tube, the content melted and became increasingly viscous within 10 min yielding polyferrocene **12d**. After further heating for 50 min, the tube was cooled down, opened and **12d** extracted with THF (Scheme 1-6).

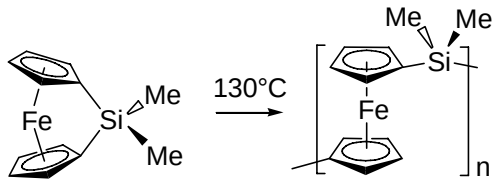

5d **12d**

Scheme 1-6. Thermal ROP of monomer **5d** to give polyferrocenylsilane **12d**.

^{1}H NMR spectra of **12d** showed a similar signal pattern to monomer **5d** but with the typical peak broadening associated with the polymer architecture. A ^{13}C NMR spectrum of **12d** displayed the high upfield shifted cyclopentadienyl *ipso* carbon resonance of monomer **5d** (33.5 ppm) at the more conventional value of 71.9 ppm. Monomer **5a** was polymerized under similar conditions than **5d** (200 °C), but the obtained polymer **12a** was insoluble, which made further characterization impossible. From GPC, a weight average molecular weight (M_w) of 5.2 x 10^5 and a number average molecular weight (M_n) of 3.4 x 10^5 was determined for **12d**, giving a polydispersity index (PDI) of 1.53. A mechanistic study was undertaken to clarify if the (C_5H_4)-Fe or the (C_5H_4)-Si bond is cleaved and if the cleavage is homolytic producing a radical species or heterolytic producing an ionic species.[64] To answer the first question, cyclopentadienyl substituted **5v** (Scheme 1-7) was thermally polymerized. If (C_5H_4)-Si bond cleavage occurred, one would expect to find three different silicon environments in the resulting polymer **12v**, namely (C_5H_4)-Si-(C_5Me_4), (C_5H_4)-Si-(C_5H_4) and (C_5Me_4)-Si-(C_5Me_4), and a single iron environment (C_5H_4)-Fe-(C_5Me_4) (Scheme 1-7). If (C_5H_4)-

Fe-(C_5Me_4) bond cleavage occurred, the opposite would be true. ThROP of **5v** at 150 °C for 1 h yielded polymer **12v** with high molecular weights of M_w = 3.4 x 10^5 and M_n = 2.3 x 10^5, PDI = 1.48. From ^{1}H and ^{29}Si NMR spectra three different signals for the $SiMe_2$ moiety were obtained, showing that thROP proceeds via cyclopentadienyl-silicon bond cleavage (Scheme 1-7).

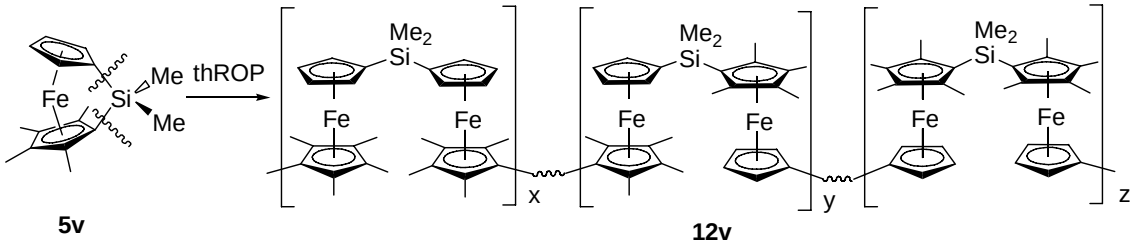

Scheme 1-7. ThROP of monomer **5v** proceeding via unselective cyclopentadienyl-silicon bond cleavage to give regioirregular polyferrocenylsilane **12v**.

In order to answer the question of homolytic vs. heterolytic cyclopentadienyl-silicon bond cleavage, **5d** was thermally polymerized in the presence of catalytic and stoichiometric amounts of the radical trap BHT (2,6-di-*tert*-butyl-4-methylphenol). In each case, high molecular weight polymers of **12d** were obtained at the same rate as without BHT. These findings strongly suggested a heterolytic cyclopentadienyl-silicon bond cleavage mechanism.

Almost all of the reported [1]MCPs that were tested as monomers showed an exothermic ring-opening at elevated temperature with subsequent polymerization. A rare example of a [1]FeCP that is not prone to thROP is complex **5f**.[18] In a DSC experiment, a sharp exotherm centered on 183 °C due to decomposition was observed (Scheme 1-8).

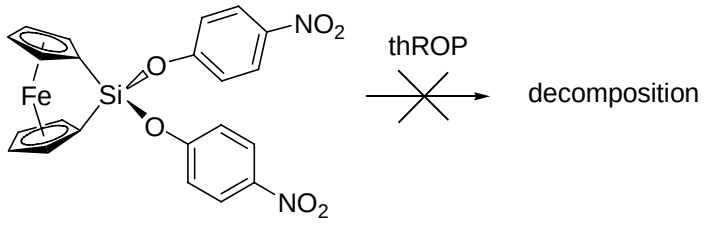

5f

Scheme 1-8. Decomposition of [1]FeCP **5f** upon heating instead of thROP.

Upon heating, **6j** (Figure 1-8, page 13) decomposed yielding intractable mixtures, and was not further investigated for ROP.[65] The zirconium-bridged [1]RuCP **2c** (Figure 1-2, page 4) showed a melt endotherm at 188 °C, but no exotherm could be detected upon further heating. In a subsequent thROP experiment in a flame-sealed tube, after heating **2c** for 4 days at 200 °C, only unconverted starting material could be recovered.[65]

1.2.2 Anionic Ring-Opening Polymerization

The first hint at the possibility of anionic initiated ring-opening polymerization (anROP) and the actual first successful anROP yielding high molecular weight polyferrocenes had been published by Seyferth *et al.* in two back-to-back reports in 1982. At the time, the authors believed a successful polycondensation had taken place, and did not realize the real mechanism of anROP that led to the formation of a high molecular weight polyferrocene.[43,66] In part 1 the synthesis of the phosphorous and arsen-bridged [1]FeCPs **8a-b** and **9a** (Figure 1-9, page 15) was described, including details of various stoichiometric ring-opening reactions with different nucleophiles like

PhLi, *t*BuLi and MeLi.[43] In part 2 the reaction of catalytic amounts (<10 mol%) of PhLi with **8a** was described yielding oligomers.[66] When a previously patented polycondensation reaction using the bi-functional monomers dilithioferrocene and $PhPCl_2$ in a 1:1 ratio was repeated under modified conditions, high molecular weight polymers of up to $M_w = 1.61 \times 10^5$ were isolated. Such a high polymer weight was never achieved before via polycondensation (see Chapter 1.2), but the result did not raise the authors' suspicion. More probable, strained **8a** formed *in situ*, which was subsequently ring-opened by dilithioferrocene, which can act as an anionic initiator, to yield high molecular weight polyferrocenylphosphine **13a** via ROP (Scheme 1-9).

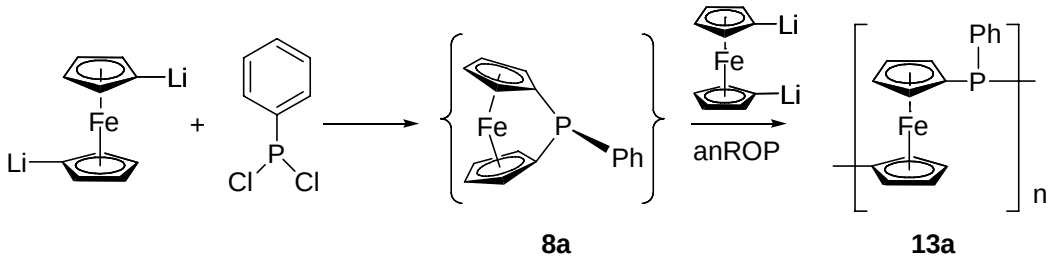

Scheme 1-9. Seyferth's attempted polycondensation that yielded high molecular weight polyferrocenylphosphine **13a** probably via *in situ* formation of **8a** and subsequent anROP initiated by dilithioferrocene.

In 1994 Manners *et al.* published two papers describing the first successful oligomerizations and living anROP using anionic initiators.[67,68] The reactions of **5d** with various ratios of monolithioferrocene (FcLi) (0.5 - 1.1 equiv.) was studied and oligomers with n = 2 - 8 repeating units were obtained.[67] Using column chromatography these oligomers were separated and thoroughly characterized by NMR spectroscopy and MS. A crystal structure for the pentamer was obtained, showing a trans planar zigzag conformation with adjacent ferrocenyl groups oriented at ca. 110° to one another. When 10 mol% of FcLi was used, a polyferrocene with $M_w = 9500$ and $M_n = 8000$, PDI = 1.19

was obtained. The first successful application of living anROP using monomer **5d** to obtain high-molecular weight, narrow-distributed polyferrocenylsilane **12d** (Scheme 1-10, page 27) was reported in the second publication.[68] FcLi, PhLi and *n*BuLi were tested as anionic initiators, with *n*BuLi giving the best results. Molecular weights could be varied in the range of M_n = 4.0 x 10^3 - 4.9 x 10^4 by changing the initiator to monomer ratio from 1:20 to 1:200. The reported PDIs of 1.02 to 1.51 were all very small, typical for a living polymerization. End group control was demonstrated by the addition of H_2O resulting in a proton terminated polymer or Me_3SiCl resulting in a trimethylsilyl terminated polymer. Also, addition of monomer **5d** to the living end of **12d** increased the polymer weight accordingly. Living anROP was demonstrated to be a powerful tool to synthesize block-copolymers. Addition of a strained, cyclic siloxane $[Me_2SiO]_3$ to a living end of **12d** yielded the well-defined, high-molecular weight block-copolymer $SiMe_2O$-*b*-**12d** (Scheme 1-10).

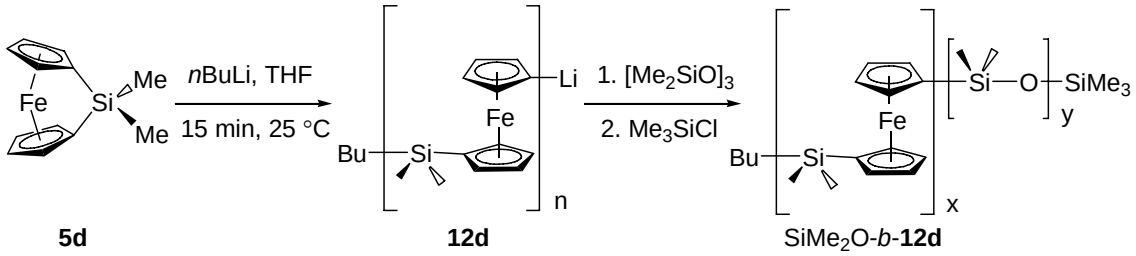

Scheme 1-10. AnROP of monomer **5d** initiated by *n*BuLi to yield living polyferrocenylsilane **12d**. Synthesis of block-copolymer $SiMe_2O$-*b*-**12d** from living polymer **12d** and a siloxane.

The mechanism is based on a (C_5H_4)-Si bond cleavage by nucleophilic attack of the anionic initiator at the silicon atom thereby ring-opening the monomer and creating a carboanionic center, in this case a cyclopentadienyl anion. The major drawback of anROP, especially living anROP, is that very stringent conditions are required,

including highly purified monomers and extremely dry solvents in order to avoid quenching of the reactive center. Also, not all functional groups are inert toward carboanions, limiting the scope of monomers. For example, in a typical anROP experiment **5d** has to be sublimed a minimum of three times to obtain purification levels required for successful anROP; glassware has to be heated and evacuated and purged with inert gas several times; solvents used require special purifications to exclude even minute amounts of moisture or oxygen (see Chapter 2); all manipulations have to be performed in a glove box.

1.2.3 Transition Metal Catalyzed Ring-Opening Polymerization

Transition metal catalyzed ring-opening polymerization (tmROP) was discovered independently by the groups of Manners and Tanaka in 1995.[69,70] Manners *et al.* tested a variety of transition metal complexes with monomer **5d**.[70] Those complexes included $[Rh(COD)(\mu\text{-}Cl)]_2$ (COD = 1,5-cyclooctadiene), $[Rh(PPh_3)_3Cl]$, $[Pd(PPh_3)_2Cl_2]$, $[Pd(CH_3CN)_2Cl_2]$, $[Pd(PPh_3)_3]$ and $[Pt(PPh_3)_3]$, which all proved to be unreactive towards tmROP. However, treatment of **5d** in C_6D_6 with catalytic amounts of $[Rh(COT)_2(\mu\text{-}Cl)]_2$ (COT = cyclooctatetraene), $[Pd(COD)Cl_2]$, $PdCl_2$ or $PtCl_2$ led to the formation of polymer **12d**. The reaction was repeated with $[Pd(COD)Cl_2]$ (1 mol%) and **5d** on a larger scale, stirring it for 24 h. After work-up **12d** was isolated in 25% yield with a molecular weight of $M_w = 1.32 \times 10^5$, $M_n = 1.22 \times 10^5$, PDI = 1.08. The dinuclear sila[1.1]FeCP **20a** was isolated in significant quantities as a side product. Tanaka *et al.* reported that phosphine free complexes of Pd and Pt like $[Pt(COD)_2]$, $[Pt(COD)Cl_2]$,

$[Pd(COD)Cl_2]$, $[Pt_2(dba)_3]$ (dba = dibenzylideneacetone) and $[Pd(dba)_2]$ yielded high molecular weight polyferrocenes using **5d** and the isostructural dimethylgermylene-bridged monomer **6c**.[69] Interestingly, when **5d** was reacted with 2 mol% of $[Pd(COD)Cl_2]$ in benzene a reaction that "was extremely rapid and within seconds an insoluble material deposited in the solution" was observed. This observation led the authors to the following conclusion, stated in Table 1 of their publication: "Rapid polymerization, insoluble polymer".[69] A similar behavior was observed for **6c**. Under almost identical conditions (1 mol% catalyst instead of 2 mol%) Manners *et al.* obtained a polymer which was very soluble and, therefore, could be fully characterized.[70] High molecular weights for **12d** between M_w = 7.0 x 10^4 and 1.7 x 10^6 and polyferrocenylgermane **14c** between M_w = 2.3 x 10^5 and 1.1 x 10^6 were reported by Tanaka et al.[69] The obtained polyferrocenes showed higher polydispersities, as could be seen from the measured PDIs of 1.5 to 9.7, than for polyferrocenes obtained from anROP or thROP. Furthermore isolated yields were high (79 - 95%). TmROP of **6c** took over 12 h whereas **5d** were completed after 3 h. Tanaka *et al.* also reported on a random copolymerization experiment of **5d** and **6c** in a 1:1 ratio using 2 mol% of $[Pt(COD)_2]$ or $[Pt_2(dba)_3]$. Surprisingly, in the case of $[Pt(COD)_2]$, the tmROP was very sluggish and did not reach completion even after 2 days. NMR spectra of the reaction mixture showed that only 20% of **5d** but 65% of **6c** had been consumed, giving an estimated ratio of $SiMe_2$ to $GeMe_2$ groups of 1:3 in the resulting copolymer.

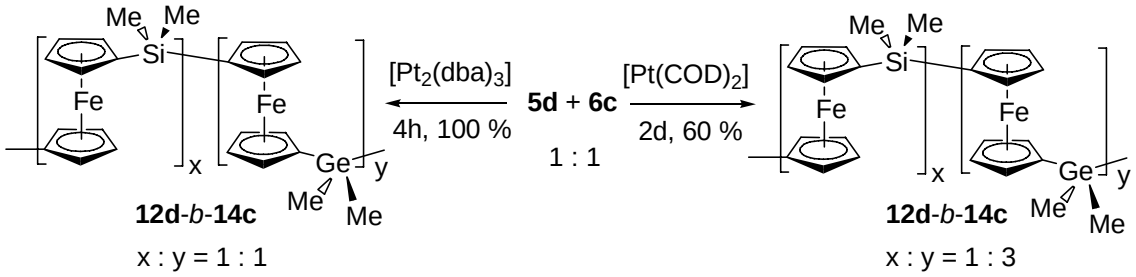

Scheme 1-11. Random copolymerization of **5d** and **6c** using transition metal initiators. If $[Pt(COD)_2]$ is used, tmROP is sluggish and **6c** is preferably incorporated into the random copolymer **12d**-*b*-**14c**. If $[Pt_2(dba)_3]$ is used, copolymerization is much faster and no monomer preference is observed.

Homo-polymerizations of **6c** generally took much longer than for **5d**, but the explanation for the preferred incorporation of **6c** over **5d** in copolymerization experiments using $[Pt(COD)_2]$ was not given. When $[Pt_2(dba)_3]$ was used, copolymerization proceeded smoothly to completion in 4 h. Spectral and analytical data indicated a 1:1 ratio of $SiMe_2$ to $GeMe_2$, with a molecular weight of $M_w = 6.8 \times 10^5$, PDI = 13.5.

A similar mechanism as the one established for strained cyclic silacyclobutanes was suggested for the tmROP of [1]MCPs.[71] There was strong evidence that the initial step is an oxidative insertion of a coordinately unsaturated metal complex fragment, requiring a ligand loss of the precursor complex. This would explain the lower reactivity of $[Rh(COD)(\mu\text{-}Cl)]_2$ over $[Rh(COT)(\mu\text{-}Cl)]_2$ in tmROP, as observed by Manners *et al,* because the more strongly bound COD ligand compared to the COT ligand does not dissociate at all in solution or not enough to induce ROP.[70] Soon thereafter, Manners *et al.* were able to isolate and crystallize the platinasila[2]ferrocenophane **5dPt'** [ER_x = $Si(Me)_2Pt(PEt_3)_2$] using $[Pt(PEt_3)_3]$ as the starting complex (Scheme 1-12).[72]

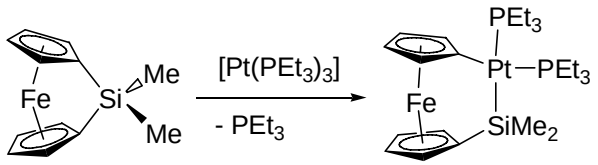

5d **5dPt'**

Scheme 1-12. Isolation of the [2]FeCP **5dPt'** from the insertion of a $[Pt(PEt_3)_2]$ fragment into the cyclopentadienyl *ipso* C-Si bond of **5d**.

Complex **5dPt'** formed at 60 °C in 4 h with an isolated yield of 60% and displayed a reduced tilt angle of α = 11.6(3)° compared to **5d** (α = 20.8(5)°). In accordance with the observation reported by Tanaka *et al.* that phosphine complexes were unreactive for tmROP,[69] **5dPt'** did not initiate tmROP of **5d** even at elevated temperatures of 95 °C. The two remaining phosphines in **5dPt'** probably do not dissociate anymore from the platinum, which would be required for the addition of a second monomer in order to initiate chain growth. Shortly after, Tanaka *et al.* independently solved a crystal structure of **5dPt'**, and pointed out that by increasing temperature conversion of **5d** to **5dPt'** increased (3 h at 80 °C gives ~95% conversion), reporting an isolated yield of **5dPt'** of 84%.[73] From previous investigations, it was known that $[Pt(PEt_3)_4]$ does dimerize silacyclobutanes, but does not induce ROP.[74] This prompted Tanaka *et al.* to screen several phosphine containing Pd and Pt complexes, and they could show that trialkylphosphine complexes of Pd cleanly dimerize **5d** to yield the sila[1.1]ferrocenophane **20a**, but do not initiate tmROP.[73] It was also observed that electron rich Pd complexes gave higher conversions, with the complex $[Pd(PCy_3)_2Cl_2]$ (Cy = cyclohexyl) giving ~100% conversion by NMR spectroscopy and 90% isolated yield of **20a**. In 2002 Manners *et al.* again observed the formation of a

cyclic dimer as a side product from tmROP experiments, which initiated a more detailed investigation into the mechanism of the formation of [1.1]FeCPs during tmROP.[31] When tmROP experiments were performed with monomer **5x** (Scheme 1-13) using Karstedt's catalyst in THF, the new sila[1.1]ferrocenophane **20d** [ER_x = SiMe(CCPh)] was isolated in significant amounts. Surprisingly the methyl and -CCPh substituents in **20d** adopted an *endo*/*exo* conformation respectively. With a bulky substituent like the -CCPh ligand in **5x**, the formation of the *exo*/*exo* isomer, with both -CCPh ligands perpendicular to the cyclopentadienyl-planes, would be expected (Scheme 1-13).

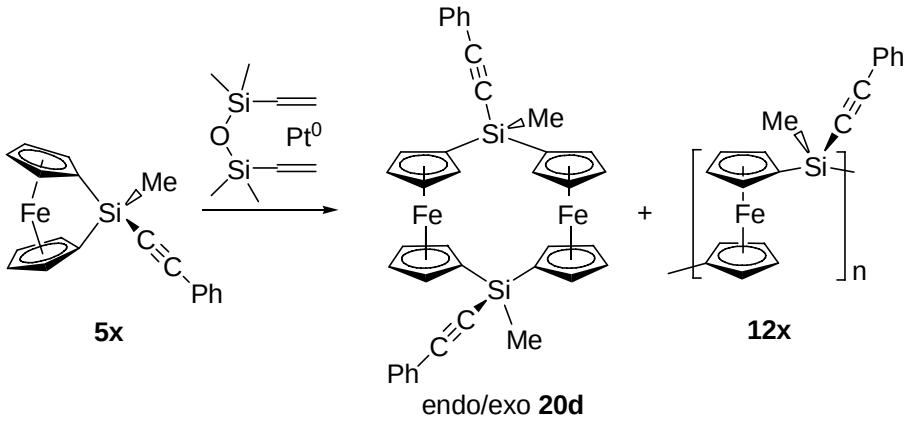

Scheme 1-13. TmROP of monomer **5x** yielding [1.1]FeCP **20d** and polyferrocenylsilane **12x**. The ratio of formation of **20d** to **12x** was found to be solvent and monomer concentration dependent. The *endo*/*exo* isomer of **20d** was formed stereoselectively.

In order to test the stereoselectivity and to get more insight into the mechanism of formation of **20d**, a series of tmROP experiments in toluene, CH_2Cl_2 and THF at various concentrations of monomer **5x** were performed. The amount of initiator was kept constant. From these experiments it was shown that the ratio of cyclic dimer to polymer **20d** : **12x** was highest in THF at low concentrations of **5x**. For example, for 50 mg of **5x** in 20 mL of THF, the ratio of **20d** : **12x** was 1:0.7, with 25% unreacted **5x** still

present after 22 h. In the non-coordinating solvents toluene or CH_2Cl_2, essentially no formation **20d** was observed. Varying the concentration of monomer **5x** did not influence the obtained molecular weight of **12x** within experimental error, but conversion of **5x** to **12x** was higher when higher concentrations of **5x** were used. Two general trends of tmROP were concluded: High monomer concentration in non-coordinating solvents favor polymerization; high dilution of monomers and coordinating solvents favor dimerization. The *endo*/*exo* isomer of **20d** was the only isomer observed in all these experiments. The exclusive formation of the *endo*/*exo* isomer over the expected, less sterically hindered *exo*/*exo* isomer was rationalized by a stereoselective formation of **20d**, but no mechanism was proposed. The stereoselectivity though decreases with increasing polymer weight, because **12x** was found to be atactic. Again, no explanation was given.

In 1997 a second fully characterized example of a platinum insertion product from the reaction of **5d** with $[Pt(COD)_2]$, the platinasila[2]ferrocenophane **5dPt*** [ER_x = $Si(Me_2)Pt(COD)$] was reported (Scheme 1-14).[75]

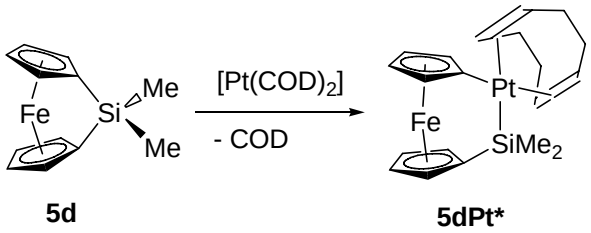

5d **5dPt***

Scheme 1-14. Isolation of the [2]ferrocenophane **5dPt*** from the insertion of $[Pt(COD)_2]$ into the cyclopentadienyl *ipso* C-Si bond of **5d**.

Complex **5dPt*** was isolated in 94% yield and shows a ring strain of α = 10.1(5)°, which is slightly less than that in **5dPt'**. More importantly, once **5dPt*** had

formed, polymerization of **5d** was initiated to give polymer **12d**. In a tmROP experiment with a ratio of **5d** to **5dPt*** of 350:1 (~0.28 mol%) 90% conversion of **5d** to **12d** was reached after 21 h at room temperature. Analysis of the polymer weight gave $M_w \approx 2 \times 10^6$ and $M_n \approx 1 \times 10^6$, which was much higher than expected based on the starting stoichiometry (expected was $M_n \approx 8.5 \times 10^4$). When the same reaction was carried out in COD, no reaction occurred at all. These observations led Manners *et al.* to propose that **5dPt*** itself is only a precatalyst, and that the active species is only present in minute amounts, thereby producing a polymer that is higher in weight than expected from the stoichiometric ratio. The reaction was monitored by NMR spectroscopy and no other species than **5d**, **12d** and **5dPt***, with the concentration of **5dPt*** being constant over time, could be detected. The structure of the active catalyst was tentatively assigned to be a "naked" platinasila[2]ferrocenophane, which requires dissociation of the remaining weakly bound COD ligand from the precatalyst **5dPt***. This would also explain why no reaction occurred when an excess of COD was present.

In 2001, an in-depth report was published by Manners *et al.* that would revise the proposed homogeneous mechanism. First, a series of short-chain model copolymers of **5d** and **5l** (Scheme 1-15) were synthesized that were short enough to be analyzed by multinuclear NMR spectroscopy using Karstedt's catalyst. If the chains are short enough, the incorporation and position of different ligands (in this case the dimethylsilane groups of **5d** vs. the methylphenylsilane groups of **5l**) can be distinguished by NMR spectroscopy. Karstedt's catalyst was chosen because it was known to show no preference for one monomer over the other. Subsequently, the unsymmetrical methylphenylsilane-bridged monomer **5l** was used to synthesize

oligomers, using **5dPt*** to see if and where in the new polyferrocene **12l** the dimethyl substituted moiety of **5d** would be incorporated. Surprisingly no evidence of incorporation of dimethylsilyl groups in these oligomers was found, only short chain homo-oligomers of pure **12l** were isolated instead (Scheme 1-15).

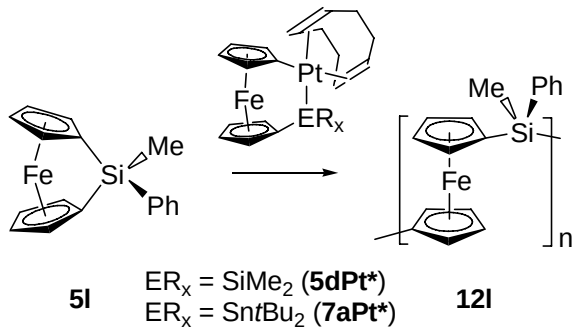

Scheme 1-15. Synthesis of homo-oligomers **12l** via tmROP of monomer **5l** using **5dPt*** or **7aPt***. No incorporation of **5d** or **7a** into **12l** could be detected.

To further confirm this result, precatalyst **7aPt*** was employed. Complex **7aPt*** was synthesized in a similar manner to **5dPt***, namely from the di(*tert*-butyl)tin-bridged monomer **7a** and $[Pt(COD)_2]$.[45] Oligomers obtained from **5l** and **7aPt*** did not contain di(*tert*-butyl)tin groups, confirming that **7a** does not get incorporated into the growing homo-polyferrocene **12l**. Since neither the ferrocenophane moiety of **5dPt*** and **7aPt*** nor Pt are incorporated into the polyferrocene, a heterogeneous mechanism was proposed, suggesting colloidal Pt^0 nanoparticles as the active catalyst.[76] To test this hypothesis, mercury was added to tmROP experiments, which is known to be a potent catalyst-toxin by alloying Pt^0. In a series of inhibition experiments, it was shown that the presence of mercury slows down the polymerization progress drastically. A tmROP using **5d** and **5dPt*** that would usually reach completion in two days showed only 40% conversion after two weeks in the presence of mercury. However, polymerization of **5d**

would not be completely inhibited, which indicates that there might be some contribution from a homogeneous catalysis.

Although tmROP has proven to be a versatile synthetic tool to obtain high molecular weight polyferrocenes under mild conditions, an average reaction takes ca. 24 h to reach complete conversion with Pt or Pd complexes. There was an interest in finding more active catalysts. In 2002, two cationic Rh(I) complexes were described, with increased catalytic activity for tmROP.[77] Complexes $[Rh(COD)_2]A$ (A = OTf or PF_6) and $[Rh(COD)(dmpe)]PF_6$ (dmpe = bis(dimethylphosphinoethane)) were investigated as tmROP initiators. When $[Rh(COD)_2]A$ (app. 1 mol%) was reacted with monomer **5d**, polymerization reached completion in less than 2 minutes, which is the time it takes to acquire a NMR spectrum. The isolated polyferrocenes **12d** showed polymer weights in the range of $M_n = 1.0 \times 10^5$ to 4.81×10^5 with PDIs from 1.40 to 2.10. It was also observed that if solutions of **12d** and $[Rh(COD)_2]A$ were left alone, depolymerization occurred after ca. 2 h. In subsequent experiments with model compounds it was shown that $[Rh(COD)_2]A$ catalyzed cyclopentadienyl C-Si bond cleavage in **12d**. The second complex studied, $[Rh(COD)(dmpe)]PF_6$, showed slightly less activity, with complete conversions reached after 4 h, but more importantly did not depolymerize **12d**, even after one week in solution. $[Rh(COD)(dmpe)]PF_6$ is also the first active phosphine containing tmROP initiator.

Another interesting report was published by Manners *et al.* concerning the control of microstructure in cyclopentadienyl substituted polyferrocenes, which also gave some additional mechanistic insight into tmROP.[78] The thROP of cyclopentadienyl substituted monomer **5v** (Scheme 1-7, page 24) had already been used to test the

mechanism of thROP.[64] As a consequence of the unselective bond cleavage of the (C_5H_4)-Si and (C_5Me_4)-Si bonds of **5v** in thROP, the obtained polymer **12v** possessed a regioirregular microstructure consisting of random repeating units (Scheme 1-7, page 24).[79] The regioirregular polyferrocene **12v** was very soluble in organic solvents and mainly amorphous as detected by wide-angle X-ray scattering (WAXS). On the other hand, if **5v** was polymerized via tmROP using $PtCl_2$ as initiator, the (C_5H_4)-Si bonds are selectively cleaved, probably due to steric reasons.[78] As a result, a regioregular polyferrocene **12v** was obtained with identical repeating units and higher crystallinity. The solubility of regioregular **12v** though was too low for polymer weight analysis by GPC.

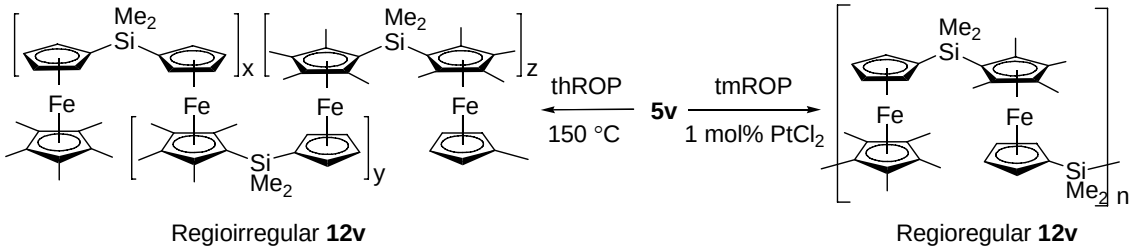

Scheme 1-16. Schematic representation of different microstructures of polyferrocene **12v** depending on initiation. Regioirregular **12v** is obtained from thROP, regioregular **12v** from tmROP.

In accordance with the proposed mechanism that (C_5Me_4)-Si bonds in **5v** are not cleaved because of steric interference, the fully methylated monomer **5s** could not be polymerized by Pt initiators at all.

1.2.4 Photolytic Ring-Opening Polymerization

Photolytic ring-opening polymerization (phROP) was the most recently discovered pathway to obtain high molecular weight polyferrocenes. So far, only phosphorous-bridged monomers **8** and silane-bridged monomers **5** have been tested and reported to undergo phROP. In the case of silane-bridged [1]FeCPs, the term photolytic assisted anionic ring-opening polymerization should be used, because an anionic initiator is required. Chain propagation occurs via a cyclopentadienyl anion, similar to anROP (see Chapter 1.2.2). However, phROP will be discussed separately from anROP because the mechanism of initiation is fundamentally different.

The first observation of phROP was reported by Miyoshi *et al.* in 2000.[51] Initially interested in P-C bond activation, complex **8a** was studied as a new type of coordinating ligand to synthesize new transition metal complexes (Scheme 1-17).[50] Upon irradiation of [**8a**→$FeCp(CO)_2$]$^+$ with UV-light to trigger photochemical elimination of one carbonyl group, a 1,2-shift was observed of one cyclopentadienyl *ipso* carbon forming a new bond to the coordinated Fe atom, resulting in ring expansion of the ferrocenophane moiety to form a ferraphospha-bridged *pseudo*[*]-[2]ferrocenophane (Scheme 1-17).

[*] The term *pseudo* is chosen, because according to IUPAC, ferrocenophanes are: "Compounds in which the two ring components of ferrocene are linked by one or more bridging chains." Although the term "chains" in the definition is not further explained, it implies σ-bonds.
http://www.chem.qmul.ac.uk/iupac/class/metal.html#08

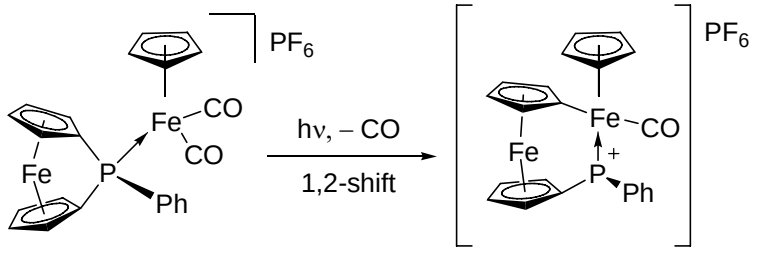

[**8a**→Fe(C_5H_5)$(CO)_2$]PF_6

Scheme 1-17. 1,2-Shift induced by UV irradiation in [**8a**→FeCp$(CO)_2]^+$.

Initial attempts by Manners *et al.* to polymerize [**8a**→FeCp$(CO)_2]^+$ or the neutral complex [**8a**→Fe$(CO)_4$] by tmROP using $PtCl_2$ and Karstedt's catalyst as initiators failed.[80] ThROP experiments for both these complexes were avoided, because the potential release of CO gas during heating in a flame sealed Pyrex tube could lead to unsafe conditions. In turn, these results prompted Miyoshi *et al.* to further investigate the reactivity of complexes [**8a**→Mn(C_5H_4R)$(CO)_2$] (R = H, Me) and [**8a**→W$(CO)_5$], and it was found that in polar solvents like THF and CH_3CN these complexes polymerize under UV-vis irradiation to give low molecular weight polymers. Also, the coordinated manganese and tungsten moieties were intact.[51] For example, when monomer [**8a**→MnCp$(CO)_2$] was dissolved in THF and irradiated for 10 min with Pyrex filtered UV-light, an oligomere with M_w = 2.2 x 10^4, PDI = 1.0 was obtained. Furthermore **8a** itself could be polymerized under these conditions, and after work-up and sulfurization, a polymer weight of M_w = 1.1x 10^4 and M_n = 1.9 x 10^3, PDI = 5.79 was measured by GPC. In 2003 Miyoshi *et al.* published results on the investigation into the mechanism of phROP.[52] Since phROP was initiated by UV irradiation in the absence of any of the established ROP initiators, a fundamentally different mechanism was suspected. When a solution of monomer **8f** in THF in the presence of an excess of

$P(OMe)_3$ was irradiated for 10 min, a ring slippage of one initially η^5-bound cyclopentadienyl ring to a η^1-bound cyclopentadienyl ring occurred with simultaneous coordination of two molecules of $P(OMe)_3$ to the Fe atom to give a piano stool-type complex (Scheme 1-18).[52]

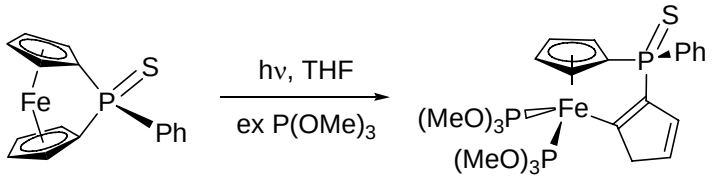

8f

Scheme 1-18. Formation of a ring slipped product by irradiating **8f** with UV-light in the presence of an excess of $P(OMe)_3$.

Precedence for a (C_5H_4)-Fe bond cleavage under UV irradiation had already been observed for bora[1]ferrocenophane **4c** (Scheme 1-2, page 5)[9] in the literature. The ring-slipped product was isolated and fully characterized by multinuclear NMR spectroscopy and X-ray crystallography (Figure 1-14). A similar product was observed by NMR spectroscopy when **8a** was used.

Figure 1-14. ORTEP plot (50% level) of the ring slipped η^5:η^1 product isolated from UV irradiation of **8f** in the presence of $P(OMe)_3$. Calculated hydrogen positions on the cyclopentadienide moiety are shown. Taken from Ref. 52.*

When the stronger donating phosphine PMe_3 was used instead of $P(OMe)_3$, a complete displacement of one cyclopentadienyl ring with coordination of three molecules of PMe_3 to the iron center occurred. The ^1H and ^{13}C NMR resonances of the displaced cyclopentadienyl ring were consistent with the formation of a cyclopentadienyl anion bound to a phosphorous atom. Based on these results, a mechanism for phROP was proposed where UV irradiation weakens the (C_5H_4)-Fe bond of the phospha[1]ferrocenophane, and in the presence of a strong donor, like THF or phosphines, displacement of one η^5-bound cyclopentadienyl ring from the iron atom occurs, generating a cyclopentadienide anion that can further attack another monomer and propagate the chain (Scheme 1-19).

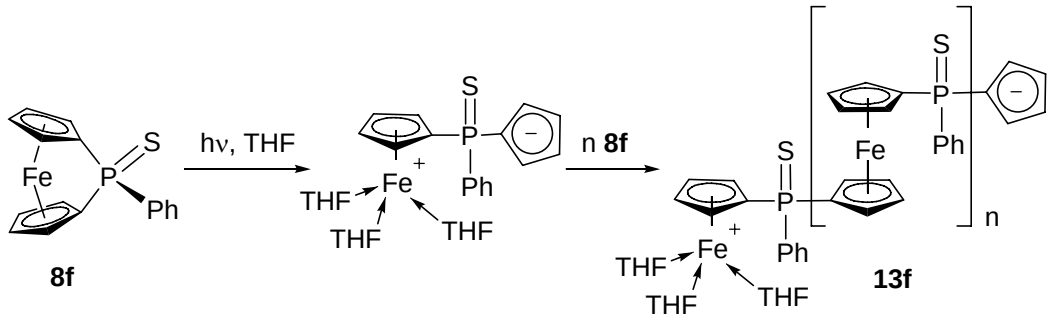

Scheme 1-19. Proposed mechanism for phROP of **8f** in a donor solvent (THF) to yield polyferrocene **13f**. Polymerization occurs via (C_5H_4)-Fe bond cleavage generating an anionic cyclopentadienid ligand that acts as the propagating center.

Further investigations supporting the proposed mechanism were published by Miyoshi *et al.* recently.[81]

In 2004, Tanabe and Manners reported on the extension of this new methodology to sila[1]ferrocenophanes.[82] Unlike **8a** or **8f**, irradiation with UV-light of **5d** in THF or CH_3CN did not lead to any identifiable ring-opened products. In the presence of a mild nucleophilic initiator like Li(C_5H_4R) (R = H, Me), which does not initiate ring-opening on its own, low molecular weight polyferrocene **12d** was obtained. High molecular weight polyferrocenes however were not accessible with Li[(C_5H_4R)] (R = H, Me) as initiator. When the more ionic initiator NaCp was used, living phROP could be achieved. Varying the monomer to NaCp ratio from 25:1 to 200:1, a linear dependency of the obtained polymer weights was found (M_n = 9.3 x 10^3 to 7.0 x 10^4) with narrow PDIs (PDI = 1.04-1.21), all consistent with a living polymerization.

A detailed mechanistic and kinetic study for silicon-bridged [1]FeCP **5d** was published by Manners *et al.*, showing that the polymerization rate is decreasing with increasing temperature.[83] Polymerizations were studied at 5, 14 and 20 °C, with the best results achieved at 5 °C, where a conversion of 83% together with the lowest PDI (<1.1)

was obtained. A feasible explanation was proposed, where photo-excited monomer **5d*** gets deactivated faster at higher temperature. In addition, the functional group tolerance of phROP was demonstrated using the reactive monomer **5w** (Scheme 1-20). Other attempts to polymerize this monomer by anROP were unsuccessful due to the high reactivity of the alkyne substituents.[83] However, **5w** was cleanly polymerized and, because of the living end generated by phROP, could be copolymerized with **5d** to give the controlled block-copolymer **12d**-*b*-**12w** (Scheme 1-20).

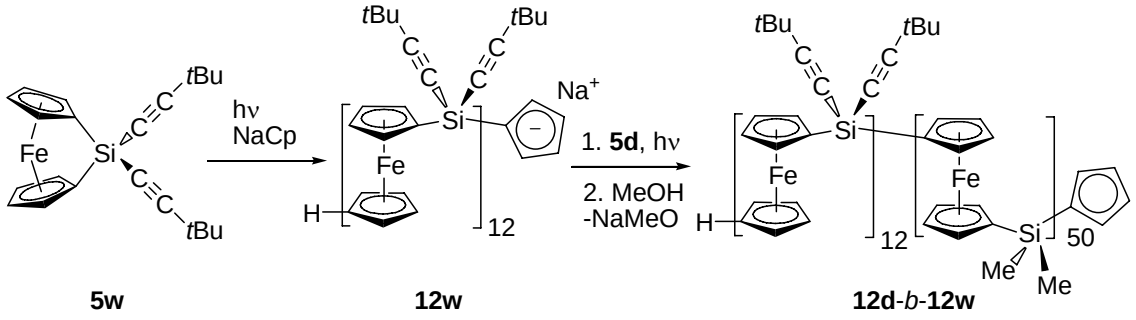

Scheme 1-20. PhROP of monomer **5w** and copolymerization of living polymer **12w** with monomer **5d** to give controlled block-copolymer **12d**-*b*-**12w**.

1.2.5 Other Ring-Opening Polymerizations

The solid state polymerization of **5d** using the radioactive γ-ray source ^{60}Co was described by Manners *et al.* in 1995.[84] The ring strain and high crystallinity of **5d** were optimal starting properties for solid state polymerization, initiated by γ-ray irradiation. The obtained polymer **12d** retained a degree of crystallinity of ~50%. This process, where the crystal structure of the product is related to the crystal structure of the reactant is called topotactic. Also, a dependence of polymer weight on irradiation time was

observed. Exposure to 2.5 MRad yielded **12d** of M_w = 2.2 x 10^5; exposure to 10 MRad yielded M_w = 2.6 x 10^5 and PDI = 1.5.

The solid state polymerization of **5l** (Scheme 1-15, page 35) has also been studied by exposure to the radioactive γ-ray source ^{60}Co.[85] Crystals of **5l** in a flame-sealed evacuated tube were exposed to a total γ-ray irradiation of 17 MRad, upon which the temperature of the sample increased to 38 °C, well below the temperature of 130 °C required for thROP.[25] Subsequent work-up yielded polymer **12l** with M_w = 9.0 x 10^5 and PDI = 1.4 measured by GPC. More interestingly, **12l** was highly syndiotactic as deduced from WAXS and NMR spectroscopy. WAXS gave three broad peaks at d = 7.81, 5.69 and 4.26 Å, whereas **12l** obtained from thROP only showed only an amorphous halo, indicating that **12l** obtained from γ-ray irradiation possessed significant crystallinity in the solid state. Only one resonance for the methyl ligand in the ^{1}H NMR spectrum and one resonance for the *ipso* carbons in the ^{13}C NMR spectrum were detected, whereas thermally obtained **12l** showed three and six resonances, respectively.

The unusual "spontaneous" ROP of tin-bridged [1]FeCPs **7a-b** in the absence of an added initiator[45] was further investigated by Manners *et al.* to elucidate the mechanism and the initiator of this "spontaneous" ROP.[47,86] In a series of experiments non-nucleophilic additives like radicals and radical traps, neutral and anionic nucleophiles, Lewis acids, protic species and cationic electrophiles were tested and the results described. In two cases, for amine nucleophiles like pyridine and for protic species like H^+ and nBu$_3$Sn$^+$, an accelerated ROP in solution was observed, which led the authors to suggest two new ROP mechanisms.[47]

The first new pathway was coined nucleophilically assisted ROP (Scheme 1-21). The greatest ROP rate acceleration was detected in the presence of pyridine, where even in excess, polymerizations of **7a** were finished in less than 90 s, the time it takes to acquire an NMR spectrum. Under the same conditions, **7b** reached a conversion of ~95% in 24 h, whereas without pyridine, conversion was less than 3%. When a catalytic amount of pyridine was added to a solution of **7b**, after 24 h at 60 °C poyferrocenylstannane **15b** was isolated in >95% yield with a polymer weight of M_n = 1.11 x 10^5 and PDI = 3.1. ROP rates did not decrease in the presence of a radical traps or UV-light, excluding a radical mechanism. Electrophiles like Me_3SiCl, a common end capping reagent, had no influence on ROP rates either, excluding a cyclopentadienyl anion as the propagating center. With all these results in hand, the following mechanism for nucleophilically assisted ROP was suggested (Scheme 1-21).

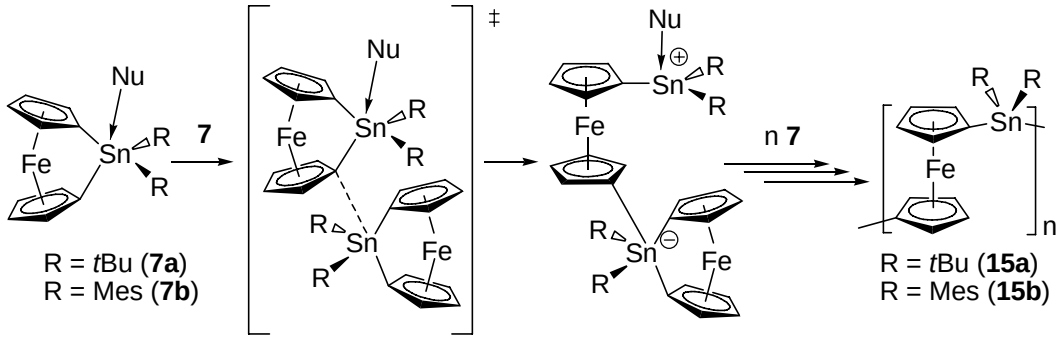

Scheme 1-21. Proposed mechanism for nucleophilically assisted ROP for tin-bridged [1]ferrocenophanes **7** to give polyferrocenylstannane **15**.

The initial step is the coordination of the nucleophile, for example pyridine, to monomer **7** to form a five-coordinated tin species. Similar as observed for complexes **5o-p** (Figure 1-6, page 8) this elongates the cyclopentadienyl *ipso* C-Sn bond *trans* to the nucleophile, which increases the nucleophilicity of this cyclopentadienyl *ipso* carbon

without generating a cyclopentadienyl anion. The enhanced nucleophilicity of the *ipso* carbon may allow for a nucleophilic attack at the tin atom of a second monomer **7**, as illustrated in the transition state in Scheme 1-21. Heterolytic C-Sn bond cleavage generates a five-coordinated stannate complex, which is known to have a lower affinity towards electrophiles compared to the corresponding lithium carbanions. This would explain why Me_3SiCl had no influence on the rate of polymerization. Based on these findings, the "spontaneous" ROP of **7a-b** therefore could be caused by trace amounts of residual TMEDA, which is used in the dilithiation of ferrocene, acting as the true initiator.

The second new pathway suggested for the "spontaneous" polymerization of tin-bridged monomers **7a-b** was cationic ring-opening polymerization initiated by protic impurities (Scheme 1-22). Addition of small quantities of HOTf or nBu$_3$SnOTf led to the formation of high molecular weight polymers. For example, when 5 mol% of HOTf were added to a solution of **7b** at -78 °C in CH_2Cl_2, polyferrocenylstannane **15b** formed within 30 min. After work-up **15b** was isolated with a polymer weight of M_n = 3.85 x 10^5 and PDI = 2.2.

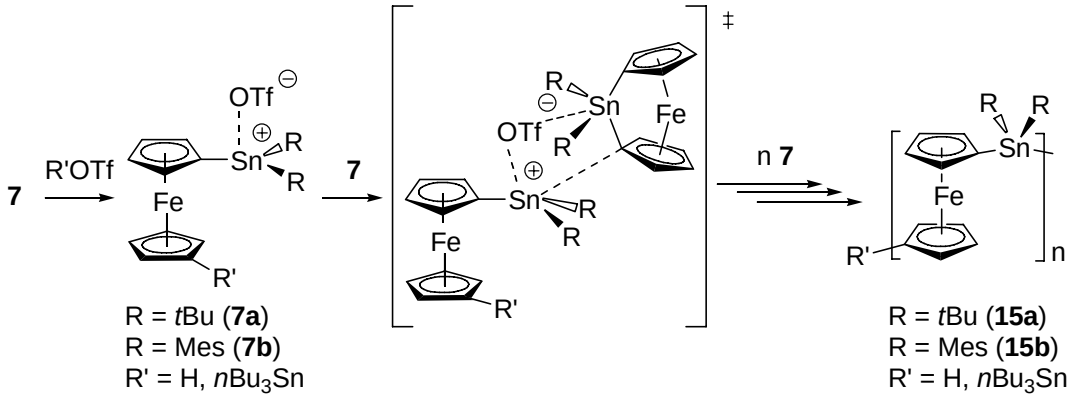

Scheme 1-22. Proposed mechanism for cationic ROP for tin-bridged [1]ferrocenophanes **7**.

Rates of polymerization were consistently faster in more polar solvents. A more polar solvent would stabilize an ionic propagating center. If a catalytic amount of R'OTf (R' = H, nBu$_3$Sn) was used together with an excess of NBu$_4$OTf (100 equiv.), polymerization was inhibited, and only low molecular weight oligomers were obtained. NBu$_4$OTf was chosen because the NBu$_4^+$ cation is not electrophilic enough to initiate ring-opening. The large excess of OTf$^-$ anions competes with the cationic propagating center thereby suppressing ROP. Both these observations support the proposed mechanism of cationic ROP.

In 2005, a second example of a cationic ROP was published by Hatanaka *et al*. An unprecedented cationic ROP of hypercoordinated complex **5n**, using a silylium salt as catalytic initiator, was observed (Scheme 1-23).[22] Polymerizations were rather sluggish, with the silylium salt giving the fastest rate of all cationic initiators tested, the polymerization still took 14 days to go to completion. Polymer **12n** was isolated in 53% yield. The polymer weight was determined by low-angle laser light scattering (LALLS) as $M_w = 9.0 \times 10^3$.

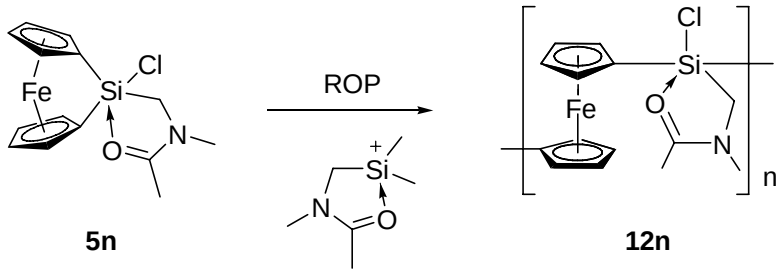

5n **12n**

Scheme 1-23. Rare example of cationic ROP of hypercoordinated monomer **5n** giving polymer **12n** using catalytic amounts of a silylium cation as an initiator.

If other Lewis acids like Me_3SiOTf, Me_3SiI or $BF_3{\cdot}OEt_2$ were used, ROP became very sluggish. [1]FeCPs with four-coordinated bridging elements (e.g. **5d**) did not yield polymeric material under the same conditions.

1.3 [1.1]Metallocenophanes

[1.1]Metallocenophanes ([1.1]MCPs) have been reported for the transition metals Fe and Ru, with the vast majority of complexes known for [1.1]ferrocenophanes ([1.1]FeCPs). They were discovered nine years earlier than [1]MCPs, when Watts reported the synthesis of the first carbon-bridged [1.1]FeCP in 1966 (see Chapter 1.3.2).[87] There are two isomers known for [1.1]FeCPs, the *syn* isomer, where both bridging elements are on the same site of the ferrocene moieties, and the *anti* isomer, where the two bridging elements adopt opposite sites of the ferrocene moieties. Furthermore, ligands on the bridging element can adopt either an *exo* position perpendicular to the plane of the cyclopentadienyl rings or an *endo* position aligned with the plane of the cyclopentadienyl ligands. In [1.1]MCps, the 2,5-protons of the cyclopentadienyl ligands are referred to as α protons (H_α) and the 3,4-protons consequently as β protons (H_β) (Scheme 1-24).

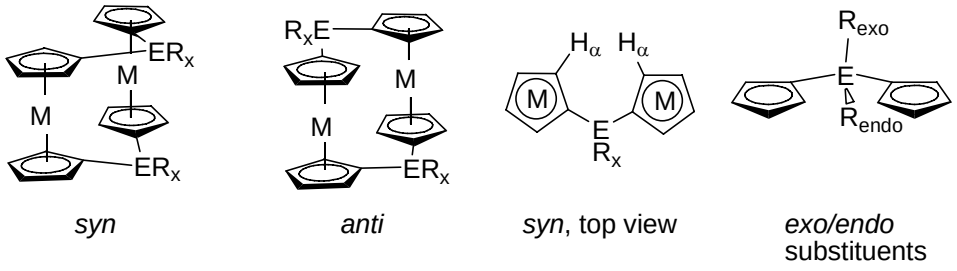

Scheme 1-24. S*yn* and *anti* isomers of [1.1]MCPs. Schematic representation of one bridging ligand with inner α protons (H_α) and *exo*/*endo* substituents (R_{exo}/R_{endo}).

Which isomer is formed mainly depends on the size of the bridging element E and the steric requirements of ligand R_x. Smaller bridging elements like boron or carbon usually prefers the *syn* conformation. The *syn* conformation shows a highly fluxional behavior in solution which has been studied in-depth.[88-90] Because of the short bond length of E-C bonds for smaller elements the inner α protons come in close contact (~0.8 Å).[87] In order to release the steric congestion of the inner α protons, usually the more flexible *syn* conformation is adopted, where one ferrocene moiety can twist out of the way (Figure 1-16, page 55). The amount of twisting can be determined by single-crystal structure analysis and is commonly described by a twisting angle. Another strategy to release steric congestion is a widening of the bridging angle C-E-C. For carbon- and phosphorous-bridged [1.1]FeCPs both *anti* and *syn* isomers have been isolated and characterized by X-ray crystallography. All the heavier bridging elements adopt the more rigid *anti* conformation in the solid state. Although the inner α protons still point directly at each other, the bond lengths between heavier elements and carbon atoms are in general longer. This bond lengthening also increases the distance between and therefore the repulsion of the inner α protons.[91] The influence of the ligand R_x is governed by its steric bulkiness. Large, bulky ligands would come in very close contact

in the *syn* conformation, where the bridging elements are stacked on top of each other, therefore favoring the *anti* conformation. Bulky ligands are usually required to protect and shield heavier bridging elements to allow for isolation of the targeted product, additionally forcing heavier element-bridged [1.1]MCPs to adopt the *anti* conformation. *Syn* isomers show a fast *syn-syn* interconversion in solution, which can be observed by NMR spectroscopy if the complex is asymmetrically substituted. An analogy to the boat-to-boat pseudorotation of cyclohexane has been suggested.[89] Although most of the metallocene moieties in [1.1]MCPs show small tilt angles of $\alpha < 6°$ as a result of proton repulsion, they are essentially unstrained and cannot be used as monomers in ROP. The tilting of the cyclopentadienyl rings in [1.1]MCPs also occurs in the opposite direction as compared to [1]MCPs, away from the bridging elements. Besides being studied for their electrochemical properties (see Chapter 1.3.4), [1.1]FeCPs also display some other interesting properties. Upon protonation with strong acids, carbon-bridged [1.1]FeCPs have been observed to produce hydrogen gas[92-95] and upon deprotonation the first evidence for an intramolecular C-H-C bond was observed.[96-98]

Bimetallic [1.1]ferroruthenocenophanes ([1.1]FeRuCPs) and [1.1]ruthenocenophanes ([1.1]RuCPs)[99-103] were published by various groups. Furthermore Mueller-Westerhoff *et al.* also mentioned the synthesis of a carbon-bridged [1.1]cobaltoferrocenophane ([1.1]CoFeCP) and a [1.1]cobaltocenophane ([1.1]CoCP), but because of the low yielding synthesis (<2%) a systematic exploration of the chemistry of these complexes was not pursued.[91]

1.3.1 Group 13-Bridged [1.1]Metallocenophanes

In 2003, a dianionic borata[1.1]ferrocenophane [ER_x = BMe_2^- (**16a**)] was published by Wagner *et al.* as a highly efficient lithium scavenger.[104] Complex **16a** was obtained from the reaction of dilithioferrocene with 1,1'-bis(dimethylboryl)ferrocene, but was not isolated (Scheme 1-25). In the presence of an excess amount of the crown ether [12]crown-4, crystals of the salt-like complex [Li([12]crown-4)$_2$][**16a-Li**] could be grown and characterized by X-ray crystallography. Complex **16a-Li** contains a "naked" lithium cation held in between the iron atoms probably by electrostatic forces (Scheme 1-25).

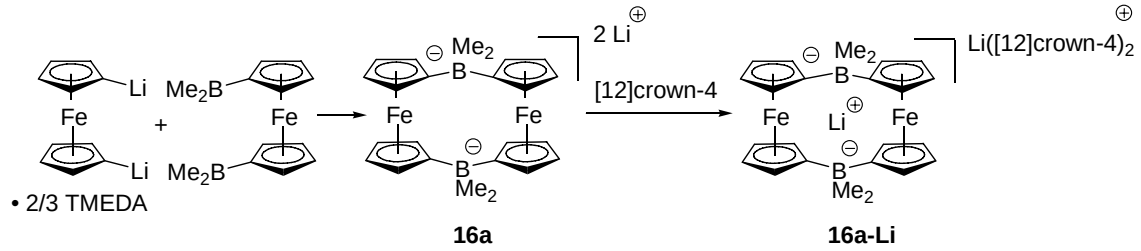

16a **16a-Li**

Scheme 1-25. Synthesis of **16a** and isolation of **16a-Li** with the help of [12]crown-4.

Alumina[1.1]ferrocenophane **17a** [ER_x = AlAr'] (Ar' = $(C_6H_4)CH_2NMe_2$) was published by Braunschweig *et al.* employing an intramolecular coordinating ligand.[105] Complex **17a** was fully characterized by X-ray crystallography and showed the *anti* conformation, expected for the larger sized element aluminum and the bulky ligand Ar' (Figure 1-15).

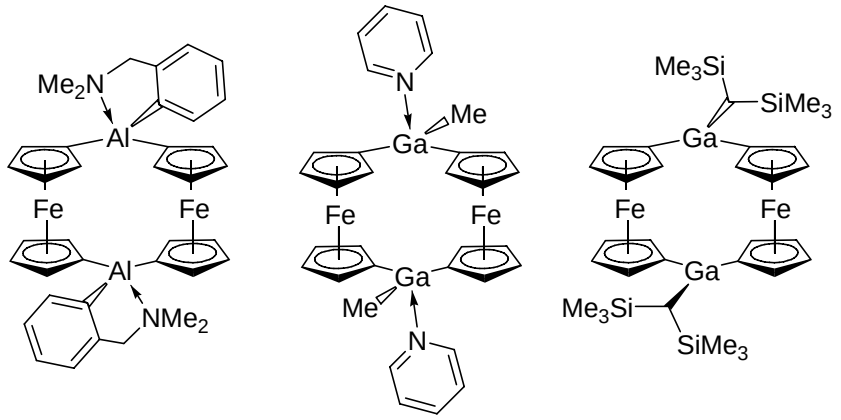

17a **18a** **18b**

Figure 1-15. Alumina[1.1]ferrocenophane **17a** and galla[1.1]ferrocenophanes **18a-b**.

The first group 13-bridged [1.1]ferrocenophanes reported contained gallium atoms in the bridging position and were published in 2001 in short succession by the groups of Jutzi[106] and Uhl.[107] The isolation of galla[1.1]ferrocenophane **18a** [ER_x = GaMe(py)] was achieved employing pyridine (py) as an external donor to satisfy the Lewis acidic gallium atom in **18a**.[106] Complex **18a** was obtained as a side product when starting material 1,1'-bis(dimethylgallyl)ferrocene was heated in toluene in the presence of external donors like pyridine or THF. Complex **18a** could be synthesized as the main product from a planned synthesis at room temperature using the same starting material and a variety of external donors.[108] A crystal structure of donor-free **18a** showed an *anti* conformation in the solid state. A small tilt angle of $\alpha = 4°$ indicated the repulsion of the inner α protons. In solution however, a highly dynamic behavior of **18a** was observed by NMR spectroscopy. Only one resonance for all α protons and all β protons, respectively, could be observed, indicating a fast pseudorotation between *anti* and *syn* conformations.

The galla[1.1]ferrocenophane **18b** [ER_x = $GaCH(SiMe_3)_2$] reported by Uhl *et al.* was obtained by first synthesizing the alkyltrichlorogallate complex $[Li(THF)][(SiMe_3)_2CHGaCl_3]$ and subsequent reaction of this gallate with dilithioferrocene.[107] Structural characterization by X-ray crystallography confirmed that **18b** contained two three-coordinated gallium atoms in an *anti* conformation. A tilt angle of α = 5.9° was measured, reflecting the constrained geometry and repulsion of the inner α protons in an *anti* conformation. Complex **18b** showed a similar dynamic behavior in solution as **18a**, where only one resonance for all α and β protons, respectively, and a single resonance for the trimethylsilyl groups and the methine protons of the ligand was detected by NMR spectroscopy.

1.3.2 Group 14-Bridged [1.1]Metallocenophanes

Investigations in the early years into the properties of [1.1]FeCPs were hampered by low yielding synthesis of [1.1]FeCPs or formation of higher oligomers. In general, two different synthetic approaches to synthesize [1.1]FeCPs were pursued (Scheme 1-26 **C** and **D**). The initial synthesis published by Watts yielded 1,12-dimethylcarba[1.1]ferrocenophane **19a** [ER_x = CHMe] (Figure 1-17, page 56) in 14-20% yield after column chromatography. An improved synthesis of **19a** was achieved by reduction of 1,1'-bis(6-methylfulvenyl)ferrocene with $LiAlH_4$ and subsequent reaction with $FeCl_2$ (Scheme 1-26 **C**, R = Me).

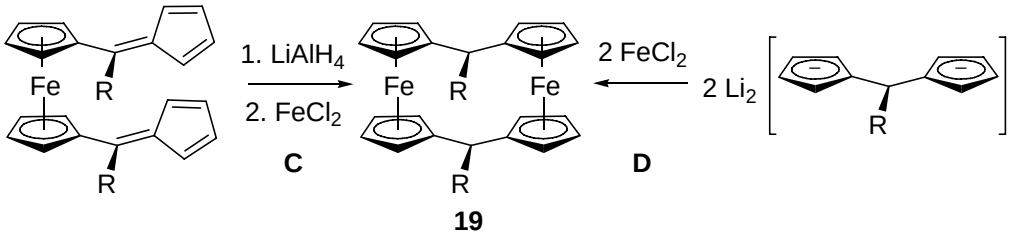

Scheme 1-26. Two synthetic approaches to yield [1.1]ferrocenophanes **19**. Reduction of 1,1'-bis(fulvenyl)ferrocene followed by cyclization **C** and bis(cyclopentadienide)methane cyclization **D**.

In a perfect coplanar arrangement of the ferrocene moieties in the *syn* conformation, the inner α protons would come too close to each other (~0.8 Å). Therefore, based on these geometric arguments, Watts tentatively assigned the two methyl groups on the bridging carbon to be *exo* and **19a** to exist in the *anti* conformation. A crystal structure of **19a** revealed that the predicted *exo* positions of the methyl groups to be correct, but an overall *syn* conformation by **19a** was adopted with twisted ferrocene moieties (Figure 1-16).[109,110] A dihedral twist angle of the two ferrocene moieties of 31° to each other was measured, together with a small tilt angle of α = 2.7°. This twisting in the *syn* conformation separates the inner α protons by an estimated 2.03 Å, which is still less than the sum of the van der Waals radii of two covalently bound hydrogen atoms of 2.4 Å (Figure 1-16).[111]

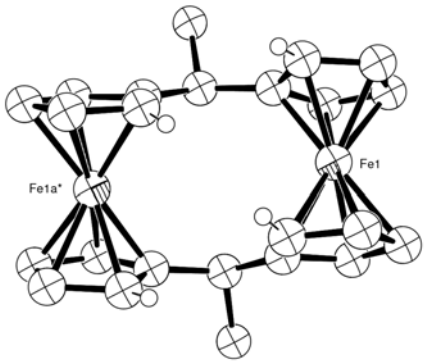

Figure 1-16. ORTEP plot of **19a** with calculated positions of inner α protons. All other H atoms are omitted for clarity. Taken from Ref. 110.*

Watts also reported an alternative synthesis of **19a** via Friedel-Crafts cyclization of 1,1'-bis[(chlorocarbonyl)]ferrocene and ferrocene.[112] This afforded a carbonyl-bridged [1.1]FeCP [ER_x = CO (**19b**)] (Figure 1-17), which was characterized by MS only. Reduction of **19b** with $LiAlH_4/AlCl_3$ yielded the carba[1.1]ferrocenophane **19c** [ER_x = CH_2] (Figure 1-17), yields were not reported. Detailed experimental results on the synthesis of **19b** and **19c** as well as three new [1.1]FeCPs were reported in 1969.[113] Complex **19b** was obtained in 3.5-7% yield via the Friedel-Crafts route, **19c** via reduction of **19b** with $LiAlH_4/AlCl_3$ in 87%. The synthesis of **19c** via route **C** was attempted, but the starting material 1,1'-bis(fulvenyl)ferrocene (Scheme 1-26 **C**, R = H) was reported to be too unstable and to polymerize before the synthesis of **19c** could be performed. Synthesis of **19c** via route **D** using *n*BuLi to deprotonate bis(cyclopentadiene)methane yielded only 3-5% of the targeted product. For **19a** an improved yield of 27% was reported via route **C**. The new carba[1.1]ferrocenophane **19d** [ER_x = CHPh] (Figure 1-17) was obtained from 1,1'-bis(6-phenylfulvenyl)ferrocene via route **C** in 9% yield. The tetramethyl

* Copyright©2002 The Cambridge Crystallographic Data Centre. All rights reserved.

carba[1.1]ferrocenophane **19e** [ER_x = CMe_2] was obtained in 2.5% yield from the reaction of 1,1'-bis(6-methylfulvenyl)ferrocene with a fivefold excess of MeLi and subsequent addition of $FeCl_2$. The methylhydroxy-bridged [1.1]FeCP **19f** [ER_x = CMeOH] was obtained in 50% yield from reduction of **19b** with MeMgI/MeI.

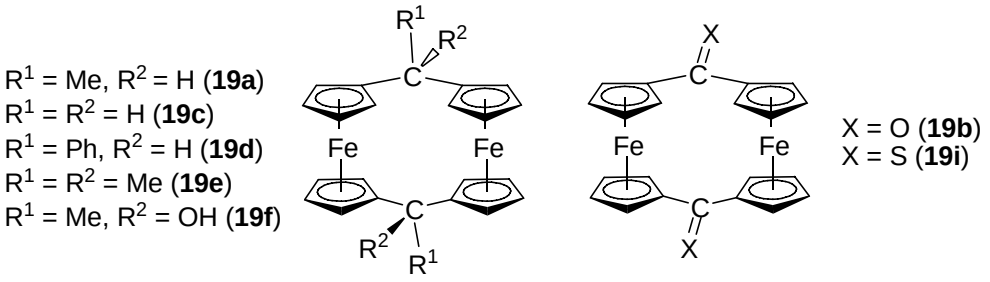

Figure 1-17. Various substituted [1.1]FeCPs **19**.

The synthesis of **19c** via route **D** was reported in 1969 by Katz *et al.* independently from Watts.[59] Bis(cyclopentadiene)methane was obtained from reaction of NaCp and CH_2Cl_2. Double lithiation with *n*BuLi yielded the dianionic precursor bis(cyclopentadienide)methane which could be cyclized with two equivalents of $FeCl_2$ to yield **19c**. However, beside complex **19c** the higher analogues [1.1.1]FeCP, [1.1.1.1]FeCP and [1.1.1.1.1]FeCP formed as byproducts and were isolated via column chromatography and analyzed by NMR spectroscopy and MS. Complex **19c** was isolated in only 1.8% yield. Katz also suggested an alternative nomenclature system with superscript indices for the higher analogues for ease of reading. Accordingly the complexes were designated as [1^2]FeCP, [1^3]FeCP etc. Full experimental details including the first spectroscopic characterization of **19b** by NMR spectroscopy were published later.[58]

Alternative routes to **19b** were published by two more groups. Ohnishi *et al.* reported the synthesis of **19b** via reaction of carbon monoxide with 1,1'-(chloromercuri)ferrocene in the presence of lithium chloropalladiate(II) (Li_2PdCl_4) as a catalyst with an isolated yield of 29%.[114] O'Connor Salazar and Cowan prepared **19b** from the reaction of 1,1'-dibromoferrocene with *n*BuLi and N,N-dimethylcarbamyl chloride ($ClC(O)NMe_2$) in 9% yield.[115]

In 1981, Mueller-Westerhoff *et al.* published an improved synthesis of [1.1]MCPs via a modified route, starting from 6-(dimethylamino)fulvene and the respective dilithiometallocene (Scheme 1-27).[116-118] Contrary to what was reported by Watts *et al.*[113] 1,1'-bis(fulvenyl)ferrocene was obtained as a stable crystalline material with a sharp melting point.[116] From 6-(dimethylamino)fulvene and dilithiometallocene, the dianion 1,1'-(6-dimethylaminofulvenyl)metallocene was obtained as a lithium salt. Upon hydrolysis dimethylamine and LiOH were eliminated to yield the precursor 1,1'-bis[(fulvenyl)]ferrocene in 85-95% yield. Reduction with $LiBH(sBu)_3$ and the subsequent addition of MCl_2 yielded the respective [1.1]MCP. Complex **19c** was isolated in up to 60% yield (Scheme 1-27).

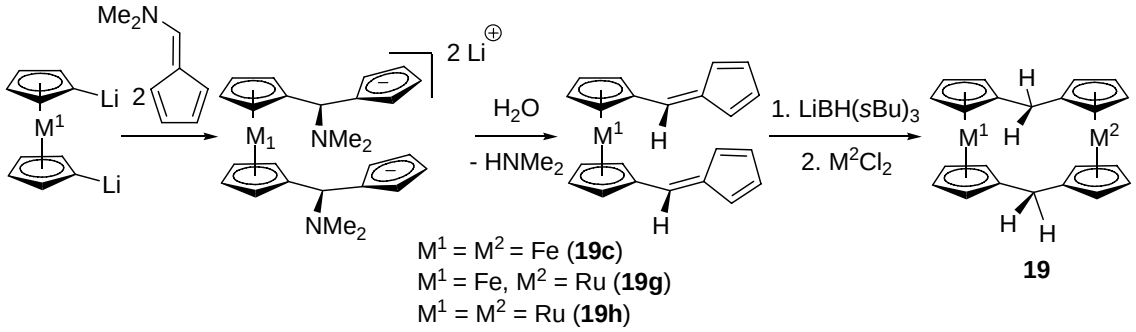

Scheme 1-27. Improved synthesis of **19c**, **19g** and **19h**.

This route was employed for the [1.1]FeRuCP **19g** [$ER_x = CH_2$] starting from dilithioferrocene and using $RuCl_2 \cdot DMSO_4$ in the last step. Carba[1.1]ruthenocenophane **19h** [$ER_x = CH_2$] was obtained starting from dilithioruthenocene.[99] The synthesis of [1.1]CoFeCP and [1.1]CoCP were mentioned, but because of the low yielding synthesis of these two complexes, no further results were published.[91] The crystal structures of **19c**, **19g** and **19h** were published in 1992.[100] All three complexes were found to exist in a twisted *syn* conformation, with **19c** showing an average twist angle of 13.3°, much smaller than that reported for **19a** (31°).[109] With the improvement in synthesis of [1.1]MCPs, the group of Mueller-Westerhoff went on to study the formation of intramolecular C-H-C bonds upon deprotonation of **19c**,[96] structural dynamics,[93,119] electrochemistry,[100,120-124] and the catalytic formation of hydrogen gas upon protonation.[94,95,125,126]

The simplicity of NMR spectra of [1.1]FeCPs like **19a** and **19c** with one resonance for all α and β protons, respectively, was recognized early on and explained by a highly fluxional behavior in solution.[91,112,116] Direct evidence for the exceptional dynamic behavior was published by Ahlberg *et al.*[90] Variable temperature NMR (VT-NMR) spectroscopy on **19c** showed a splitting of the *endo*/*exo* bridge protons and α/β protons at 133 K. An analogy was drawn to the pseudorotation of cyclohexane, by which the cyclohexane ring undergoes a boat-to-boat interconversion which exchanges the axial and equatorial substituents. The coalescence temperature for this pseudorotation for **19c** was determined at 150 K (500 MHz), with an estimated free energy of activation of 28 ± 4 kJ/mol. This flexibility was not only observed in solution, but also in the solid state. From a crystal structure analysis of **19c** a different crystal

phase to the previously reported one was revealed. This new phase showed a *syn* isomer with an approximate C_{2v} symmetry of the complex, displaying an average twist angle of only 2.4°.[127] To release steric repulsion of the inner α protons in this new phase of a *syn* conformation, the C-CH_2-C bridge angles were widened (121°) compared to the crystal phase of **19c** determined before.

In the same year, Ahlberg *et al.* also reported on the isolation of **19a** in an *anti* conformation.[128] Up to this point, carbon-bridged [1.1]FeCPs were believed to be stable only in the flexible *syn* conformation, because in the rigid *anti* conformation, the repulsion of the inner α protons could not be relieved.[91] However, a crystal structure analysis showed a distorted *anti* conformation with both methyl groups in *exo* positions. Whilst one ferrocene moiety displayed a conventional tilt angle of α = 4.1°, the second ferrocene moiety displayed a tilt angle of α = 22.7°. In addition, an average twist angle of 35° was measured (Figure 1-18).[128]

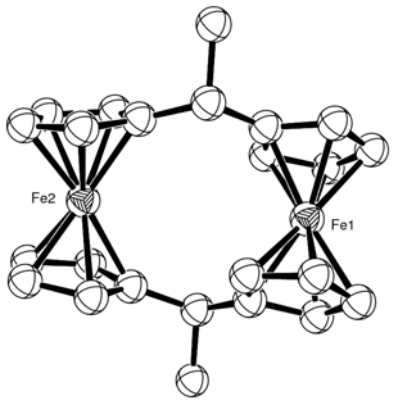

Figure 1-18. ORTEP plot (50% level) of **19a** in the *anti* conformation. H atoms are omitted for clarity. Taken from Ref. 129.*

The only other example of a [1.1]FeCP in an *anti* conformation at the time, tin-bridged [1.1]FeCP **21a** [ER_x = Sn(*n*Bu)$_2$], was published by Seyferth *et al.*, and showed an undistorted approximate C_{2h} symmetry in the solid state.[129]

In 1995, Löwendahl and Håkansson reported on the isolation of a third isomer of **19a**, the *exo*/*endo syn* isomer of **19a**.[89] A crystal structure analysis yielded an average twist angle of 38.8° and an average tilt angle of α = 6.7° (Figure 1-19).

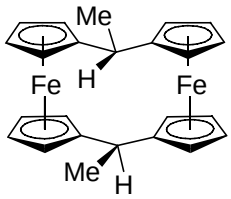

exo/endo syn **19a**

Figure 1-19. The *exo*/*endo syn* isomer of **19a**.

Furthermore, an in-depth discussion on all the possible conformational and configurational isomers of **19a** and their possible interconversion mechanisms was provided. The group of Ahlberg also investigated various metallation[97,98,130-133] and protonation[134] reactions of [1.1]FeCPs.

An interesting contribution to the studies of dynamic behavior of [1.1]FeCPs was published by Sato and Asai.[103] The sulfurization of **19b** using Lawesson's reagent (2,4-bis(4-methoxyphenyl)-2,4-dithioxo-1,3,2,4-dithiadiphosphetane) was investigated in order to synthesize the new [1.1]ferrocenophane **19i** [ER_x = CS] (Figure 1-17, page 56) and the dynamics in solution were investigated by VT-NMR spectroscopy. The starting material **19b** was also reinvestigated by VT-NMR spectroscopy, which had been reported to show one multiplet for all α and β protons, respectively, at room temperature.[58] At -41 °C the static spectrum of **19b** was observed corresponding to the

fixed *syn* conformation with four multiplets for the ferrocene protons (400 MHz). More importantly though, at the same temperature a second set of four multiplets with minor intensities (~13%) also was observed, that coalesced with the main set of multiplets at 10 °C. The authors attributed the minor set of multiplets to the *anti* conformation, suggesting that [1.1]FeCPs cannot only undergo *syn-syn* interconversion but also *syn-anti* interconversion.[103] Six years later, however, Watanabe *et al.* published their results on some oxidation chemistry of [1.1]FeCPs and [1.1]FeRuCPs and revised their conclusions on the dynamics in solution.[101] The complexes **19b** and [1.1]FeRuCP **19j** [ER_x = CO] were investigated. The synthesis of **19j** was reported earlier with little analytical data.[135] A crystal structure determination of **19j** revealed its *syn* conformation, with a tilt angle for the ferrocene moiety of $\alpha = 2.5°$ and for the ruthenocene moiety of $\alpha = 3.6°$.[101] VT-NMR spectra of **19b** and **19j** revealed similar signal splitting at lower temperatures with the appearance of a minor set of signals. This minor set of signals was originally assigned to the *anti* conformation,[103] but now the authors revised their assignment as probably due to the twist-conformation, stating as one of their reasons the fact that no other *syn-anti* interconversions had been published in literature.[101] The twist-conformation had been suggested by Mueller-Westerhoff as an intermediate conformation halfway through the *syn-syn* interconversion, where both bridging groups undergo a synchronized pseudorotation (Scheme 1-28).[91]

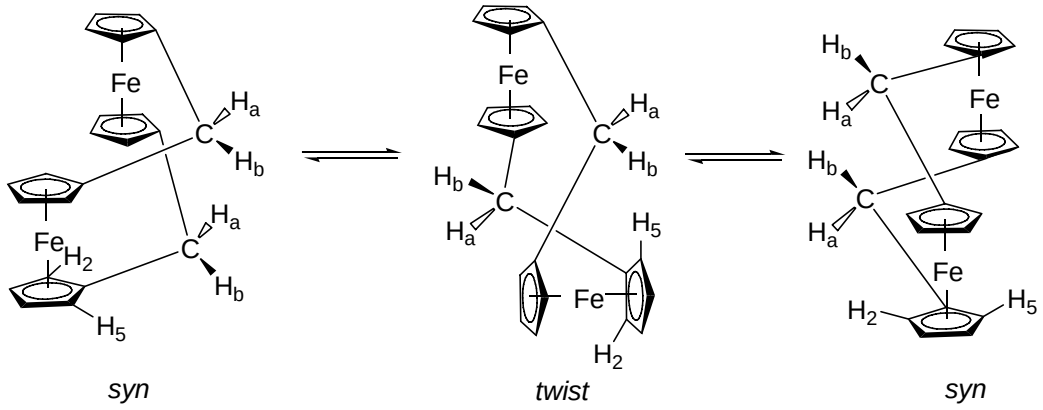

Scheme 1-28. Proposed intervonversion of *syn* **19c** via an intermediate *twist* conformation which results in exchange of bridging ligands (H_a and H_b) and the cyclopentadienyl protons (only α protons H_2 and H_5 shown).

Interestingly, five years before Watanabe *et al.* published their revised findings,[101] Rudziński and Osawa published a theoretical investigation of the *syn-syn* interconversion of **19c**, concluding that Mueller-Westerhoffs proposed synchronized twist-conformation constitutes a local maximum on the energy surface and is therefore very unlikely to occure.[136] The *syn-syn* interconversion rather proceeds via a sequential flipping of one methylene bridge first, leading to an *anti* conformation local minimum on the energy surface (Scheme 1-29).

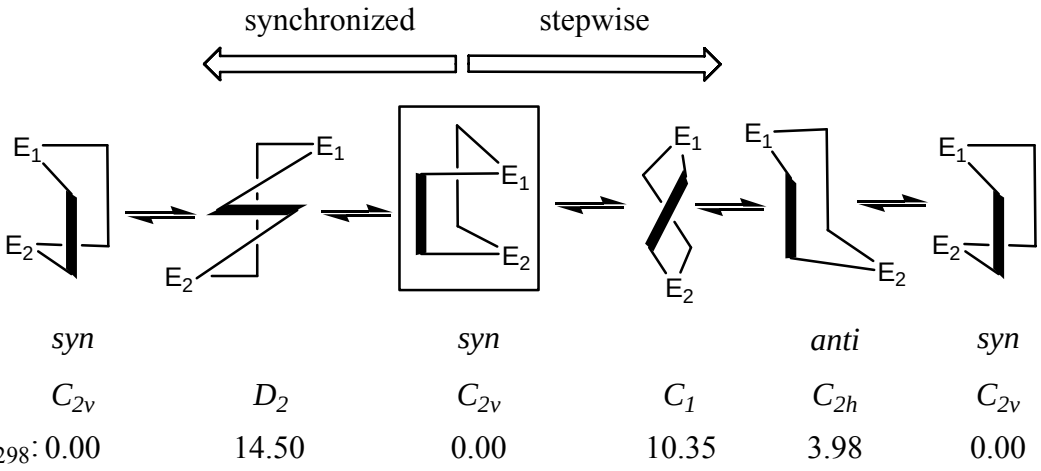

Scheme 1-29. Illustration of two proposed mechanisms for *syn-syn* interconversion of [1.1]MCPs. Optimized structures calculated at the MM2'-level. Synchronized interconversion (left) occurs via a simultaneous flip of the bridging elements (E_1 and E_2) and is a local maximum on the energy surface. Stepwise interconversion occurs via a sequential flip of bridging groups (E_1 first, then E_2) and is a local minimum on the energy surface. Relative free energies ΔG at 298 K are in kcal/mol. Taken from Ref. 136.

It also has been shown that *syn-syn* interconversion can be inhibited or completely suppressed, if the cyclopentadienyl rings in [1.1]FeCPs are substituted. For example, an ethyl group in the 3 position did not inhibit the interconversion, substitution in the 2 position completely suppressed it.[119] The hybrid complexes [1.1]FeCP **19k** [$ER_x = CH_2$] and [1.1]FeCP **19m** [$ER_x = CH_2$] (Figure 1-20), where one ferrocene moiety is also bridged intramolecularly by a propyl group in the 2,2' and 3,3' position, respectively (Figure 1-20).[137]

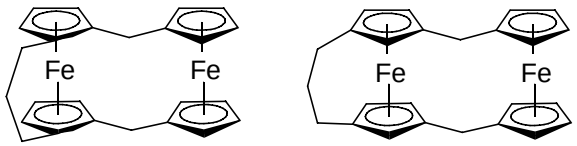

19k **19m**

Figure 1-20. Hybrid [1.1]FeCP **19k** and [1.1]FeCP **19m**.

Complexes **19k-m** were synthesized using published procedures and full structural details were obtained from X-ray crystallography, which showed that both complexes adopt the *syn* conformation in the solid state. In solution, **19k-m** showed a significantly different behavior, reflected by the NMR resonances of the methylene bridge protons. Whereas the 3,3'-isomer **19m** showed a sharp singlet indicating rapid *syn-syn* interconversion that led to fast *endo-exo* exchange of the bridging methylene protons on the NMR timescale, the bridging methylene protons in the 2,2'-isomer **19k** were split into an AB quartet. Substitution in the 2 position obviously leads to steric congestion in the transition state of the *syn-syn* interconversion.

The first silicon-bridged [1.1]FeCP [ER_x = $SiMe_2$ (**20a**)], was isolated and published independently by the groups of Chang[138] and Manners[139]. Chang *et al.* obtained **20a** as the main product from an attempted polycondensation reaction of the dilithium salt of bis(cyclopentadienide)dimethylsilane and $FeCl_2$ in 21.3% yield, together with 7.3% yield of the polymer **12d**. The molecular structure of **20a** was established by X-ray crystallography, showing that **20a** adopts the *anti* conformation, with a tilt angle of α = 4.7°. Manners *et al.* obtained **20a** from a directed five-step synthesis in an overall yield of 14% (Scheme 1-30). Starting from dilithioferrocene and $Me_2(NEt_2)SiCl$, the product 1,1'-bis(diethylaminedimethyl)silylferrocene was obtained.

Substitution of the amine groups with chlorine by acetyl chloride afforded 1,1'-bis(chlorodimethylsilyl)ferrocene. Reaction with LiCp, double deprotonation with *n*BuLi and subsequent reaction with $FeCl_2$ yielded **20a** (Scheme 1-30).

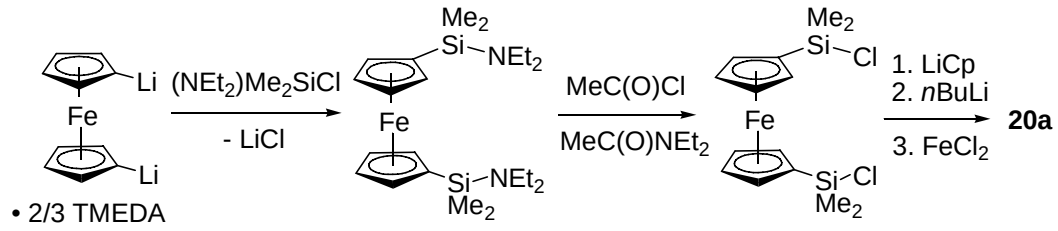

Scheme 1-30. Stepwise synthesis of the [1.1]FeCP **20a** starting from dilithioferrocene.

A crystal structure analysis revealed essentially the same results as obtained by Chang; complex **20a** adopts the *anti* conformation in the solid state with a tilt angle of α = 4.9(3)°. The potential use of **20a** as a monomer for ROP was also investigated. As expected for an unstrained complex, experiments showed that **20a** did not undergo thROP at elevated temperatures. Manners *et al.* also reported on the identification of **20a** as a side product in tmROP experiments of **5d** with $[Pd(COD)Cl_2]$.[70] As already mentioned in Chapter 1.2.3, Tanaka *et al.* found that phosphine containing Pd and Pt complexes cleanly dimerize **5d** to yield **20a**.[73] In 2000, Manners *et al.* reported that the di(ferrocenyl)silane-bridged [1]FeCP **5g** gave the insoluble polymer **12g** in thROP experiments at 250 °C, but at 200 °C predominantly produced the new sila[1.1]ferrocenophane (**20b**) [ER_x = $SiFc_2$].[19] Complex **20b** was characterized by NMR spectroscopy and MS (Scheme 1-31).

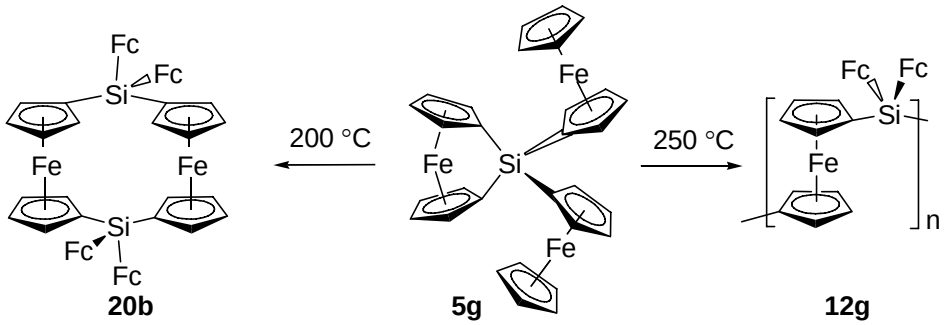

Scheme 1-31. Formation of [1.1]FeCP **20b** or polyferrocenylsilane **12g** from monomer **5g** depending on temperature. [Fc = $(C_5H_4)Fe(C_5H_5)$]

The $SiCl_2$-bridged [1.1]FeCP **20c** [$ER_x = SiCl_2$] was isolated as the byproduct of a thROP experiment of monomer **5e** in 17% yield by Cerveau *et al.*[140] A crystal structure analysis of **20c** showed an undistorted *anti* conformation in the solid state with a tilt angle of α = 3.5°. More interestingly, NMR spectroscopy of **20c** at room temperature showed only one multiplet for all α and β protons, respectively.

In 2002, Manners *et al.* reported the isolation of an acetylide substituted [1.1]FeCP [ER_x = SiMe(CCPh) (**20d**)] as a side product from tmROP experiments with monomer **5x** (Scheme 1-13, page 32).[31] X-ray crystal structure analysis established a distorted *anti* conformation in the solid state, with similar distortions than those reported for the *anti* conformation of **19a**.[128] One ferrocene moiety in **20d** was essentially unstrained with a tilt angle of α = 1.7(2)°, whereas the other one showed a tilt angle of α = 10.3(3)°. The twist angle, although clearly present, was not mentioned by the authors. More interestingly, the methyl and acetylide substituents on the silicon bridges adopt an *endo*/*exo* conformation, a result of a stereoselective synthesis.

Hatanaka *et al.* published the isolation of a hypercoordinated sila[1.1]ferrocenophane, that was surprising in many ways.[141] Pentacoordinated

monomer **5n** was dimerized to obtain [1.1]FeCP **20e** [ER_x = SiClO'] (O' = $CH_2N(Me)C(Me)=O$) via an established route using $[PdCl_2(PCy_3)_2]$.[73] Surprisingly, $PdCl_2$, an otherwise potent tmROP initiator, also cleanly gave **20e** as the sole product, with no formation of polymers detected (Scheme 1-32).

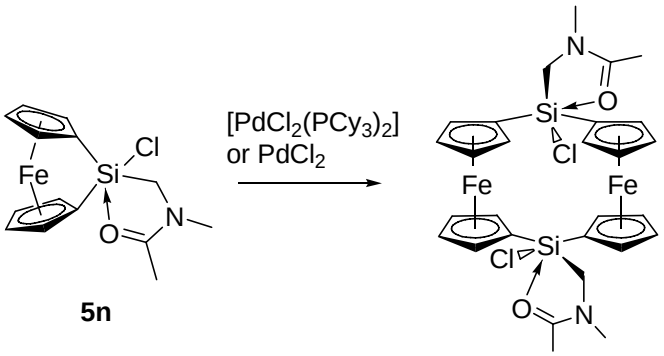

5n **20e**

Scheme 1-32. Transition metal catalyzed dimerization of **5n** to yield **20e**.

The most surprising result was the crystal structure obtained from X-ray crystallography of **20e**. Although the authors state that **20e** adopts the *anti* conformation in the solid state and make several structural comparisons of **20e** with the previously published structure of **20a**, it must have escaped their attention that the ferrocene moieties in **20e** are not coplanar, but rotated to each other by almost 90° (Figure 1-21).

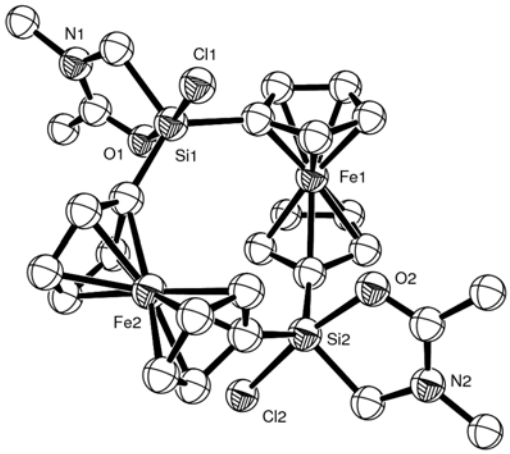

Figure 1-21. ORTEP plot (50% level) of **20e**. H atoms omitted for clarity. Taken from Ref 141.*

This important structural feature, which was not mentioned in the discussion of structure **20e** by the authors with a single word,[141] might constitute direct evidence for the proposed twist-conformation,[91,119] an intermediate conformation in the *syn-syn*, *syn-anti*[103,142] and possible *anti-anti*[143,144] interconversions of [1.1]MCPs. The highly fluxional behavior of **20e** in solution, which also was not further investigated by the authors, is evident from the reported NMR spectrum.[141] Only one multiplet for all α and β protons, respectively, and three singlets for protons of the O' ligand were detected. In a hypothetical rigid twist-conformation, as found in the crystal structure for **20e**, with an approximate C_2 symmetry, the equivalency of the cyclopentadienyl protons cannot be explained, and must therefore be the result of a dynamic behavior in solution.

The only example of a sila[1.1]ruthenocenophane [ER_x = $SiMe_2$ (**20f**)] was published by Bärtl and Herberhold in 1995 and was obtained in very low yield (1.4%) from the reaction of bis(cyclopentadienide)dimethylsilane and $RuCl_2 \cdot 4DMSO$.[102]

* Copyright©2002 The Cambridge Crystallographic Data Centre. All rights reserved.

Complex **20f** was characterized by MS and NMR spectroscopy and showed one resonance for all α and β protons, respectively, in the ^{1}H NMR spectrum.

Germanium-bridged [1.1]MCPs have not been reported in literature.

The first stanna[1.1]ferrocenophanes were mentioned as the only identifiable products from unsuccessful attempts to synthesize a tin-bridged [1]FeCP.[43] The [1.1]FeCPs **21a** [ER_x = Sn(*n*Bu)$_2$] and **21b** [ER_x = $SnEt_2$] were identified by their MS, UV-vis and NMR spectra and CHN analyses. A year later, the crystal structure of **21a** was reported.[129] Complex **21a** adopted an undistorted *anti* conformation in the solid state with an approximate C_{2h} symmetry. The ferrocene moieties were coplanar and almost perfectly eclipsed; the dihedral angle between staggered carbon atoms in the cyclopentadienyl rings was measured as 2.5°.

Stanna[1.1]ferrocenophane **21c** [ER_x = SnI(*n*Bu)] was obtained by reaction of **21a** with I_2.[143] A crystal structure analysis showed that **21c** adopts the *anti* conformation, with the *n*Bu substituents in the *endo* and the iodine substituents in the *exo* position. A tilt angle of α = 3.38° was measured, no yield was reported. The NMR spectrum at room temperature again only showed one multiplet for α and β protons, respectively, which was explained by the authors with an *anti-anti* interconversion. [143]

Two more stanna[1.1]ferrocenophanes, [ER_x = Sn(*t*Bu)$_2$ (**21d**), $SnMes_2$ (**21e**)] (Mes = 2,4,6-trimethylphenyl), were isolated and reported by Manners *et al.* as a side product from the solution polymerization of their respective [1]FeCPs **7a-b** (Scheme 1-21, page 45). Both complexes adopted an undistorted *anti* conformation in the solid state, together with small tilt angles. For **21d** a tilt angle of α = 5.0(2)°; for **21e** a tilt angle of α = 3.3(2)° was reported.

The only plumba[1.1]ferrocenophane [ER_x = $PbPh_2$ (**22a**)] was reported in 1990 by Schwarzhans *et al.* (in German).[144] A rather unusual synthetic strategy was employed, with the goal to synthesize a mixture of various ferrocenylplumbanes in one pot, literally, with subsequent separation. To a mixture of Ph_2PbCl_2 (4.174 g, 9.66 mmol) and Ph_3PbCl (0.453 g, 0.95 mmol) in 1.4 L of benzene a mixture (4.6 g) of dilithioferrocene and monolithioferrocene, with the latter being a 6% impurity in dilithioferrocene, was added by spatula over a period of 80 h to avoid polymerization reactions. After filtration and concentration of the reaction mixture, **22a** precipitated first, and 600 mg (0.55 mmol, 11% yield) of **22a** could be isolated. Complex **22a** was characterized by multinuclear NMR spectroscopy, CHN analysis and MS. Although a crystal structure analysis of **22a** was not performed, an *anti* conformation in the solid state **22a** was reasonably postulated. This assumption was supported by the fact that all other structurally characterized heavier group 14 element-bridged [1.1]MCPs (E = Si, Sn) with bulky ligands also adopted the *anti* conformation. It was further pointed out that the obtained ^{1}H NMR spectrum with only two mulitplets in the cyclopentadienyl region could not be explained by a rigid *anti* conformation, but only by a fluxional *anti-anti* interconversion. In order to test this assumption, a VT-NMR experiment was performed. Although the expected splitting of the signals caused by a freezing the *anti* isomer could not be observed even at - 89 °C, the half-width of the multiplet assigned to the α protons increased from 3.92 Hz at room temperature to 20.27 Hz at -89 °C. This broadening was explained with a slowing down of the conformational flexibility of the molecule at low temperatures.

1.3.3 Group 15-Bridged [1.1]Metallocenophanes

The first reported phospha[1.1]FeCP [ER_x = P(-)Men (**23a**)] was obtained from the low-temperature reaction (- 40 °C) of dilithioferrocene and the chiral phosphine (-)$MenPCl_2$ (Figure 1-11, page 17).[53] From a crystal structure analysis it was shown that **23a** adopt a slightly distorted *anti* conformation. Small tilt angles for both ferrocene moieties of α = 2.12° and α = 6.11° respectively with an average twist angle of 13.4° were measured. The C-P-C angle was widened to 107.51(19)° to release repulsion by the inner α protons.

In 2000, Miyoshi *et al.* reported on their discovery of phROP of phospha[1]ferrocenophanes like **8a** (see Chapter 1.2.4).[51] Additionally, it was mentioned that after sulfurization, masses were detected by GPC consistent with cyclic dimers and trimers. In 2005, full experimental details were reported on this new phospha[1.1]ferrocenophanes.[142] Monomer **8a** was photolytically ring-opened to yield a mixture of cyclic dimers, trimers and polyferrocene **13a**. The reaction mixture was sulfurized with elemental sulfur to avoid oxidation by air and was separated by column chromatography, yielding phospha[1.1]ferrocenophane **23b** [ER_x = P(S)Ph] in 9% yield. Interestingly, when the authors crystallized the product, they were able to isolate and characterize both an *anti* and a *syn* isomer. *Anti* **23b** showed a relative undistorted *anti* conformation, with a tilt angle of α = 2.91(7)°, a twist angle of 2.91(7)°, and the phenyl groups in *exo* positions. *Syn* **23b** was more distorted with a twist angle of 42.5(1)°, a tilt angle α = 8.2(1)°, with the phenyl groups in the *exo* positions. The high degree of distortion was rationalized by the repulsion of not only the inner α protons, but also of

the two sulfur atoms in the *endo* positions. The authors also showed that *syn* **23b** could be cleanly desulfurized with Si_2Cl_6 in refluxing benzene to give the [1.1]FeCP **23c** [ER_x = PPh]. A crystal structure analysis proved that **23c** had retained the distorted *syn* conformation, with a twist angle of 24.81(7)° and a tilt angle of α = 3.68(7)°. When *anti* **23b** was desulfurized under the same conditions, a ^{31}P NMR spectrum of the product revealed that *anti* **23b** had isomerized to *syn* **23c**. Desulfurization under stereo-chemical retention was achieved in benzene at room temperature using $CF_3SO_3Me/P(NMe_2)_3$ (Scheme 1-33).

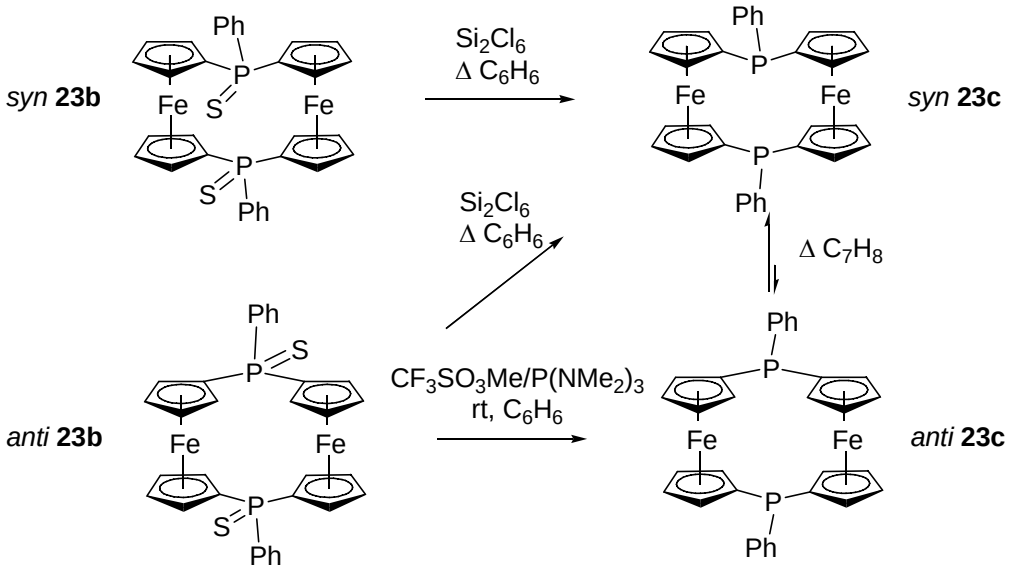

Scheme 1-33. Desulfurization and interconversion of *syn* and *anti* isomers of phospha[1.1]ferrocenophanes.

However, *anti* **23c** proved to be highly insoluble in common solvents, but after resulfurization, identical NMR spectra than *anti* **23b** were obtained. A crystal structure for *anti* **23c** was not reported. The isomerization of *anti* **23b** to *syn* **23c** was explained by the higher thermodynamic stability of the *syn* conformation of **23c** over the *anti* conformation of **23c**. When a solution of pure *anti* **23c** was refluxed in toluene, a

complete isomerization to *syn* **23c** was observed, whereas a solution of pure *syn* **23c** after refluxing in toluene showed only trace amounts of *anti* **23c**. In this respect, it is interesting to compare the ^{1}H NMR spectra of sulfurized *anti* and *syn* **23b**. *Anti* **23b** shows four multiplets for all cyclopentadienyl protons reflecting the C_{2h} symmetry also displayed in the solid state. *Syn* **23b** showed three multiplets in the expected cyclopentadienyl range, two integrating for 4 protons and one integrating for 8 protons. If the overlap of the one multiplet integrating for 8 protons is magnetic coincidence or the result of a dynamic process was neither mentioned nor investigated by the authors. A *syn*-*syn* interconversion of **23b** should be unlikely because the initially *exo*/*exo* phenyl substituents would interconvert to *endo*/*endo*, a very unfavorable situation. *Syn* **23c** also showed four well resolved multiplets in the cyclopentadienyl region, which would indicate a rigid conformation in solution. *Anti* **23c** was too insoluble to obtain NMR spectra. In order to increase the yield of **23c**, the dimerization of **8a**, similar to the previously reported dimerization of **20a** from **5d**, using phosphine containing Pd and Pt complexes was attempted.[73] However, addition of $[Pd(PPh_3)_4]$ to a solution of **8a** did not yield the desired product **23c**, which was explained by the strong coordination of **8a** to the metal moiety. Improvement of the yield of **23c** was achieved by UV irradiation of a solution of **8a** in Et_2O, which is a less donating solvent than THF, in higher dilution, both which favored the formation of shorter oligomers over polymers. The yield of **23c** thereby could be increased to 23%. The strong donating property of **23c** towards transition metals was further investigated. Complex *syn* **23c** was probed as a new phosphine containing chelating ligand. Co(II) was chosen because it was known to tolerate a wide range of bite angles from diphosphine chelates. Reaction of $CoCl_2$ with

syn **23c** in THF afforded the new complex [**23c**→$CoCl_2$] in quantitative yield (Scheme 1-34).

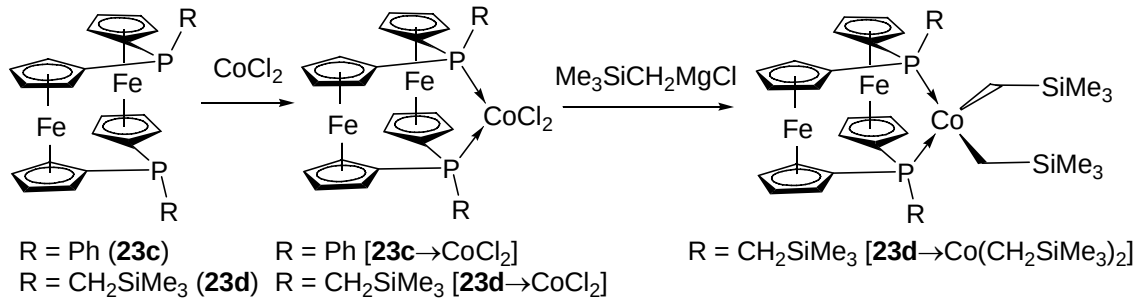

Scheme 1-34. Coordination of the [1.1]FeCps **23c** and **23d** to $CoCl_2$ with subsequent alkylation of the Co atom.

A crystal structure analysis of [**23c**→$CoCl_2$] showed the cobalt atom to be tetrahedrally coordinated by *syn* **23c** with a P-Co-P bite angle of 95.62(2)°. The group of Miyoshi was interested in the potential of [**23c**→$CoCl_2$] in Heck reactions. In 2006, Miyoshi *et al.* reported the alkylation of [**23c**→$CoCl_2$], a suspected intermediate in cobalt catalyzed Heck reactions.[145] Using the Grignard reagent Me_3SiCH_2MgCl, the monoalkylated complex [**23c**→$CoCl(CH_2SiMe_3)$] was isolated and fully characterized and the dialkylated complex [**23c**→$Co(CH_2SiMe_3)_2$] was also identified in solution, but was not crystallized. After modifying the ligands on the phosphorous atoms, the new trimethylsilylmethylene substituted phospha[1.1]ferrocenophane **23d** [ER_x = PCH_2SiMe_3] was obtained (Scheme 1-34). Subsequent reaction with $CoCl_2$ afforded the new complex [**23d**→$CoCl_2$] which could be alkylated by the same protocol to yield the fully alkylated complex [**23d**→$Co(CH_2SiMe_3)_2$] which could be crystallized. Full synthetic details for **23d** were not mentioned.

1.3.4 Electrochemistry of [1.1]Metallocenophanes

[1.1]MCPs represent a class of compounds with two redox active sites that are linked to each other. In [1.1]MCPs the linking units are the two elements in the bridge between the metallocene moieties, which are symmetrically equivalent. In general, for compounds that contain ions of the same element in different formal oxidation states a classification system has been devised by Robin and Day to describe the electrochemistry of such compounds.[146] Although metallocenophanes were not mentioned (the chapter was published in 1967), the Robin and Day classification can be used with some modifications. For [1.1]FeCPs the electrochemistry of the iron centers can be described as shown in Scheme 1-35.

$$[Fe^{II}\text{-}Fe^{II}] \underset{Red}{\overset{Ox}{\rightleftharpoons}} [Fe^{II}\text{-}Fe^{III}]^{+} \underset{Red}{\overset{Ox}{\rightleftharpoons}} [Fe^{III}\text{-}Fe^{III}]^{2+}$$

Scheme 1-35. Illustration of fully reversible stepwise oxidation of [1.1]ferrocenophanes.

Initially there is no preference for which one of the two available Fe^{II} atoms is oxidized. After the first oxidation, a mixed-valent complex is formed. The Robin and Day classification applies to this mixed-valent compound and distinguishes between three classes. Class I complexes show no delocalization at all, because the redox active centers are either removed from each other by two or more relatively non-interacting ligands or have very different coordination symmetry. With respect to [1.1]FeCPs this means their electrochemistry is similar to the parent ferrocene, with both ferrocenyl moieties being oxidized at the same potential. Since both iron atoms in [1.1]FeCPs are

symmetrically equivalent, the delocalization has to depend only on the electronic nature of the bridging element.

Class II defines cases in which delocalization takes place, but the two types of sites are still distinguishable, because the optical electron does not spend equal amounts of time on them. In [1.1]FeCPs infrared spectra can give definite information about the oxidation state of the iron atom. A diagnostic band assigned to the C-H bend of the cyclopentadienyl ligand in ferrocene can be seen at 815 cm^{-1}, whereas in ferrocinium triiodide this band is shifted to 851 cm^{-1}.[147] In Class II [1.1]FeCPs, both bands can be observed in the mixed-valent complex. If full delocalization of the optical electron would occur, an average band at ca. 830 cm^{-1} would be observed. All [1.1]FeCPs discussed in Chapter 1.3.4 belong to Class II, showing moderate delocalization. Class III compounds consequently show full delocalization in the mixed-valent state, with the mixed-valent sites being indistinguishable from each other. The analytical tool of choice is cyclic voltammetry (CV), where the potential is swept through the anodic and cathodic region and the peak currents are recorded. Class II compounds like [1.1]FeCPs show two fully reversible, one-electron oxidations, with the midway potential for each reversible redox event being the halfway potential $E_{1/2}$ (Figure 1-22).

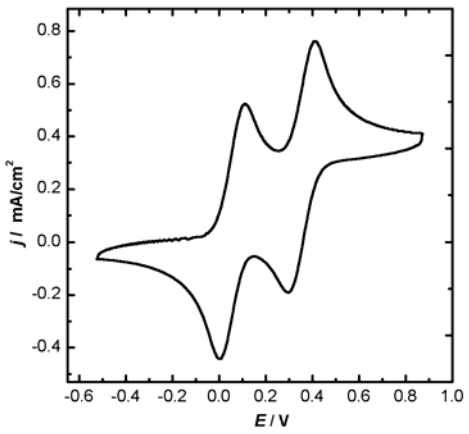

Figure 1-22. Typical cyclic voltammogram of a Class II [1.1]FeCP (see Chapter 8).

The separation between the two redox events, the $\Delta E_{1/2}$, gives a measurement of the amount of delocalization of the optical electron between the iron atoms. It was also shown that for the series of group 14-bridged [1.1]FeCPs $\Delta E_{1/2}$ increases with increasing Fe-Fe distance.[45] This observation strongly suggests a bridge-mediated mechanism for the delocalization in the mixed-valent state over a through-space mechanism.

The electrochemistry of ruthenocene is quite different from that of ferrocene. Whereas ferrocene is reversibly oxidized and reduced, oxidation of ruthenocene involves an irreversible two-electron oxidation. The electrochemistry of [1.1]FeRuCP **19g** and [1.1]RuCP **19h** has been described by Mueller-Westerhoff *et al.*[120] Complex **19g** showed a ferrocene centered reversible one-electron oxidation and a ruthenocene centered irreversible two-electron oxidation, thereby showing independence of the two metallocene units in **19g**, typical for a Class I compound. For complex **19h**, a quasi-reversible one step two-electron oxidation was observed, which initially created a RuIV-RuII dicationic complex. The oxidized RuIV atom subsequently reacts with the RuII atom to form a single bond between the two Ru atoms.[124] Overall, two quasi-reversible

oxidations well below the oxidation potential of ruthenocene were observed that yielded a diamagnetic, oxidized complex.

1.4 Research Objectives

The primary goal of this PhD project was to explore the synthesis of heavier group 13-bridged [1]FeCPs (E = Al, Ga, In) and their application as potential monomers for ROP. Before this project was started in February 2004, [1]MCPs bridged by heavier group 13 elements were unknown in the literature. Based on the research background of the Müller group, the concept of intramolecular coordinating ligands to satisfy the Lewis acidic group 13 elements was applied in order to obtain monomeric, well-defined starting group 13 element dihalides. The synthesis and electrochemical investigations of [1.1]FeCPs developed as a secondary project over the course of the investigations. One example of a borata[1.1]ferrocenophane[104] and two examples of galla[1.1]ferrocenophanes[107,108] were published in literature at the time. Since the electrochemistry of [1.1]ruthenocenophane is distinctly different (see Chapter 1.3.4), no attempts were made to synthesize such complexes.

This PhD project was purely academic in nature. The primary goal was to investigate if [1]MCPs with heavier group 13 elements in bridging positions can be synthesized. [1]MCPs have shown to be interesting starting compounds for the synthesis of high-molecular weight polyferrocenes. Polyferrocenes are a new type of organometallic polymers that already showed some new and unusual properties that might some day lead to conducting or magnetic polymers. The incorporation of different bridging elements does influence these properties. Therefore, we hoped that by synthesizing heavier group 13-bridged [1]MCPs and polymerize them, we could contribute to the growing field and development of organometallic polymers.

1.5 References

(1) Green, J. C. *Chem. Soc. Rev.* **1998**, *27*, 263-272.
(2) Neuse, E. W.; Rosenberg, H. *J. Macromol. Sci., Rev. Macromol. Chem.* **1970**, *4*, 1-145.
(3) Butler, I. R.; Cullen, W. R.; Ni, J.; Rettig, S. J. *Organometallics* **1985**, *4*, 2196-2201.
(4) Arnold, R.; Matchett, S. A.; Rosenblum, M. *Organometallics* **1988**, *7*, 2261-2266.
(5) Broussier, R.; Da Rold, A.; Gautheron, B.; Dromzee, Y.; Jeannin, Y. *Inorg. Chem.* **1990**, *29*, 1817-1822.
(6) Vogel, U.; Lough, A. J.; Manners, I. *Angew. Chem., Int. Ed. Engl.* **2004**, *43*, 3321-3325.
(7) Braunschweig, H.; Dirk, R.; Müller, M.; Nguyen, P.; Resendes, R.; Gates, D. P.; Manners, I. *Angew. Chem., Int. Ed. Engl.* **1997**, *36*, 2338-2340.
(8) Wiberg, N. *Inorganic Chemistry*; 1st Ed in English ed.; Academic Press: San Diego, 2001.
(9) Berenbaum, A.; Braunschweig, H.; Dirk, R.; Englert, U.; Green, J. C.; Jäkle, F.; Lough, A. J.; Manners, I. *J. Am. Chem. Soc.* **2000**, *122*, 5765-5774.
(10) Osborne, A. G.; Whiteley, R. H. *J. Organomet. Chem.* **1975**, *101*, C27-C28.
(11) Osborne, A. G.; Whiteley, R. H.; Meads, R. E. *J. Organomet. Chem.* **1980**, *193*, 345-357.
(12) MacLachlan, M. J.; Lough, A. J.; Geiger, W. E.; Manners, I. *Organometallics* **1998**, *17*, 1873-1883.
(13) Stoeckli-Evans, H.; Osborne, A. G.; Whiteley, R. H. *J. Organomet. Chem.* **1980**, *194*, 91-101.
(14) Fischer, A. B.; Kinney, J. B.; Staley, R. H.; Wrighton, M. S. *J. Am. Chem. Soc.* **1979**, *101*, 6501-6506.
(15) Finckh, W.; Tang, B. Z.; Foucher, D. A.; Zamble, D. B.; Ziembinski, R.; Lough, A.; Manners, I. *Organometallics* **1993**, *12*, 823-829.
(16) Wrighton, M. S.; Palazzotto, M. C.; Bocarsly, A. B.; Bolts, J. M.; Fischer, A. B.; Nadjo, L. *J. Am. Chem. Soc.* **1978**, *100*, 7264-7271.
(17) Zechel, D. L.; Hultzsch, K. C.; Rulkens, R.; Balaishis, D.; Ni, Y.; Pudelski, J. K.; Lough, A. J.; Manners, I.; Foucher, D. A. *Organometallics* **1996**, *15*, 1972-1978.
(18) Nguyen, P.; Stojcevic, G.; Kulbaba, K.; MacLachlan, M. J.; Liu, X. H.; Lough, A. J.; Manners, I. *Macromolecules* **1998**, *31*, 5977-5983.
(19) MacLachlan, M. J.; Zheng, J.; Thieme, K.; Lough, A. J.; Manners, I.; Mordas, C.; LeSuer, R.; Geiger, W. E.; Liable-Sands, L. M.; Rheingold, A. L. *Polyhedron* **2000**, *19*, 275-289.
(20) Pudelski, J. K.; Rulkens, R.; Foucher, D. A.; Lough, A. J.; MacDonald, P. M.; Manners, I. *Macromolecules* **1995**, *28*, 7301-7308.
(21) Chan, W. Y.; Lough, A. J.; Manners, I. *Acta Crystallogr., Sect. E* **2005**, *61*, m375-m376.
(22) Hatanaka, Y.; Okada, S.; Minami, T.; Goto, M.; Shimada, K. *Organometallics* **2005**, *24*, 1053-1055.

(23) Bourke, S. C.; Jäkle, F.; Vejzovic, E.; Lam, K.-C.; Rheingold, A. L.; Lough, A. J.; Manners, I. *Chem., Eur. J.* **2003**, *9*, 3042-3054.
(24) Foucher, D. A.; Lough, A. J.; Manners, I.; Rasburn, J.; Vancso, J. G. *Acta Crystallogr., Sect. C* **1995**, *51*, 580-582.
(25) Foucher, D.; Ziembinski, R.; Petersen, R.; Pudelski, J.; Edwards, M.; Ni, Y.; Massey, J.; Jaeger, C. R.; Vancso, G. J.; Manners, I. *Macromolecules* **1994**, *27*, 3992-3999.
(26) Jaekle, F.; Vejzovic, E.; Power-Billard, K. N.; MacLachlan, M. J.; Lough, A. J.; Manners, I. *Organometallics* **2000**, *19*, 2826-2828.
(27) Masson, G.; Beyer, P.; Cyr, P. W.; Lough, A. J.; Manners, I. *Macromolecules* **2006**, *39*, 3720-3730.
(28) Pudelski, J. K.; Foucher, D. A.; Honeyman, C. H.; Lough, A. J.; Manners, I.; Barlow, S.; O'Hare, D. *Organometallics* **1995**, *14*, 2470-2479.
(29) Schultz, M.; Sofield, C. D.; Walter, M. D.; Andersen, R. A. *New J. Chem.* **2005**, *29*, 919-927.
(30) Power-Billard, K. N.; Manners, I. *Macromolecules* **2000**, *33*, 26-31.
(31) Berenbaum, A.; Lough, A. J.; Manners, I. *Organometallics* **2002**, *21*, 4415-4424.
(32) Calleja, G.; Carre, F.; Cerveau, G.; Corriu, R. J. P. *C. R. l'Academie. Sci., Ser. II Univers* **1998**, *1*, 285-291.
(33) Nguyen, P.; Lough, A. J.; Manners, I. *Macromol. Rapid Commun.* **1997**, *18*, 953-959.
(34) Chan, W. Y.; Berenbaum, A.; Clendenning, S. B.; Lough, A. J.; Manners, I. *Organometallics* **2003**, *22*, 3796-3808.
(35) Butler, I. R.; Cullen, W. R.; Rettig, S. J. *Can. J. Chem.* **1987**, *65*, 1452-1456.
(36) Peckham, T. J.; Foucher, D. A.; Lough, A. J.; Manners, I. *Can. J. Chem.* **1995**, *73*, 2069-2078.
(37) Blake, A. J.; Mayers, F. R.; Osborne, A. G.; Rosseinsky, D. R. *J. Chem. Soc., Dalton Trans.* **1982**, 2379-2383.
(38) Foucher, D. A.; Manners, I. *Makromol. Chem., Rapid Commun.* **1993**, *14*, 63-66.
(39) Foucher, D. A.; Edwards, M.; Burrow, R. A.; Lough, A. J.; Manners, I. *Organometallics* **1994**, *13*, 4959-4966.
(40) Kapoor, R. N.; Crawford, G. M.; Mahmoud, J.; Dementiev, V. V.; Nguyen, M. T.; Diaz, A. F.; Pannell, K. H. *Organometallics* **1995**, *14*, 4944-4947.
(41) Castruita, M.; Cervantes-Lee, F.; Mahmoud, J. S.; Zhang, Y.; Pannell, K. H. *J. Organomet. Chem.* **2001**, *637-639*, 664-668.
(42) Zurcher, S.; Gramlich, V.; Togni, A. *Inorg. Chim. Acta* **1999**, *291*, 355-364.
(43) Seyferth, D.; Withers, H. P. *Organometallics* **1982**, *1*, 1275-1282.
(44) Rulkens, R.; Lough, A. J.; Manners, I. *Angew. Chem., Int. Ed. Engl.* **1996**, *35*, 1805-1807.
(45) Jäkle, F.; Rulkens, R.; Zech, G.; Foucher, D. A.; Lough, A. J.; Manners, I. *Chem., Eur. J.* **1998**, *4*, 2117-2128.
(46) Sharma, H. K.; Cervantes-Lee, F.; Mahmoud, J. S.; Pannell, K. H. *Organometallics* **1999**, *18*, 399-403.
(47) Baumgartner, T.; Jakle, F.; Rulkens, R.; Zech, G.; Lough, A. J.; Manners, I. *J. Am. Chem. Soc.* **2002**, *124*, 10062-10070.

(48) Butler, I. R.; Cullen, W. R.; Einstein, F. W. B.; Rettig, S. J.; Willis, A. J. *Organometallics* **1983**, *2*, 128-135.
(49) Honeyman, C. H.; Foucher, D. A.; Dahmen, F. Y.; Rulkens, R.; Lough, A. J.; Manners, I. *Organometallics* **1995**, *14*, 5503-5512.
(50) Mizuta, T.; Yamasaki, T.; Nakazawa, H.; Miyoshi, K. *Organometallics* **1996**, *15*, 1093-1100.
(51) Mizuta, T.; Onishi, M.; Miyoshi, K. *Organometallics* **2000**, *19*, 5005-5009.
(52) Mizuta, T.; Imamura, Y.; Miyoshi, K. *J. Am. Chem. Soc.* **2003**, *125*, 2068-2069.
(53) Brunner, H.; Klankermayer, J.; Zabel, M. *J. Organomet. Chem.* **2000**, *601*, 211-219.
(54) Pudelski, J. K.; Gates, D. P.; Rulkens, R.; Lough, A. J.; Manners, I. *Angew. Chem., Int. Ed. Engl.* **1995**, *34*, 1506-1508.
(55) Rulkens, R.; Gates, D. P.; Balaishis, D.; Pudelski, J. K.; McIntosh, D. F.; Lough, A. J.; Manners, I. *J. Am. Chem. Soc.* **1997**, *119*, 10976-10986.
(56) Odian, G. *Principles of Polymerization*; 4 ed.; Wiley-Interscience: Hoboken, N.J., 2004.
(57) Katz, T. J.; Slusarek, W. *J. Am. Chem. Soc.* **1979**, *101*, 4259-4267.
(58) Katz, T. J.; Acton, N.; Martin, G. *J. Am. Chem. Soc.* **1973**, *95*, 2934-2939.
(59) Katz, T. J.; Acton, N.; Martin, G. *J. Am. Chem. Soc.* **1969**, *91*, 2804-2805.
(60) Manners, I. In *Advances in Organometallic Chemistry, Vol 37* 1995; Vol. 37, p 131-168.
(61) Rehahn, M. *Acta Polym.* **1998**, *49*, 201-224.
(62) Arimoto, F. S.; Haven, A. C. *J. Am. Chem. Soc.* **1955**, *77*, 6295-6297.
(63) Foucher, D. A.; Tang, B. Z.; Manners, I. *J. Am. Chem. Soc.* **1992**, *114*, 6246-6248.
(64) Pudelski, J. K.; Manners, I. *J. Am. Chem. Soc.* **1995**, *117*, 7265-7266.
(65) Togni, A., unpublished results.
(66) Withers, H. P.; Seyferth, D.; Fellmann, J. D.; Garrou, P. E.; Martin, S. *Organometallics* **1982**, *1*, 1283-1288.
(67) Rulkens, R.; Lough, A. J.; Manners, I. *J. Am. Chem. Soc.* **1994**, *116*, 797-798.
(68) Rulkens, R.; Ni, Y.; Manners, I. *J. Am. Chem. Soc.* **1994**, *116*, 12121-12122.
(69) Reddy, N. P.; Yamashita, H.; Tanaka, M. *J. Chem. Soc., Chem. Commun.* **1995**, 2263-2264.
(70) Ni, Y.; Rulkens, R.; Pudelski, J. K.; Manners, I. *Macromol. Rapid Commun.* **1995**, *16*, 637-641.
(71) Cundy, C. S.; Eaborn, C.; Lappert, M. F. *J. Organomet. Chem.* **1972**, *44*, 291-297.
(72) Sheridan, J. B.; Lough, A. J.; Manners, I. *Organometallics* **1996**, *15*, 2195-2197.
(73) Reddy, N. P.; Choi, N.; Shimada, S.; Tanaka, M. *Chem. Lett.* **1996**, 649-650.
(74) Yamashita, H.; Tanaka, M.; Honda, K. *J. Am. Chem. Soc.* **1995**, *117*, 8873-8874.
(75) Sheridan, J. B.; Temple, K.; Lough, A. J.; Manners, I. *J. Chem. Soc., Dalton Trans.* **1997**, *5*, 711-714.
(76) Temple, K.; Jakle, F.; Sheridan, J. B.; Manners, I. *J. Am. Chem. Soc.* **2001**, *123*, 1355-1364.
(77) Temple, K.; Dziadek, S.; Manners, I. *Organometallics* **2002**, *21*, 4377-4384.

(78) Gómez-Elipe, P.; Resendes, R.; Macdonald, P. M.; Manners, I. *J. Am. Chem. Soc.* **1998**, *120*, 8348-8356.
(79) Pudelski, J. K.; Foucher, D. A.; Honeyman, C. H.; Macdonald, P. M.; Manners, I.; Barlow, S.; O'Hare, D. *Macromolecules* **1996**, *29*, 1894-1903.
(80) Peckham, T. J.; Lough, A. J.; Manners, I. *Organometallics* **1999**, *18*, 1030-1040.
(81) Imamura, Y.; Kubo, K.; Mizuta, T.; Miyoshi, K. *Organometallics* **2006**, *25*, 2301-2307.
(82) Tanabe, M.; Manners, I. *J. Am. Chem. Soc.* **2004**, *126*, 11434-11435.
(83) Tanabe, M.; Vandermeulen, G. W. M.; Wing, Y. C.; Cyr, P. W.; Vanderark, L.; David, A. R.; Manners, I. *Nat. Mater.* **2006**, *5*, 467-470.
(84) Rasburn, J.; Petersen, R.; Jahr, R.; Rulkens, R.; Manners, I.; Vancso, G. J. *Chem. Mater.* **1995**, *7*, 871-877.
(85) Rasburn, J.; Foucher, D. A.; Reynolds, W. F.; Manners, I.; Vancso, G. J. *J. Chem. Soc., Chem. Commun.* **1998**, 843-844.
(86) Jaekle, F.; Rulkens, R.; Zech, G.; Massey, J. A.; Manners, I. *J. Am. Chem. Soc.* **2000**, *122*, 4231-4232.
(87) Watts, W. E. *J. Am. Chem. Soc.* **1966**, *88*, 855-856.
(88) Karlsson, A.; Löwendahl, M.; Hilmersson, G.; Davidsson, O.; Ahlberg, P. *J. Phys. Org. Chem.* **1996**, *9*, 436-438.
(89) Löwendahl, J. M.; Hakansson, M. *Organometallics* **1995**, *14*, 4736-4741.
(90) Löwendahl, M.; Davidsson, O.; Ahlberg, P. *J. Chem. Res., Synop.* **1993**, 40-41.
(91) Mueller-Westerhoff, U. T. *Angew. Chem., Int. Ed. Engl.* **1986**, *25*, 702-717.
(92) Bitterwolf, T. E.; Ling, A. C. *J. Organomet. Chem.* **1973**, *57*, C15-C18.
(93) Gavini, B. G.; Haas, T. J.; Plourde, K. L.; Mueller-Westerhoff, U. T. *Synth. React. Inorg. Met.-Org. Chem.* **1992**, *22*, 481 - 486.
(94) Waleh, A.; Loew, G. H.; Mueller-Westerhoff, U. T. *Inorg. Chem.* **1984**, *23*, 2859-2863.
(95) Mueller-Westerhoff, U. T.; Nazzal, A. *J. Am. Chem. Soc.* **1984**, *106*, 5381-5382.
(96) Mueller-Westerhoff, U. T.; Nazzal, A.; Proessdorf, W. *J. Am. Chem. Soc.* **1981**, *103*, 7678-7681.
(97) Ahlberg, P.; Davidsson, O.; Hilmersson, G.; Löwendahl, M.; Hakansson, M. *Journal of the Chemical Society-Chemical Communications* **1994**, 1573-1574.
(98) Ahlberg, P.; Davidsson, O. *J. Chem. Soc., Chem. Commun.* **1987**, 623-624.
(99) Mueller-Westerhoff, U. T.; Nazzal, A.; Tanner, M. *J. Organomet. Chem.* **1982**, *236*, C41-C44.
(100) Rheingold, A. L.; Mueller-Westerhoff, U. T.; Swiegers, G. F.; Haas, T. J. *Organometallics* **1992**, *11*, 3411-3417.
(101) Watanabe, M.; Sato, M.; Nagasawa, A.; Motoyama, I.; Takayama, T. *Bull. Chem. Soc. Jpn.* **1998**, *71*, 2127-2136.
(102) Bärtl, T.; Herberhold, M. *Z. Naturforsch., B: Chem. Sci.* **1995**, *50*, 1692-1698.
(103) Sato, M.; Asai, M. *J. Organomet. Chem.* **1992**, *430*, 105-110.
(104) Scheibitz, M.; Winter, R. F.; Bolte, M.; Lerner, H.-W.; Wagner, M. *Angew. Chem., Int. Ed. Engl.* **2003**, *42*, 924-927.
(105) Braunschweig, H.; Burschka, C.; Clentsmith, G. K. B.; Kupfer, T.; Radacki, K. *Inorg. Chem.* **2005**, *44*, 4906-4908.

(106) Jutzi, P.; Lenze, N.; Neumann, B.; Stammler, H.-G. *Angew. Chem., Int. Ed. Engl.* **2001**, *40*, 1423-1427.
(107) Uhl, W.; Hahn, I.; Jantschak, A.; Spies, T. *J. Organomet. Chem.* **2001**, *637-639*, 300-303.
(108) Althoff, A.; Jutzi, P.; Lenze, N.; Neumann, B.; Stammler, A.; Stammler, H. G. *Organometallics* **2003**, *22*, 2766-2774.
(109) McKechnie, J. S.; Bersted, B.; Paul, I. C.; Watts, W. E. *J. Organomet. Chem.* **1967**, *8*, P29-P31.
(110) McKechnie, J. S.; Maier, C. A.; Bersted, B.; Paul, I. C. *J. Chem. Soc., Perkin Trans. 2* **1973**, 138-143.
(111) Pauling, L. *Nature of the Chemical Bond*; 3 ed.; Cornell University Press: Ithaca, 1960.
(112) Watts, W. E. *J. Organomet. Chem.* **1967**, *10*, 191-192.
(113) Barr, T. H.; Lentzner, H. L.; Watts, W. E. *Tetrahedron* **1969**, *25*, 6001-6013.
(114) Kasahara, A.; Izumi, T.; Ohnishi, S. *Bull. Chem. Soc. Jpn.* **1972**, *45*, 951-952.
(115) O'Connor Salazar, D. C.; Cowan, D. O. *J. Organomet. Chem.* **1991**, *408*, 219-225.
(116) Cassens, A.; Eilbracht, P.; Nazzal, A.; Proessdorf, W.; Mueller-Westerhoff, U. T. *J. Am. Chem. Soc.* **1981**, *103*, 6367-6372.
(117) Cassens, A.; Eilbracht, P.; Mueller-Westerhoff, U. T.; Nazzal, A.; Neuenschwander, M.; Prossdorf, W. *J. Organomet. Chem.* **1981**, *205*, C17-C20.
(118) Mueller-Westerhoff, U. T.; Nazzal, A.; Prossdorf, W. *J. Organomet. Chem.* **1981**, *205*, C21-C23.
(119) Kansal, V. K.; Watts, W. E.; Mueller-Westerhoff, U. T.; Nazzal, A. *J. Organomet. Chem.* **1983**, *243*, 443-449.
(120) Diaz, A. F.; Mueller-Westerhoff, U. T.; Nazzal, A.; Tanner, M. *J. Organomet. Chem.* **1982**, *236*, C45-C48.
(121) Moore, M. F.; Wilson, S. R.; Hendrickson, D. N.; Mueller-Westerhoff, U. T. *Inorg. Chem.* **1984**, *23*, 2918-2920.
(122) Waleh, A.; Cher, M. L.; Loew, G. H.; Mueller-Westerhoff, U. T. *Theoretical Chemistry Accounts: Theory, Computation, and Modeling (Theoretica Chimica Acta)* **1984**, *65*, 167-177.
(123) Moore, M. F.; Wilson, S. R.; Cohn, M. J.; Dong, T. Y.; Mueller-Westerhoff, U. T.; Hendrickson, D. N. *Inorg. Chem.* **1985**, *24*, 4559-4565.
(124) Mueller-Westerhoff, U. T.; Rheingold, A. L.; Swiegers, G. F. *Angew. Chem., Int. Ed. Engl.* **1992**, *31*, 1352-1354.
(125) Mueller-Westerhoff, U. T.; Haas, T. J.; Swiegers, G. F.; Leipert, T. K. *J. Organomet. Chem.* **1994**, *472*, 229-246.
(126) Waleh, A.; Cher, M. L.; Loew, G. H.; Muellerwesterhoff, U. T. *Theor. Chim. Acta* **1984**, *65*, 167-177.
(127) Hakansson, M.; Löwendahl, M.; Davidsson, O.; Ahlberg, P. *Organometallics* **1993**, *12*, 2841-2844.
(128) Löwendahl, M.; Davidsson, O.; Ahlberg, P.; Hakansson, M. *Organometallics* **1993**, *12*, 2417-2419.
(129) Clearfield, A.; Simmons, C. J.; Withers, H. P.; Seyferth, D. *Inorg. Chim. Acta* **1983**, *75*, 139-144.

(130) Karlsson, A.; Hilmersson, G.; Davidsson, O.; Löwendahl, M.; Ahlberg, P. *Acta Chem. Scand.* **1999**, *53*, 693-698.
(131) Ahlberg, P.; Davidsson, O.; Löwendahl, M.; Hilmersson, G.; Karlsson, A.; Hakansson, M. *J. Am. Chem. Soc.* **1997**, *119*, 1745-1750.
(132) Ahlberg, P.; Karlsson, A.; Davidsson, O.; Hilmersson, G.; Lowendahl, M. *J. Am. Chem. Soc.* **1997**, *119*, 1751-1757.
(133) Davidsson, O.; Lowendahl, M.; Ahlberg, P. *J. Chem. Soc., Chem. Commun.* **1992**, 1004-1005.
(134) Karlsson, A.; Hilmersson, G.; Ahlberg, P. *J. Phys. Org. Chem.* **1997**, *10*, 590-592.
(135) Watanabe, M.; Sano, H. *Bull. Chem. Soc. Jpn.* **1990**, *63*, 777-784.
(136) Rudziński, J. M.; Osawa, E. *J. Phys. Org. Chem.* **1993**, *6*, 107-112.
(137) Singletary, N. J.; Hillman, M.; Dauplaise, H.; Kvick, A.; Kerber, R. C. *Organometallics* **1984**, *3*, 1427-1434.
(138) Park, J.; Seo, Y.; Cho, S.; Whang, D.; Kim, K.; Chang, T. *J. Organomet. Chem.* **1995**, *489*, 23-25.
(139) Zechel, D. L.; Foucher, D. A.; Pudelski, J. K.; Yap, G. P. A.; Rheingold, A. L.; Manners, I. *J. Chem. Soc., Dalton Trans.* **1995**, 1893-1899.
(140) Calleja, G.; Carre, F.; Cerveau, G.; Labbé, P.; Coche-Guérente, L. *Organometallics* **2001**, *20*, 4211-4215.
(141) Bao, M.; Hatanaka, Y.; Shimada, S. *Chem. Lett.* **2004**, *33*, 520-521.
(142) Mizuta, T.; Imamura, Y.; Miyoshi, K.; Yorimitsu, H.; Oshima, K. *Organometallics* **2005**, *24*, 990-996.
(143) Dong, T.-Y.; Hwang, M.-Y.; Wen, Y.-s.; Hwang, W.-S. *J. Organomet. Chem.* **1990**, *391*, 377-385.
(144) Utri, G.; Schwarzhans, K.-E.; Allmaier, G. M. *Z. Naturforsch., B: Chem. Sci.* **1990**, *45*, 755-762.
(145) Imamura, Y.; Mizuta, T.; Miyoshi, K.; Yorimitsu, H.; Oshima, K. *Chem. Lett.* **2006**, *35*, 260-261.
(146) Robin, M. B.; Day, P. In *Adv. Inorg. Chem. Radiochem.*; Academic Press: New York and London, 1967; Vol. 10, p 247-422.
(147) Rulkens, R.; Lough, A. J.; Manners, I.; Lovelace, S. R.; Grant, C.; Geiger, W. E. *J. Am. Chem. Soc.* **1996**, *118*, 12683-12695.

CHAPTER 2
EXPERIMENTAL SECTION

2.1 Synthesis

All manipulations were carried out using standard Schlenk techniques, if not noted differently. For synthesis solvents were dried using a MBraun Solvent Purification System (SPS) and stored under nitrogen over 4 Å molecular sieves. Benzene and cyclohexane were refluxed over sodium metal using benzophenone as an indicator.

$AlCl_3$ and $GaCl_3$ were sublimed prior to use. Liquid reactants were degassed prior to use (freeze-pump-thaw cycles), reactive solid reactants were transferred to a Schlenk flask under inert atmosphere or moved into the glovebox directly. Deuterated solvents like C_6D_6, $CDCl_3$ and C_7D_8 were degassed prior to use and stored under nitrogen over 4 Å molecular sieves. ^1H, ^{13}C and ^{27}Al NMR spectra were recorded on a Bruker 500 MHz Avance spectrometer; ^1H and ^{13}C chemical shifts were referenced to the deuterated solvent (C_6D_6: ^1H δ 7.15, ^{13}C δ 128.0; $CDCl_3$: ^1H δ 7.26, ^{13}C δ 77.0; C_7D_8: $–CD_3$ ^1H δ 2.10, ^{13}C δ 20.4); ^{27}Al was referenced to $[Al(acac)_3]$ in C_6D_6 (^{27}Al δ 0.0) . Mass spectra were measured on a VG 70SE in EI^+ mode and were reported in the form M (%I) [F], where M is the mass observed, %I is the intensity of the peak relative to the most intense peak in the spectrum and F is the molecular ion or fragment; Elemental analysis was performed on a Perkin Elmer 2400 CHN Elemental Analyzer; samples were prepared in a glove-box and V_2O_5 was added to promote combustion.

2.2 Ring-Opening Polymerization

For polymerization and dynamic light scattering (DLS) experiments solvents were vacuum transferred from solutions containing the deep red 1,1-diphenylhexyllithium (DPH-Li) as an indicator. The collected solvents were moved into the glovebox. All manipulations were carried out in the glovebox; glassware and NMR tubes for flame-sealing experiments were stored in an oven at 200 °C for at least one hour and moved directly into the glovebox. THF solutions for DLS (~5 mg/ml) were prepared in the glovebox, filtered a minimum of two times through Millex-FG13 PTFE syringe filter with 0.2 μm pore size directly into a 12 μl quartz cuvette capped with a plastic lid and sealed with para-film. DLS measurements were performed on a DynamPro-MS800 at 25 °C.

2.3 Electrochemistry

All experiments were conducted with 660B CH Instruments Inc. A gold working electrode (BAS, 2 mm) or glassy carbon (BAS, 3 mm) were employed. Quasi-reference electrode was a silver wire immersed in 0.1 M tetrabutylammonium hexafluorophosphate (TBAPF) in EtOH solution separated by a Vycor® tip or a silver wire. Platinum wire was used as the auxiliary electrode. In each case, IR compensation was applied. Samples were prepared in dry dichloromethane (1 mM, SPS) with 0.1 M TBAPF as supporting electrolyte. Scan rate for all cyclic voltammograms (CV) and differential pulse voltammograms (DPV) reported was 100 mV/s. Experiments were conducted under strict inert conditions to exclude decomposition by oxygen and moisture (glovebox, vacuum pump and nitrogen purging). All measurements were

carried out in a nitrogen purged electrochemical cell. Measurements were taken at room temperature.

Electrochemical quartz crystal microbalance (EQCM) experiments were conducted with CHI 440 CH Instruments Inc., and quartz crystal (8 MHz) covered with 100 Å Ti and 1000 Å Au was used as a working electrode (commercially available from CH Instruments). The gold electrode area was 0.205 cm^2.

The principal work was carried out at the research labs of the Müller group at the University of Saskatchewan from February 2004 to August 2007. Electrochemical experiments were performed in collaboration with the Kraatz group at the University Of Saskatchewan. Initial work on ROP of [1]FeCPs was carried out in collaboration with the Rehahn group at the TU Darmstadt, Germany, during a research stay in July 2006.

CHAPTER 3
PUBLICATION 1

The following chapter is a verbatim copy of a communication published in December 2004 in *Organometallics*[*] and describes the first synthesis of an aluminum-bridged [1]ferrocenophane. The co-authors on this paper are Clinton L. Lund, who synthesized the ligand Pytsi, J. Wilson Quail, who did the single-crystal X-ray analysis, and my supervisor Jens Müller. Written permission was obtained from all contributing authors to include this material within this thesis.

[*] Reproduced with permission from Organometallics. © 2005 American Chemical Society

3. Synthesis and Characterization of the First Aluminum-Bridged [1]Ferrocenophane

Jörg A. Schachner,[‡] Clinton L. Lund,[‡] J. Wilson Quail,[§] Jens Müller[‡,*]

[‡] *Department of Chemistry and* [§] *Saskatchewan Structural Sciences Centre,University of Saskatchewan, 110 Science Place, Saskatoon, SK S7N 5C9 Canada*

Received December 15, 2004

3.1 Summary

The first example of a [1]ferrocenophane with a heavier group 13 element in the bridging position is described. The [1]aluminaferrocenophane, with the aluminum atom equipped with a bulky and intramolecularly stabilizing ligand, has been synthesized and structurally characterized by NMR spectroscopy and single-crystal X-ray analysis.

3.2 Introduction

In 1975 Osborn and Whiteley described the first [1]ferrocenophane, a strained organometallic compounds that contains silicon in the bridging position (ER_x = $SiPh_2$; Figure 3-1).[1] Three decades later, Manners *et al*. discovered that ring-opening polymerization (ROP) of [1]silaferrocenophanes provides access to poly(ferrocenylsilanes) with high molecular weights.[2] Today, [1]ferrocenophanes with main-group elements in the bridging position are known from group 16 (S, Se),[3,4] 15 (P, As),[5-8] 14 (Si, Ge, Sn),[1,2,5,6,9-11] and 13 (B)[12,13] elements, with the [1]boraferrocenophanes being the most recent examples in this series (ER_x = $BN(SiMe_3)_2$, $BN(SiMe_3)$*t*Bu, BN*i*Pr_2). However, [1]ferrocenophanes with bridging

heavier group 13 elements are unknown today. Surprisingly, even simpler compounds such as ferrocenylalanes[14,15] or gallanes are very rare, with some interesting ferrocenylgallanes being characterized recently.[16-18] Within this report we describe the synthesis and structural characterization of the first [1]aluminaferrocenophane.

3.3 Results and Discussion

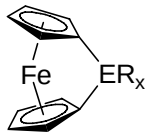

Figure 3-1. ER_x-bridged [1]ferrocenophane

On the basis of our experience with organic ligands that are capable of intramolecular donation,[19-21] we decided to attach a trisyl ligand[22] in which one of the methyl groups is replaced by a 2-pyridyl group to aluminum (trisyl = tris(trimethylsilyl)methyl, $C(SiMe_3)_3$; commonly denoted as Tsi). The ligand $C(SiMe_3)_2(SiMe_2C_5H_4N\text{-}2)$ was described for the first time in 2000,[23] and since then investigations have been published dealing with new compounds equipped with this ligand.[23-27] Very recently, the first compounds with group 13 elements containing this unique ligand were reported, including the two alanes $(Pytsi)AlCl_2$ and $(Pytsi)AlMe_2$ (Pytsi = $C(SiMe_3)_2(SiMe_2C_5H_4N\text{-}2)$).[28] Independent from this publication, we had started to exploit the chemistry of 'pytrisyl' alanes recently.

A slurry of dilithioferrocene · ⅔ (TMEDA)[29] in toluene was slowly added to a solution of $(Pytsi)AlCl_2$ to a give the aluminum-bridged ferrocenophane **1**. Compound **1** was isolated from hexane solution as red crystals in a moderate yield of 31% (eq 3-1).[30]

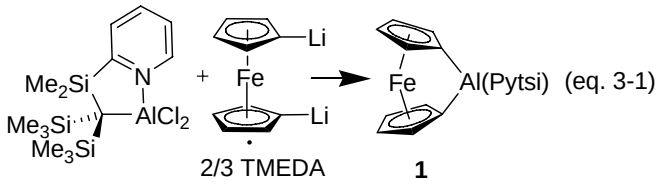

(eq. 3-1)

Suitable single crystals for X-ray structural analysis of compound **1** were grown from hexane solutions at ambient temperatures.[31]

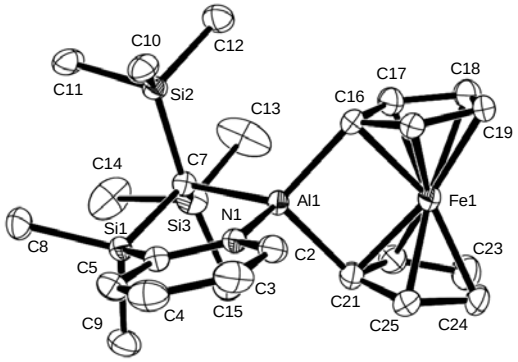

Figure 3-2. Molecular structure of **1** with thermal ellipsoids drawn at a 30% probability level. H atoms and ½ $FeCp_2$ are omitted for clarity (see supporting information for details).

Figure 3-2 shows the molecular structure of compound **1** in the crystal lattice. The aluminum-bridged ferrocenophane **1** crystallizes in the space group $P2_1/c$ with half of a molecule of $FeCp_2$ in the asymmetric unit. However, we could not find any unusually short intermolecular distances in the lattice that would indicate additional chemical interactions. Aluminum is distorted tetrahedrally surrounded by C7, N1, C16, and C21. The 'tetrahedral' angles cover a wide range with the smallest angle of 95° dictated by the ferrocene moiety (C16–Al1–C21) and the largest with 125° for C21–Al1–C7 (see Figure 3-2). As expected, the five-membered ring exhibits an envelope conformation with C7 being 0.613(5) Å away from the least-squares plane Si1–C6–N1–

Al1. The four bonds around the aluminum atom are very similar in length and the values of 1.981(4) Å for Al1–N1 and 2.026(5) Å for Al1–C7 are slightly larger than those of 1.94 and 1.98 Å determined for the respective bonds in (Pytsi)$AlCl_2$.[28] Commonly, key structural features of a [1]ferrocenophane are described by a set of different angles as illustrated in Figure 3-3.

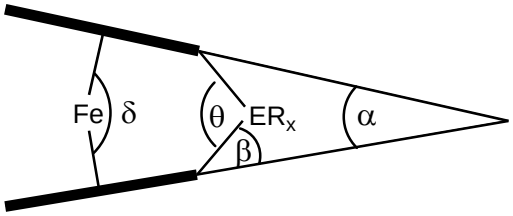

Figure 3-3. Common set of angles to describe [1]ferrocenophanes [data for **1**: α = 14.9(3)°, β = 43.1°, δ =167.9°, θ = 94.7(2)°]

The ferrocenophane **1** is a strained compound with the tilt angle α = 14.9(3)° (Figure 3-3). On the basis of pure geometric considerations, one would expect that a [1]aluminaferrocenophane would exhibit ring tilt values that are between those of germanium- and tin-bridged species.[32] One of the first structurally characterized ferrocenophanes was a germanium compound with $GePh_2$ as the bridging unit.[5,6] A few years later, a ferrocenophane bridged by $GeMe_2$ was characterized, followed by a report of the first [1]stannaferrocenophane. The tilt angles α were determined to be 16.6(15)° ($GePh_2$),[5,6] 19.0(9)° ($GeMe_2$),[9] 14.1(2)° (Sn*t*Bu_2),[10] and 15.2(2)° ($SnMes_2$)[11] illustrating that the [1]aluminaferrocenophane **1** with α = 14.9(3)° falls in the expected range.

The ^{1}H-NMR spectrum of the isolated product **1** clearly reveals a 1:1 ratio between a 1,1'-ferrocenyl moiety and a $C(SiMe_3)_2(SiMe_2C_5H_4N$-2) ligand, plus the presence of a 2-fold symmetry element. For example, the Cp range of the spectrum

consists of four *pseudo*-triplets between δ of 3.91 and 4.68. In addition, the sharp singlet at δ = 3.99 indicates the presence of half of an equivalent of $FeCp_2$. Differences between the *pseudo*-triplets are commonly taken as an indication for a [1]ferrocenophane, and one might interpret the large splitting of Δδ = 0.77 in **1** as being due to a highly strained ferrocenophane. However, the lower symmetry of **1** compared to that of ferrocenophanes with ER_2 bridging units (E = group 14 element) might contribute to the large splitting. In ^{13}C NMR spectra of [1]ferrocenophanes, the most informative chemical shifts are those of the *ipso*-C atoms of the Cp rings. It is known that their ^{13}C NMR values are shifted upfield with respect to the parent ferrocene (δ 68) with typical values of δ 33.1 ($SiMe_2$), 30.0 ($GeMe_2$), 34.9 (Sn*t*Bu_2), and 38.2 ($SnMes_2$).[11] Boron-bridged [1]ferrocenophanes are the highest strained ferrocenophanes known today, but surprisingly their *ipso*-C atoms resonate at relatively low field (δ 44–45; B(NRR')).[12,13] This effect was attributed to the electropositive nature of the boron atom. The ^{13}C NMR spectrum of **1** can be rationalized by assuming a C_s-symmetrical compound. NMR peaks of ^{13}C atoms which are directly bound to Al are often broad and sometimes difficult to detect, which is caused by the electric quadrupole moment of aluminum. A broad peak for **1** at δ 53 measured at ambient temperature sharpens at -40 ºC, clearly indicating the vicinity of aluminum. The signal unequivocally is due to the *ipso*-C atoms of the Cp rings. The value of δ 53 is shifted downfield in comparison with those *ipso*-C resonances of the known [1]ferrocenophanes mentioned before, but it is still significantly upfield shifted with respect to the parent ferrocene (δ 68). The detected ^{27}Al NMR resonance of δ 141 is in the expected range for tetracoordinated aluminum species.[33,34]

3.4 Conclusions

It seems that the 'pytrisyl' ligand shields the Al center through the bulky $C(SiMe_3)_2$ unit and stabilizes it by the pyridine donor and presumably through α-silyl effects. We started to change the stabilizing ligand systematically to illuminate the factors that are important to obtain [1]ferrocenophanes with bridging heavier group 13 elements. Further investigations are underway to find out if one can take advantage of the strain in compound **1** to get access to new polymers via ROP. We will report on the results shortly.

Acknowledgement. We thank the Natural Sciences and Engineering Research Council of Canada (NSERC Discovery Grant), the Department of Chemistry, and the University of Saskatchewan for their generous support.

Supporting Information Available: Text detailing the instruments and techniques used for the experimental preparation and structural determination of **1** · ½ $FeCp_2$ and crystallographic data as a CIF file. This material is available free of charge via the Internet at http://pubs.acs.org. Crystallographic data for **1** · ½ $FeCp_2$ have also been deposited with the Cambridge Crystallographic Data Centre (CCDC-253088) and can be obtained free of charge via www.ccdc.ac.uk/conts/retrieving.html (or from the Cambridge Crystallographic Data Centre, 12 Union Road, Cambridge CB2 1EZ, U.K.; fax: (+44)1223-336-033; or deposit@ccdc.cam.ac.uk).

3.5 References

(1) Osborne, A. G.; Whiteley, R. H. *J. Organomet. Chem*. **1975**, *101*, C27-C28.
(2) Foucher, D. A.; Tang, B. Z.; Manners, I. *J. Am. Chem. Soc*. **1992**, *114*, 6246-6248.
(3) Pudelski, J. K.; Gates, D. P.; Rulkens, R.; Lough, A. J.; Manners, I. *Angew. Chem. Int. Ed. Engl*. **1995**, *34*, 1506-1508.
(4) Rulkens, R.; Gates, D. P.; Balaishis, D.; Pudelski, J. K.; McIntosh, D. F.; Lough, A. J.; Manners, I. *J. Am. Chem. Soc*. **1997**, *119*, 10976-10986.
(5) Stoecklievans, H.; Osborne, A. G.; Whiteley, R. H. *J. Organomet. Chem*. **1980**, *194*, 91-101.
(6) Osborne, A. G.; Whiteley, R. H.; Meads, R. E. *J. Organomet. Chem*. **1980**, *193*, 345-357.
(7) Seyferth, D.; Withers, H. P. *Organometallics* **1982**, *1*, 1275-1282.
(8) Butler, I. R.; Cullen, W. R.; Einstein, F. W. B.; Rettig, S. J.; Willis, A. J. *Organometallics* **1983**, *2*, 128-135.
(9) Foucher, D. A.; Edwards, M.; Burrow, R. A.; Lough, A. J.; Manners, I. *Organometallics* **1994**, *13*, 4959-4966.
(10) Rulkens, R.; Lough, A. J.; Manners, I. *Angew. Chem. Int. Ed. Engl*. **1996**, *35*, 1805-1807.
(11) Jäkle, F.; Rulkens, R.; Zech, G.; Foucher, D. A.; Lough, A. J.; Manners, I. *Chem., Eur. J*. **1998**, *4*, 2117-2128.
(12) Braunschweig, H.; Dirk, R.; Müller, M.; Nguyen, P.; Resendes, R.; Gates, D. P.; Manners, I. *Angew. Chem. Int. Ed. Engl*. **1997**, *36*, 2338-2340.
(13) Berenbaum, A.; Braunschweig, H.; Dirk, R.; Englert, U.; Green, J. C.; Jäkle, F.; Lough, A. J.; Manners, I. *J. Am. Chem. Soc*. **2000**, *122*, 5765-5774.
(14) Atwood, J. L.; Shoemaker, A. L. *J. Chem. Soc., Chem. Commun.* **1976**, 536-537.
(15) Rogers, R. D.; Cook, W. J.; Atwood, J. L. *Inorg. Chem*. **1979**, *18*, 279-282.
(16) Althoff, A.; Jutzi, P.; Lenze, N.; Neumann, B.; Stammler, A.; Stammler, H.-G. *Organometallics* **2002**, *21*, 3018-3022.
(17) Jutzi, P.; Lenze, N.; Neumann, B.; Stammler, H. G. *Angew. Chem. Int. Ed. Engl*. **2001**, *40*, 1424-1427.
(18) Althoff, A.; Jutzi, P.; Lenze, N.; Neumann, B.; Stammler, A.; Stammler, H. G. *Organometallics* **2003**, *22*, 2766-2774.
(19) Müller, J.; Englert, U. *Chem. Ber*. **1995**, *128*, 493-497.
(20) Müller, J.; Fischer, R. A.; Sussek, H.; Pilgram, P.; Wang, R.; Pritzkow, H.; Herdtweck, E. *Organometallics* **1998**, *17*, 161-166.
(21) Müller, J.; Schröder, R.; Wang, R. M. *Eur. J. Inorg. Chem*. **2000**, 153-157.
(22) Eaborn, C.; Smith, J. D. *J. Chem. Soc., Dalton Trans*. **2001**, 1541-1552.
(23) Al-Juaid, S. S.; Eaborn, C.; Hitchcock, P. B.; Hill, M. S.; Smith, J. D. *Organometallics* **2000**, *19*, 3224-3231.
(24) Eaborn, C.; Hill, M. S.; Hitchcock, P. B.; Smith, J. D. *J. Chem. Soc., Chem. Commun.* **2000**, 691-692.

(25) Al-Juaid, S. S.; Avent, A. G.; Eaborn, C.; El-Hamruni, S. M.; Hawkes, S. A.; Hill, M. S.; Hopman, M.; Hitchcock, P. B.; Smith, J. D. *J. Organomet. Chem*. **2001**, *631*, 76-86.
(26) Al-Juaid, S. S.; Avent, A. G.; Eaborn, C.; Hill, M. S.; Hitchcock, P. B.; Patel, D. J.; Smith, J. D. *Organometallics* **2001**, *20*, 1223-1229.
(27) Eaborn, C.; Hill, M. S.; Hitchcock, P. B.; Smith, J. D. *J. Chem. Soc., Dalton Trans.* **2002**, 2467-2472.
(28) Howson, J.; Eaborn, C.; Hitchcock, P. B.; Hill, M. S.; Smith, D. J. *J. Organomet. Chem*. **2005**, in press.
(29) Butler, I. R.; Cullen, W. R.; Ni, J.; Rettig, S. J. *Organometallics* **1985**, *4*, 2196-2201.
(30) Synthesis of **1**: $Cl_2AlC(SiMe_3)_2(SiMe_2C_5H_4N\text{-}2)$ (1.49 g, 3.80 mmol) was dissolved in toluene (30 mL) and chilled to -10 °C. A suspension of $[Fe(\eta^5\text{-}C_5H_4Li)_2]\cdot$ ⅔ TMEDA (1.05 g, 3.81 mmol) in toluene (30 mL) was added dropwise via tubing. After stirring for 16 h, the color of the solution changed to purple. After filtration, the solvent was removed at high vacuum (25 °C/0.01 mbar) to yield a dark purple, viscous oil. The residue was extracted with hexane (2×10 mL). After removal of some hexane, product **1** was obtained as **1** • ½ $FeCp_2$ as red crystals at room temperature (0.701 g, 31 % with respect to $(Pytsi)AlCl_2$). NMR spectra in C_6D_6 at 25 °C, unless noted differently: ^{1}H NMR (500 MHz; C_6D_6 at 25 °C): δ = 0.41 (s, 18H, $SiMe_3$), 0.45 (s, 6H, CH_3), 3.91, 4.31, 4.64, 4.68 (pst, 8H, C_5H_4), 3.99 (s, 5H, $FeCp_2$), 6.44, 6.84 (t, 2H, C_6H_4N), 6.98, 8.73 (d, 2H, C_6H_4N); ^{13}C NMR (125.8 MHz): δ = 0.71 (Si-$C(SiMe_3)_2$-Al, -40 °C, C_7D_8), 3.67 (Si-CH_3), 6.52 ($SiMe_3$), 52.92 (ipso-C of C_5H_4-Al, -40 °C, C_7D_8), 68.30 ($FeCp_2$), 75.64, 75.69, 76.94, 77.27 (C_5H_4-Al), 124.18, 129.50, 138.93, 147.48 (2-C_6H_4N), 174.54 (ipso-C of 2-C_6H_4N); ^{27}Al NMR (130.3 MHz, C_7D_8, 60 °C): δ = 141 (h½ = 2000 Hz); MS (70 eV): m/z (%): 295 (35) [$C_{14}H_{29}Si_3N^+$], 280 (100) $C_{13}H_{26}Si_3N^+$], 264 (6) [$C_{12}H_{22}Si_3N^+$], 186 (12) [Cp_2Fe^+], 73 (9) [$SiMe_3^+$]; elemental analysis (%): calcd for $C_{29}H_{41}AlFe_{1.5}NSi_3$ (598.66): C 58.18, H 6.90, N 2.34; found C 58.81, H 7.52, N 2.39.
(31) Crystal data for **1** • ½ $FeCp_2$: $C_{29}H_{41}AlFe_{1.5}NSi_3$; monoclinic; space group $P2_1/c$; unit cell dimensions: a = 19.3070(5) Å, b = 11.8720(4) Å, c = 13.5850(3) Å, α = 90°, β = 94.113(2)°, γ = 90°; V = 3105.83(15) Å^3; Z = 4; density (calculated) = 1.280 mg/m^3; T = 173(2) K; λ = 0.71073 Å; reflections collected = 18974; independent reflections = 5488 [R_{int} = 0.1079]; completeness to θ of 25.03° = 99.9 %; absorption correction = none; refinement method = full-matrix least-squares on F^2; data / restraints / parameters = 5488 / 61 / 372; GOF = 1.072; final R1 = 0.0678, wR2 = 0.1347 [I>2σ(I)] and R1 = 0.1166, wR2 = 0.1530 (all data).
(32) Covalent radii: Al (1.25 Å for CN = 3), Ge (1.22 Å for CN = 4), Sn (1.40 Å for CN = 4), taken from Holleman-Wiberg *Inorganic Chemistry*; 1. English ed.; Academic Press: San Diego, London, **2001**.
(33) Benn, R.; Rufinska, A. *Angew. Chem*. **1986**, 98, 851-871.
(34) Benn, R.; Janssen, E.; Lehmkuhl, H.; Rufinska, A. *J. Organomet. Chem*. **1987**, 333, 155-168.

CHAPTER 4
PUBLICATION 2

The following chapter is a verbatim copy of an article published in *Organometallics*[*] in May 2005 and describes the first synthesis of a gallium-bridged [1]ferrocenophane. Attempts to synthesize the first indium-bridged [1]ferrocenophane are also described. The co-authors on this paper are Clinton L. Lund, who synthesized the ligand Pytsi, J. Wilson Quail, who did all structure determinations by single-crystal X-ray analysis, and my supervisor Jens Müller. Written permission was obtained from all contributing authors to include this material within this thesis.

[*] Reproduced with permission from Organometallics. © 2005 American Chemical Society

4. Synthesis and Characterization of Heavier Group 13 Element Ferrocenophanes: The First Gallium-Bridged [1]Ferrocenophane and an Unusual Indium Species

Jörg A. Schachner[‡], Clinton L. Lund[‡], J. Wilson Quail[§] and Jens Müller[‡,*]

Department of Chemistry and Saskatchewan Structural Sciences Centre, University of Saskatchewan, 110 Science Place, Saskatoon, Saskatchewan S7N 5C9, Canada

Received May 17, 2005

4.1 Abstract

On the basis of our previous results with aluminum, we herein report the synthesis of the first gallium-bridged [1]ferrocenophane. The attempt to synthesize the respective indium compound resulted in an unusual ferrocenophane containing an In-(μ-$Cl)_2$-In group in the bridging position. All compounds have been characterized by NMR spectroscopy and single-crystal X-ray structural determination.

4.2 Introduction

Since their discovery in 1975 by Osborne and Whiteley,[1] strained [1]ferrocenophanes containing metals in the bridging position (Figure 4-1) have sparked much interest throughout the scientific community. Manners *et al.* showed that strained [1]ferrocenophanes can serve as monomers for polymetallocenes via ring-opening polymerization (ROP).[2] Until recently, strained [1]ferrocenophanes containing a bridging group 13 element were only known for boron (ER_x = $BN(SiMe_3)_2$, $BN(SiMe_3)$*t*Bu, $BNiPr_2$).[3] Very recently, we successfully synthesized the first

[1]ferrocenophane containing the heavier group 13 element aluminum. The [1]aluminaferrocenophane ([1]Al-FCP), equipped with the stabilizing "pytrisyl" ligand [ER_x = Al(Pytsi) with Pytsi = $C(SiMe_3)_2SiMe_2(2\text{-}C_5H_4N)$], was characterized by a single-crystal X-ray analysis.[4] The pytrisyl ligand, derived from the parent trisyl ligand $C(SiMe_3)_3$ by a formal substitution of one methyl group with a pyridyl ring, provides intramolecular coordination via the N atom of the pyridine ring and steric shielding through the trimethylsilyl groups. The pytrisyl ligand was introduced in 2000[5] and has mainly been used for transition metal chemistry.[6]

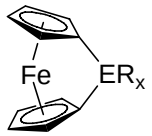

Figure 4-1. ER_x-bridged [1]ferrocenophane.

Unstrained [1.1]ferrocenophanes, formal dimers of [1]ferrocenophanes, where two ferrocene moieties are bridged by two metals, are investigated for their redox properties as model compounds for electronic interactions of iron centers.[7] So far, [1.1]ferrocenophanes containing group 13 elements have been known for boron[7] and gallium.[8] Very recently, we characterized the first aluminum-containing [1.1]ferrocenophane by single-crystal X-ray analysis.[9] Within this publication we report on our results to synthesize gallium- and indium-bridged [1]ferrocenophanes.

4.2 Results and Discussion

The successful synthesis of the first [1]Al-FCP was achieved by reaction of dilithioferrocene with $(Pytsi)AlCl_2$.[4] To apply the same method to gallium and indium,

the respective starting compounds (Pytsi)ECl_2 [E = Ga (**1**), In (**3**)] were needed. The aluminum compound (Pytsi)$AlCl_2$ was described in 2005,[10] and the same publication described the attempted synthesis of the dihalides (Pytsi)$GaBr_2$ and (Pytsi)$InCl_2$ (**3**). However, only partly hydrolyzed compounds of the type (Pytsi)$EX_x(OH)_y$ could be isolated, and the authors speculated that this was due to partly hydrolyzed starting materials.[10] We encountered no problems in isolating analytically pure **1** and **3** in good yields by using readily available $GaCl_3$ and $InCl_3$ (see Experimental Section for details).

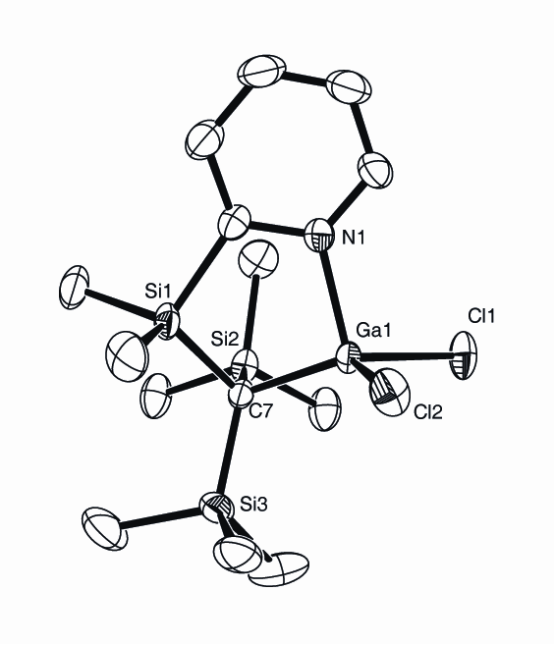

Figure 4-2. Molecular structure of **1** with thermal ellipsoids at the 50% probability level. H atoms are omitted for clarity. Selected bond length (Å) and angles (º): Ga1-N1 = 2.004(2), Ga1-C7 = 1.988(2), Ga1-Cl1 = 2.1816(7), Ga1-Cl2 = 2.2016(7), N1-Ga1-C7 = 98.03(9), N1-Ga1-Cl1 = 104.91(7), N1-Ga1-Cl2 = 98.95(7), Cl1-Ga1-Cl2 = 103.73(3), Cl2-Ga1-C7 = 121.49(8), C7-Ga1-Cl1 = 124.77(8).

As expected, the starting gallane **1** is a monomeric species in the solid state (Figure 4-2, Table 4-1). The Ga-N bond length of 2.004(2) Å is slightly shorter than that of 2.047(5) Å found in the (Pytsi)GaBr(OH),[10] , with a similar difference found for the Ga-C bond lengths [1.988(2) Å for **1** and 2.008(5) Å for (Pytsi)GaBr(OH)]. As

expected, the M-N bond of the respective dichloro alane (Pytsi)$AlCl_2$, at 1.9383(16) Å, significantly shorter,[10] exemplifying the well-known fact that a $GaCl_2$ moiety is the weaker Lewis acceptor for a hard Lewis donor compared to an $AlCl_2$ group.

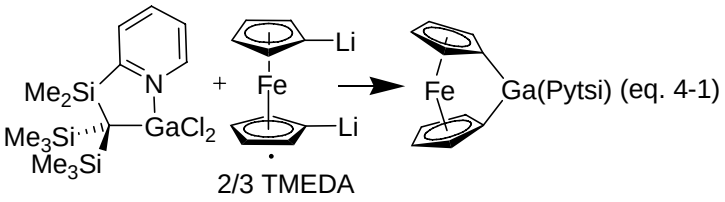

1 **2**

A slurry of dilithioferrocene · 2/3 TMEDA in toluene was slowly added to a cooled solution of **1** in toluene to give the gallium-bridged [1]ferrocenophane **2** (eq 4-1). Compound **2** was isolated as deep red crystal from hexane in a yield of 59%. Compound **2** is a gallium-bridged [1]ferrocenophane, which is clearly revealed by its NMR data. It shows similar signal pattern and shifts in the ^{1}H- and ^{13}C NMR spectra similar to those of the [1]Al-FCP;[4] both ferrocenophanes are time-averaged C_s symmetrical species in solution.

Table 4-1. Crystal and Structural Refinement Data for compounds **1**, **3**, and **4**.

	1	**3**	**4** · 2.5 toluene
empirical formula	$C_{14}H_{28}Cl_2GaNSi_3$	$C_{28}H_{56}Cl_4In_2N_2Si_6$	$C_{55.50}H_{84}Cl_2FeIn_2N_2Si_6$
formula weight	435.26	960.7318	1304.18
wavelength, Å	0.71073	0.71073	0.71073
crystal system	triclinic	monoclinic	triclinic
space group (No.)	P-1 (2)	P 2_1/c (14)	P-1 (2)
Z	2	2	2
a, Å	9.0460(2)	9.2181(2)	14.1309(9)
b, Å	10.0441(2)	24.3893(5)	14.7231(11)
c, Å	11.8243(3)	12.5633(3)	16.135(2)
α, deg	84.7182(10)	90	72.624(4)
β, deg	89.2236(10)	131.6290(10)	77.960(6)
γ, deg	87.5315(10)	90	87.868(4)
vol, $Å^3$	1068.74(4)	2111.22(9)	3132.1(5)
d (calc), mg/m^3	1.353	1.511	1.383
temp, K	173(2)	173(2)	173(2)
abs coefficient, mm^{-1}	1.700	1.537	1.194
theta range, deg	2.04 to 27.65	2.32 – 27.47	2.90 – 25.03
refl collected	9350	8767	40880
indep refl	4911	4810	11048
abs correction	none	semi-empirical from equivalents	
ref method	full-matrix least-squares on F^2		
data / restr / params	4911 / 0 / 198	4810 / 0 / 198	11048 / 242 / 638
goodness-of-fit on F^2	1.030	1.061	1.102
final R indices [I>2sigma(I)]	R1 = 0.0373, wR2 = 0.0793	R1 = 0.0334, wR2 = 0.0653	R1 = 0.0595, wR2 = 0.1030
R indices (all data)	R1 = 0.0587, wR2 = 0.0888	R1 = 0.0481, wR2 = 0.0709	R1 = 0.0882, wR2 = 0.1114
largest diff. peak and hole, $e.Å^{-3}$	0.382 and -0.467	0.493 and -0.688	0.988 and -0.793

So far, several attempts to solve the structure of **2** by single-crystal X-ray analysis ended in partially solved structures (Figure 4-3; see Experimental Section for details). The best solution shows four molecules in the asymmetric unit ($P2_1$) with an *R*

value of 14.3%. The crystals of **2** diffracted very poorly, and the data does not give a complete crystal structure of **2** with accurate bond lengths and bond angles, but shows with certainty the presence of the targeted [1]Ga-FCP (Figure 4-3). A set of tilt angles is commonly used to describe strained [1]ferrocenophanes (Figure 4-4).[11] The asymmetric unit of compound **2** exhibits four molecules with tilt angles α of 13.6(2.1), 15.0(1.6), 15.4(1.9), and 18.8(1.8)º, resulting in an average of 15.7º. This is a very reasonable value if compared with α = 14.9(3)º found for the [1]Al-FCP.[4]

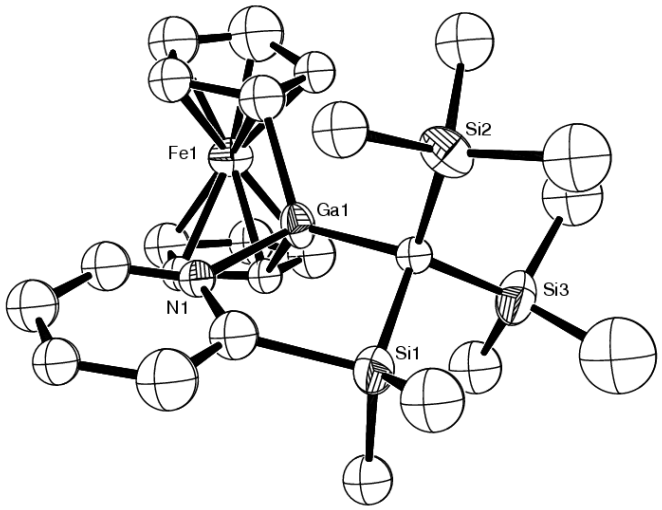

Figure 4-3. Molecular framework structure of **2**. One of four independent molecules is shown (see experimental part for details).

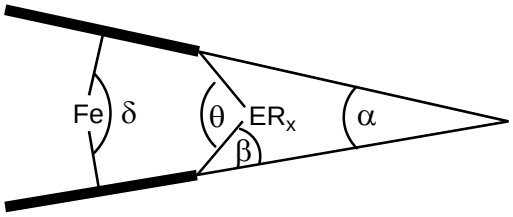

Figure 4-4. Common set of tilt angles to describe [1]ferrocenophanes.

It is common practice to deduce the amount of ring strain present in [1]ferrocenophanes from two NMR parameters: the difference in the splitting of the Cp protons (denoted as Δδ) and the upfield shift of the two *ipso*-C atoms of each Cp ring in the ^{13}C NMR spectra. The ^{1}H NMR spectra of **2** shows four pseudotriplets at δ = 4.08, 4.45, 4.61, and 4.65, corresponding to a Δδ = 0.57, and the resonance of the *ipso*-C is found at δ = 47.24. The respective values for the [1]Al-FCP are 0.77 (Δδ) and 52.92 (*ipso*-C). For comparison, the highly strained sulfur-bridged [1]ferrocenophane (ER_x = S), with the large tilt angle of α = 31.05(10)°, shows a splitting of the two pseudotriplets of Δδ = 0.65 and the *ipso*-C resonates at δ = 14.6.[12] From first glance, the comparable large Δδ of the less strained compound **2** and [1]Al-FCP, respectively, might indicate highly strained molecules. However, most of the [1]ferrocenophanes are C_{2v} symmetrical species resulting in two pseudotriplets. Consequently, the Δδ value expresses the splitting between the two Cp protons adjacent to the bridge and the two Cp protons away from the bridge. To obtain a more realistic splitting value Δδ, we assigned all four pseudotriplets to Cp protons in compound **2** using NOE experiments (Figure 4-5). The difference between average chemical shifts of Cp protons adjacent to gallium (H_a and $H_{a'}$) and away from gallium (H_b and $H_{b'}$) amounts to Δδ = 0.37; a similar procedure gives a Δδ of 0.49 ppm for the [1]Al-FCP.[4] Still, compared with other [1]ferrocenophanes such as [1]Si-FCP (ER_x = $SiMe_2$; α = 20.8(5)º; Δδ = 0.40),[13] [1]Ge-FCP (ER_x = $GeMe_2$; α = 19.0(9)º; Δδ = 0.26),[13] [1]Sn-FCP (ER_x = Sn*t*Bu_2; α = 14.1(2)º; Δδ = 0.22; ER_x = $SnMes_2$; α = 15.2(2)º; Δδ = 0.13),[13] and [1]B-FCP (ER_x = $BN(SiMe_3)_2$; α = 32.4(2)º; Δδ = 0.50; ER_x = BN*i*Pr_2; α = 31.0(2) and 31.4(2)º; Δδ =

0.39)[3] the splitting in **2** and [1]Al-FCP, respectively, are large and do not correlate nicely with the small ring tilt.

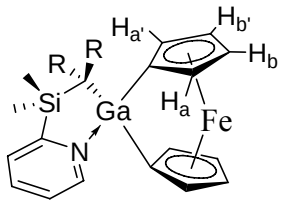

Figure 4-5. Assignment of the Cp protons via NOE experiment (R = $SiMe_3$): δ = 4.08 (H_a), 4.45 ($H_{a'}$), 4.61 (H_b), 4.65 ($H_{b'}$).

As an indication for ring strain, the *ipso*-C shift seems more reliable, because it is not dependent on the overall symmetry of the [1]ferrocenophane. The values for the *ipso*-C atoms in **2** (δ = 47.24) and [1]Al-FCP (δ = 52.92) are significantly upfield shifted with respect to parent ferrocene (δ = 68). However, they are only slightly downfield from the value of the known [1]B-FCP (δ = 44 - 45), which does not correlate with the tremendous difference in the ring tilt.[3b] The boron-bridged compounds exhibit the highest known ring tilt in ferrocenophanes, but their *ipso*-C resonances are compared with the similar strained [1]S-FCP (δ = 14.6) appearing at unexpected low field.[3b] Braunschweig and Manners suggested that this is a result of the electropositive nature of the bridging boron atom.[3b] Silicon is more electropositive than boron, but the *ipso*-C atoms of less-strained [1]Si-FCP are found at higher fields (ER_x = $SiMe_2$; δ = 33.1).[13] In summary, one can say that an upfield shift of the *ipso*-C atom resonances compared to the parent ferrocene indicates tilted Cp rings, but a simple correlation for all known [1]ferrocenophanes seems not to be existing.

In a similar manner to that described for the gallane **2**, we attempted to synthesize an indium-bridged [1]ferrocenophane. We synthesized the required starting

complex (Pytsi)$InCl_2$ (**3**) from $InCl_3$ and Li(thf)(Pytsi)[5] (see Experimental Section for details). As revealed by a single-crystal X-ray analysis, compound **3** forms dimers in the solid state (Figure 4-6; Table 4-1). This is not surprising, because indium prefers higher coordination numbers than 4.

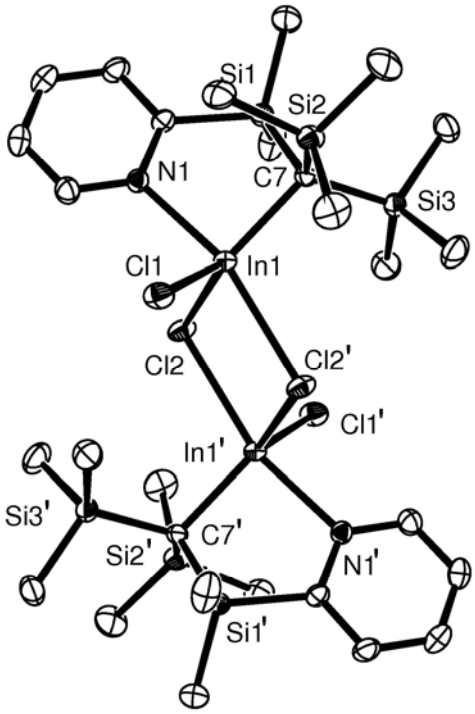

Figure 4-6. Molecular structure of **3** with thermal ellipsoids at the 50% probability level. H atoms are omitted for clarity. Primed atoms are generated by –x, -y, -z operation. Selected bond length (Å) and angles (º): In1-Cl1 = 2.3845(7), In1-Cl2 = 2.4812(7), In1-Cl2' = 2.7706(7), In1-C7 = 2.195(3), In1-N1 = 2.307(2), Cl1-In1-C7 = 124.01(8), Cl2-In1-C7 = 126.80(8), Cl1-In1-Cl2 = 109.10(3), N1-In1-Cl2' = 162.50(6), N1-In1-C7 = 90.07(9), N1-In1-Cl1 = 90.25(6), N1-In1-Cl2 = 86.53(6), Cl2'-In1-C7 = 105.89(7), Cl2'-In1-Cl1 = 86.73(3), Cl2'-In1-Cl2 = 78.21(2)

Each indium atom is 5-fold coordinated, with two chlorine atoms bridging the two metal centers and two terminal chlorine ligands, which are *trans* to each other (Figure 4-6). Both indium atoms are in a center of a distorted trigonal bipyramid with

both polyhedra sharing the Cl2–Cl2' edge to form a centrosymmetric dimer. For example, In1 is coordinated by Cl1, Cl2, and C7 in the equatorial position (angle sum = 359.9º) and by N1 and Cl2' in the axial position (N1–In1–Cl2' = 162.50(6)º) (Figure 4-6). Both chlorine bridges are asymmetric, e. g., with a long In1-Cl2' bond of 2.7706(7) Å and a short In1-Cl2 bond of 2.4812(7) Å.

The dimer **3** (C_i point group symmetry) is very flexible in solution. The ^{1}H and ^{13}C NMR spectra show only one type of pytrisyl ligand, which is C_s symmetrical in solution, e. g., only one singlet for $SiMe_2$ and one singlet for the $SiMe_3$ groups. These NMR data could be interpreted in several ways, and one can speculate that a fast monomer-dimer equilibrium occurs in solution.

Similar to the synthesis of compound **2** (eq 4-1), a synthesis of an [1]In-FCP was attempted. The only isolatable product from this batch was the unexpected ferrocenophane **4**, and consequently, we changed the In to Fe ration to 2:1 to optimize the synthesis of the novel compound **4** (eq 4-2).

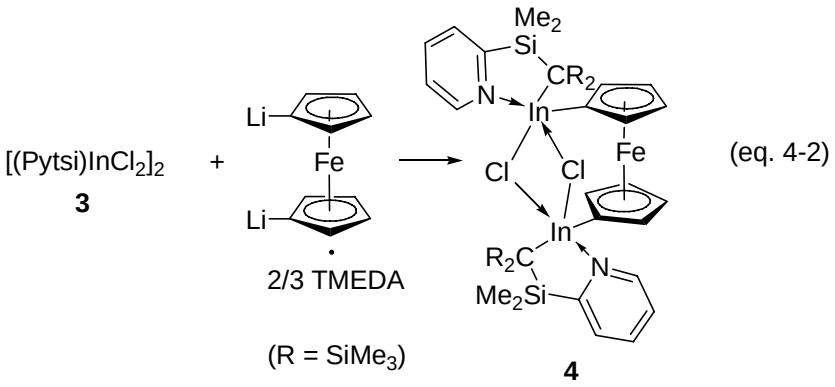

Dropwise addition of the poorly soluble complex **3** in toluene to a cooled slurry of dilithioferrocene 2/3 TMEDA[16] in toluene and subsequent filtration yielded an orange solution, which was concentrated, resulting in a crystallization of **4** at -10 °C (see

Experimental Section for details). Suitable crystals for X-ray diffraction were taken directly out of the toluene solution (Figure 4-7; Table 4-1).

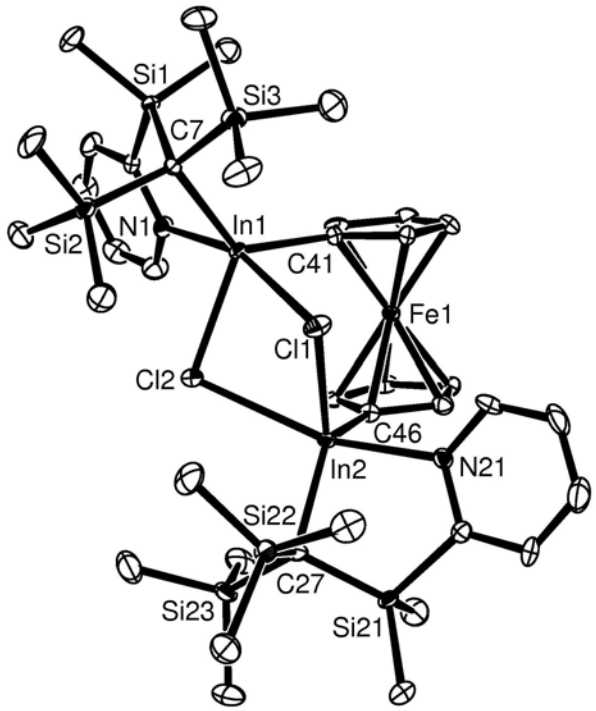

Figure 4-7. Molecular structure of **4** with thermal ellipsoids at the 50% probability level. H atoms and solvent molecules are omitted for clarity. Selected bond length (Å) and angles (º): In1-Cl1 = 2.8322(15), In2-Cl2 = 2.8655(15), In1-Cl2 = 2.5087(14), In2-Cl1 = 2.5072(15), In1-C7 = 2.236(5), In2-C27 = 2.227(5), In1-N1 = 2.364(5), In2-N21 = 2.358(4), In1-C41 = 2.155(6), In2-C46 = 2.136(6), Cl2-In1-C7 = 120.58(14), Cl1-In2-C27 = 120.61(15), C7-In1-C41 = 128.1(2), C27-In2-C46 = 128.2(2), C41-In1-Cl2 = 111.30(15), C46-In2-Cl1 = 111.12(15), N1-In1-Cl1 = 162.37(11), N21-In2-Cl2 = 161.86(12), N1-In1-C7 = 87.29(18), N21-In2-C27 = 86.72(18), N1-In1-Cl2 = 84.69(12), N21-In2-Cl1 = 84.83(12), N1-In1-C41 = 95.17(19), N21-In2-C46 = 95.22(19), Cl1-In1-C7 = 102.66(14), Cl2-In2-C27 = 103.95(14), Cl1-In1-Cl2 = 77.73(5), Cl1-In2-Cl2 = 77.12(5), Cl1-In1-C41 = 90.09(15), Cl2-In2-C46 = 89.66(15).

The isolated ferrocene **4** contains a similar In-(μ-Cl)$_2$-In unit as the starting indane **3**, but in contrast to compound **3**, there is not a 2-fold symmetry element that renders the two molecular halves of **4** identical. However, the molecular geometry of

compound **4** is very close to C_2 point group symmetry. Each indium atom is trigonal bipyramidally surrounded. In each case, a set of two C atoms and one Cl atom define the equatorial plane (angle sum = 359.9º for In1 and In2, respectively); N and Cl atoms are coordinated at the axial positions (N1-In1-Cl1 = 162.37(11) and N21-In2-Cl2 = 161.86(12)°; Figure 4-7). As for **3**, the In-(μ-Cl)$_2$-In moiety shows a short [In1-Cl2 = 2.5087(14) and In2-Cl1 = 2.5072(15) Å] and a long [In1-Cl1 = 2.8322(15) and In2-Cl2 = 2.8655(15) Å] indium chlorine bond. These distances are slightly longer than those found in **3** [In1-Cl2 = 2.4812(7) Å, and In1-Cl2' = 2.7706(7) Å; Figure 4-6], which might reflect the weaker Lewis-acidity of indium in **4**, caused by fewer chloride substituents. Compound **4** is unstrained, as revealed by a tilt angle α = 2.10(45)°; the Cp rings are staggered at an average angle of 29.12(38)° to each other. It seems that the rotational flexibility of the Cp ligands in ferrocene allows for an ideal adjustment to fit in an In-(μ-Cl)$_2$-In unit.

The NMR spectra of **4** can be interpreted as being caused by C_2 symmetrical molecules with a chlorine-bridged structure similar to that revealed in the crystal lattice: one set of signals for asymmetric pytrisyl ligands and one set of signals for asymmetric Cp groups. These C_2 symmetrical species must be a racemic mixture of molecules with the same relative configuration at each In atom, the *rac* isomers. There are no signs of the presence of diastereomers with opposite configurations at each In atom, the *meso* isomers. The molecular structure of **4** in the crystal lattice gives the impression that a respective *meso* isomer with an In-(μ-Cl)$_2$-In moiety is impossible for steric reasons. If the two molecular halves are *not* linked through Cl bridges, a mixture of *rac* and *meso* isomers should be present. The fact that this is not the case supports the interpretation of

the NMR data as being caused by compound **4** with a similar structure similar to that in the crystal lattice. Interestingly the four pseudotriplets of the Cp groups resonate at δ of 3.44, 4.18, 4.43, and 5.18 resulting in a very large splitting of $\Delta\delta = 1.74$ ppm. However, the ^{13}C NMR spectrum displays the *ipso*-C at δ 67.71, clearly indicating an unstrained ferrocenophane. In the course of assigning ^{1}H NMR peaks to protons in **4** by NOESY experiments we found that compound **4** fluctuates in solution (Figure 4-8; see Experimental Section for details). If one methyl of the $SiMe_2$ group, the methyl groups of a $SiMe_3$ moiety, or one CH proton is irradiated, one can observe, in addition to nuclear Overhauser effects, magnetization transfer to respective diastereotopic protons (Figure 4-8; Me_a to $Me_{a'}$, R to R', H_a to $H_{a'}$, H_b to $H_{b'}$ and vice versa). This clearly indicates that the two enantiomers of the *rac* isomer form an equilibrium.

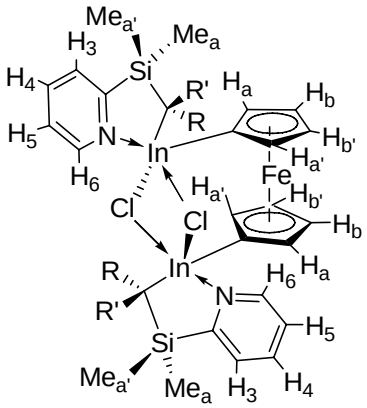

Figure 4-8. Assignment of the ^{1}H NMR peaks for **4** (R and R' = $SiMe_3$; none-primed groups R and Me_a are on the same side of the ferrocene moiety; primed groups R' and $Me_{a'}$ are on the opposite side of the ferrocene moiety (see experimental for details)

The equilibration between the R/R isomer and the S/S isomer is slow at ambient temperature, and signals do not coalesce in a ^{1}H NMR spectrum (500 MHz). In the temperature range of 25 to 80 °C coalescence between the primed and none-primed

atoms and groups, respectively, is observed, indicating a time-averaged C_{2v} symmetrical molecule. Besides exhibiting dynamic behavior, compound **4** is temperature sensitive. After one series of variable-temperature experiments, new signals appeared in the ^{1}H NMR spectrum remeasured at ambient temperature, indicating unidentified thermolysis products. We have no experimental evidence on how the equilibration takes place. It is known for 4- and 5-fold coordinated indium species that the donor bond between In atoms and the dimethylamino group from the chelating "one-arm" phenyl ligand 2-$Me_2NCH(Z)C_6H_4$ (Z = H, Me)[14] breakes and re-forms in solution. We assume that a similar process takes place with the pyridine donor groups in compound **4**, and it is feasible that both pyridine ligands are lifted off the In atoms, followed by rotations of the pytrisyl ligand around the In-C bonds, and are reattached which results in inversions of both metal centers. A process like this could explain the observed equilibration.

4.4 Conclusions

Like the aluminum-bridged [1]ferrocenophane, the pytrisyl ligand provides the right combination of steric bulkiness and intramolecular coordination to allow the synthesis of the first example of a gallium-bridged [1]ferrocenophane (**2**). For the heavier homologue indium, we isolated the first example of an ferrocene molecule bridged by an indium-containing moiety (**4**). Interestingly, the synthesis is diastereoselective and the resulting product fluctuates in solution. It is evident from solution NMR experiments that the two Cp ligands in compound **4** are bridged by a In-$(\mu$-$Cl)_2$-In unit; the molecular structure of **4** in solution is similar to that found in the solid state. IUPAC defines ferrocenophanes as "compounds in which the two ring

components of ferrocene are linked by one or more bridging chains".[15] Because of the linkage between the Cp ligands, compound **4** is clearly a ferrocenophane. However, the bridging In-(μ-Cl)$_2$-In unit is not a simple chain, and therefore, an IUPAC name for species **4** as a ferrocenophane is not defined.

The bridging In-(μ-Cl)$_2$-In unit of the starting indane **3** is preserved in the product **4**, which suggests that a monomerization of the starting indium dihalide might open the door to the targeted [1]In-FCP. We are currently increasing the bulkiness of the pytrisyl ligand by introducing sterically demanding groups in position 6 of the pyridine ring. This might prevent dimerization and, therefore, change the course of the reaction with dilithioferrocene. We hope to report on the outcome shortly.

4.5 Experimental Section

General Procedures. All manipulations were carried out using standard Schlenk techniques, if not noted differently. Solvents were dried using a Braun Solvent Purification System and stored under Argon over a 4 Å molecular sieve. C_6D_6 and C_7D_8 were degassed prior to use and stored under argon over a 4 Å molecular sieve. $GaCl_3$ and $InCl_3$ were purchased from VWR and used as received. ^1H and ^{13}C NMR spectra were recorded on a Bruker 500 MHz Avance spectrometer; chemical shifts were referenced to the residual protons of the deuterated solvent. All NMR spectra were recorded in C_6D_6 at 25 °C, unless noted differently. Mass spectra were measured on a VG 70SE and were reported in the form M (%I) [F], where M is the mass observed, %I is the intensity of the peak relative to the most intense peak in the spectrum and F is the molecular ion or fragment. Only ions with intensities higher than 10% are listed.

Elemental analysis was performed on a Perkin-Elmer 2400 CHN Elemental Analyzer; samples were prepared in a glovebox, and V_2O_5 was added to promote combustion.

Synthesis of 1. Li(thf)(Pytsi) (1.939 g, 5.19 mmol)[5] dissolved in Et_2O (30 mL) was cooled to –80 ºC and added to a stirring solution of $GaCl_3$ (0.920 g, 5.22 mmol) in Et_2O (40 mL; –80 ºC). The reaction mixture was stirred at –80 ºC for 20 min before being warmed to ambient temperature with stirring continued for 16 h to give a yellow solution. Subsequently, the solvent was removed from the filtered solution. The remaining white solid was then sublimed at 130 ºC at high vacuum to yield **1** as a white crystalline solid (1.672 g, 74%). ^{1}H NMR (500 MHz): δ = 0.29 (s, 18H, $SiMe_3$), 0.36 (s, 6H, $SiMe_2$), 6.37 (pst, 1H, 5-H), 6.82-6.84 (m, 2H, 3-H, 4-H), 8.42 (d, 1H, 6-H). ^{13}C NMR (125.8 MHz): δ = 3.25 ($SiMe_2$), 5.84 ($SiMe_3$), 125.64 (5-C), 129.37 (3-C), 139.93 (4-C), 146.29 (6-C), 169.27 (*ipso*-C, C_5H_4N). Carbon attached to gallium was obscured in baseline. MS (70 eV, EI+): *m/z* (%): 420 (27) [M^+ - Me], 264 (100) [$Pytsi^+$ - 2 Me]. Anal. Calcd for $C_{14}H_{28}Cl_2GaNSi_3$ (435.264): C, 38.63; H, 6.48; N, 3.22. Found: C, 38.74; H, 6.49; N, 3.07.

Synthesis of 2. (Pytsi)$GaCl_2$ (**1**) (0.621 g, 1.42 mmol) was dissolved in toluene (15 mL) and chilled to -10°C. A suspension of dilithioferrocene · 2/3 TMEDA (0.506 g, 1.83 mmol)[16] in toluene (15 mL) was added dropwise via tubing. After stirring for 16 h, the color of the solution changed to red. After filtration, the solvent was removed at high vacuum (25 °C/0.01 mbar) to yield red, viscous oil. The residue was extracted with hexane (2 × 10 mL). After concentration, product **2** (0.460 g, 59%) was obtained as red crystals at ambient temperature. ^{1}H NMR (500 MHz): δ = 0.38 (s, 18H, $SiMe_3$), 0.43 (s, 6H, $SiMe_2$), 4.08 (H_a), 4.45 ($H_{a'}$), 4.61 (H_b), 4.65 ($H_{b'}$) (pst, 8H, Cp, see Figure 4-5),

6.46 (pst, 1H, 4-H or 5-H), 6.85 (pst, 1H, 4-H or 5-H), 6.96 (d, 1H, 3-H), 8.73 (d, 1H, 6-H). ^{13}C NMR (125.8 MHz): δ = 1.27 (Si-C(SiMe$_3$)$_2$-Ga), 3.22 (SiMe$_2$), 5.94 (SiMe$_3$), 47.24 (*ipso*-C, Cp), 75.39, 75.53, 76.71, 77.19 (Cp), 124.22 (5-C), 129.40 (3-C), 138.21 (4-C), 147.87 (6-C), 172.74 (*ipso*-C, C_5H_4N). MS (70 eV, EI+): *m/z* (%): 547 (100) [M^+], 532 (69) [M^+ –Me], 293 (91) [Pytsi$^+$ – H], 278 (69) [Pytsi$^+$ – H – Me], 264 (42) [Pytsi$^+$ – 2 Me], 73 (10) [SiMe$_3^+$]. Anal. Calcd for $C_{24}H_{36}GaFeNSi_3$ (548.379): C, 52.57; H, 6.62; N, 2.55. Found: C, 53.22; H, 6.80; N, 2.31.

Synthesis of 3. Li(thf)(Pytsi) (1.901 g, 5.09 mmol) was dissolved in THF (20 mL, –80 ºC) and added to a solution of $InCl_3$ (1.125 g, 5.09 mmol) in THF (40 mL; –80 ºC). The reaction mixture was stirred at –80 ºC for 20 min before slowly being warmed to ambient temperature with stirring continued for 16 h to give a green solution initially, and finally a yellow solution. Subsequently, the solvent was removed, and the residue washed with hexane (2 x 30 mL) and filtered. Upon removal of all volatiles at ambient temperature, a white solid remained, which was then sublimed at 135 ºC at high vacuum (0.01 mbar) to yield **3** as a white crystalline solid (1.634 g, 67%). ^{1}H NMR (500 MHz): δ = 0.20 (s, 18H, SiMe$_3$), 0.32 (s, 6H, SiMe$_2$), 6.30 (pst, 1H, 5-H), 6.74 (pst, 1H, 4-H), 6.81 (d, 1H, 3-H), 8.30 (d, 1H, 6-H). ^{13}C NMR (125.8 MHz): δ = 3.13 (SiMe$_2$), 6.31 (SiMe$_3$), 125.46 (5-C), 129.54 (3-C), 139.16 (4-C), 148.40 (6-C), 170.14 (*ipso*-C, C_5H_4N). Carbon attached to indium was obscured in baseline. MS (70 eV, EI+): *m/z* (%): 464 (15) [M^+ – Me], 444 (16) [M^+ – Cl], 264 (100) [Pytsi$^+$ – 2 Me]. Anal. Calcd for $C_{14}H_{28}Cl_2InNSi_3$ (480.364): C, 35.01; H, 5.88; N, 2.92 Found: C, 35.62; H, 5.97; N, 2.31.

Synthesis of 4. A suspension of **3** (1.562 g, 1.62 mmol) in toluene (50 mL) and was added dropwise via tubing to a suspension of dilithioferrocene · 2/3 TMEDA (0.448 g, 1.62 mmol)[16] in toluene (20 mL) that was chilled to -10 °C. After stirring for 16 h, the color of the solution had changed to orange. After filtration and concentration at high vacuum (25 °C/0.01 mbar), crystallization occurred at -10 °C (0.990 g, 57.0%). Single-crystal X-ray analysis was performed on a toluene wet crystal. ^{1}H NMR (500 MHz; see Figure 4-8 for assignments): δ = 0.22 (s, 3H, Me_a of $SiMe_2$), 0.34 (s, 9H, R' = $SiMe_3$), 0.48 (s, 3H, $Me_{a'}$ of $SiMe_2$), 0.59 (s, 9H, R = $SiMe_3$), 3.44 (H_a), 4.18 (H_b), 4.43 ($H_{b'}$), 5.18 ($H_{a'}$) (pst, 4H, Cp), 6.62 (pst, 1H, 5-H), 6.92 (pst, 1H, 4-H), 7.03 (d, 1H, 3-H), 9.25 (d, 1H, 6-H). ^{13}C NMR (125 MHz): δ = 0.57, 3.01 ($SiMe_2$), 4.60, 4.96 ($SiMe_3$), 5.32 (Si-C($SiMe_3$)$_2$-In, –40 °C, C_7D_8), 67.71 (*ipso*-C, Cp), 69.61, 70.21, 74.26, 75.76 (Cp), 122.73, 127.84, 136.09, 147.47, 169.48 (aromatic, C_5H_4N). MS (70 eV, EI+): *m/z* (%): 629 (22) [MH^+ – (Pytsi)In(Cl)], 444 (32) [(Pytsi)InCl^+], 264 (100) [Pytsi$^+$ – 2 Me], 115 (11) [In^+]. Anal. Calcd for $C_{38}H_{64}Cl_2FeIn_2N_2Si_6$ (1073.843): C, 42.50; H, 6.01; N, 2.61; Found: C, 43.61; H, 6.12; N, 2.59.

X-ray structural analysis for 1, 2, 3, and 4. Data were collected at -100 °C on a Nonius Kappa CCD diffractometer, using the COLLECT program.[17] Cell refinement and data reductions used the programs DENZO and SCALEPACK.[18] The program SIR97[19] was used to solve the structure and SHELXL97[20] was used to refine the structure. All H atoms were placed in calculated positions, with C-H distances in the range 0.95 – 0.99 Å, and included in a riding model approximation. For compound **1**, U_{iso}(H) was constrained to be 1.2 U_{eq}(C) for all protons. For **3** and **4**, U_{iso}(H) was

constrained to be 1.2 U_{eq}(C) for all aromatic protons and 1.5 U_{eq}(C) for all methyl protons.

The crystals of **2** diffracted very poorly, and data could be obtained only to a maximum diffraction angle of 22º using Mo radiation. The unit cell had three angles near 90º with cell edges of 14.342, 18.200 and 20.442 Å. Systematic absences suggested $P2_12_12_1$ or $P2_12_12$, but neither SIR97[19] nor SHELXS97[20] could find a solution in either of these space groups. The data were processed as triclinic and solved with SIR97[19] to give an eight molecule solution, and refined using SHELXL97[20] using rigid models of the Al analolgue of **2**[4] to complete the molecules. The eight molecules were examined using Platon[21] and conversion to $P2_1$ was suggested. In $P2_1$ the asymmetric unit had four molecules. All atoms were refined isotropically with no constraints, and the structures of the four molecules were maintained. The Ga, Fe, and Si atoms were then refined anisotropically. The number of data did not allow all atoms to be refined anisotropically, but H atoms were placed in calculated positions with U_{iso} constrained to be 1.2 times U_{eq} of the carrier atom for aromatic protons and 1.5 times U_{eq} of the carrier atoms for methyl hydrogen atoms. The *R* value refined to 0.143. All four molecules maintained their geometry. No further symmetry elements could be identified. The angles between the cyclopentadienyl rings for the four molecules are 13.6(2.1), 15.0(1.6), 15.4(1.9), and 18.8(1.8)º for an average of 15.7º. An ORTEP diagram of one of the molecules is shown in Figure 4-3. The data does not give a complete crystal structure of **2** with accurate bond lengths and bond angles, but they do determine the arrangement of the atoms of **2**.

Acknowledgement. We thank the Natural Sciences and Engineering Research Council of Canada (NSERC Discovery Grant, J.M.), the Department of Chemistry, the Saskatchewan Structural Sciences Centre, and the University of Saskatchewan for their generous support.

Supporting Information Available. Crystallographic data for **1**, **3**, and **4** in CIF file format. This material is available free of charge via the Internet at http://pubs.acs.org.

4.6 References

(1) Osborne, A. G.; Whiteley, R. H. *J. Organomet. Chem*. **1975**, *101*, C27-C28.
(2) Nguyen, P.; Gómez-Elipe, P.; Manners, I. *Chem. Rev.* **1999**, *99*, 1515-1548.
(3) (a) Braunschweig, H.; Dirk, R.; Müller, M.; Nguyen, P.; Resendes, R.; Gates, D. P.; Manners, I. *Angew. Chem., Int. Ed. Engl.* **1997**, *36*, 2338-2340. (b) Berenbaum, A.; Braunschweig, H.; Dirk, R.; Englert, U.; Green, J. C.; Jäkle, F.; Lough, A. J.; Manners, I. *J. Am. Chem. Soc. 2000*, 122, 5765-5774.
(4) Schachner, J. A.; Lund, C. L.; Quail, J. W.; Müller, J. *Organometallics* **2005**, *24*, 785-787.
(5) Al-Juaid, S. S.; Eaborn, C.; Hitchcock, P. B.; Hill, M. S.; Smith, J. D. *Organometallics* **2000**, *19*, 3224-3231.
(6) (a) Eaborn, C.; Hill M. S.; Hitchcock P. B.; Smith J. D. *J. Chem. Soc., Chem. Commun.* **2000**, 691-692. (b) Al-Juaid, S. S.; Avent A. G.; Eaborn, C.; El-Hamruni, S. M.; Hawkes, S. A.; Hill, M. S.; Hitchcock, P. B.; Smith, J. D. *J. Organomet. Chem.* **2001**, *631*, 76-86. (c) Al-Juaid, S. S.; Avent A. G.; Eaborn, C.; Hill, M. S.; Hitchcock, P. B.; Patel, D. J.; Smith, J. D. *Organometallics* **2001**, *20*, 1223-1229. (d) Eaborn, C.; Hill, M. S.; Hitchcock, P. B.; Smith, J. D. *J. Chem. Soc., Dalton Trans.* **2002**, 2467-2472.
(7) Scheibitz, M.; Winter, R. F.; Bolte, M.; Lerner, H-W.; Wagner, M. *Angew. Chem., Int. Ed. Engl.* **2003**, *42*, 924-927.
(8) (a) Uhl, W.; Hahn, I.; Jantschak, A.; Spies, T. *J. Organomet. Chem.* **2001**, *637*, 300-303. (b) Althoff, A.; Jutzi, P.; Lenze, N.; Neumann, B.; Stammler, A.; Stammler, H-G. *Organometallics* **2002**, *21*, 3018-3022. (c) Jutzi, P.; Lenze, N.; Neumann, B.; Stammler, H-G. *Angew. Chem., Int. Ed. Engl.* **2001**, *40*, 1424-1427. (d) , A.; Jutzi, P.; Lenze, N.; Neumann, B.; Stammler, A.; Stammler, H-G. *Organometallics* **2003**, *22*, 2766-2774.
(9) Schachner, J. A.; Lund, C. L.; Quail, J. W.; Müller, *J. Acta Crystallogr.* **2005**, *E61*, m682-m684.
(10) Howson, J.; Eaborn, C.; Hitchcock, P. B.; Hill, M. S.; Smith, J. D. *J. Organomet. Chem*. **2005**, *690*, 69-75.

(11) Rulkens, R.; Gates, D. P.; Balaishis, D.; Pudelski, J. K.; McIntosh, D. F.; Lough, A. J.; Manners, I. *J. Am. Chem. Soc.* **1997**, *119*, 10976-10986.
(12) Pudelski, J. K.; Gates, D. P.; Rulkens, R.; Lough, A. J.; Manners, I. *Angew. Chem., Int. Ed. Engl.* **1995**, *43*, 1506-1508.
(13) Jäkle, F.; Rulkens, R.; Zech, G.; Foucher, D. A.; Lough, A. J.; Manners, I. *Chem., Eur. J.* **1998**, *4*, 2117-2128, and references therein.
(14) Jastrzebski, J. T. B. H.; van Koten, G.; Tuck, D. G.; Meinema, H. A.; Noltes, J. G. *Organometallics* **1982**, *1*, 1492-1495.
(15) online version of the IUPAC Compendium of Chemical Terminology (www.iupac.org/publications/compendium/)
(16) Butler, I. R.; Cullen, W. R.; Ni, J.; Rettig, S. J. *Organometallics* **1985**, *4*, 2196-2201.
(17) Nonius; Nonius BV, Delft, The Netherlands, **1998**.
(18) Otwinowski, Z.; Minor, W. In *Macromolecular Crystallography, Part A*; Carter, C. W., Sweet, R. M., Eds.; Academic Press: London, **1997**; Vol. 276, pp 307-326.
(19) Altomare, A.; Burla, M. C.; Camalli, M.; Cascarano, G.; Giacovazzo, C.; Guagliardi, A.; Moliterni, A. G. G.; Polidori, G.; Spagna, R. *J. Appl. Crystallogr.* **1999**, *32*, 115-119.
(20) Sheldrick, G. M.; *SHELXS97 and SHELXL97*, University of Göttingen, Germany, 1997.
(21) Spek, A. L.; *PLATON, A Multipurpose Crystallographic Tool*, University of Utrecht, The Netherlands, 2003.

CHAPTER 5
PUBLICATION 3

The following chapter is a verbatim copy of an article published in *Organometallics*[*] in August 2006 and describes an improved synthesis of [1]ferrocenophanes bridged by Al and Ga using the ligand Me_2Ntsi which stands for $C(SiMe_3)_2SiMe_2NMe_2$. The authors of this paper are Clinton L. Lund, who did the work on [1]chromarenophanes and [1]vandarenophanes, myself, who did the synthesis and characterization of the new [1]ferrocenophanes, J. Wilson Quail, who did all structure determinations by single-crystal X-ray analysis, and my supervisor Jens Müller. Written permission was obtained from all contributing authors to include this material within this thesis.

[*] Reproduced with permission from Organometallics. © 2006 American Chemical Society

5. [1]Ferrocenophanes, [1]Chromarenophanes, and [1]Vanadarenophanes with Aluminium and Gallium in Bridging Positions

Clinton L. Lund,[‡] Jörg A. Schachner,[‡] J. Wilson Quail,[§] Jens Müller[‡,]*

Department of Chemistry and Saskatchewan Structural Sciences Centre, University of Saskatchewan, 110 Science Place, Saskatoon, Saskatchewan S7N 5C9, Canada

Received August 14, 2006

5.1 Abstract

Aluminium- and gallium-bridged [1]ferrocenophanes (**4a**, **4b**), [1]chromarenophanes (**5a**, **5b**), and [1]vanadarenophanes (**6a**, **6b**) were synthesized from the respective dilithiated sandwich compounds with element dichlorides $(Me_2Ntsi)ECl_2$ [E = Al, Ga; $Me_2Ntsi = C(SiMe_3)_2(SiMe_2NMe_2)$] in moderate to high isolated yields (54 – 97%). The new intramolecularly stabilized aluminum compound $(Me_2NCH_2tsi)AlCl_2$ (**2a**) was synthesized, but was proven to be unreactive with respect to $[Fe(LiC_5H_4)_2]\cdot 2/3$ TMEDA. The diamagnetic species **2a**, **4a**, **4b**, **5a**, and **5b** were characterized by NMR spectroscopy (^1H, ^{13}C, ^{27}Al), CHN elemental analysis, and mass spectrometry, whereas the paramagnetic compounds **6a** and **6b** were characterized by IR spectroscopy, CHN elemental analysis, and mass spectrometry. In addition, the molecular structures of compounds **2a**, **4a**, **4b**, **5a**, **5b**, **6a**, and **6b** were determined by single-crystal X-ray analysis. All [1]cyclophanes are strained species as revealed by the following tilt angles α [°]: 14.33(14) (**4a**), 15.83(19) (**4b**), 11.81(9) (**5a**), 13.24(13) (**5b**), 14.65(14) (**6a**), and 15.63(14) (**6b**).

5.2 Introduction

Since their discovery in 1975 by Osborne and Whiteley,[1] strained [1]ferrocenophanes containing main-group elements in the bridging position have sparked a lot of interest throughout the scientific community. Manners *et al.* showed that [1]ferrocenophanes ([1]FCPs) produce high molecular weight polyferrocenes via ring-opening polymerization (ROP).[2] Because of the incorporation of metals into the backbone of the polymer chain, these materials show interesting new properties (e.g., redox, magnetic, electrical, and chemical).[3-5] Over the last two decades, new [1]ferrocenophanes with bridging elements ranging from group 13 to 16 were synthesized and their use for polymer synthesis was explored.[6] However, group 13 [1]ferrocenophane chemistry was restricted to boron.[7-9]

Recently, by reactions of intramolecularly coordinated element dichlorides (Pytsi)ECl_2 [E = Al, Ga; Pytsi = $C(SiMe_3)_2SiMe_2(2\text{-}C_5H_4N)$] with dilithioferrocene, we isolated the first alumina[1]ferrocenophane (Al[1]FCP)[10] and the first galla[1]ferrocenophane (Ga[1]FCP)[11] (Figure 5-1).

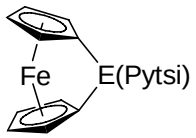

E = Al (**1a**), Ga (**1b**)

Figure 5-1. Al- and Ga[1]FCP [Pytsi = $C(SiMe_3)_2SiMe_2(2\text{-}C_5H_4N)$].

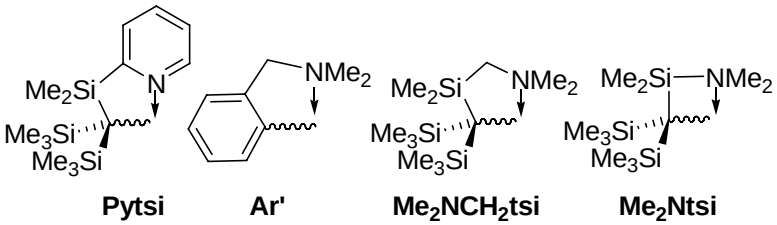

Figure 5-2. Intramolecularly coordinating ligands.

The Pytsi ligand, derived from the well-known trisyl ligand $C(SiMe_3)_3$ by a formal substitution of one methyl group with a pyridyl ring, provides intramolecular coordination via the pyridyl moiety and steric shielding through the trimethylsilyl groups (Figure 5-2).[12]

In order to use strained [1]FCP as monomers for ROP, ideally, they should be accessible in high yields and high purities. In light of these requirements, the preparations of the Al[1]FCP **1a** and the Ga[1]FCP **1b** were unsatisfactory (Figure 5-1); yields were low to moderate and significant amounts of ferrocene were always produced during the synthesis. The aluminum compound **1a** (Figure 5-1) even crystallized with half of a molecule of $FeCp_2$ in the asymmetric unit.[10] Consequently, we focused our attention on improving the synthesis of Al- and Ga[1]FCPs by altering the ligand that remains attached at the bridging element. Furthermore, we started to explore the possibilities of using intramolecularly coordinated alanes and gallanes for the synthesis of strained [1]metalloarenophanes. Our first results are described in this paper.

5.3 Results and Discussion

If the popular "one-armed phenyl" ligand (Ar′, Figure 5-2) is applied instead of the Pytsi ligand, [1.1]FCPs are produced exclusively (E = Al,[13,14] Ga,[14] In[14]). In our first

attempt to improve the synthesis of an Al[1]FCP, we formally replaced the pyridyl donor of the Pytsi ligand by the saturated CH_2NMe_2 "arm" of the Ar′ ligand (Figure 5-2). By adapting known procedures, we synthesized the aluminum compound $(Me_2NCH_2tsi)AlCl_2$ (**2a**) (see Experimental Section for details). As expected, the molecular structure of compound **2a** reveals no surprises (Figure 5-3).

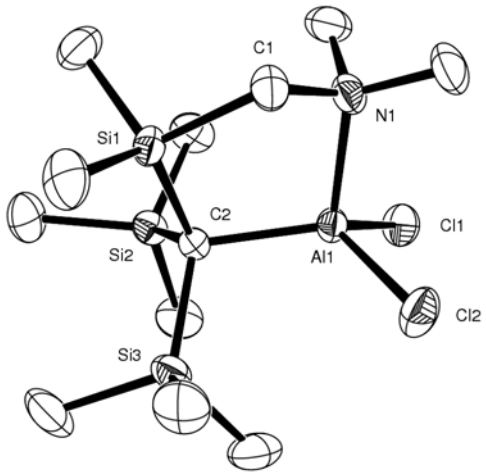

Figure 5-3. Molecular structure of **2a** with thermal ellipsoids at the 50% probability level. H atoms are omitted for clarity. Selected bond lengths [Å] and angles [º]: Al1-N1 = 1.9783(12), Al1-C2 = 1.9805(13), Al1-Cl1 = 2.1501(5), Al1-Cl2 = 2.1661(5), N1-Al1-C2 = 103.80(5), N1-Al1-Cl1 = 106.42(4), N1-Al1-Cl2 = 100.24(4), C2-Al1-Cl1 = 119.03(4), C2-Al1-Cl2 = 117.37(4).

The Al atom in **2a** is similarly coordinated to that in the known compound $(Pytsi)AlCl_2$.[15] For both species, the central metal atom is surrounded by C-, N-, and two Cl atoms with bond lengths of 1.9783(12) Å (Al-N), 1.9805(13) Å (Al-C), 2.1501(5) Å (Al-Cl), and 2.1661(5) Å (Al-Cl) for compound **2a** (Figure 5-3) compared with 1.9383(16) Å (Al-N), 1.9784(19) Å (Al-C), 2.1295(8) Å (Al-Cl), and 2.1529(8) Å (Al-Cl) for $(Pytsi)AlCl_2$.[15] For both species, the set of four atoms around the Al atom form a similarly distorted tetrahedron. On the basis of this comparison, we expected a similar

reactivity of **2a** relative to (Pytsi)$AlCl_2$. However, reaction of **2a** with dilithioferrocene, under similar conditions to those we applied for the syntheses of the [1]FCPs **1a** and **1b**,[10,11] revealed that the dichloride **2a** was significantly less reactive than (Pytsi)$AlCl_2$. ^{1}H NMR spectra taken from the reaction mixtures showed only small peaks in the typical range for Cp groups, indicating the presence of substituted ferrocenes; ca. 90% of the dichloride **2a** was still present in solution. None of the ^{1}H NMR signals indicated the presence of the targeted Al[1]FCP.

A drastic change in reactivity can be observed if, instead of $MeNCH_2$tsi ligand, the shorter Me_2Ntsi is employed (Figure 5-2). Alanes and gallanes of the type (Me_2Ntsi)ECl_2 were already synthesized by Eaborn and Smith *et al.*[16] Reaction of (Me_2Ntsi)$AlCl_2$ (**3a**) with dilithioferrocene gave the new Al[1]FCP **4a** in an isolated yield of 97% (Scheme 5-1). Similarly, we synthesized the Ga[1]FCP **4b**. Encouraged by these results, we were able to synthesize the first aluminum- and gallium-bridged [1]chromarenophanes (**5a**,**b**) and the respective vanadium compounds (**6a**,**b**; Scheme 5-1).

Scheme 5-1.

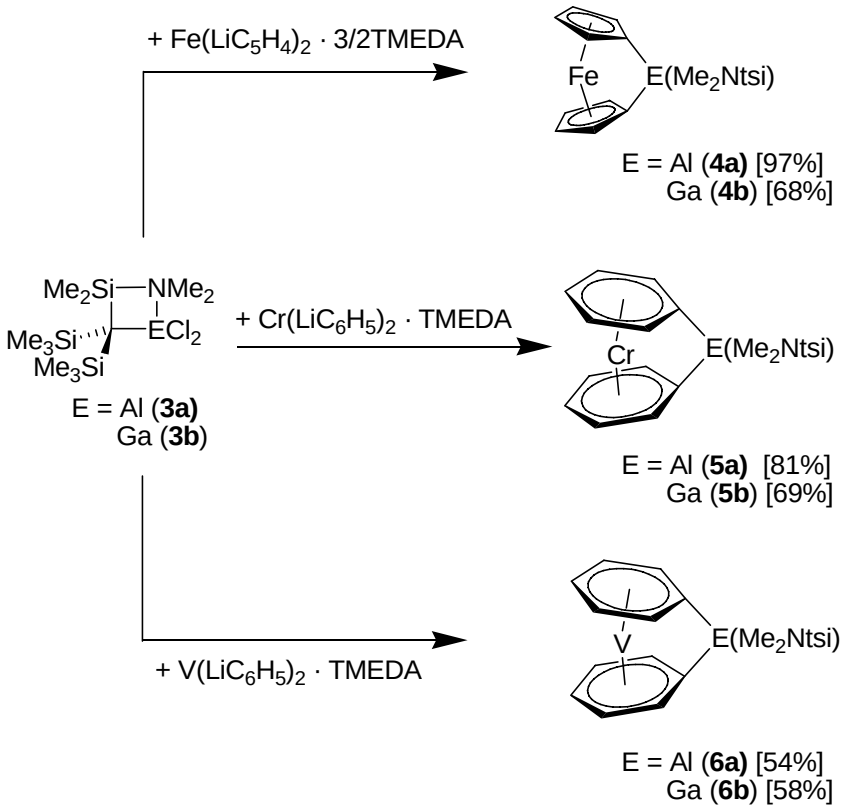

5.3.1 [1]Ferrocenophanes.

Compounds **4a** and **4b** both show signal patterns in the ^{1}H- and ^{13}C NMR spectra that can be interpreted as being caused by [1]FCPs with time-averaged C_s symmetry. For example, the ^{1}H NMR spectrum of **4a** shows three pseudo triplets for the C_5H_4 rings with a 1 : 1 : 2 intensity ratio at δ 3.76 (α-H), 4.24 (α-H), and 4.58 (β-H). This signal pattern is similar to that of the Pytsi species **1a**,[10] except for the fact that the splitting of the β-protons in **4a** is so small that their signals overlap. The most indicative spectroscopic data to prove that indeed strained [1]FCPs were formed comes from ^{13}C NMR spectroscopy. The signal of the *ipso*-C atoms of the cyclopentadienyl ligands should be shifted upfield with respect to that of the $FeCp_2$ (δ 68). The detected shifts for

4a (δ 53.0) and **4b** (δ 47.3) match very well with those of the [1]FCPs **1a** (δ = 52.9)[10] and **1b** (δ 47.2)[11].

The new [1]FCPs **4a** and **4b** are isomorphous and crystallized with half of a molecule of C_6H_6 in the asymmetric unit (Table 5-1); the molecular structure of the aluminum species **4a** is depicted in Figure 5-4 (ORTEP plot of **4b** see Supporting Information).

Table 5-1. Crystal and Structural Refinement Data for Compounds **2a**, **4a**, and **4b**.

	2a	**4a** · ½ C_6H_6	**4b** · ½ C_6H_6
empirical formula	$C_{12}H_{32}AlCl_2NSi_3$	$C_{24}H_{41}AlFeNSi_3$	$C_{24}H_{41}FeGaNSi_3$
formula weight	372.54	510.68	553.42
wavelength, Å	0.71073	0.71073	0.71073
crystal system	monoclinic	triclinic	triclinic
space group (No.)	$P2_1/c$ (14)	P-1 (2)	P-1 (2)
Z	4	2	2
a, Å	14.5558(2)	9.0703(2)	9.0689(3)
b, Å	10.5318(2)	9.1867(2)	9.1768(3)
c, Å	14.0477(2)	18.8627(3)	18.9466(6)
α, deg	90	79.4549(12)	79.2406(18
β, deg	101.3318(12)	85.2343(11)	85.294(2)
γ, deg	90	61.3777(10)	61.6414(16)
vol, $Å^3$	2111.51(6)	1356.36(5)	1363.14(8)
d (calc), mg/m^3	1.172	1.250	1.348
temp, K	173(2)	173(2)	173(2)
abs coeff., mm^{-1}	0.510	0.733	1.664
theta range, deg	2.43 to 30.04	2.56 to 30.51	2.69 to 27.60
refl collected	12031	35005	18573
indep refl	6185 [R(int) = 0.0187]	8264 [R(int) = 0.0615]	6232 [R(int) = 0.0538]
abs correction	none	psi-scan	psi-scan
ref method	Full-matrix least-squares on F^2		
data / restr / params	6185 / 0 / 182	8264 / 0 / 281	6232 / 0 / 281
goodness-of-fit on F^2	1.024	1.025	1.040
final R indices [I>2sigma(I)]	R1 = 0.0340, wR2 = 0.0829	R1 = 0.0449, wR2 = 0.0942	R1 = 0.0403, wR2 = 0.0805
R indices (all data)	R1 = 0.0452, wR2 = 0.0886	R1 = 0.0739, wR2 = 0.1070	R1 = 0.0623, wR2 = 0.0900
max diff. peak-hole, $e.Å^{-3}$	0.340 and -0.353	0.333 and -0.534	0.371 and -0.541

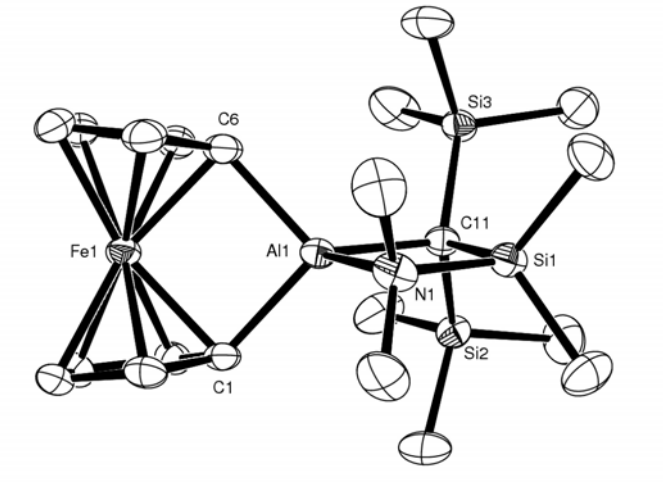

Figure 5-4. Molecular structure of **4a** with thermal ellipsoids at the 50% probability level. H atoms and ½ benzene are omitted for clarity. ORTEP plot for **4b** see Supporting Information. Selected atom-atom distances [Å] and bond angles [º] for **4a**: Al1-N1 2.0123(17), Al1-C1 2.000(2), Al1-C6 1.988(2), Al1-C11 2.0301(19), Al1-Fe1 2.7708(6), C1-Al1-C6 94.51(8), N1-Al1-C11 86.71(7). Selected atom-atom distances [Å] and bond angles [º] for **4b**: Ga1-N1 2.105(2), Ga1-C1 2.008(3), Ga1-C6 2.017(3), Ga1-C11 2.048(3), Ga1-Fe1 2.8184(5), C1-Ga1-C6 92.75(11), N1-Ga1-C11 84.98(10).

In both cases, the bridging element is part of a planar, four-membered ring [rms deviations from planarity [Å] are: 0.0074 (**4a**), 0.0068 (**4b**)] and surrounded by one N atom and three C atoms. As expected, the E–C bonds are very similar for both species [Al1–C1 2.000(2), Al1–C6 1.988(2), Al1–C11 2.0301(19) Å, for **4a**; Ga1–C1 2.008(3), Ga1–C6 2.017(3), Ga1–C11 2.048(3) Å for **4b**] and the E–N bonds are significantly different [Al1–N1 2.0123(17) and Ga1–N1 2.105(2) Å]. The extent of strain present in [1]FCPs can be expressed by a set of angles, among which the tilt angle α is the most common one (Figure 5-5).[17]

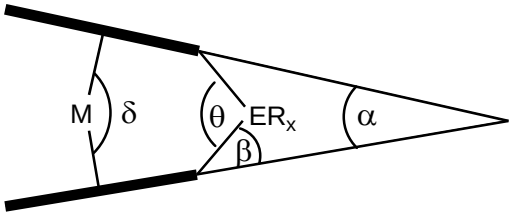

Figure 5-5. Set of angles to describe deformations in [1]metallocenophanes and [1]metalloarenophanes.

We determined tilt angles α of 14.33(14)° for **4a** and 15.83(19)° for **4b**. The value for **4a** is very close to that of 14.9(3)° determined for the Pytsi containing Al[1]FCP **1a** (Figure 5-1).[10] Compound **4b** is the first fully characterized Ga[1]FCP; the structural analysis of its Pytsi containing counterpart **1b**[11] (Figure 5-1) did not allow the extraction of structural details like bond lengths and angles. The tilt angles α for **4a** and **4b** are similar as those determined for Sn[1]FCP [Sn*t*Bu$_2$ α = 14.1(2)°,[18] SnMes$_2$ α = 15.2(2)°[19]] and significantly smaller than those found for B[1]FCP, with the latter holding the record with 32.4(2)° for the largest known tilt angle in [1]FCP.[8] Even though the difference in the tilt of **4a** and **4b** is small, it is significant within three estimated standard deviations.

5.3.2 [1]Chromarenophanes and [1]Vanadarenophanes.

Compared to [1]FCPs, only few examples of [1]chromarenophanes ([1]CAPs) and the [1]vanadarenophanes ([1]VAPs) are known in the literature. The first [1]CAPs and the first [1]VAPs were published in 1990 by Elschenbroich *et al.* (SiPh$_2$ moieties in bridging positions).[20] Since then, [1]CAPs had been described with silicon,[21-23] germanium,[24] zirconium,[25] and boron[26] in bridging positions.[27] Strained [1]VAPs are

known with the bridging elements silicon,[20-22] germanium,[24] and zirconium[25]. Very recently, highly strained cyclophanes of cycloheptrienyl-cyclopentadienyl sandwich compounds, isoelectronic species to bis(benzene) complexes, had been characterized.[28-32]

We have synthesized the first aluminum- and gallium-bridged [1]chromarenophanes ([1]CAPs) and [1]vanadarenophanes ([1]VAPs) in isolated yields of 54–81% from slurries of dilithiated metalloarenes and the dihalogen species **3a** and **3b**, respectively (Scheme 5-1). Usually, we apply ^{1}H NMR spectroscopy to check on the progress of a new reaction. However, the vanadium compounds are paramagnetic and inaccessible for NMR spectroscopy, and, consequently, we started with the syntheses of the chromium compounds. The optimized synthetic procedures for **5a** and **5b** were then adapted for the syntheses of the vanadium compounds **6a** and **6b**.

The [1]CAPs **5a** and **5b** show the expected signal pattern for time-averaged C_s symmetrical species in the ^{1}H and ^{13}C NMR spectra. For example, the aluminum compound **5a** exhibits five signals for the benzene rings [δ 3.74 and 4.35 (*o*-H), 4.53 and 4.60 (*m*-H), and 4.87 (*p*-H)] whereas in the case of the gallium counterpart **5b** a coincidental equivalency of the *meta*- and *para* protons results in just three signals [δ 3.69 and 4.18 (*o*-H), 4.74 (*m*-H and *p*-H)]. All these proton signals are relatively broad, and their width depends on how often a particular compound had been manipulated. ^{1}H NMR spectra with the smallest peak width and best resolved structure of the aromatic protons were obtained from freshly synthesized samples. Elschenbroich *et al.* described a similar phenomenon for $[(Ph_3SiC_6H_5)_2Cr]$. It was proposed that the presence of the paramagnetic chromium(I) species $[(Ph_3SiC_6H_5)_2Cr]^{+}$ leads to a fast electron transfer

with the neutral species $[(Ph_3SiC_6H_5)_2Cr]$ resulting in line broadening.[20] Electron exchange reactions of this type had been investigated before.[33] On the basis of these results, and in the absence of direct experimental evidence, we can only speculate that small amounts of the paramagnetic chromium(I) species **5a**$^+$ and **5b**$^+$, respectively, are responsible for the observed line broadening. The ^{13}C NMR spectra clearly reveal that both products **5a** and **5b** are strained [1]CAP. The resonances of the *ipso*-C atoms at δ 62.1 (**5a**) and 56.6 (**5b**) are significantly upfield shifted with respect to the parent bis(benzene)chromium (δ 74.8).[34] More pronounced upfield shifts are exhibited by the known [1]CAPs with $SiMe_2$ (δ 39.5),[23] $GeMe_2$ (δ 37.5),[24] $GePh_2$ (δ 36.4),[24] and $Zr(tBuC_5H_4)_2$ (δ 30.7)[25].

The [1]CAPs **5a** and **5b** and the [1]VAPs **6a** and **6b** all crystallized with half of a molecule of benzene in the asymmetric unit; all four compounds are isomorphous. Table 5-2 compiles crystal and structural refinement data and Figures 5-6 and 5-7 depict their molecular structures of the aluminum species (ORTEP plots of the gallium compounds **5b** and **6b** see Supporting Information).

Table 5-2. Crystal and Structural Refinement Data for Compounds **5a-b** and **6a-b**.

	5a · ½ C_6H_6	**5b** · ½ C_6H_6	**6a** · ½ C_6H_6	**6b** · ½ C_6H_6
	$C_{26}H_{43}AlCrNSi_3$	$C_{26}H_{43}CrGaNSi_3$	$C_{26}H_{43}AlNSi_3V$	$C_{26}H_{43}GaNSi_3V$
M_r	532.86	575.60	531.80	574.54
wave-length, Å	0.71073			
crystal system	triclinic			
space group (No.)	P-1 (2)			
Z	2	2	2	2
a, Å	8.96730(10)	8.9883(2)	8.9681(3)	8.9868(3)
b, Å	9.16420(10)	9.1772(2)	9.1579(3)	9.1721(3)
c, Å	19.6077(3)	19.6458(4)	19.6320(5)	19.6692(5)
α, deg	81.9412(11)	81.3833(14)	82.0285(18)	81.577(2)
β, deg	89.5973(11)	89.3431(14)	89.204(2)	89.047(2)
γ, deg	63.0923(11)	63.0831(11)	63.2623(17)	63.324(2)
vol, $Å^3$	1419.78(3)	1425.74(6)	1423.90(8)	1430.88(8)
d (calc), mg/m^3	1.246	1.341	1.240	1.334
temp, K	173(2)	173(2)	173(2)	173(2)
abs coeff., mm^{-1}	0.575	1.467	0.520	1.408
theta range, deg	2.52 to 30.50	2.52 to 30.51	2.52 to 27.58	2.52 to 27.54
refl collected	36806	39640	20973	21117
indep refl	8649 [R(int) = 0.0563]	8694 [R(int) = 0.0741]	6521 [R(int) = 0.0766]	6560 [R(int) = 0.0602]
abs correction	Psi-scan			
ref method	Full-matrix least-squares on F^2			
data / restr / params	8649 / 0 / 299	8694 / 0 / 299	6521 / 0 / 299	6560 / 0 / 299
goodness-of-fit on F^2	1.026	1.036	1.027	1.034
final R indices [I>2sigma(I)]	R1 = 0.0425, wR2 = 0.0984	R1 = 0.0469, wR2 = 0.0932	R1 = 0.0510, wR2 = 0.1034	R1 = 0.0403, wR2 = 0.0820
R indices (all data)	R1 = 0.0608, wR2 = 0.1089	R1 = 0.0776, wR2 = 0.1067	R1 = 0.0874, wR2 = 0.1205	R1 = 0.0610, wR2 = 0.0918
largest diff. peak and hole, $e.Å^{-3}$	0.384 and -0.609	0.564 and -0.722	0.333 and -0.455	0.362 and -0.537

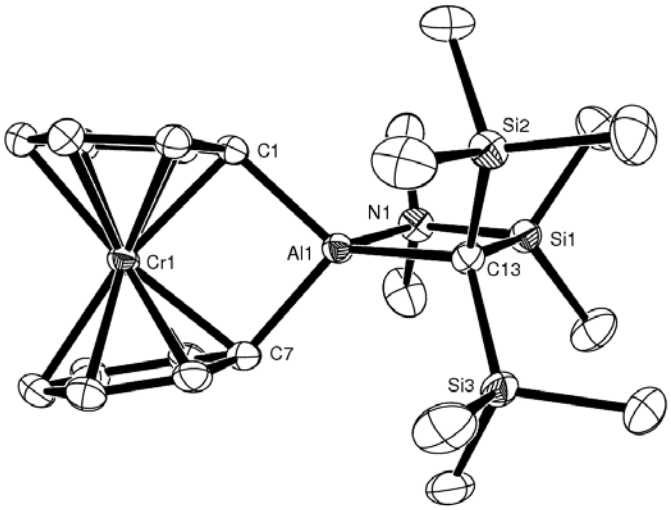

Figure 5-6. Molecular Structure of **5a** with thermal ellipsoids drawn at 50 % probability level. H atoms and ½ benzene are omitted for clarity. ORTEP plot for **5b** see Supporting Information. Selected atom-atom distances [Å] and bond angles [º] for **5a**: Al1-N1 = 2.0257(15), Al-C1 = 1.9979(17), Al1-C7 = 1.9940(17), Al1-C13 = 2.0412(16), Al1-Cr1 = 2.9740(5), C7-Al-C1 = 91.93(7), C7-Al1-N1 = 118.15(7), C1-Al1-N1 = 110.54(7), C7-Al1-C13 = 122.40(7), C1-Al-C13 = 129.30(7), N1-Al1-C13 = 86.47(6). Selected bond lengths (Å), atom-atom distances [Å], and angles [º] for **5b**: Ga1-N1 = 2.121(2), Ga-C1 = 2.017(2), Ga1-C7 = 2.012(3), Ga1-C13 = 2.055(2), Ga1-Cr1 = 3.0256(5), C7-Ga-C1 = 89.77(10), C7-Ga1-N1 = 117.79(9), C1-Ga1-N1 = 109.85(9), C7-Ga1-C13 = 124.90(10), C1-Ga1-C13 = 131.70(10), N1-Ga1-C13 = 86.50(9).

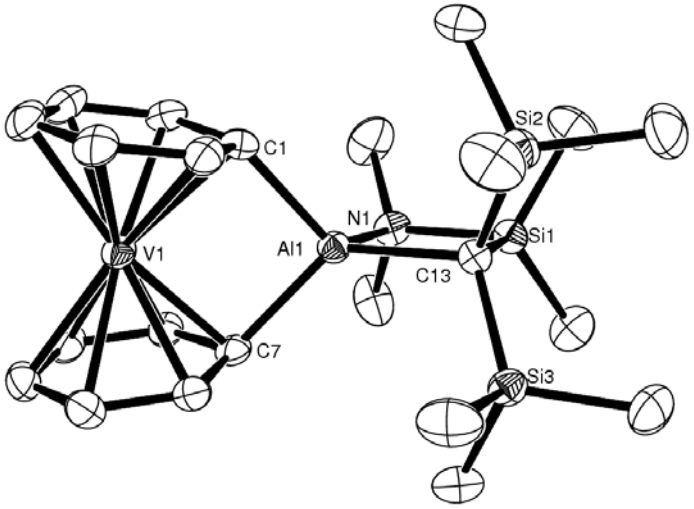

Figure 5-7. Molecular Structure of **6a** with thermal ellipsoids drawn at 50 % probability level. H atoms and ½ benzene are omitted for clarity. ORTEP plot for **6b** see Supporting Information Selected atom-atom distances [Å] and bond angles [º] for **6a**: Al1-N1 = 2.020(2), Al-C1 = 1.985(3), Al1-C7 = 1.995(3), Al1-C13 = 2.039(3), Al1-V1 = 2.9805(9), C7-Al-C1 = 93.78(11), C7-Al1-N1 = 110.27(11), C1-Al1-N1 = 117.52(11), C7-Al1-C13 = 128.51(11), C1-Al-C13 = 121.77(11), N1-Al1-C13 = 86.50(10). Selected atom-atom distances [Å] and bond angles [º] for **6b**: Ga1-N1 = 2.122(2), Ga-C1 = 2.017(3), Ga1-C7 = 2.007(3), Ga1-C13 = 2.053(2), Ga1-V1 = 3.0212(5), C7-Ga-C1 = 92.37(10), C7-Ga1-N1 = 117.21(11), C1-Ga1-N1 = 109.29(10), C7-Ga1-C13 = 124.15(10), C1-Ga1-C13 = 130.34(11), N1-Ga1-C13 = 84.53(9).

As in the case of the [1]FCPs **4a** and **4b** described before, the [1]CAPs and [1]VAPs show planar heterocycles containing the bridging elements aluminum and gallium, respectively [rms deviations from planarity [Å] are: 0.0082 (**5a**), 0.0042 (**5b**), 0.0050 (**6a)**, 0.0042 (**6b**)]. The bridging elements are distorted tetrahedrally surrounded by three C- and one N atom. Al–C distances are slightly shorter than respective Ga–C distances; respective E–C bond lengths are similar for the chromium and the vanadium species (Figure 5-6 and 5-7). Expectedly, E–N donor bonds are significantly shorter for aluminum than for gallium [Al1-N1 = 2.0257(15) (**5a**), Ga1-N1 = 2.121(2) (**5b**), Al1-N1

= 2.020(2) (**6a**), Ga1-N1 = 2.122(2) (**6b**)], which exemplifies that the lighter group 13 element is the stronger Lewis acid with respect to the NMe_2 donor group.

The alumina- and galla[1]metalloarenophanes **5** and **6** are strained species. Table 5-3 shows the set of common deformation angles α, θ, and δ (Figure 5-5) for the four species.

Table 5-3. Deformation angles α, θ, and δ [º] of **5** and **6** (see Figure 5-5).

	5a [**5b**]	**6a** [**6b**]
α	11.81(9) [13.24(13)]	14.65(14) [15.63(14)]
θ	91.93(7) [89.77(10)]	93.78(11) [92.37(10)]
δ[a]	170.63(7) [169.43(11)]	168.43(11) [167.30(11)]

[a] It was assumed that the δ angle have similar esd's as found for respective C-M-C angles (M = Cr, V; C: aromatic C atoms). The largest esd of C-M-C angles was taken for δ.

For the chromium and the vanadium compounds, respectively, the benzene rings are more tilted for the gallium-bridged species than for the aluminum-bridged species. The differences between the angles α for the [1]CAPs **5a** and **5b** of 1.4°, and for the [1]VAPs **6a** and **6b** of 1.0° are small but significant. A similar trend was observed for the [1]FCPs **4a** and **4b** discussed before (1.5°). The α angles of known [1]CAPs are 14.4° ($SiPh_2$),[20] 16.6(3)° ($SiMe_2$),[23] 14.4(2)° ($GePh_2$),[24] and 26.6(3)° [BN*i*Pr($SiMe_3$)][26]; those of [1]VAPs are 20.8° [SiRR'],[21] 19.9° [$Si(CH_2)_3$],[22] and 8º [$Zr(tBuC_5H_4)_2$][25].

5.4 Conclusions

Six new strained organometallic species were synthesized and structurally characterized. For all six species, the bridging Al- and Ga atom, respectively, are equipped with the same trisyl based ligand Me_2Ntsi (Figure 5-2). Hence, within the pairs

of compounds **4a**–**b**, **5a**–**b**, and **6a**–**b**, respectively, only the bridging element differs and this close relation allows revealing the influence of aluminum versus gallium as a bridging element. Commonly, the tilt angle α is taken as a measure of the extent of strain in cyclophanes (Figure 5-5). One major factor that governs α is the size of the bridging element. On the basis of covalent radii of 1.25 Å for aluminum and of 1.26 Å for gallium alone (singly bound, 3-fold coordinated elements),[35] a similar or a slightly higher tilt angle for the aluminum-bridged species **4a**, **5a**, and **6a** in comparison with the respective gallium-bridged species would be expected; surprisingly, just the opposite is the case. However, a glance at the neighboring group 14 elements Si and Ge reveals a similar situation, if only those molecules are compared that are equipped with the same set of ligands at the bridging element. On the basis of covalent radii of 1.17 Å for Si and of 1.22 Å for Ge alone (singly bound tetracoordinated elements),[35] smaller angles of α are expected for germanium-bridged species. However, for [1]CAPs with $SiPh_2$ and $GePh_2$ in bridging positions, respectively, the same value of α was detected [14.4(2)°].[24] Similarly, for [1]FCPs with $SiMe_2$ [α = 20.8(5)°][36] and $GeMe_2$ [α = 19.0(9)°][37] bridging moieties, the tilt angles α are the same within three estimated standard deviations. Causes for these small structural differences are unknown today.

With the synthesis of the new strained molecules **4** – **6** on hand, we started to explore their chemistry, in particular, with respect to polymerizations. Initial DSC measurements for **4a** and **4b**, respectively, showed exothermic peaks above 210°C, a typical indication that ROP occurred.

5.5 Experimental Section

General Procedures. All manipulations were carried out using standard Schlenk techniques. Solvents were dried using a Braun Solvent Purification System and stored under nitrogen over 4 Å molecular sieves. All solvents for NMR spectroscopy were degassed prior to use and stored under nitrogen over 4 Å molecular sieves. $[Fe(LiC_5H_4)_2] \cdot 2/3$ TMEDA,[38] $[Cr(C_6H_6)_2]$,[39] $[V(C_6H_6)_2]$,[40] $AlCl_2[C(SiMe_3)(SiMe_2NMe_2)]$ (**3a**),[16] and $GaCl_2[C(SiMe_3)(SiMe_2NMe_2)]$ (**3b**)[16] were synthesized as described in the literature. ^1H, ^{13}C, and ^{27}Al NMR spectra were recorded on a Bruker 500 MHz Avance at 25 ^oC, unless noted differently. ^1H chemical shifts were referenced to the residual protons of the deuterated solvents (C_6D_6 at δ 7.15); ^{13}C chemical shifts were referenced to the C_6D_6 signal at δ 128.0; ^{27}Al NMR spectra were referenced to $[Al(acac)_3]$ dissolved in C_6D_6. Mass spectra were measured on a VG 70SE (m/z > 10% are listed for signals of the most abundant ions). Elemental analyses were performed on a Perkin-Elmer 2400 CHN Elemental Analyzer using V_2O_5 to promote complete combustion.

$HC(SiMe_3)_2SiMe_2CH_2NMe_2$ (Me_2NCH_2tsiH). $HC(SiMe_3)_2Si(Me_2)Br$[41] (3.697 g, 12.4 mmol) in diethyl ether (30 mL) was added to $LiCH_2NMe_2$[42] (0.800 g, 12.3 mmol) in diethyl ether (20 mL) at −78 ^oC. The dry ice bath was removed and the solution stirred for 1 h to give a yellow solution. Volatiles were removed in vacuum, and the product was extracted with hexane (3 x 10 mL). After removal of hexane in vacuum, a yellow oil of $HC(SiMe_3)_2SiMe_2CH_2NMe_2$ was left behind (3.41 g, 99%). ^1H NMR (500 MHz): δ -0.56 (s, 1H, CH), 0.17 (s, 18H, $SiMe_3$), 0.23 (s, 6H, $SiMe_2$), 1.83 (s, 2H, CH_2), 2.15 (s, 6H, NMe_2).

(Me_2NCH_2tsi)$AlCl_2$ (2a). Due to an unsuccessful usage of **2a** as a starting material for [1]FCPs, the following procedure was not optimized. MeLi (11.5 mL, 1.0 M in THF, 11.5 mmol) was added to $HC(SiMe_3)_2SiMe_2CH_2NMe_2$ (2.87 g, 10.4 mmol) in THF (15 mL) at ambient temperature. After stirring for 1 h all volatiles were removed in vacuum to give an orange solid. Diethyl ether (20 mL) was added and $AlCl_3$ (1.42 g, 10.6 mmol) in diethyl ether (30 mL) was added at –78 °C. The mixture was stirred for 16 h at ambient temperature and filtered, and the solids were washed with 20 mL of diethyl ether. The combined filtrates were concentrated to 20 mL, and crystallization at app. –30°C gave yellow cubes of **2a** (1.41 g, 36%). ^{1}H NMR (500 MHz): δ 0.10 (s, 6H, $SiMe_2$), 0.44 (s, 18 H, $SiMe_3$), 1.48 (s, 2H, CH_2), 1.99 (s, 6H, NMe_2). ^{13}C NMR: δ 4.1 ($SiMe_2$), 5.8 (CSi_3), 7.4 ($SiMe_3$), 49.9 (NMe_2), 54.6 (CH_2). ^{27}Al NMR (130.3 MHz): δ 131 ($h_{½}$ = 800 Hz). MS (70 eV): *m/z* (%) = 356 (100) [M^+ – Me], 244 (62) [$C_{10}H_{26}NSi_3^+$], 73 (50) [$SiMe_3^+$]. Anal. Calcd. for $C_{12}H_{32}AlCl_2NSi_3$ (372.536): C, 38.69; H, 8.66; N, 3.76; Found: C, 38.45; H, 8.93; N, 3.11.

Al[1]FCP (4a). A suspension of dilithioferrocene · 2/3 TMEDA (0.874 g, 3.17 mmol)[38] in toluene (15 mL) was added dropwise via tubing to a solution of **3a** (1.04 g, 2.90 mmol)[16] in toluene (15 mL; -20 °C). After stirring for 16 h at ambient temperature, the red solution was filtered and all volatiles were removed at high vacuum (25 °C/0.01 mbar), upon which crystallization of pure **4a** occurred (1.33 g, 2.82 mmol, 97%). Single crystals of **4a** · ½ C_6H_6 for X-ray analysis were grown from benzene solutions at ca. 8 °C. ^{1}H NMR (500 MHz): δ 0.18 (s, 6H, $SiMe_2$), 0.45 (s, 18H, $SiMe_3$), 2.11 (s, 6H, NMe_2), 3.76, 4.24 (pst, 4H, C_5H_4), 4.58 (pst, 4H, C_5H_4). ^{13}C NMR (125.8 MHz): δ 2.9 ($SiMe_2$), 7.7 ($SiMe_3$), 40.9 (NMe_2), 53.0 (*ipso*-C, C_5H_4, -40 °C, C_7D_8), 75.4, 75.6, 75.9,

76.1 (C_5H_4); signal of *C*($SiMe_3$)$_2$ not detected. ^{27}Al NMR (130.3 MHz): δ 154 ($h_{½}$ = 4300 Hz). MS (70 eV): *m/z* (%) = 471 (100) [M^+], 456 (27) [M^+ – Me], 186 (12) [$FeCp_2^+$], 73 (10) [$SiMe_3^+$]. Anal. Calcd for $C_{21}H_{38}AlFeNSi_3$ (471.62): C, 53.48; H, 8.12; N, 2.97; Found: C, 53.65; H, 8.35; N, 2.70.

Ga[1]FCP (4b). As described for **4a**, dilithioferrocene · 2/3 TMEDA (1.17 g, 4.25 mmol)[38] in toluene (20 mL) and **3b** (1.70 g, 4.24 mmol)[16] in toluene (20 mL; -20 °C) resulted in a crude product of **4b**. Re-crystallization from toluene yielded red, needle shaped crystals of **4b** (1.48 g, 2.88 mmol, 68%). Single crystals of **4b** · ½ C_6H_6 for X-ray analysis were grown from benzene solutions at ca. 8 °C. ^{1}H NMR (500 MHz): δ 0.19 (s, 6H, $SiMe_2$), 0.42 (s, 18H, $SiMe_3$), 2.15 (s, 6H, NMe_2), 3.90, 4.24 (pst, 4H, C_5H_4), 4.54 (pst, 4H, C_5H_4). ^{13}C NMR (125.8 MHz): δ 3.0 ($SiMe_2$), 6.7 ($SiMe_3$), 41.9 (NMe_2), 47.2 (*ipso*-C, C_5H_4), 75.3, 76.2, 76.5 (C_5H_4); signal of *C*($SiMe_3$)$_2$ not detected. MS (70 eV): *m/z* (%) = 513 (10) [M^+], 186 (100) [$FeCp_2^+$], 121 (22) [$FeCp^+$], 73 (6) [$SiMe_3^+$], 58 (16) [Fe^+]. Anal. Calcd for $C_{21}H_{38}GaFeNSi_3$ (514.361): C, 49.04; H, 7.45; N, 2.72. Found: C, 49.93; H, 7.70; N, 2.42.

Al[1]CAP (5a). *n*BuLi (3.2 mL, 2.6 M in hexanes, 8.3 mmol) was added dropwise to a refluxing solution of [$Cr(C_6H_6)_2$] (0.638 g, 3.06 mmol) and TMEDA (1.217 g, 10.47 mmol) in cyclohexane (30 mL).[20] After refluxing for 1 h, the red reaction mixture was cooled to 0 ^{o}C, the liquid phase was removed via syringe, and the residual solid was dried on high vacuum (0.646 g, 1.92 mmol). A slurry of this solid in diethyl ether (30 mL, –20 ^{o}C) was added to a solution of **3a** (0.690 g, 1.92 mmol) in diethyl ether (10 mL, –20 ^{o}C). The reaction mixture was stirred for 16 h at ambient temperature and filtered, and additional product was extracted with diethyl ether (2 x 10

mL) from the filter cake. From the combined organic phases, all volatiles were removed in vacuum resulting in a crude solid, which was washed with hexane (3 x 15 mL) to give **5a** as a red-brown solid (0.490 g). Concentration of the washings to 10 mL gave an additional 0.272 g of **5a** (overall yield 0.762 g, 81%). Single crystals of **5a** · ½ C_6H_6 for X-ray analysis were grown from benzene solutions at ca. 8 °C. ^{1}H NMR (500 MHz, C_6D_6): δ 0.20 (s, 6H, $SiMe_2$), 0.49 (s, 18 H, 2 $SiMe_3$), 2.14 (s, 6H, NMe_2), 3.74 (d, 2H, *o*-H), 4.35 (d, 2H, *o*-H), 4.53 (pst, 2H, *m*-H), 4.60 (pst, 2H, *m*-H), 4.87 (pst, 2H, *p*-H). ^{13}C NMR: δ 3.0 ($SiMe_2$), 7.9 (2 $SiMe_3$), 9.2 ($AlCSiMe_3$) 40.6 (NMe_2), 62.1 (*ipso*-C), 77.6 (*p*-C), 77.9 (*o*-C), 78.4 (*o*-C), 80.7 (*m*-C), 81.2 (*m*-C). ^{27}Al NMR: δ 154 ($h_{1/2}$ = 3400 Hz); MS (70 eV): m/z (%) 493 (100) $[C_{23}H_{40}CrAlNSi_3]^+$, 450 (18) $[C_{21}H_{35}AlCrSi_3]^+$, 364 (95) $[C_{17}H_{35}AlNSi_3]^+$, 319 (16) $[C_{15}H_{28}AlSi_3]^+$, 287 (32) $[C_{11}H_{30}AlNSi_3]^+$, 247 (18), 230 (39) $[C_9H_{24}NSi_3]^+$, 201 (20) $[C_8H_{21}Si_3]^+$, 187 (18) $[C_7H_{19}Si_3]^+$, 175 (25), 129 (16) $[C_5H_{13}Si_2]^+$, 78 (32) $[C_6H_6]^+$, 73 (39) $[C_3H_9Si]^+$, 69 (49), 59 (13). Anal. Calcd for $C_{23}H_{40}AlCrNSi_3$ (493.810): C, 55.94; H, 8.16; N, 2.84; Found: C, 54.80; H, 8.58; N, 2.82.

Ga[1]CAP (5b). As described for **5a**, *n*BuLi (3.8 mL, 2.6 M in hexanes, 9.8 mmol), [$Cr(C_6H_6)_2$] (0.8112 g, 3.89 mmol), TMEDA (1.339 g, 8.64 mmol) and cyclohexane (25 mL)[20] resulted in a solid (0.923 g, 2.74 mmol). A slurry of this solid in benzene (30 mL, 0°C) and **3b** (1.063 g, 2.65 mmol) in benzene (10 mL, 0 °C) resulted in red-brown crystals of **5b** · ½ C_6H_6 (1.076 g, 69%) after crystallization from benzene. ^{1}H NMR (500 MHz, C_6D_6, 298 K): δ 0.21 (s, 6H, $SiMe_2$), 0.47 (s, 18 H, 2 $SiMe_3$), 2.16 (s, 6H, NMe_2), 3.69 (br. s, 2H, *o*-H), 4.18 (br. s, 2H, *o*-H), 4.74 (br. s, 6H, *m*-H, *p*-H). ^{13}C NMR: δ 3.1 ($SiMe_2$), 7.3 ($SiMe_3$), 12.4 ($GaCSi_3$) 41.8 (NMe_2), 56.6 (br, *ipso*-C), 78.0

(*p*-C), 78.4 (br, *o*-C) 82.4 (br, *m*-C). MS (70 eV): m/z (%) 535 (42) $[C_{23}H_{40}CrGaNSi_3]^+$, 406 (27) $[C_{17}H_{35}GaNSi_3]^+$, 290 (22), 230 (61) $[C_9H_{24}NSi_3]^+$, 187 (52) $[C_7H_{19}Si_3]^+$, 175 (32), 129 (41) $[C_5H_{13}Si_2]^+$, 73 (100) $[C_3H_9Si]^+$. Anal. Calcd for $C_{26}H_{43}CrGaNSi_3$ (575.605): C, 54.25; H, 7.53; N, 2.43; Found: C, 54.05; H, 8.07; N, 2.28.

Al[1]VAP (6a). As described for **5a**, *n*BuLi (2.8 mL, 2.6 M in hexanes, 7.3 mmol), $[V(C_6H_6)_2]$ (0.6019 g, 2.905 mmol), TMEDA (1.127 g, 9.70 mmol) and cyclohexane (25 mL) resulted in a solid (0.797 g, 2.38 mmol).[20] A slurry of this solid in diethyl ether (30 mL, –20 ^oC) and **3a** (0.863 g, 2.41 mmol) in diethyl ether (10 mL, –20 ^oC) resulted in dark-red crystals of **6a** · ½ C_6H_6 (0.678 g, 54%) after crystallization from benzene. IR (KBr; selected value are given): 846 (s), 1012 (w), 1251 (m), 2898 (w), 2953 (w). MS (70 eV): m/z (%) 492 (100) $[C_{23}H_{40}CrGaNSi_3]^+$, 449 (26) $[C_{21}H_{35}AlSi_3V]^+$, 364 (39) $[C_{17}H_{35}AlNSi_3]^+$, 302 (26) $[C_{12}H_{33}AlNSi_3]^+$, 246 (34), 230 (26) $[C_9H_{24}NSi_3]^+$, 219 (40), 217 (17) $[C_8H_{24}AlNSi_2]^+$, 207 (11) $[C_{12}H_{12}V]^+$, 203 (21), 129 (24) $[C_4H_{12}AlNSi]^+$, 102 (19) $[C_4H_{12}NSi]^+$, 78 (52) $[C_6H_6]^+$, 73 (40) $[C_3H_9Si]^+$. Anal. Calcd for $C_{23}H_{40}AlNSi_3V$ (531.812): C, 58.72; H, 8.15; N, 2.63; Found: C, 58.73; H, 8.60; N, 2.43;

Ga[1]VAP (6b). As described for **5a**, *n*BuLi (3.0 mL, 2.6 M in hexanes, 7.8 mmol) , $[V(C_6H_6)_2]$ (0.6508 g, 3.141 mmol), TMEDA (1.362 g, 11.7 mmol) and cyclohexane (25 mL) resulted in a solid (0.839 g, 2.50 mmol).[20] A slurry of this solid in diethyl ether (30 mL, –20 ^oC) and **3b** (1.011 g, 2.51 mmol) in diethyl ether (10 mL, –20 ^oC) resulted in dark-red crystals of **6b** · ½ C_6H_6 (0.830 g, 58%) after crystallization from benzene. IR (KBr; selected value are given): 676 (w) 845 (s), 997 (w), 1249 (m), 1458 (w), 2896 (w), 2953 (w). MS (70 eV): m/z (%) 534 (80) $[C_{23}H_{40}GaNSi_3V]^+$, 390 (25)

$[C_{16}H_{31}GaNSi_3]^+$, 344 (25), 247 (21), 230 (14) $[C_9H_{24}NSi_3]^+$ 102 (13) $[C_4H_{12}NSi]^+$, 78 (100) $[C_6H_6]^+$, 73 (21) $[C_3H_9Si]^+$, 59 (13). Anal. Calcd for $C_{26}H_{43}GaNSi_3V$ (574.550): C, 54.35; H, 7.54; N, 2.44; Found: C, 54.82; H, 7.78; N, 2.41.

Acknowledgement. We thank the Natural Sciences and Engineering Research Council of Canada (NSERC Discovery Grant, JM), the Department of Chemistry, the Saskatchewan Structural Sciences Centre, and the University of Saskatchewan for their generous support. We thank the Canada Foundation for Innovation (CFI) and the government of Saskatchewan for funding of the X-ray and NMR facilities in the Saskatchewan Structural Sciences Centre. We thank Alan J. Lough (University of Toronto) for a helpful discussion about tilt angles.

X-ray structural analysis for 2a, 4a, 4b, 5a, 5b, 6a, and 6b. Data was collected at -100 °C on a Nonius Kappa CCD diffractometer, using the COLLECT program.[43] Cell refinement and data reductions used the programs DENZO and SCALEPACK.[44] The program SIR97[45] was used to solve the structure and SHELXL97[46] was used to refine the structure. ORTEP-3 for Windows[47] was used for molecular graphics, and PLATON[48] was used to prepare material for publication. H atoms were placed in calculated positions with U_{iso} constrained to be 1.2 times U_{eq} of the carrier atom for the methylene protons and 1.5 times U_{eq} of the carrier atom for methyl hydrogen atoms.

Supporting Information Available. Crystallographic data for **2a**, **4a**, **4b**, **5a**, **5b**, **6a**, and **6b** in CIF file format. ORTEP plots for compounds **4b**, **5b**, and **6b**. This material is available free of charge via the Internet at http://pubs.acs.org.

5.6 References

(1) Osborne, A. G.; Whiteley, R. H. *J. Organomet. Chem*. **1975**, *101*, C27-C28.
(2) Foucher, D. A.; Tang, B. Z.; Manners, I. *J. Am. Chem. Soc*. **1992**, *114*, 6246-6248.
(3) Manners, I. *J. Chem. Soc., Chem. Commun*. **1999**, *10*, 857-944.
(4) Manners, I. *Science* **2001**, *294*, 1664-1666.
(5) Nguyen, P.; Gomez-Elipe, P.; Manners, I. *Chem. Rev*. **1999**, *99*, 1515-1548.
(6) Tanabe, M.; Vandermeulen, G. W. M.; Chan, W. Y.; Cyr, P. W.; Vanderark, L.; Rider, D. A.; Manners, I. *Nature Materials* **2006**, *5*, 467-470 and references therein.
(7) Berenbaum, A.; Braunschweig, H.; Dirk, R.; Englert, U.; Green, J. C.; Jäkle, F.; Lough, A. J.; Manners, I. *J. Am. Chem. Soc*. **2000**, *122*, 5765-5774.
(8) Braunschweig, H.; Dirk, R.; Müller, M.; Nguyen, P.; Resendes, R.; Gates, D. P.; Manners, I. *Angew. Chem., Int. Ed. Engl*. **1997**, *36*, 2338-2340.
(9) Braunschweig, H.; Breitling, F. M.; Gullo, E.; Kraft, M. *J. Organomet. Chem*. **2003**, *680*, 31-42.
(10) Schachner, J. A.; Lund, C. L.; Quail, J. W.; Müller, J. *Organometallics* **2005**, *24*, 785-787.
(11) Schachner, J. A.; Lund, C. L.; Quail, J. W.; Müller, J. *Organometallics* **2005**, *24*, 4483-4488.
(12) Eaborn, C.; Smith, J. D. *J. Chem. Soc., Dalton Trans*. **2001**, 1541-1552.
(13) Braunschweig, H.; Burschka, C.; Clentsmith, G. K. B.; Kupfer, T.; Radacki, K. *Inorg. Chem*. **2005**, *44*, 4906-4908.
(14) Schachner, J. A.; Orlowski, G. A.; Quail, J. W.; Kraatz, H.-B.; Müller, J. *Inorg. Chem*. **2006**, *45*, 454-459.
(15) Howson, J.; Eaborn, C.; Hitchcock, P. B.; Hill, M. S.; Smith, D. J. *J. Organomet. Chem*. **2005**, *690*, 69-75.
(16) Al-Juaid, S. S.; Eaborn, C.; El-Hamruni, S. M.; Hitchcock, P. B.; Smith, J. D. *Organometallics* **1999**, *18*, 45-52.
(17) See for example: Herberhold, M. *Angew. Chem., Int. Ed. Engl*. **1995**, *34*, 1837-1839.
(18) Rulkens, R.; Lough, A. J.; Manners, I. *Angew. Chem., Int. Ed. Engl*. **1996**, *35*, 1805-1807.
(19) Jäkle, F.; Rulkens, R.; Zech, G.; Foucher, D. A.; Lough, A. J.; Manners, I. *Chem., Eur. J*. **1998**, *4*, 2117-2128.
(20) Elschenbroich, C.; Hurley, J.; Metz, B.; Massa, W.; Baum, G. *Organometallics* **1990**, *9*, 889-897.
(21) Elschenbroich, C.; Bretschneider-Hurley, A.; Hurley, J.; Massa, W.; Wocadlo, S.; Pebler, J.; Reijerse, E. *Inorg. Chem*. **1993**, *32*, 5421-5424.
(22) Elschenbroich, C.; Bretschneider-Hurley, A.; Hurley, J.; Behrendt, A.; Massa, W.; Wocadlo, S.; Reijerse, E. *Inorg. Chem*. **1995**, *34*, 743-745.
(23) Hultzsch, K. C.; Nelson, J. M.; Lough, A. J.; Manners, I. *Organometallics* **1995**, *14*, 5496-5502.
(24) Elschenbroich, C.; Schmidt, E.; Gondrum, R.; Metz, B.; Burghaus, O.; Massa, W.; Wocadlo, S. *Organometallics* **1997**, *16*, 4589-4596.
(25) Elschenbroich, C.; Schmidt, E.; Metz, B.; Harms, K. *Organometallics* **1995**, *14*, 4043-4045.

(26) Braunschweig, H.; Homberger, M.; Hu, C. H.; Zheng, X. L.; Gullo, E.; Clentsmith, G.; Lutz, M. *Organometallics* **2004**, *23*, 1968-1970.
(27) For an historical overview and leading references about bis(benzene)chromium chemistry see: Seyferth, D. *Organometallics* **2002**, *21*, 1520-1530.
(28) Elschenbroich, C.; Paganelli, F.; Nowotny, M.; Neumüller, B.; Burghaus, O. *Z. Anorg. Allg. Chem.* **2004**, *630*, 1599-1606.
(29) Tamm, M.; Kunst, A.; Bannenberg, T.; Herdtweck, E.; Sirsch, P.; Elsevier, C. J.; Ernsting, J. M. *Angew. Chem., Int. Ed. Engl*. **2004**, *41*, 5530-5534.
(30) Braunschweig, H.; Lutz, M.; Radacki, K. *Angew. Chem., Int. Ed. Engl*. **2005**, *44*, 5647-5651.
(31) Bartole-Scott, A.; Braunschweig, H.; Kupfer, T.; Lutz, M.; Manners, I.; Nguyen, T.-l.; Radacki, K.; Seeler, F. *Chem., Eur. J.* **2006**, *12*, 1266-1273.
(32) Braunschweig, H.; Lutz, M.; Radacki, K.; Schaumlöffel, A.; Seeler, F.; Unkelbach, C. *Organometallics* **2006**, *25*, 4433-4435.
(33) Elschenbroich, C.; Zenneck, U. *J. Organomet. Chem*. **1978**, *160*, 125-137.
(34) Elschenbroich, C.; Koch, J. *J. Organomet. Chem*. **1982**, *229*, 139-158.
(35) Holleman-Wiberg *Inorganic Chemistry*; 1. English ed.; Academic Press: San Diego, London, **2001**, p 1756.
(36) Finckh, W.; Tang, B. Z.; Foucher, D. A.; Zamble, D. B.; Ziembinski, R.; Lough, A.; Manners, I. *Organometallics* **1993**, *12*, 823-829.
(37) Foucher, D. A.; Edwards, M.; Burrow, R. A.; Lough, A. J.; Manners, I. *Organometallics* **1994**, *13*, 4959-4966.
(38) Butler, I. R.; Cullen, W. R.; Ni, J.; Rettig, S. J. *Organometallics* **1985**, *4*, 2196-2201.
(39) *Synthetic methods of organometallic and inorganic chemistry* Herrmann, W. A., Ed.; Georg Thieme Verlag Stuttgart: New York, **1997**; Vol. 8.
(40) Fischer, E. O.; Reckziegel, A. *Chem. Ber*. **1961**, *94*, 2204-2208.
(41) Al-Juaid, S. S.; Eaborn, C.; Hitchcock, P. B.; Hill, M. S.; Smith, J. D. *Organometallics* **2000**, *19*, 3224-3231.
(42) Steinborn, D.; Becke, F.; Boese, R. *Inorg. Chem*. **1995**, *34*, 2625-2628.
(43) *Nonius*; Nonius BV, Delft, The Netherlands: **1998**.
(44) Otwinowski, Z.; Minor, W. In *Macromolecular Crystallography, Part A*; Carter, C. W., Sweet, R. M., Eds.; Academic Press: London, **1997**; Vol. 276, p 307-326.
(45) Altomare, A.; Burla, M. C.; Camalli, M.; Cascarano, G.; Giacovazzo, C.; Guagliardi, A.; Moliterni, A. G. G.; Polidori, G.; Spagna, R. *J. Appl. Crystallogr*. **1999**, 32, 115-119.
(46) Sheldrick, G. M.; University of Göttingen, Germany: **1997**.
(47) Farrugia, L. J. *J. Appl. Crystallogr*. **1997**, 30, 565.
(48) Spek, A. L.; University of Utrecht, The Netherlands: **2001**.

CHAPTER 6
PUBLICATION 4

The following chapter is a verbatim copy of an article which was published in *Organometallics*[*] on June 28, 2007. The article describes the synthesis of [1]ruthenocenophanes bridged by Al and Ga using the ligand Me_2Ntsi which stands for $C(SiMe_3)_2SiMe_2NMe_2$. In addition, initial results on ring-opening polymerization (ROP) of six different monomers, including four previously published [1]ferrocenophanes and the two new [1]ruthenocenophanes are described. This ROP work was done in collaboration with the Rehahn group at the TU Darmstadt, Germany. The authors of this paper are myself, who did the synthesis and characterization of the new [1]ruthenocenophanes and the work on ROP, Stefan Tockner, who worked with me on the ROP, Clinton L. Lund, who originally synthesized the ligands Pytsi and Me_2Ntsi, J. Wilson Quail, who did all structure determinations by single-crystal X-ray analysis, Matthias Rehahn, who is S.T. supervisor, and my supervisor Jens Müller. Written permission was obtained from all contributing authors to include this material within this thesis.

[*] Reproduced with permission from Organometallics. © 2007 American Chemical Society

6. [1]Metallocenophanes (M = Fe, Ru) of Heavier Group 13 Elements (E = Al, Ga): Synthesis, Characterization and Ring-Opening Polymerization

Jörg A. Schachner,[‡] Stefan Tockner,[†] Clinton L. Lund,[‡] J. Wilson Quail,[§] Matthias Rehahn[†] and Jens Müller[‡] *

Department of Chemistry and Saskatchewan Structural Sciences Centre, University of Saskatchewan, 110 Science Place, Saskatoon, Saskatchewan S7N 5C9, Canada, and Ernst-Berl Institute for Chemical Engineering and Macromolecular Science, Darmstadt University of Technology, Petersenstr. 22, D-64287 Darmstadt, Germany.

Received May 1, 2007

6.1 Abstract

Two new [1]ruthenocenophanes, Ru(η^5-C_5H_4)$_2$E(Me_2tsi) (Me_2Ntsi = C($SiMe_3$)$_2$$SiMe_2$$NMe_2$, E = Al, Ga), bridged by aluminum (**3a**) and gallium (**3b**) were synthesized by reaction of dilithioruthenocene with (Me_2Ntsi)ECl_2 in good to moderate yields (**3a**: 80%, **3b**: 36%). Both species were analyszed by standard techniques (multinuclear NMR spectroscopy, elemental analysis, UV-vis, MS) and their molecular structures were deduced from single-crystal X-ray analysis. Compared to the analogous [1]ferrocenophanes **2a**,**b**, compounds **3a**,**b** showed an increased ring tilt as indicated by the tilt angle α (**2a**, α = 14.33(14)°, **3a**, α = 20.31(19)°; **2b**, α = 15.83(19)°, **3b**, α = 20.91(19)°). Ring-Opening Polymerization (ROP) experiments with previously published aluminum- and gallium-bridged [1]ferrocenophanes Fe(η^5-C_5H_4)$_2$E(Pytsi)

(Pytsi = $C(SiMe_3)_2SiMe_2(2\text{-}C_6H_4N)$, E = Al (**1a**), Ga (**1b**)) and $Fe(\eta^5\text{-}C_5H_4)_2E(Me_2tsi)$ (E = Al (**2a**), Ga (**2b**)), and the [1]ruthenocenophanes **3a**,**b** (this paper) has been shown to be very sluggish or unsuccessful. Only the ROP of **1b** with $[Pd(dba)_2]$ (2 mol%, toluene, 25 °C, 48 h) resulted in polymeric material (GPC analysis: M_w = 2.11 x 10^4, PDI = 3.0).

6.2 Introduction

Since the discovery by Manners *et al*. that strained, ring-tilted [1]ferrocenophanes ([1]FeCPs) yield well-defined organometallic polymers via Ring-Opening Polymerization (ROP), most research in this area has focused on the ferrocene system.[1,2] Two reviews spanning both synthesis of strained metallacenophanes by Manners and properties of polyferrocenylsilanes by Rehahn appeared very reccently.[3,4] Examples of other [1]metallacyclophanes had been restricted to the bis-benzene complexes [1]vanadarenophanes and [1]chromarenophanes.[5,6] Recently, the field of strained [1]metallacyclophanes was expanded to heteroleptic sandwich complexes containing a five-membered cyclopentadienyl and seven-membered cycloheptatrienyl ring. The first example, a silicon bridged vanadium complex, was published by Elschenbroich *et al.*,[7] followed shortly by a report about a titanium complex published by Tamm *et al*.[8a] Since then, derivatives of $[Cr(C_5H_5)(C_7H_7)]$ bridged by silicon[9], of $[V(C_5H_5)(C_7H_7)]$ bridged by boron[10], and of $[Ti(C_5H_5)(C_7H_7)]$ bridged by Ge[8b] had been described. Very recently, the first bridged species of a benzene-cyclopentadienyl complex containing manganese was published by Braunschweig *et al*.[11] All the above-mentioned strained compounds contain 3d metals. The only strained sandwich

complexes containing a 4d metal are [1]ruthenocenophanes ([1]RuCPs) bridged by Zr- and Sn containing moieties, respectively.[12] The propensity towards ROP is directly related to the inherent ring strain of a [1]metallacyclophane. The release of ring strain and relaxation back to the coplanar arrangement of the cyclic ligands had been shown to be the driving force for ROP. An indication of the extent of the strain present can be accomplished by a crystallographic measurement of the α angle, which is the angle between the two planes of the tilted cyclic ligands (Figure 6-1). For a given transition-metal sandwich compound, the amount of ring tilting mainly depends on the size of the bridging element, where a small bridging element results in a larger α angle. To this day, the largest ring tilt of α = 32.4(2)° was found for a boron-bridged [1]FeCP.[13] The incorporation of the group 13 elements Al and Ga into [1]FeCPs, as in **1a**,**b** and **2a**,**b** (Figure 6-1), resulted in moderate ring tilt in the range of α = 14.33(14)° to 15.83(19)°,[14-16] comparable values as exhibited by tin-bridged [1]FeCPs ($SntBu_2$, α = 14.1(2)°;[17] $SnMes_2$, α = 15.2(2)°[18]). In contrast, the prototypical $SiMe_2$-bridged [1]FeCP shows a significant strain with α = 20.8(5)°.[19] Since the size of the bridging elements Al and Ga is invariant, we intended to increase the overall ring strain and therefore facilitate ROP by moving to a larger transition metal, namely ruthenium.

Within this paper, we describe the first aluminum- and gallium-bridged [1]ruthenocenophanes and our attempts to polymerize aluminum- and gallium-bridged [1]metallocenophanes.

6.3 Results and Discussion

Recently, we reported on the improved synthesis of alumina- and galla[1]ferrocenophanes by employing the intramolecular coordinating ligand Me_2Ntsi ($Me_2Ntsi = C(SiMe_3)_2SiMe_2NMe_2$) instead of Pytsi (Pytsi = $C(SiMe_3)_2SiMe_2(2\text{-}C_6H_4N)$) (Figure 6-1).[16]

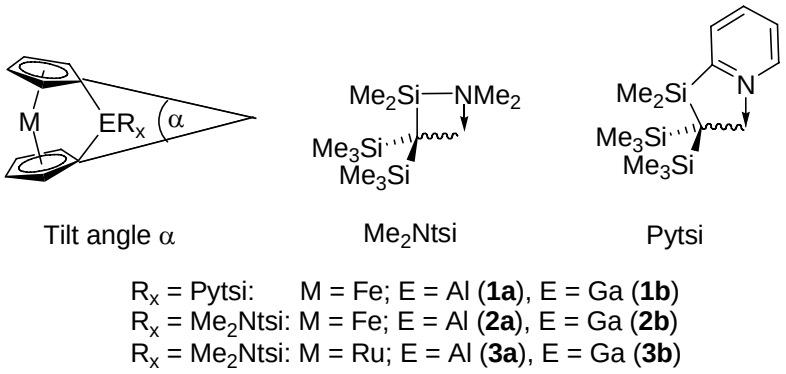

Figure 6-1. [1]Metallocenophanes stabilized with intramolecular coordinating ligands $Me_2N(tsi)$ and Py(tsi).

The ligand Me_2Ntsi, derived from the well-known trisyl ligand -$C(SiMe_3)_3$ by a formal substitution of one methyl group with a Me_2N group, provides intramolecular coordination via the nitrogen donor and steric shielding through the trimethylsilyl groups. Element dichlorides $(Me_2Ntsi)ECl_2$ of aluminum and gallium are easily accessible in five steps from readily available starting materials.[20] The [1]FeCPs of aluminum (**2a)** and gallium (**2b)** had been obtained from reaction with 1,1'-dilithioferrocene in very good yields (**2a** 96%, **2b** 68%).[16] The stabilizing Me_2Ntsi ligand also allowed for the isolation of the first aluminum- and gallium-bridged bis-benzene complexes of vanadium and chromium.[16]

Reaction of 1,1'-dilithioruthenocene with the respective dichloride of $(Me_2Ntsi)ECl_2$ in benzene yielded the new aluminum-bridged [1]RuCP **3a** and the gallium-bridged [1]RuCP **3b** in good to moderate yields (80% and 36%; eq 6-1).

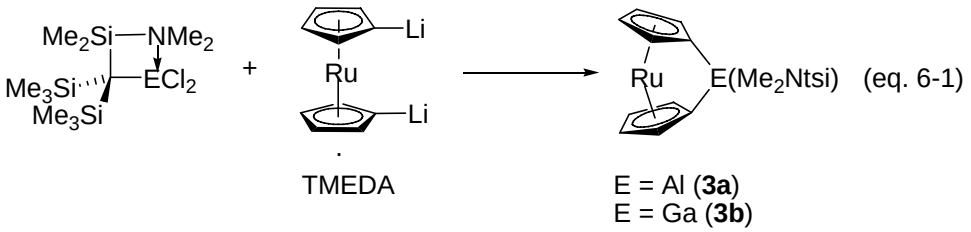

(eq. 6-1)

Both complexes can be crystallized from n-hexane or benzene, resulting in half of a solvent molecule in the asymmetric unit, as revealed by single-crystal X-ray crystallography (Table 6-2, Figure 6-2 and 6-3).

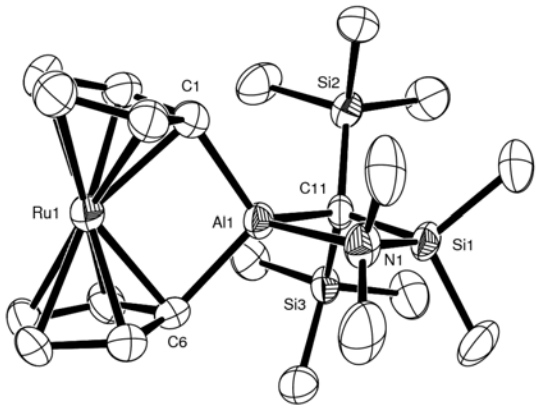

Figure 6-2. ORTEP plot of **3a** (thermal ellipsoids drawn at a 50 % probability level). H atoms and half a molecule of cyclohexane are omitted for clarity. Selected bond lengths [Å] and angles [°]: Al1-C1 = 2.018(5), Al1-C6 = 2.007(6), Al1-C11 = 2.034(5), Al1-N1 = 2.015(4), Al1-Ru1 = 2.7534(16), C1-Al1-C6 = 101.3(2), N1-Al1-C11 = 86.4(2), α = 20.31(19).

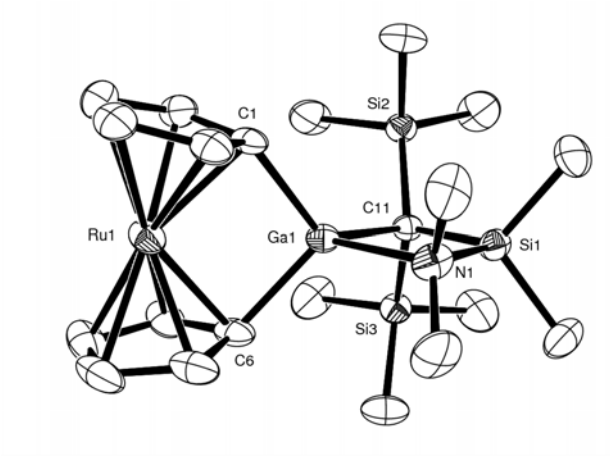

Figure 6-3. ORTEP plot of **3b** (thermal ellipsoids drawn at a 50 % probability level). H atoms and half a molecule of benzene are omitted for clarity. Selected bond lengths [Å] and angles [°]: Ga1-C1 = 2.047(3), Ga1-C6 = 2.037(3), Ga1-C11 = 2.054(3), Ga1-N1 = 2.107(3), Ga1-Ru1 = 2.8230(5), C1-Ga1-C6 = 98.42(13), N1-Ga1-C11 = 84.62(12), α = 20.91(19).

The bridging group 13 element in **3a** and **3b** is 4-fold coordinated with bond lengths and angles similar to those found for the respective [1]FeCPs.[16] Expectedly, the main difference between the new [1]RuCPs and the known [1]FeCPs is revealed by the tilt angle α. The gallium compound **3b** with α = 20.91(19)° seems to be slightly higher strained than **3a** with α = 20.31(20)°. Compared to the previously published [1]FeCPs [α = 14.33(14)° (**2a**); 15.83(19)° (**2b**)][16] this means an increase of the tilt angle of 42% (5.98°) for **3a** and of 32% (5.08°) for **3b**. The tilt angles α for **3a**,**b** are comparable to those of the prototypical Me_2Si-bridged [1]FeCPs **4** (α = 20.8(5)°).[19] The extent of the tilt in **2a,b** and **3a,b** are also reflected by a typical red-shift and increase in absorption coefficient of the lowest absorption band in the visible spectrum (Table 6-1).[18,21]

Table 6-1. UV-vis data of **2a,b** and **3a,b**[a].

Fe	λ_{max}	ε	α	Ru	λ_{max}	ε	α
Cp_2Fe	440	99	-	Cp_2Ru	322	160	-
2a	477	140	14.3	**3a**	357	560	20.3
2b	479	155	15.8	**3b**	358	365	20.9
Me_2Si[b]	482	375	20.8	Mes_2Sn[c]	363	436	20.6

[a] Units: λ_{max}, nm; ε, l/mol·cm; α, deg.[b] data taken from ref. 22.[c] data taken from ref 12.

Table 6-2. Crystal and structural refinement data for **3a**,**b**.

	3a · ½ C_6H_{14}	**3b** · ½ C_6H_6
empirical formula	$C_{24}H_{45}AlNRuSi_3$	$C_{24}H_{41}GaNRuSi_3$
formula weight	559.93	598.64
wavelength, Å	0.71073	0.71073
crystal system	triclinic	triclinic
space group (No.)	P-1	P-1
Z	2	2
a, Å	9.0629(6)	9.0977(3)
b, Å	12.8123(9)	9.1156(3)
c, Å	13.6050(7)	19.1531(7)
α, deg	110.401(4)	79.084(2)
β, deg	90.731(4)	84.375(2)
γ, deg	98.070(4)	62.2079(17)
vol, $Å^3$	1462.87(17)	1379.65(8)
d (calc), mg/m^3	1.271	1.441
temp, K	173(2)	173(2)
abs coeff., mm^{-1}	0.700	1.666
theta range, deg	2.63 to 26.00	2.53 to 27.41
refl collected	17766	22122
indep refl	5714 [R(int) = 0.0931]	6195 [R(int) = 0.0549]
abs correction	Psi-scan	Psi-scan
ref method	full-matrix least-squares on F^2	
data / restr / params	5714/168/339	6195 / 0 / 282
goodness-of-fit on F^2	1.028	1.044
final R indices [I>2sigma(I)]	R1 = 0.0574, wR2 = 0.1219	R1 = 0.0386, wR2 = 0.0813
R indices (all data)	R1 = 0.0920, wR2 = 0.1385	R1 = 0.0552, wR2 = 0.0894
largest diff. peak and hole, $e.Å^{-3}$	1.310 and -0.652	0.955 and -1.043

6.3.1 Ring-Opening Polymerization

We started to explore the application of compounds **1-3** as monomers in ROPs. Thermal, anionic, transition-metal catalyzed, and photocontrolled ROP are the four major pathways to synthesize high-molecular-weight polyferrocenes.[1-4] To test the ability of ring opening of a new monomer, usually a differential scanning calorimetry (DSC) experiment is performed. This experiment can provide a melting point (endothermic peak), the onset temperature for thermal-ROP, and the enthalpy of ring strain release.

Table 6-3. Comparison of DSC data.

	1a	**1b**	**2a**	**2b**	**3a**	**3b**	**4** [c]
m.p. (°C)	*a*	*a*	177	183	*a*	*a*	78
Onset (°C)	180	173	212	220	216	*b*	120
ΔH (kJ/mol)	-30	-55	-59	-43	-55	*b*	-80

[a] No melting point detected.[b] No exotherm detected.[c] Fe(η^5-C_5H_4)$_2$SiMe$_2$ (**4**), data taken from ref 19.

Compounds **1a**-**3a** all showed exothermic peaks, which we interpret as the result of ring opening (Table 6-3). Compounds **2a**,**b** also showed a sharp melting point without decomposition. Interestingly, **3b** showed a featureless spectrum in repeated DSC experiments up to 300 °C, indicating that neither melting nor ring opening occurred (see Supporting Information). To date, we cannot explain this unusual behaviour of **3b**. Even though the DSC results looked promising with respect to preparing new polymers via thermal ROP, all preparative attempts to obtain new polymers failed. In addition, we tested our monomers of types **1-3** with respect to anionic, transition-metal catalyzed, and photocontrolled ROP; however, preliminary

results showed that only the transition-metal-catalyzed ROP resulted in polymeric material (see below). All other attempts proved to be either sluggish or unsuccessful and full experimental details are given in the Supporting Information.

The most promising results were obtained with transition-metal(0) complexes as catalysts. For **1b** we did a series of experiments using 2 mol% [$Pd(dba)_2$] (dba = dibenzylideneacetone) in toluene or THF at ambient temperature or 40 °C for 48 h and analyzed the samples via GPC (Figure 6-4). In all cases, polymeric material was found independent of solvent or temperature.

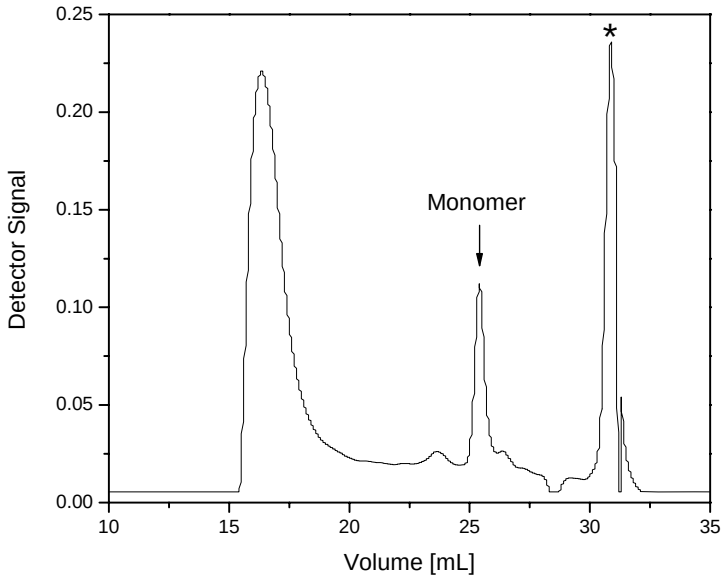

Figure 6-4. GPC trace obtained from polymerization of **1b** with [$Pd(dba)_2$] (2 mol%, toluene, 25 °C, 48 h; The asterisk indicates the internal standard toluene).

The solvent was removed from the reaction mixture on a rotaevaporator and directly injected into the GPC. The polymer fraction was eluted between 15 and 20 mL, giving a calculated polymer weight M_w of 2.11 x 10^4 with a PDI of 3.0. Interestingly,

under these conditions, unreacted monomer could be detected (V = 26 mL). We are currently working on optimizing the reaction conditions, including a workup procedure to purify the polymer from lower molecular weight oligomers and unreacted monomer. We also started to employ light scattering methods to unambiguously analyze polymer weights.

6.4 Conclusions

Within this paper we presented the synthesis of the first strained [1]RuCPs bridged by the group 13 elements aluminum (**3a)** and gallium (**3b**). Both compounds are very similar to their 3d metal counterparts **2a**,**b**,[171] with the main difference being the expected larger ring tilt in [1]RuCPs. Preliminary results on the ring-opening polymerization of aluminum- and gallium-bridged [1]metallocenophanes **1a**,**b**, **2a,b,** and **3a,b** were discussed. All strained complexes except for **3b** showed an exothermic ring opening at elevated temperatures as measured by DSC. However, out of attempted thermal, anionic, photocontrolled, and transition-metal-catalyzed ROP, only the latter method using [$Pd(dba)_2$] and monomer **1b** gave the first evidence of the formation of polymeric material. In conclusion, there might be three contributing factors to the little success of ROP so far. First, it seems that the intramolecular coordinating ligand Me_2Ntsi is too bulky and protects the C_5H_4 bridging element bonds from nucleophilic attack or oxidative insertion of an ROP initiator. Second, it is known that side group interactions between sterically demanding substituents cause a substantial destabilization of the targeted polymer, resulting in a significant decrease of polymerization enthalpy.[23] Third, although the monomers seem to thermally ring open, the Al–C or Ga–C bond formation in the propagation step might be hampered. It should

be mentioned that attempts to polymerize the only other example of a group 13 bridged [1]metallocenophane, a boron-bridged [1]FeCP, by thermal ROP and transition-metal-catalyzed ROP were also sluggish or unsuccessful.[23] To date, the only reported, well-characterized polyferrocene containing a group 13 element was obtained by polycondensation of an unstrained ferrocenylborane followed by derivatization to make the material soluble and less air sensitive.[24] The material was then analyzed by GPC and MALDI TOF-TOF and showed a polymerization degree of 21 repeating units.

6.5 Experimental Section

General Procedures. All manipulations were carried out using standard Schlenk techniques, if not noted differently. For synthesis the solvents were dried using a Braun Solvent Purification System and stored under nitrogen over a 4 Å molecular sieves. C_6D_6 and C_7D_8 were degassed prior to use and stored under nitrogen over a 4 Å molecular sieves. $AlCl_3$ and $GaCl_3$ were purchased from VWR, and $AlCl_3$ was sublimed prior to use. $RuCl_3 \cdot xH_2O$ (~41 % Ru) was purchased from Alfa Aesar and used as received. [$Pd(dba)_2$] was purchased from Acros Chemicals (16-21 % Pd). ^1H, ^{13}C and ^{27}Al NMR spectra were recorded on a Bruker 500 MHz Avance spectrometer; ^1H and ^{13}C chemical shifts were referenced to the deuterated solvent (C_6D_6: ^1H δ 7.15, ^{13}C δ 128.0; C_7D_8: $-CD_3$ ^1H δ 2.10, ^{13}C δ 20.4); ^{27}Al was referenced to [$Al(acac)_3$] in C_6D_6 (^{27}Al δ 0.0) . All NMR spectra were recorded in C_6D_6 at 25°C, unless noted differently. Mass spectra were measured on a VG 70SE and were reported in the form M (I) [F], where M is the mass observed, I (%) is the intensity of the peak relative to the most intense peak in the spectrum and F is the molecular ion or fragment. Elemental analysis

was performed on a Perkin-Elmer 2400 CHN Elemental Analyzer; samples were prepared in a glovebox and V_2O_5 was added to promote combustion.

For polymerization and light scattering experiments solvents were vacuum transferred from solutions containing the deep red 1,1-diphenylhexyllithium as an indicator. These so-prepared solvents were moved into a glovebox. All manipulations were carried out in a glovebox; glassware and NMR tubes for flame-sealing experiments were stored in an oven at 200 °C for at least one hour and moved directly into the antechamber of a glovebox. THF solutions for DLS (~5 mg/mL) were prepared in a glovebox, filtered a minimum of two times through Millex-FG13 PTFE syringe filter with 0.2 μm pore size directly into a 12 μl quartz cuvette capped with a plastic lid and sealed with para-film. DLS measurements were performed on a DynamPro-MS800.

Ruthenocene[25] and 1,1'-dilithioruthenocene · TMEDA[26] were synthesized according to literature.

Synthesis of 3a. A solution of $(Me_2Ntsi)AlCl_2$ (0.465 g, 1.27 mmol) in benzene (10 mL) was added dropwise via tubing to a suspension of dilithioruthenocene · TMEDA (0.457 g, 1.27 mmol) in benzene (10 mL). After stirring for 16 h, the color of the solution had changed to gold-brown. After filtration, the reaction mixture was concentrated upon which crystallization of pure **3a** occurred at 8 °C (0.53 g, 80%). These crystals contain half a molecule of benzene in the asymmetric unit. X-ray quality crystals were obtained through recrystallization from n-hexane. ^{1}H NMR (500 MHz): δ = 0.16 (s, 6H, $SiMe_2$), 0.43 (s, 18H, $SiMe_3$), 2.00 (s, 6H, NMe_2), 3.98, 4.48 (pst, 4H, C_5H_4), 5.21 (pst, 4H, C_5H_4). ^{13}C NMR (125.8 MHz): δ = 2.7 ($SiMe_2$), 7.7 ($SiMe_3$), 40.7 (NMe_2), 50.3 (*ipso*-C, C_5H_4, -40 °C, C_7D_8), 75.6, 76.2, 77.9, 78.2 (C_5H_4), one C is

obscured. ^{27}Al NMR (130.3 MHz): δ = 149 ($h_{½}$ = 2800 Hz). MS (70 eV, EI+): *m/z* (%): 517 (49) [M^+], 502 (46) [M^+ – Me], 459 (47) [M^+ – $SiMe_2$], 401 (30) [MH^+ – Me_2NSiMe_2], 232 (31) [$RuCp_2^+$], 73 (100) [$SiMe_3^+$]. UV (THF): λ_{max} [nm (ε)] 357 (560). Anal. Calcd for $C_{21}H_{38}AlRuNSi_3 \cdot 0.5\ C_6H_6$ (555.89): C, 51.85; H, 7.43; N, 2.52. Found: C, 50.36; N, 7.40; H, 2.71.

Synthesis of 3b. A solution of $(Me_2Ntsi)GaCl_2$ (0.564 g, 1.39 mmol) in benzene (10 mL) was added dropwise via tubing to a suspension of dilithioruthenocene · TMEDA (0.500 g, 1.39 mmol) in benzene (10 mL). After stirring for 16 h, the color of the solution had changed to gold-brown. After filtration, the reaction mixture was concentrated upon which crystallization of pure **3b** occurred at 8 °C (0.30 g, 36%). These crystals contain half a molecule of benzene in the unit cell. ^{1}H NMR (500 MHz): δ = 0.16 (s, 6H, $SiMe_2$), 0.40 (s, 18H, $SiMe_3$), 2.03 (s, 6H, NMe_2), 3.99, 4.38 (pst, 4H, C_5H_4), 5.22 (pst, 4H, C_5H_4). ^{13}C NMR (125.8 MHz): δ = 2.7 ($SiMe_2$), 6.9 ($SiMe_3$), 40.8 (*ipso*-C, C_5H_4, -40 °C, C_7D_8), 41.8 (NMe_2), 75.0, 75.6, 78.1 (C_5H_4), one C is obscured. MS (70 eV, EI+): *m/z* (%): 559 (1.7) [M^+], 246 (67) [Me_2NtsiH^+ - Me], 232 (22) [$RuCp_2^+$], 102 (27) [$SiMe_2NMe_2^+$], 78 (100) [$C_6H_6^+$], 73 (48) [$SiMe_3^+$]. UV (THF): λ_{max} [nm (ε)] 358 (365). Anal Calcd for $C_{21}H_{38}GaNRuSi_3 \cdot 0.5\ C_6H_6$ (598.64): C, 48.15; H, 6.90; N, 2.34. Found: C, 49.32; H, 8.36; N, 3.67.

Crystal structure determination. The crystal data of **3a,b** was collected at -100 °C on a Nonius Kappa CCD diffractometer, using the COLLECT program.[27] Cell refinement and data reductions used the programs DENZO and SCALEPACK.[28] SIR97[29] was used to solve the structure and SHELXL-97[30] was used to refine the structure. ORTEP-3 for Windows[31] was used for molecular graphics and PLATON[32]

was used to prepare material for publication. H atoms were placed in calculated positions with U_{iso} constrained to be 1.2 times U_{eq} of the carrier atom for aromatic protons. U_{iso} is constrained to be 1.5 times U_{eq} for methyl protons. For compound **3a**, a solvent n-hexane molecule was found disordered around a centre of symmetry. It was modelled in two different positions. The atoms were highly constrained to acceptable n-hexane geometries. After the n-hexane molecule had settled in positions, the positions and anisotropic displacement factors were frozen to complete the refinement.

Acknowledgement. We thank Dr. Andrew Ross and Doug Olson at NRC-PBI for measuring MALDI-TOF mass spectra. We thank the Natural Sciences and Engineering Research Council of Canada (NSERC Discovery Grant, J.M.), the Department of Chemistry, the Saskatchewan Structural Sciences Centre, and the University of Saskatchewan for their generous support. We thank the Canada Foundation for Innovation (CFI) and the government of Saskatchewan for funding of the X-ray and NMR facilities in the Saskatchewan Structural Sciences Centre (SSSC).

Supporting Information Available. Crystallographic data for **3a-b** in CIF file format; details on analysis of polymers (GPC, DLS, MALDI-TOF); experimental details on attempts with thermal-, anionic-, and photocontrolled-ROP. This material is available free of charge via the Internet at http://pubs.acs.org.

6.6 References

(1) Manners, I. *Science* **2001**, *294*, 1664-1666.
(2) Nguyen, P.; Gómez-Elipe, P.; Manners, I. *Chem. Rev*. **1999**, *99*, 1515-1548.
(3) Herbert, D. E.; Mayer, U. F. J.; Manners, I. *Angew. Chem. Int. Ed. Engl.* **2007**, *46*, asap
(4) Bellas, V.; Rehahn, M. *Angew. Chem., Int. Ed. Engl.* **2007**, *46*, asap
(5) Elschenbroich, C.; Hurley, J.; Metz, B.; Massa, W.; Baum, G. *Organometallics* **1990**, *9*, 889-897.

(6) Hultzsch, K. C.; Nelson, J. M.; Lough, A. J.; Manners, I. *Organometallics* **1995**, *14*, 5496-5502.
(7) Elschenbroich, C.; Paganelli, F.; Nowotny, M.; Neumüller, B.; Burghaus, O. *Z. Anorg. Allg. Chem.* **2004**, *630*, 1599-1606.
(8) (a) Tamm, M.; Kunst, A.; Bannenberg, T.; Herdtweck, E.; Sirsch, P.; Elsevier, C. J.; Ernsting, J. M. *Angew. Chem., Int. Ed. Engl.* **2004**, *43*, 5530-5534. (b) Tamm, M.; Kunst, A.; Bannenberg, T.; Randoll, S.; Jones, P. G. *Organometallics* **2007**, *26*, 417-424.
(9) Bartole-Scott, A.; Braunschweig, H.; Kupfer, T.; Lutz, M.; Manners, I.; Nguyen, T.-l.; Radacki, K.; Seeler, F. *Chem., Eur. J.* **2006**, *12*, 1266-1273.
(10) Braunschweig, H.; Lutz, M.; Radacki, K.; Schaumlöffel, A.; Seeler, F.; Unkelbach, C. *Organometallics* **2006**, *25*, 4433-4435.
(11) Braunschweig, H.; Kupfer, T.; Radacki, K. *Angew. Chem., Int. Ed. Engl.* **2007**, *46*, 1630-1633.
(12) Vogel, U.; Lough, A. J.; Manners, I. *Angew. Chem. Int. Ed. Engl* **2004**, *43*, 3321-3325.
(13) Braunschweig, H.; Dirk, R.; Müller, M.; Nguyen, P.; Resendes, R.; Gates, D. P.; Manners, I. *Angew. Chem., Int. Ed. Engl.* **1997**, *36*, 2338-2340.
(14) Schachner, J. A.; Lund, C. L.; Quail, J. W.; Müller, J. *Organometallics* **2005**, *24*, 785-787.
(15) Schachner, J. A.; Lund, C. L.; Quail, J. W.; Müller, J. *Organometallics* **2005**, *24*, 4483-4488.
(16) Lund, C. L.; Schachner, J. A.; Quail, J. W.; Müller, J. *Organometallics* **2006**, *25*, 5817-5823.
(17) Rulkens, R.; Lough, A. J.; Manners, I. *Angew. Chem., Int. Ed. Engl.* **1996**, *35*, 1805-1807.
(18) Jäkle, F.; Rulkens, R.; Zech, G.; Foucher, D. A.; Lough, A. J.; Manners, I. *Chem., Eur. J.* **1998**, *4*, 2117-2128.
(19) Foucher, D. A.; Tang, B. Z.; Manners, I. *J. Am. Chem. Soc.* **1992**, *114*, 6246-6248.
(20) Al-Juaid, S. S.; Eaborn, C.; El-Hamruni, S. M.; Hitchcock, P. B.; Smith, J. D. *Organometallics* **1999**, *18*, 45-52.
(21) Rulkens, R.; Gates, D. P.; Balaishis, D.; Pudelski, J. K.; McIntosh, D. F.; Lough, A. J.; Manners, I. *J. Am. Chem. Soc.* **1997**, *119*, 10976-10986.
(22) Pudelski, J. K.; Foucher, D. A.; Honeyman, C. H.; Lough, A. J.; Manners, I.; Barlow, S.; O'Hare, D. *Organometallics* **1995**, *14*, 2470-2479.
(23) Berenbaum, A.; Braunschweig, H.; Dirk, R.; Englert, U.; Green, J. C.; Jäkle, F.; Lough, A. J.; Manners, I. *J. Am. Chem. Soc.* **2000**, *122*, 5765-5774.
(24) Heilmann, J. B.; Scheibitz, M.; Qin, Y.; Sundararaman, A.; Jäkle, F.; Kretz, T.; Bolte, M.; Lerner, H.-W.; Holthausen, M. C.; Wagner, M. *Angew. Chem., Int. Ed. Engl.* **2006**, *45*, 920-925.
(25) Winter, C. H.; Pirzad, S.; Graf, D. D.; Cao, D. H.; Heeg, M. J. *Inorg. Chem.* **1993**, *32*, 3654-3659.
(26) Arnold, R.; Matchett, S. A.; Rosenblum, M. *Organometallics* **1988**, *7*, 2261-2266.
(27) Nonius; Nonius BV, Delft, The Netherlands: 1998.

(28) Otwinowski, Z.; Minor, W. In *Macromolecular Crystallography, Part A*; Carter, C. W., Sweet, R. M., Eds.; Academic Press: London, 1997; Vol. 276, p 307-326.
(29) Altomare, A.; Burla, M. C.; Camalli, M.; Cascarano, G.; Giacovazzo, C.; Guagliardi, A.; Moliterni, A. G. G.; Polidori, G.; Spagna, R. *J. Appl. Crystallogr.* **1999**, *32*, 115-119.
(30) Sheldrick, G. M.; University of Göttingen, Germany: 1997.
(31) Farrugia, L. J. *J. Appl. Crystallogr.* **1997**, *30*, 565.
(32) Spek, A. L.; University of Utrecht, The Netherlands: 2001.

CHAPTER 7
PUBLICATION 5

The following chapter is a verbatim copy of an electronic communication published in *Acta Crystallographica E*[*] in March 2005 and describes the synthesis of the first aluminum-bridged [1.1]ferrocenophane (Jörg A. Schachner, Clinton L. Lund, J. Wilson Quail, Jens Müller, *Acta Crystallogr.* **2005**, *E61*, m682-m684). The co-authors of this paper are Clinton L. Lund, who synthesized the ligand Pytsi, J. Wilson Quail, who did the structure determination by single-crystal X-ray analysis, and my supervisor Jens Müller. Written permission was obtained from all contributing authors and from IUCr to include this material within this thesis.

[*] Reproduced with permission from IUCr. http://journals.iucr.org/ © 2005 International Union of Crystallography

7. The First Aluminum-Bridged [1.1]Ferrocenophane

Jörg A. Schachner,[a] Clinton L. Lund,[a] J. Wilson Quail[b] and Jens Müller[a]*

[a]*Department of Chemistry, University Of Saskatchewan, 110 Science Place, Saskatoon, Saskatchewan, Canada, S7N 5C9, and* [b]*Saskatchewan Structural Sciences Center, University Of Saskatchewan, 110 Science Place, Saskatoon, Saskatchewan, Canada, S7N 5C9*

Received March 02, 2005

The structure of the title compound, bis(μ-ferrocene-1,1'-diyl)bis[chloro(N,N,N',N'-tetramethylethylenediamine)-aluminium], $[Al_2Fe_2Cl_2(C_2H_4)_4(C_4H_{16}N_2)_2]$, possesses a center of inversion and an *anti* conformation. Bound to each Al atom in the bridging position are one Cl atom and one molecule of N,N,N',N'-tetramethylethylenediamine (TMEDA). The angle between the least-squares planes of the two cyclopentadienyl (Cp) ligands is 3.6(3)°. The five C atoms in the Cp rings are staggered on average at an angle of 10.3(5)°

7.1 Comment

Recently, we synthesized the first alumina[1]ferrocenophane, (I), by a metathesis reaction of 1,1'-dilithioferrocene·0.67-TMEDA and (Pytsi)$AlCl_2$ [Pytsi = $C(SiMe_3)_2SiMe_2(2\text{-}C_2H_4N)$ and TMEDA = N,N,N',N'-tetramethylethylenediamine] using toluene as a solvent. Compound (I) was isolated as a crystalline material with one half-molecule of ferrocene ($FeCp_2$) in the asymmetric unit (Schachner et al., 2005). We assume that $FeCp_2$ results from the protolysis of 1,1'-dilithioferrocene, with toluene

being the source of protons. Consequently, we substituted toluene by the less acidic solvent hexane with the intention of optimizing the synthesis of (I). However, the title compound, (II), was the only isolable product from this reaction (isolated yield 9%).

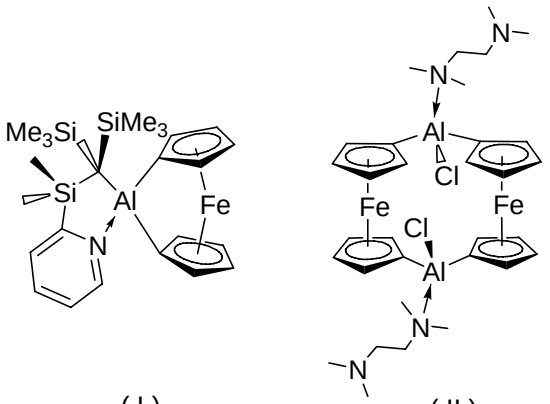

(I) (II)

Compound (II) is a [1.1]dialuminaferrocenophane in which each Al atom still carries one Cl atom and is coordinated by one molecule of TMEDA. So far, we could neither clarify how compound (II) is formed nor optimize its synthesis by a rational approach starting from 1,1'-dilithioferrocene·0.67-TMEDA and $AlCl_3$. To the best of our knowledge, there are no reports in the literature of other alumina[1.1]-ferrocenophanes; only similar bora (Scheibitz et al., 2003) and galla[1.1]ferrocenophanes (Uhl et al., 2001; Jutzi et al., 2001; Althoff et al., 2002, 2003) are described.

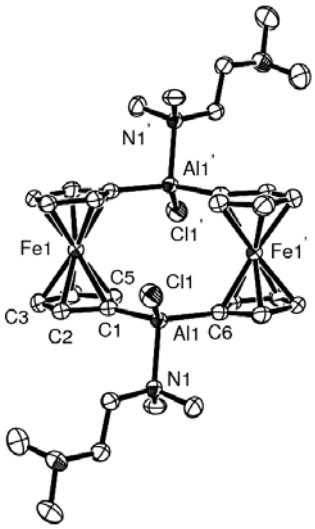

Figure 7-1. An ORTEP-3 view (Farrugia, 1997) of molecule (II), with displacement ellipsoids at the 50 % probability level. H atoms have been omitted for clarity. [Symmetry code: (') -x, -y,-z].

7.2 Experimental

A slurry of 1,1'-dilithioferrocene·0.67-TMEDA (582 mg, 2.11 mmol) in hexane (20 mL) was added drop-wise to a cooled (263 K) slurry of (Pytsi)$AlCl_2$ (826 mg, 2.10 mmol) in hexane (60 mL) and stirred for 72 h at room temperature. The resulting mixture was filtered to yield a light-red solution. After removal of some hexane in vacuum, orange crystals of (II) formed at 240 K (68 mg; 9%). ^{1}H NMR (500 MHz, C_6D_6, 298 K): δ 0.93–2.29 (m, 16H, TMEDA), 4.39 (m, 2H, Cp), 4.51 (m, 2H, Cp), 4.68 (m, 2H, Cp), 5.16 (m, 2H, Cp).

Crystal data	
$[Al_2Fe_2Cl_2(C_2H_4)_4(C_4H_{16}N_2)_2]$	Z = 1
M_r = 725.30	D_x = 1.419 mg m^{-3}
Triclinic *P*1	Mo *K*α radiation
a 7.8491(2) Å	Cell parameters from 3725
b = 10.2612(3) Å	reflections
c = 11.2111(5) Å	θ = 1.0-27.5°
α = 78.5212(12)°	μ = 1.09 mm^{-1}
β = 89.0564(12)°	T = 173(2) K
γ = 73.722(2)°	Chip, orange
V = 848.68(5) $Å^3$	0.20 x 0.20 x 0.12 mm

Data collection	
Nonius KappaCCD diffractometer	R_{int} = 0.045
φ scans, and ω scans with κ offsets	θ_{max} = 27.5
Absorption correction: none	h = -10 → 10
7256 measured reflections	k = -13 → 13
3869 independent reflections	l = -14 → 14
2697 reflections with I >2□(I)	

Refinement	
Refinement on F^2	$w = 1/[\sigma^2 (F_0^2) + (0.047P)^2$
$R[F^2 > 2\sigma(F^2)] = 0.047$	+ 0.4054P]
$wR(F^2) = 0.120$	where $P = (F_0^2 + 2F_c^2)/3$
S = 1.04	$(\Delta/\sigma)_{max} < 0.001$
3869 reflections	$\Delta\rho_{max}$ = 0.76 e $Å^{-3}$
194 parameters	$\Delta\rho_{min}$ = -0.51 e $Å^{-3}$
H-atom parameters constrained	

Table 7-1. Selected geometric parameters (Å,°).

Al1—C1	1.954 (3)	Fe1—C2	2.034 (3)
Al1—C6	1.958 (3)	Fe1—C3	2.038 (3)
Al1—N1	2.040 (3)	Fe1—C4	2.044 (3)
Al1—Cl1	2.1594 (12)	Fe1—C5	2.053 (3)
Fe1—C1	2.081 (3)		
C1—Al1—C6	119.59 (14)	C6—Al1—Cl1	112.74 (10)
C1—Al1—N1	101.62 (12)	N1—Al1—Cl1	101.45 (8)
C6—Al1—N1	103.03 (11)		
C1—Al1—Cl1	114.94 (10)		
C6—Al1—C1—C2	179.6 (3)	Cl1—Al1—C1—C2	41.4 (3)
N1—Al1—C1—C2	67.2 (3)		

H atoms were placed in calculated positions, with C—H distances ranging from 0.95 to 0.99 Å, and included in the refinement in the riding-model approximation, with U_{iso}(H) values constrained to be 1.2 times U_{eq} of the carrier atom.

Data collection: COLLECT (Nonius, 1998); cell refinement: SCALEPACK (Otwinowski & Minor, 1997); data reduction: SCALEPACK and DENZO (Otwinowski & Minor, 1997); program(s) used to solve structure: SIR97 (Altomare et al., 1999); program(s) used to refine structure: SHELXL97 (Sheldrick, 1997); molecular graphics: ORTEP-3 for Windows (Farrugia, 1997); software used to prepare material for publication: PLATON (Spek, 2003).

We thank the Natural Sciences and Engineering Research Council of Canada (NSERC Discovery Grant), the Department of Chemistry and the University of Saskatchewan for their generous support. The authors also thank the Canadian Foundation for Innovation and the Government of Saskatchewan for funding of the X-ray laboratory.

7.3 References

Althoff, A., Jutzi, P., Lenze, N., Neumann, B., Stammler, A. & Stammler, H.-G. (2002). Organometallics, 21, 3018–3022.
Althoff, A., Jutzi, P., Lenze, N., Neumann, B., Stammler, A. & Stammler, H.-G. (2003). Organometallics, 22, 2766–2774.
Altomare, A., Burla, M. C., Camalli, M., Cascarano, G., Giacovazzo, C., Guagliardi, A., Moliterni, A. G. G., Polidori, G. & Spagna, R. (1999). J. Appl. Cryst. 32, 115–119.
Farrugia, L. J. (1997). J. Appl. Cryst. 30, 565.
Jutzi, P., Lenze, N., Neumann, B. & Stammler, H.-G. (2001). Angew. Chem. Int. Ed. 40, 1424–1427.
Nonius (1998). COLLECT. Nonius BV, Delft, The Netherlands.
Otwinowski, Z. & Minor, W. (1997). Methods in Enzymology, Vol. 276, Macromolecular Crystallography, Part A, edited by C. W. Carter Jr & R. M. Sweet, pp. 307–326. New York: Academic Press.
Schachner, J. A., Lund, C. L., Quail, J. W. & Müller, J. (2005). Organometallics, 24, 785–787.

Scheibitz, M., Winter, R. F., Bolte, M., Lerner, H.-W. & Wagner, M. (2003). Angew. Chem. Int. Ed. 42, 924–927.
Sheldrick, G. M. (1997). SHELXL97. University of Göttingen, Germany.
Spek, A. L. (2003). J. Appl. Cryst. 36, 7–13.
Uhl, W., Hahn, I., Jantschak, A. & Spies, T. (2001). J. Organomet. Chem. 637, 300–303.

CHAPTER 8
PUBLICATION 6

This chapter is a verbatim copy of a published article in *Inorganic Chemistry*[*] from September 2005 and describes the synthesis, characterization and electrochemistry of three isostructural [1.1]ferrocenophanes bridged by Al, Ga and In, with the latter two being new complexes. The intramolecular ligand employed was N,N-dimethylbenzylamine (Ar' = 2-(Me_2NCH_2)C_6H_4). It was shown that these three complexes have significantly different electrochemical properties. This project was done in collaboration with the Kraatz group. The co-authors on this paper are Grzegorz A. Orlowski, who I did the electrochemical measurements with, J. Wilson Quail, who did all structure determinations by single-crystal X-ray analysis, Heinz-Bernhard Kraatz, who is G. A. O. supervisor, and my supervisor Jens Müller. Written permission was obtained from all contributing authors to include this material within this thesis.

[*] Reproduced with permission from Inorganic Chemistry. © 2006 American Chemical Society

8. Synthesis, Chacterization, and Electrochemical Studies on [1.1]Ferrocenophanes Containing Aluminum, Gallium and Indium

Jörg A. Schachner[‡] , Grzegorz A. Orlowski[‡], J. Wilson Quail[§], Heinz-Bernhard Kraatz[‡] and Jens Müller[‡,]*

Department of Chemistry and Saskatchewan Structural Sciences Centre, University of Saskatchewan, 110 Science Place, Saskatoon, Saskatchewan S7N 5C9, Canada

Received September 20, 2005

8.1 Abstract

The synthesis, characterization, structure, and electrochemistry of [1.1]ferrocenophanes, bridged by the heavier group 13 elements aluminum (**1a**), gallium (**1b**) and indium (**1c**) are described and discussed. Compounds **1a-c** have been synthesized from dilithioferrocene and intramolecularly coordinated group 13 element dihalides Ar'EX_2 (Ar' = 2-(Me_2NCH_2)C_6H_4; EX_2 = $AlCl_2$, $GaCl_2$, InI_2). Although the synthesis and characterization of **1a** by single-crystal X-ray analysis has been described recently (Braunschweig, H.; Burschka, C.; Clentsmith, G. K. B.; Kupfer, T.; Radacki, K. *Inorg. Chem.* **2005**, *44*, 4906), compounds **1b** and **1c** are described for the first time. The galla (**1b**) and the inda (**1c**) [1.1]ferrocenophane have been characterized by single-crystal X-ray determination [**1b**: $C_{38}H_{40}Fe_2Ga_2N_2$, monoclinic, $P2_1/c$, a = 10.3467(5) Å, b = 11.6311(4) Å, c = 14.0747(7) Å, β = 105.931(2)°, Z = 2; **1c**: $C_{38}H_{40}Fe_2In_2N_2$, monoclinic, $P2_1/c$, a = 10.5522(7) Å, b = 11.8476(8) Å, c = 13.9855(9) Å, β = 104.990(3)°, Z = 2]. All three compounds **1a-c** are *anti* conformers with *trans*

orientations of the two donating NMe_2 groups. For the [1.1]ferrocenophane **1a**, an unprecedented fully reversible two-electron redox process was observed by cyclic voltammetry, whereas the corresponding Ga and In species exhibit a more conventional stepwise redox chemistry. According to the Robin-Day classification, **1a** is a class I, and **1b** and **1c** are class II species. In addition to the reversible processes, compound **1a** shows an irreversible oxidation at higher voltages accompanied by adsorption processes. The irreversible adsorption process was investigated with an electrochemical quartz crystal microbalance (EQCM).

8.2 Introduction

During the last two decades, inorganic polymers containing metals in their backbones have attracted considerable interest because of their wide range of tunable properties (e.g., redox, magnetic, electrical, and chemical). The main route to these polymers is via ring opening polymerization (ROP) of strained [1]ferrocenophanes (Figure 8-1, **I**) developed by Manners and coworkers.[1] The formal dimer of a [1]ferrocenophane is an unstrained [1.1]ferrocenophane, where two ferrocene moieties are linked by two ER_x groups (Figure 8-1, **II**).

To date, [1.1]ferrocenophanes with various R groups have been reported for elements of groups 13 (B, Al, Ga),[2-4] 14 (C, Si, Sn, Pb),[5-8] and 15 (P).[9] The conformation of a dimer largely depends on the size of the bridging element E and the bulkiness of the substituents R. All reported group 13 bridged [1.1]ferrocenophanes adopt an *anti* conformation. Although not useable for ROP, because of the lack of intrinsic ring strain, [1.1]ferrocenophanes have attracted significant interest for different reasons. The methylene-bridged *syn*-[1.1]ferrocenophane ($ER_x = CH_2$) catalyzes the

formation of H_2 upon protonation.[10] Furthermore, the deprotonation of the *syn*-[1.1]ferrocenophane resulted in a carbanion with an unprecedented hydrogen bond between the two bridging carbon atoms.[10]

The electronic interaction between the two ferrocene redox centers in [1.1]ferrocenophanes can be classified according to the Robin-Day scheme.[11] In class I compounds, no interaction between the redox centers exists, and thus the molecule displays the properties of the isolated redox centers. For classes II and III, the two redox centers influence each other, which is noticeable in the redox properties and spectroscopic properties of the dimer. For class II systems, the interactions are moderate interactions, whereas for class III systems, the redox centers interact strongly.[11] At present, all of the reported [1.1]ferrocenophanes display two fully reversible one-electron oxidation waves. This is generally interpreted by the sequential oxidation of the two ferrocene centers, initially generating a monocation, which in a separate step is oxidized at a higher oxidation potential to generate a dicationic species. In general, [1.1]ferrocenophanes are classified as class II compounds exhibiting moderate electronic interactions between the two redox centers.

In the course of our investigation of ferrocenophanes equipped with the heavier group 13 elements Al, Ga, and In, we employed two different intramolecularly coordinating ligands (Figure 8-2).

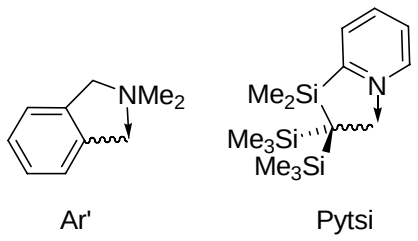

Figure 8-2. Intramolecularly coordinating ligands.

The "pytrisyl" ligand is derived from the parent trisyl ligand $C(SiMe_3)_3$ by formal substitution of one methyl group with a pyridyl ring. This bulky ligand with donor capability was introduced by Eaborn and Smith in 2000.[12] Recently, we have shown that reaction of dilithioferrocene with (Pytsi)ECl_2 (E = Al,[13] Ga[14]) gives access to [1]ferrocenophanes, the first [1]metallocenophanes with aluminum and gallium in the bridging position. In the case of the indium compound (Pytsi)$InCl_2$, an unusual ferrocenophane with an In–(μ-Cl)$_2$–In moiety was characterized.[14]

Within this report, we describe the synthesis and electrochemical analysis of [1.1]ferrocenophanes with bridging elements Al, Ga, and In (Figure 8-1). As the ligand R attached to the group 13 element we used the intramolecularly coordinating "one-armed" phenyl substituents, 2-(Me_2NCH_2)C_6H_4 (Ar', Figure 8-2).

8.3 Results and Discussion

Reaction of dilithioferrocene·with Ar'EX_2 (Ar' = 2-(Me_2NCH_2)C_6H_4; EX_2 = $AlCl_2$, $GaCl_2$, InI_2) gave the respective [1.1]ferrocenophanes in moderate yields (eq 8-1).

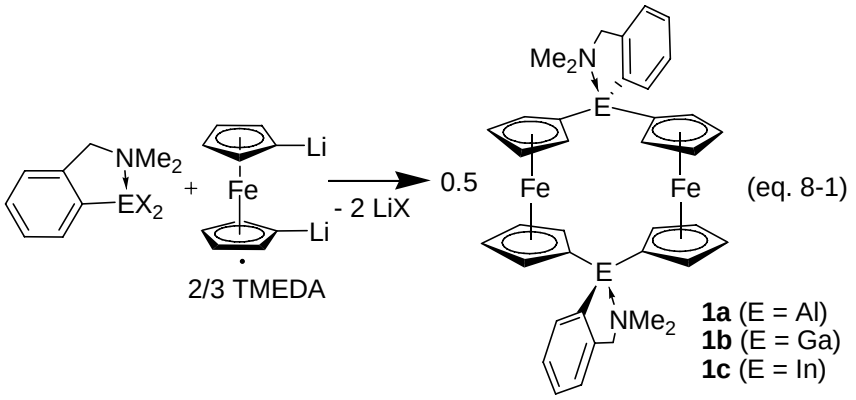

In the course of our investigations, the synthesis and molecular structure of the [1.1]ferrocenophane **1a** have been published by Braunschweig *et al*.[3b] Their published data agree very well with ours, including that of a structure determination by a single-crystal X-ray analysis. The molecular structures of compounds **1b** and **1c** are depicted in Figures 8-3 and 8-4; the crystal and structural refinement data are compiled in Table 8-1. All three [1.1]ferrocenophanes **1a-c**[3b] are isostructural and *anti* conformers (Figure 8-1). In addition to the relative orientation of the bridging elements, which is described by the prefixes *anti* and *syn* (see Figure 8-1), the dimethyl amino groups, in principle, could exhibit two different orientations each. For all three species **1a**–**c**, the amino moieties are pointing away from each other. Each amino group is outside the space provided by the two ferrocene units, which have a *trans* orientation.

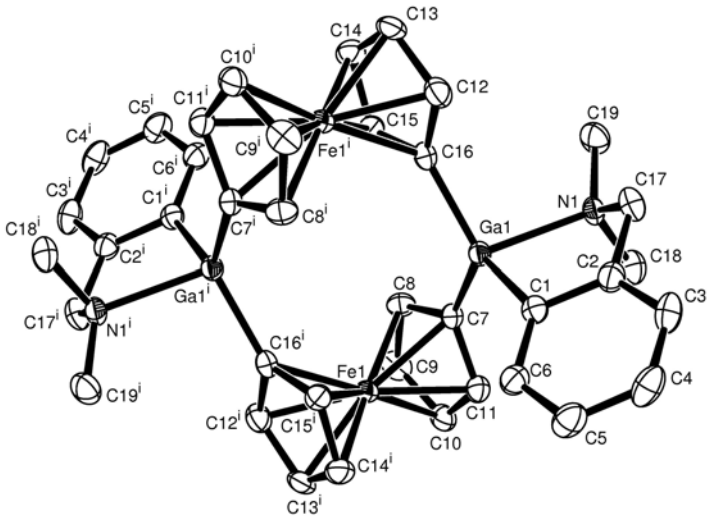

Figure 8-3. ORTEP plot of compound **1b**. Thermal ellipsoids are drawn at the 50% probability level. H atoms are omitted for clarity. X^i atoms are generated by -x, -y, -z operation.

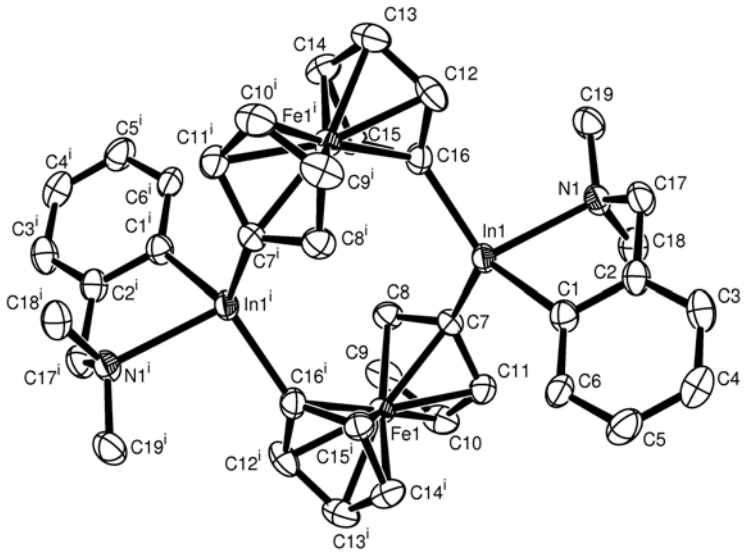

Figure 8-4. ORTEP plot of compound **1c**. Thermal ellipsoids are drawn at the 50% probability level. H atoms are omitted for clarity. X^i atoms are generated by -x, -y, -z operation.

Like those in **1a**, the E-C and E-N bond lengths and the angles around the metal centers of **1b** and **1c** are unremarkable (**1a**:[3b] Al-N = 2.0748(14) Å; Al-C: 1.9571(16), 1.9599(17), 1.9856(17) Å; **1b** : Ga1-N1 = 2.178(3) Å, Ga-C1, -C7, -C16 = 1.988(3), 1.951(4), 1.963(3) Å; ∠ C1-Ga1-C16 = 123.20(15)°, C7-Ga1-C16 = 117.71(15)°, C1-Ga1-C7 = 115.37(15)°; **1c**: In1-N1 = 2.386(4) Å, In1-C1, -C7, -C16 = 2.178(5), 2.150(5), 2.136(5) Å; ∠ C1-In1-C16 = 126.03(18)°, C7-In1-C16 = 116.32(17)°, C1-In1-C7 = 115.63(17)°). With respect to a possible Fe-Fe interaction in these species, the Fe-Fe distances are worth mentioning. As expected, the Al compound **1a** (5.443 Å)[3b] and the Ga species **1b** (5.462 Å) exhibit a similar Fe-Fe distance, whereas that of **1c** is slightly longer (5.724 Å).

^{1}H and ^{13}C NMR spectra of compounds **1a-c** show signal patterns for one type of Ar' and one type of C_5H_4 ligand. These spectra can be interpreted as being caused by time-averaged C_{2h} symmetrical species. This indicates that the molecular structures of **1a-c** in solution are similar to those in the solid state, taking into account the well-known, fast inversion of the five-membered rings of the coordinated Ar' ligands.[15]

Table 8-1. Crystal and structural refinement data for compounds **1b** and **1c**.

	1b	**1c**
empirical formula	$C_{38}H_{40}Fe_2Ga_2N_2$	$C_{38}H_{40}Fe_2In_2N_2$
formula weight	775.85	866.06
wavelength, Å	0.71073	0.71073
crystal system	monoclinic	monoclinic
space group (No.)	$P2_1/c$	$P2_1/c$
Z	2	2
a, Å	10.3467(5)	10.5522(7)
b, Å	11.6311(4)	11.8476(8)
c, Å	14.0747(7)	13.9855(9)
α, deg	90	90
β, deg	105.931(2)	104.990(3)
γ, deg	90	90
vol, Å^3	1628.75(13)	1688.94(19)
d (calc), mg/m^3	1.582	1.703
temp, K	173(2)	173(2)
abs coefficient, mm^{-1}	2.540	2.219
theta range, deg	2.69 to 26.37	3.02 to 25.98
refl collected	6339	19945
indep refl	3325 [R(int) = 0.0520]	3304 [R(int) = 0.0891]
abs correction	none	psi-scan, T_{min} = 0.269, T_{max} = 0.350
ref method	full-matrix least-squares on F^2	
data / restr / params	3325 / 0 / 201	3304 / 0 / 201
goodness-of-fit on F^2	1.021	1.086
final R indices [I>2sigma(I)]	R1 = 0.0394, wR2 = 0.0711	R1 = 0.0448, wR2 = 0.1019
R indices (all data)	R1 = 0.0708, wR2 = 0.0817	R1 = 0.0560, wR2 = 0.1107
largest diff. peak and hole, e.Å^{-3}	0.563 and -0.528	2.056 and -1.635

We expected to find that compounds **1a**–**c** exhibit essentially the same electrochemistry and display weak electronic communication between the redox centers (class II compounds). However, to our surprise the redox properties examined by cyclic voltammetry (CV) of the Al, Ga, and In species are significantly different. The redox properties of compounds **1a-c** are summarized in Table 8-2.

The CV of the Al species **1a** shows two oxidation waves and one reduction wave (Figure 8-5). The first redox wave ($E_{1/2}$ = 0.36 V vs Ag/AgCl) is fully reversible and corresponds to a two-electron process. To calculate the number of electrons involved in the oxidation step, we measured the Cottrell constant via chronocoulometry on a Pt electrode by assuming the same diffusion coefficient as that measured for **1b** (D = 2.4 x 10^{-5} cm^2/s, assuming $n = 2e^-$).[16] The gallium compound **1b** displays two reversible one-electron processes at $E_{1/2}$ = 0.05 and $E_{1/2}$ = 0.35 V (Figure 8-6). However, the redox behavior of the In compound **1c** is more complex (Figure 8-7, Table 8-2). Because the half-wave potentials $E_{1/2}$ could not be obtained reliably, we would like to report the oxidation potentials E_{ox} for **1c** instead. The voltammogram is composed of two major oxidation waves at E_{ox1} = 0.12 V and E_{ox2} = 0.39 V and two poorly resolved minor oxidation waves around E'_{ox1} = 0.0 V and E'_{ox2} = 0.2 V (Figure 8-7, Table 8-2). Importantly, the redox waves of all species are fully reversible, and have a ratio of the peak currents that is close to unity.

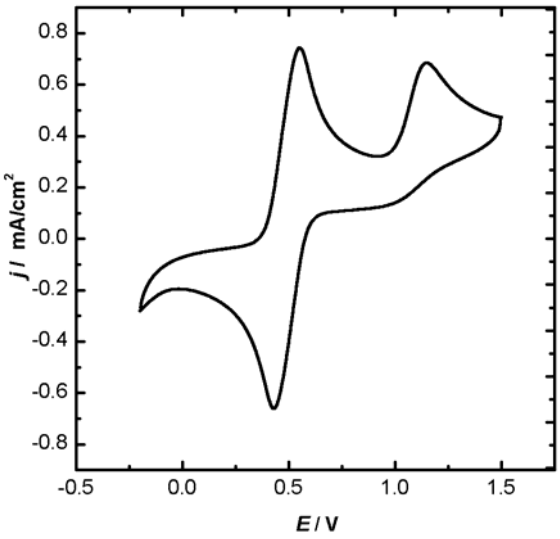

Figure 8-5. Cyclic Voltammogram of **1a**.

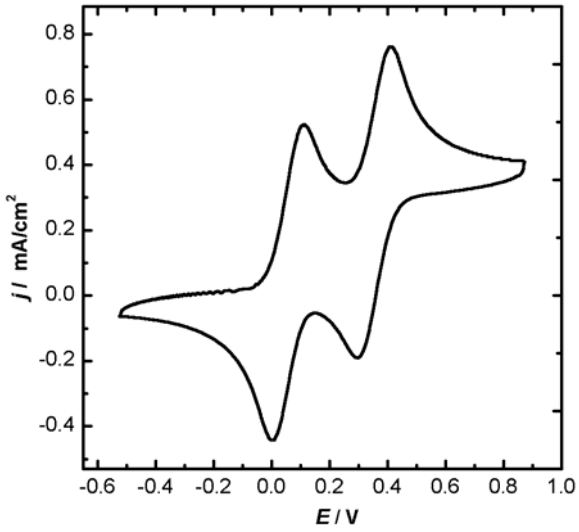

Figure 8-6. Cyclic Voltammogram of **1b**.

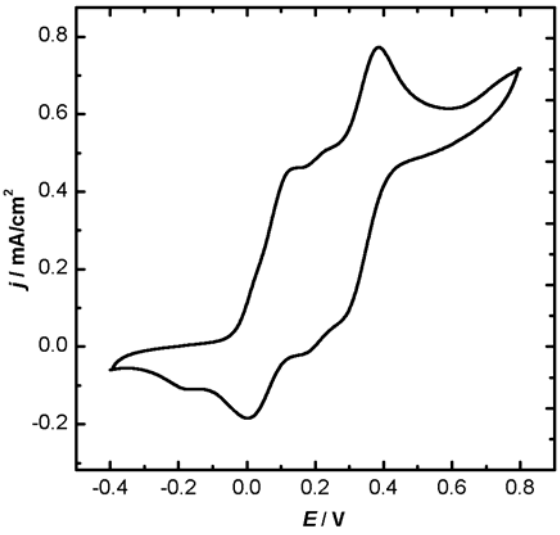

Figure 8-7. Cyclic voltammogram of compound **1c**.

Table 8-2. Oxidation potentials and classification of the three [1.1]ferrocenophanes studied.[a]

	$E_{1/2}$ [V]		E_{ox1} [V]	E_{ox2} [V]	Robin-Day Class
1a	0.36	–	0.54	–	I
1b	0.05	0.35	0.11	0.41	II
1c	–[b]	–[b]	0.12	0.39	II
			(0.0)	(0.2)	

[a] values in brackets for **1c** correspond to the two minor oxidation waves.
[b] $E_{1/2}$ could not be determined for **1c** reliably.

Compound **1a** displays the redox chemistry of isolated Fe centers lacking any electronic communication, thus belonging to class I, according to the Robin-Day classification.[11] To the best of our knowledge, this is an unprecedented behavior for [1.1]ferrocenophanes. In contrast, the Ga species **1b** displays the expected stepwise oxidation, showing moderate electronic interaction between the two ferrocene moieties. The separation between the oxidation potentials in **1b** ΔE_{ox} is 0.30 V, from which an exchange constant of K_c = 118000 was obtained,[17] indicating class II behavior. The two major and two minor oxidation waves for the In compound **1c** hint at the presence of

two different species in solution (Figure 8-7). It is feasible that compound **1c** consists of a mixture of two isomers that can be differentiated in solution by CV. This speculation is supported by the fact that at -80 °C in C_7D_8, a second set of signals emerges in the ^1H NMR spectrum of **1c.** We assume that the major redox waves belong to an isomer with a structure similar to that found for **1c** in the crystal lattice. We do not have experimental evidence about the nature of the minor species; however, the NMR spectrum of **1c** at room temperature reveals only one species, as it shows only one set of signals.

In addition to the reversible two-electron wave, compound **1a** displays a second but irreversible oxidation process at 1.2 V (Figure 8-5). Furthermore, we observed a white precipitate that was produced during extensive cycling, which prompted us to carry out studies with an electrochemical quartz crystal microbalance (EQCM). It can be seen in Figure 8-8 that the Al dimer **1a** showed significant adsorption to the gold electrode, corresponding to an increase in mass on the quartz crystal starting around 1.0 V (Figure 8-5 and Figure 8-8, b).

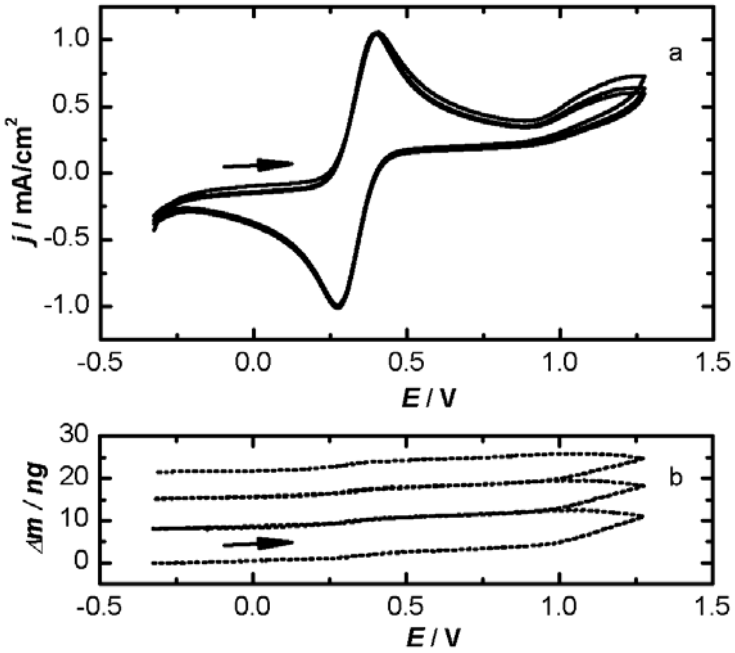

Figure 8-8. a) Cyclic voltammogram of compound **1a** (gold disc on quartz crystal as a working electrode) b) QCM response. Significant increase in mass (aprox.10 ng) starting around 1.0 V indicates deposition of **1a** onto the electrode.

When the sweep was reversed at 0.9 V, compound **1a** showed full redox reversibility without any adsorption to the electrode. To obtain some information about the deposited material, we analyzed the topography of the gold electrode by atomic force microscopy (AFM, see the Supporting Information) and the elemental composition by X-ray photoelectron spectroscopy (XPS) and Auger electron spectroscopy (AES). For the AFM measurement, we examined samples for which a constant potential of 1.3 V for 5, 15, and 30 min had been applied. After 30 min, the current leveled out to zero, indicating that the surface of the electrode was completely covered, corresponding to a total deposition of a few hundred nanograms. After 5 min, an islandlike growth of deposited material on the surface was observed by AFM. After 15 min, the gold surface

was largely covered, and after 30 min the surface was completely covered with multiple layers of material.

From XPS and AES, the five most abundant elements of the deposited material are C, O, Fe, Al, and N. It is fair to assume that oxygen was introduced through an exposure of the sample to air after deposition. With respect to the four elements C, Fe, Al, and N, the elemental composition found for the deposited material reflects the overall composition of the initial ferrocenophane **1a** (see Experimental Section).

Because the two ferrocene moieties in **1a** are already oxidized at the same potential ($E_{1/2}$ = 0.36 V and E_{ox1} = 0.54 V), the occurrence of the second irreversible oxidation at 1.2 V must be due to an oxidation somewhere else in **1a**. Aluminum alkyl species exhibit highly polar Al-C bonds, and are known to be reducing agents. We assume that at higher voltage, C atoms bound to aluminum become oxidized, which must result in a breakage of the respective Al-C bond, obviously an irreversible process. To to test this hypothesis, we recorded an EQCM of Ar'$AlMe_2$ (Figure 8-9). This compound serves as a ferrocene-free model for **1a**, because it shows aluminum with a first coordination sphere similar to that in **1a**.

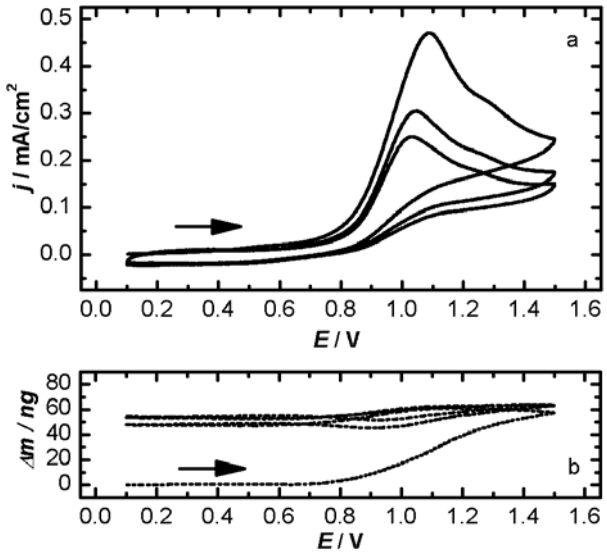

Figure 8-9. (a) Cyclic Voltammogram of Ar'$AlMe_2$. (b) QCM response. Large increase in mass (~50 ng) strating around 0.8 V indicates a decomposition process.

The model compound Ar'$AlMe_2$ displays an irreversible oxidation wave similar to that of **1a**, at a comparable potential and with an even larger adsorption to the electrode. The first sweep already deposited more than 50 ng of material, which almost completely covered the electrode disk. Deposited material withstood multiple washings with various solvents, and is rather soft.

8.4 Conclusion

Heavier group 13 element-containing compounds equipped with the intramolecularly coordinating "one-armed" phenyl ligand Ar' (Figure 8-2) give access to the [1.1]ferrocenophanes **1a-c**. Although the aluminum species **1a** was published very recently,[3b] and the gallium compound **1b** is another example of a [1.1]digallaferrocenophane,[4] **1c** is the first indium-bridged [1.1]ferrocenophane. In the

solid state, **1a-c** display the expected *anti* conformation. Interestingly, similar reactions with pytrisyl-containing starting compounds yielded strained [1]ferrocenophanes (Pytsi, Figure 8-2).[13,14]

The three isostructural [1.1]ferrocenophanes **1a-c** display distinctively different electrochemical behavior, as revealed by cyclic voltammetry. Only the [1.1]digallaferrocenophane **1b** shows the expected voltagramm, with two separated, fully reversible one electron oxidation steps. The [1.1]dialuminaferrocenophane **1a** shows a fully reversible two-electron oxidation step. Furthermore, at a higher potential, it shows an irreversible oxidation step, which is accompanied by adsorption processes on the gold electrode. On the other hand, the [1.1]diindaferrocenophane **1c** exhibits a more complex cyclic voltagramm, with four reversible oxidation steps. We attribute this to the presence of conformational isomers in solution. To the best of our knowledge, the Al species **1a** is the first [1.1]ferrocenophane in which the two Fe atoms act independently (class I). So far, the reasons for this exceptional behavior remain unclear. Further investigations to illuminate the origins of the different properties of Al-bridged ferrocenophanes compared to those of Ga-bridged ferrocenophanes are currently underway.

8.5 Experimental Section

Electrochemistry. All experiments were conducted with a CH Instruments, Inc., model 660B electrochemical analyzer. A gold working electrode (BAS, 2 mm) was employed. The quasi-reference electrode was a silver wire immersed in 0.1 M tetrabutylammonium hexafluorophosphate (TBAPF) in EtOH solution separated by a Vycor tip (the potential of which is 75 mV vs. a standard hydrogen electrode (SHE)).

Platinum wire was used as the auxiliary electrode. In each case, IR compensation was applied. Solutions of **1a-c** (1 mM) were prepared in dry dichloromethane with 0.1 M TBAPF as supporting electrolyte. The scan rate for all CVs reported was 100 mV/s. Experiments were conducted under strict inert conditions to exclude interactions with oxygen and moisture (glovebox, vacuum pump, and nitrogen purging). All measurements were carried out in a nitrogen-purged electrochemical cell. Measurements were taken at room temperature (22 ^{o}C).

EQCM experiments were conducted with a CH Instruments, Inc., model series CHI 440 EQCM instrument. An 8 MHz quartz crystal covered with 100 Å of Ti and 1000 Å of Au was used as a working electrode (commercially available from CH Instruments). The gold electrode area was 0.205 cm^2.

Synthesis. All manipulations were carried out using standard Schlenk techniques. Solvents were dried using a Braun Solvent Purification System, and were stored under argon over a 4 Å molecular sieve. C_6D_6 and C_7D_8 were degassed prior to use and were stored under argon over a 4 Å molecular sieve. $GaCl_3$ (99.99%, Aldrich) and InI_3 (99.999%, Alpha Aesar) were purchased and used as received. ^{1}H and ^{13}C NMR spectra were recorded on a Bruker 500 MHz Avance spectrometer; chemical shifts were referenced to the residual protons of the deuterated solvent. All NMR spectra are in C_6D_6 at 25°C, unless noted differently. Mass spectra were measured on a VG 70SE mass spectrometer and were reported in the form *M* (%*I*) [*F*], where *M* is the mass observed, %*I* is the intensity of the peak relative to the most intense peak in the spectrum, and *F* is the molecular ion or fragment. Only ions with intensities greater than 10% are listed. Elemental analysis was performed on a Perkin-Elmer 2400 CHN

Elemental Analyzer; samples were prepared in a glovebox and V_2O_5 was added to promote combustion.

The compounds Ar'$AlCl_2$,[15] Ar'Me_2,[15] Ar'$GaCl_2$,[18] and Ar'InI_2[19] were synthesized according to literature procedures (Ar' = 2-(Me_2NCH_2)C_6H_4). In the course of our investigations, the synthesis and characterization of **1a** was published;[3b] the synthetic procedure we used for compound **1a**, is described in the Supporting Information.

Synthesis of 1b. A solution of Ar'$GaCl_2$ (1.025 g, 3.73 mmol) in toluene (30 mL) was chilled to -10 °C and was added dropwise via tubing to a chilled (-10 °C) suspension of dilithioferrocene·2/3TMEDA (1.027 g, 3.73 mmol) in toluene (30 mL). After being stirred for 16 h, the solution changed in color to red. After being filtered, the solution was concentrated by evacuation until crystallization started. To promote crystallization, we cooled the solution to 6 °C (0.215 g, 0.28 mmol, 15%). ^{1}H NMR (500 MHz): δ = 1.70 (s, 12H, NMe_2), 3.24 (s, 4H, -CH_2-), 3.99, 4.37, 4.48, 5.07 (pst, 16H, C_5H_4), 6.99 (d, 2H, C_6H_4), 7.28 (pst, 2H, C_6H_4), 7.42 (pst, 2H, C_6H_4), 8.45 (d, 2H, C_6H_4). ^{13}C NMR (125.8 MHz): δ = 45.61 (NMe_2), 66.40 (-CH_2-), 70.91 (*ipso*-C, C_5H_4), 70.76, 71.05, 74.79, 75.20 (C_5H_4), 124.99, 127.42, 127.59, 130.08, 144.59, 150.99 (C_6H_4). Anal. Calcd for $C_{38}H_{40}Fe_2Ga_2N_2$ (775.87): C, 58.82; H, 5.20; N, 3.61. Found: C, 59.62; H, 5.35; N, 3.80. MS (70 eV, EI+): *m/z* (%): 776 (100) [M^+], 571 (5.6) [M^+ – Ar'Ga], 388 (14) [½M^+ + H].

Synthesis of 1c. Ar'InI_2 (0.880 g, 1.75 mmol) was dissolved in THF (15 mL), chilled to -10 °C and added dropwise via tubing to a chilled (-10 °C) suspension of dilithioferrocene·2/3TMEDA (0.482 g, 1.75 mmol) in THF (15 mL). After being stirred

for 16 h, the solution changed in color to red. The solvent was removed under high vacuum to give a sticky orange-brown solid. This solid was redissolved in benzene (20 mL), and was filtered. At 6 °C orange crystals of **1c** precipitated (0.440 g, 0.51 mmol, 58%). ^{1}H NMR (500 MHz): δ = 1.81 (s, 12H, NMe_2), 3.24 (s, 4H, -CH_2-), 4.04, 4.45, 4.53, 4.97 (pst, 16H, C_5H_4), 7.01 (d, 2H, C_6H_4), 7.25 (pst, 2H, C_6H_4), 7.35 (pst, 2H, C_6H_4), 8.37 (d, 2H, C_6H_4); ^{13}C NMR (125.8 MHz): δ = 45.38 (NMe_2), 67.55 (-CH_2-), 68.30 (*ipso*-C, C_5H_4), 71.30, 71.64, 75.44, 76.35 (C_5H_4), 126.35, 127.37, 127.75, 139.11, 145.37, 155.71 (C_6H_4). Anal. Calcd for $C_{38}H_{40}Fe_2In_2N_2$ (866.06): C, 52.70; H, 4.66; N, 3.23. Found: C, 50.06; H, 4.75; N, 3.10. MS (70 eV, EI+): *m/z* (%): 866 (100) [M^+], 619 (7.3) [M^+ – Ar'In], 433 (14) [½M^+], 383 (23) [Ar'$_2$In$^+$], 115 (37) [In^+].

X-ray structural analysis for 1b and 1c. Data were collected at -100 °C on a Nonius Kappa CCD diffractometer, using the COLLECT program.[20] Cell refinement and data reductions used the programs DENZO and SCALEPACK.[21] The program SIR97[22] was used to solve the structure and SHELXL97[23] was used to refine the structure. All H atoms were placed in calculated positions, with C-H distances in the range 0.95 – 0.99 Å, and were included in a riding model approximation. U_{iso}(H) was constrained to be 1.2 U_{eq}(C) for all aromatic protons and 1.5 U_{eq}(C) for all methyl protons.

Surface analysis. X-ray photoelectron spectroscopy (XPS) and Auger electron spectroscopy (AES) were done at the Alberta Center for Surface Engineering and Science (ACSES) using a Kratos Axis 165 spectrometer. Several spots of the sample were analyzed by XPS and all spectra showed C, O, and Fe as the three elements with the highest mass concentrations. A representative analysis (aperture 120 μm) for just

five elements (set to 100%) gave C (1s, 50.6%), O (1s, 24.7%), Fe (2p, 17.9%), Al (2p, 5.0%), N (1s, 1.8%); if only four elements (set to 100%) are used, the results are: C (1s, 67.2%), Fe (2p, 23.7%), Al (2p, 6.6%), N (1s, 2.4%). Several different positions of the sample previously analyzed by XPS were analyzed by AES. Representative results for three different positions are C (70.5, 71.0, 68.1%), O (13.3, 12.8, 15.2%), Fe (10.6, 9.7, 9.3%), Al (3.4, 4.5, 5.5%), N (2.2, 2.0, 1.8%); if only four elements (set to 100%) are used, the results are C (80.7, 81.4, 80.3%), Fe (12.2, 11.1, 11.0%), Al (3.9, 5.2, 6.5 %), N (2.5, 2.3, 2.1%). The results from XPS and AES compare well with the mass concentrations of the four elements C, Fe, Al, and N in **1a** (set to 100%): C (70.21%), Fe (17.18%), Al (8.30%), N (4.31%).

Acknowledgement. We thank the Natural Sciences and Engineering Research Council of Canada (NSERC Discovery Grant), the Department of Chemistry, and the University of Saskatchewan for their generous support. We thank the Canada Foundation for Innovation (CFI) and the government of Saskatchewan for funding of the X-ray and NMR facilities in the Saskatchewan Structural Sciences Centre (SSSC). We thank Dr. D. Karpuzov of the Alberta Center for Surface Engineering and Science (ACSES) for obtaining the XPS and AES data. H.-B.K. is the Canada Research Chair in Biomaterials.

Supporting Information Available. Text detailing the synthesis and characterization of compound **1a**; crystallographic data for **1b** and **1c** in CIF file format, picture of the electrochemical cell, and AFM images of adsorbed material. This material is available free of charge via the Internet at http://pubs.acs.org.

8.6 References

(1) (a) Nguyen, P.; Gomez-Elipe, P.; Manners, I. *Chem. Rev.* **1999**, *99*, 1515. (b) Manners, I. *Chem. Comm.* **1999**, 857. (c) Manners, I. *Science*, **2001**, *294*, 1664.
(2) Scheibitz, M.; Winter, R. F.; Bolte, M.; Lerner, H.-W.; Wagner, M. *Angew. Chem. Int. Ed. Engl.* **2003**, *42*, 924.
(3) (a) Schachner, J. A.; Lund, C. L.; Quail, J. W.; Müller, J *Acta Crystallogr.*. **2005**, *E61*, m682. (b) Braunschweig, H.; Burschka, C.; Clentsmith, G. K. B.; Kupfer, T.; Radacki, K. *Inorg. Chem.* **2005**, *44*, 4906.
(4) (a) Uhl, W.; Hahn, I.; Jantschak, A.; Spies, T. *J. Organomet. Chem.* **2001**, *637*, 300. (b) Jutzi, P.; Lenze, N.; Neumann, B.; Stammler, H. G. *Angew. Chem., Int. Ed. Engl.* **2001**, *40*, 1424. (c) Althoff, A.; Jutzi, P.; Lenze, N.; Neumann, B.; Stammler, A.; Stammler, H.-G. *Organometallics* **2002**, *21*, 3018. (d) Althoff, A.; Jutzi, P.; Lenze, N.; Neumann, B.; Stammler, A.; Stammler, H. G. *Organometallics* **2003**, *22*, 2766.
(5) (a) Watts, W. E. *J. Am. Chem. Soc.* **1966**, *88*, 855. (b) Watts, W. E. *J. Organomet. Chem.* **1967**, *10*, 191.
(6) (a) Berenbaum, A.; Lough, A. J.; Manners, I. *Organometallics* **2002**, *21*, 4415. (b) Calleja, G.; Carré, F.; Cerveau, G.; Labbé, P.; Coche-Guérente, L. *Organometallics* **2001**, *20*, 4211. (c) Zechel, D. L.; Foucher, D. A.; Pudelski, J. K.; Yap, G. P. A.; Rheingold, A. L.; Manners, I. *J. Chem. Soc., Dalton Trans.* **1995**, 1893. (d) Park, J.; Seo, Y.; Cho, S.; Whang, D.; Kim, K.; Chang, T. *J. Organomet. Chem.* **1995**, *489*, 23.
(7) (a) Rulkens, R.; Lough, A. J.; Manners, I. *Angew. Chem., Int. Ed. Engl.* **1996**, *35*, 1805. (b) Jaekle, F.; Rulkens, R.; Zech, G.; Foucher, D. A.; Lough, A. J.; Manners, I. *Chem. Eur. J.* **1998**, *4*, 2117.
(8) Utri, G.; Schwarzhans, K.-E.; Allmaier, G. M. *Z. Naturforsch. B* **1990**, *45*, 755.
(9) Brunner, H.; Klankermayer, J.; Zabel, M. *J. Organomet. Chem.* **2000**, *601*, 211.
(10) Mueller-Westerhoff, U. T., *Angew. Chem., Int. Ed. Engl.* **1986**, *25*, 702.
(11) Robin, M. B.; Day, P. *Adv. Inorg. Chem. Radiochem.* **1967**, *10*, 247.
(12) Al-Juaid, S. S.; Eaborn, C.; Hitchcock, P. B.; Hill, M. S.; Smith, J. D. *Organometallics* **2000**, *19*, 3224.
(13) Schachner, J. A.; Lund, C. L.; Quail, J. W.; Müller, J *Organometallics* **2005**, *24*, 785.
(14) Schachner, J. A.; Lund, C. L.; Quail, J. W.; Müller, J *Organometallics* **2005**, *24*, 4483.
(15) Müller, J.; Englert, U. *Chem. Ber.* **1995**, *128*, 493.
(16) Cottrell constant: $it^{1/2} = 1.77nFAD^{1/2}C^*$, where n is the amounts of electrons transferred, F is the Faraday constant, A is the area of the electrode, D is the diffusion coefficient and C* is the bulk concentration of the electrochemical reactant.
(17) Creutz, C. *Prog. Inorg. Chem.* **1983**, *30*, 1.
(18) Brown, D. S.; Decken, A.; Cowley, A. H. *J. Am. Chem. Soc.* **1995**, *117*, 5421.
(19) Gabbaie, F. P.; Isom, H. S.; Decken, A.; Culp, R. D.; Cowley, A. H. *Main Group Chemistry* **1995**, *1*, 9.
(20) Nonius; Nonius BV, Delft, The Netherlands, **1998**.
(21) Otwinowski, Z.; Minor, W. In *Macromolecular Crystallography, Part A*; Carter, C. W., Sweet, R. M., Eds.; Academic Press: London, **1997**; Vol. 276, pp 307-326.

(22) Altomare, A.; Burla, M. C.; Camalli, M.; Cascarano, G.; Giacovazzo, C.; Guagliardi, A.; Moliterni, A. G. G.; Polidori, G.; Spagna, R. *J. Appl. Crystallogr.* **1999**, *32*, 115.
(23) Sheldrick, G. M.; *SHELXS97 and SHELXL97*, University of Göttingen, Germany, 1997.

CHAPTER 9
SUMMARY and CONCLUSIONS

The successful synthesis of heavier group 13-bridged [1]metallocenophanes ([1]MCPs) and [1.1]ferrocenophanes ([1.1]FeCPs) was achieved by employing intramolecular coordinating ligands. The ligands utilized amine functionalities as donors to satisfy the Lewis-acidic group 13 element.

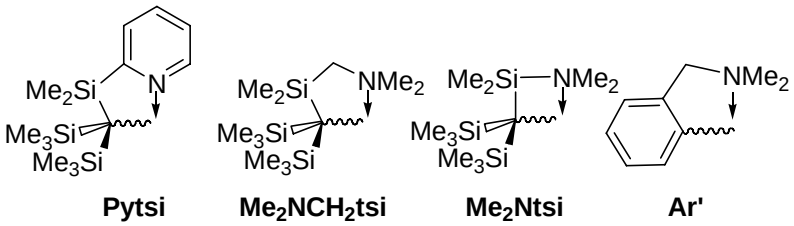

Figure 9-1. Intramolecular coordinating ligands used in this PhD project.

A series of four new aluminum- and gallium-bridged [1]ferrocenophanes employing both the Pytsi (see Chapters 3 and 4) and Me_2Ntsi ligand (see Chapter 5) as well as two new [1]ruthenocenophanes employing only the Me_2Ntsi ligand (see Chapter 6) were synthesized. In addition, the first aluminum-bridged [1.1]ferrocenophane (see Chapter 7) and a novel gallium- and the first indium-bridged [1.1]ferrocenophanes employing the Ar' ligand (see Chapter 8) were synthesized.

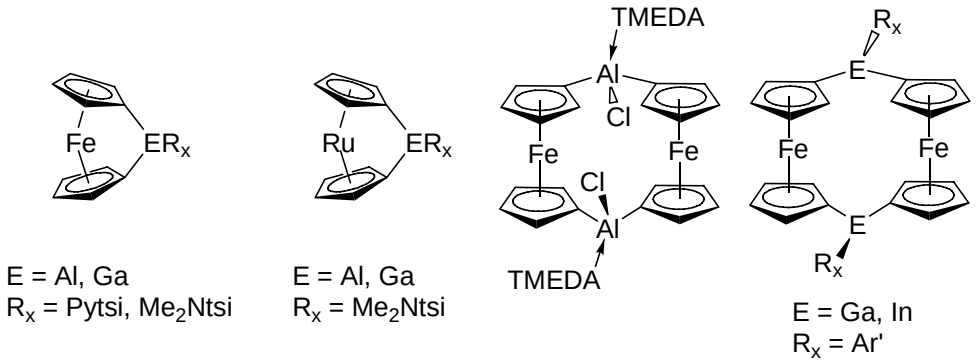

Figure 9-2. New metallocenophanes synthesized during this PhD project.

Figure 9-2 shows all the novel compounds published during the duration of this PhD project. The [1]MCPs are the first examples of heavier group 13 bridged [1]MCPs. The aluminum- and indium-bridged[1.1]ferrocenophanes were previously unpublished. The aluminum-bridged [1.1]ferrocenophane employing the Ar' ligand and two other examples of gallium-bridged [1.1]ferrocenophanes had been previously published in literature (see Chapter 1.3.1, **17a**, **18a-b**). All complexes were fully characterized by single-crystal X-ray crystallography. Furthermore, the new [1]MCPs were investigated as potential monomers in ROP, and the Ar' containing aluminum-, gallium-, and indium-bridged [1.1]ferrocenophanes yielded interesting insight into the electrochemistry of these complexes.

It is interesting to note that the trisyl-based ligands, namely Me_2Ntsi and Pytsi, preferably yielded strained [1]ferrocenophanes ([1]FeCPs) and [1]ruthenocenophanes ([1]RuCPs), whereas the benzylamine ligand Ar' yielded preferably [1.1]FeCPs. We mainly attribute this difference in reactivity to the presence of the bulkier trimethylsilyl groups in the trisyl-based ligands, compared to the slimmer Ar' ligand. This becomes especially obvious when the reactivity of

Me_2Ntsi and Ar' are compared, both of which use the same donor, a dimethylamine group. The aromatic groups (pyridine in Pytsi and a phenyl group in Ar') do not offer a lot of steric protection above and below their respective planes, whereas the bulky trimethylsilyl groups do. The previously unpublished ligand Me_2NCH_2tsi proved to be surprisingly unreactive (see Chapter 5). Me_2NCH_2tsi is formally extended by a methylene group compared to Me_2Ntsi to form a five-membered heterocycle when coordinated to a group 13 element. Under similar reaction conditions that yielded [1]FeCPs in high yields with Me_2Ntsi, [(Me_2NCH_2tsi)$AlCl_2$] showed a conversion of only 10 % to give unidentified ferrocenophanes (see Chapter 5).

The Me_2Ntsi ligand offered some advantages in the synthesis of [1]MCPs. The overall synthesis was reduced by two steps compared to Pytsi (5 steps vs. 7 steps) with an overall higher yield. Synthesis of [1]MCPs containing the Me_2Ntsi ligand also produced higher yields with a significant ease in crystallizing the products, a major advantage because all complexes obtained were purified by crystallization (see Chapter 5). For (Me_2Ntsi)Al[1]FeCP almost quantitative yields were obtained. Me_2Ntsi also gave access to a series of strained [1]metallarenophanes, which could not be synthesized with Pytsi (see Chapter 5).

Although Pytsi and Me_2Ntsi allowed for the first successful isolation of heavier group 13 bridged [1]MCPs with Al and Ga in the bridging position, initial ROP experiments were rather unsuccessful (see Chapter 6). Only in the case of transition metal catalyzed ROP, using [$Pd(dba)_2$] (dba = dibenzylideneacetone) as initiator and the monomer Pytsi[1]FeCPs, polymeric material was obtained.

Thermal, anionic, and photolytic ROP were unsuccessful. Since other [1]MCPs with similar ring strain (e.g. stanna[1]MCPs) showed a high propensity towards ROP, the reason for the lower reactivity of aluminum- and gallium-bridged [1]MCPs must have different explanations, which have yet to be examined in detail. All novel [1]MCPs except galla[1]RuCP (α [°]: Ga: 20.91(19)) showed an exothermic ring-opening in Differential Scanning Calorimetry (DSC) experiments. At this point it is unknown why galla[1]RuCP did not ring-open at elevated temperatures, but rather decomposed (see Chapter 6). The similar ring-tilted alumina[1]RuCP (α [°]: Al 20.31(19)) does show exothermic ring-opening. Me_2Ntsi containing [1]FeCPs did not yield polymeric material after heating to 240 °C for 20 h. When common anionic initiators like *n*BuLi were used, Pytsi containing [1]FeCPs showed an unexpected alkylation at the *para* position of the pyridine ring, but no ring-opened products could be identified. [1]MCPs equipped with the Me_2Ntsi ligand showed no reaction at all under various conditions. Photolytic induced ROP with Me_2Ntsi containing [1]MCPs also showed no reaction under various conditions in the strong donor solvent THF. Photolytic induced ROP has been reported so far only for phospha[1]FeCPs and sila[1]FeCPs, and a strong correlation between their tilt angle α and their treactivity was observed. Phospha[1]FeCP showed ring-opening under UV irradiation already in strong donor solvents like THF or CH_3CN, whereas sila[1]FeCPs showed no reactivity under the same conditions. Phospha[1]FeCP generally display a ring tilt of α ~ 26-27° which is more strained compared to sila[1]FeCPs with general ring tilts of α ~ 20-21°. Sila[1]FeCPs could be photolytically ring-opened in the presence of a mild initiator like LiCp, but better

results were obtained when the more nucleophilic initiator NaCp was used. For the novel aluminum- and gallium-bridged [1]FeCPs which possess a ring tilt of $\alpha \sim 14$-15°, the ring strain might not be large enough to induce ring-opening in the presence of NaCp. The incorporation of the 4d metal ruthenium to give [1]RuCP increases the ring tilt as expected. However, (Me_2Ntsi)Al[1]RuCP ($\alpha = 20.31°$) showed a similar ring-opening enthalpy in DSC experiments than the less tilted [1]FeCPs ($\alpha = 14$-15°). Together with the general low reactivity of [1]RuCPs in ROP experiments, which is similar to the [1]FeCPs, it can be concluded that the overall ring strain did not increase in [1]RuCPs compared to [1]FeCPs. This can be explained by a weaker π-bonding between ruthenium and the (C_5H_4) ligands, which is reflected by longer Ru-(C_5H_4) bonds in the crystal structure, which results in a higher flexibility. Therefore the ring strain for a given [1]MCP mainly depends on the size of the bridging element, with smaller size elements resulting in higher ring strains (see Chapter 6).

The electrochemistry of novel [1.1]ferrocenophanes yielded further evidence that the charge delocalization in the mixed-valent complex is bridge-mediated, not mediated through-space (see Chapter 8). This becomes obvious when the isostructural aluminum- and gallium-bridged [1.1]FeCPs containing the Ar' ligand are compared. The aluminum-bridged complex behaved as an unprecedented Class I complex, with no charge delocalization between the two iron atoms in the mixed-valent state. The gallium-bridged [1.1]FeCP on the other hand showed the expected behavior of a Class II complex with moderate coupling in the mixed-valent state. These observations pose an interesting question with respect to polyferrocenes

containing bridging aluminum and gallium atoms. From a simplified point of view, [1.1]FeCPs can be regarded as the shortest model compound for a polyferrocene. From a mechanistic standpoint, the formation of [1.1]FeCPs is equivalent to backbiting after addition of one monomer unit, thereby terminating the growing chain. The electrochemistry of various oligomers and polymers of polyferrocenylsilanes have been investigated, and it was found that iron atoms get oxidized at alternating sites first because of charge delocalization, with the oxidation of the iron atoms in between occurring at higher potential. Since polyferrocenes are expected to show novel properties compared to polyolefins, for example electric conductivity, a polyferrocenylalane could potentially behave as an insulator, because no charge transport should occur between the iron atoms (see Chapter 8).

The novel indium-bridged [1.1]FeCP equipped with the Ar' ligand showed a more complex electrochemistry (see Chapter 8). This was explained by an isomerization in solution which was further studied by variable temperature and 2D NMR experiments. The complex adopted an anti-conformation in the solid state, which was expected from the size of the bridging element and the bulkiness of the ligands Ar'. *Syn* isomers of [1.1]FeCPs are known to undergo a fast *syn-syn* isomerization in solution. *Anti* isomers have also been postulated to undergo a similar *anti-anti* isomerization, and we could obtain some additional evidence for this from EXSY NMR experiments. An *anti-syn* isomerization has also been postulated in literature, and for carbon- and phosphorous-bridged [1.1]FeCPs both anti- and syn-isomers have been isolated. Variable temperature NMR experiments

with (Ar')In[1.1]FeCP did yield evidence for the *syn* isomer. At - 80 °C, a second set of signals emerged, as expected for the *syn* isomer (see Chapter 8).